National Aeronautics and
Space Administration

CxP 72067

DRAFT

RELEASE DATE: TBD

Constellation Program

Draft Maturity 100%
August 31, 2006

ARES-I SYSTEM STRUCTURAL DYNAMICS, LOADS, AND MODEL DATA BOOK

TABLE OF CONTENTS

LIST OF FIGURES

LIST OF TABLES

1.0 Scope

This document provides an official reference of the Loads Cycle 1A design limit loads and applies to the DAC-1 Integrated Stack CLV and CLV Elements for their design activities. The document includes the supporting analysis details for the design limit loads published in memorandum EV31-06-006 and updates to the analysis results since publication of the memorandum. If there is a conflict between EV31-06-006, this document supercedes.

2.0 Purpose

The purpose of this System Structural Dynamics, Loads, and Models Databook is to present the defined design loads and structural dynamic characteristics for the integrated CLV, CEV, and Launch Pad System. Each individual system element is presumed to have its own Databook to document that element's unique requirements. The scope of these Databooks must be carefully coordinated to assure the inclusion of all credible loading events.

This document provides references to data sources along with pertinent and summary data for inputs and results. Detailed information is stored in the Vehicle Integration Loads Team database located on the ICE server, Reference 1. This database contains all tools, data, and models used in this analysis. All input data files and program files needed to reconstruct the analysis are contained in the database. Detailed result files are also contained there

Section 4.0 is a very brief description of the CEV/CLV integrated stack configuration.

Section 5.0 of this document summarizes and references all the detailed inputs used to assess the system load conditions and conduct the system level loads analyses.

Section 6.0 of this document summarizes the element and system finite element models (FEM's) used to conduct the system level loads analysis.

Section 7.0 of this document summarizes the development and assumptions of the different system load cases analyzed.

Section 8.0 of this document summarizes the integrated system loads analysis results.

Section 9.0 of this document summarizes the recommended design loads. This also includes a discussion of any uncertainty factors used in generating these design loads. Unless otherwise specified all loadings are to be considered limit loads.

Section 10.0 of this document summarizes additional trades and studies completed based on the FEM's and results of the system loads analysis documented here.

3.0 Documents

3.1 Applicable Documents

3.2 References

1) NASA, Exploration Systems Integrated Collaborative Environment (ICE-Windchill), Path =”CLV - Vehicle Integration / (03) Integrated Design & Analysi... / E) Groups and Panels / 1) AFS Integration Group / PANELS / Loads Struc Dyn Panel / VI Loads & Dynamics Team / Load_Cycle_1A/Analysis Archive”.
2) “Terrestrial Environment (Climatic) Criteria Handbook for Use in Aerospace Vehicle Development,” NASA-HDBK-1001, August 11, 2000.
3) NASA, Exploration Systems Integrated Collaborative Environment (ICE-Windchill), Path =”CLV - Vehicle Integration / (03) Integrated Design & Analysi... / E) Groups and Panels / 1) AFS Integration Group / PANELS /Ascent Perf Panel / Trajectory Perf Working Group / DAC/DAC-0/ POST_CLV-5_DAC0_Rev1”
4) NASA, Exploration Systems Integrated Collaborative Environment (ICE-Windchill), Path =”CLV - Vehicle Integration / (03) Integrated Design & Analysi... / E) Groups and Panels / 1) AFS Integration Group /AFSIG Meetings/2006-05-11/ DAC1Rev2MonteCarloResults (Greg Dukeman)”
5) NASA, Exploration Systems Integrated Collaborative Environment (ICE-Windchill), Path =”CLV - Vehicle Integration / (03) Integrated Design & Analysi... / E) Groups and Panels / 1) AFS Integration Group / PANELS /Aero Panel Database Releases / Current / DAC-1 Force and Moment Database/ Initial Release of DAC-1 F&M Database/ CLV5_dac1_new_aero_R1.xls “
6) NASA, Exploration Systems Integrated Collaborative Environment (ICE-Windchill), Path =”CLV - Vehicle Integration / (03) Integrated Design & Analysi... / E) Groups and Panels / 1) AFS Integration Group / PANELS /Aero Panel Database Releases / Current /DAC-1 Loads R1.0 dac1_load_dist_M163_R1.0/ dac1_load_dist_M163_R1.0.xls”
7) NASA, Exploration Systems Integrated Collaborative Environment (ICE-Windchill), Path =”CLV - Vehicle Integration / (03) Integrated Design & Analysi... / E) Groups and Panels / 1) AFS Integration Group / PANELS / Loads Struc Dyn Panel/Loads Panel All / Meetings / 2006-03-29/CLV Loads Cycle 1a - Aero Database/CLV Loads Cycle 1a.ppt “
8) “NLS On-Pad Aerodynamic Data Base,” NASA/MSFC Memorandum, ED35-114-91, September 12, 1991.
9) “Pre-Launch Ground Winds,” NASA SP-8008, 1966.
10) MSFC/ER42 PowerPoint presentation, “feb23_06_J2X_thrust_osc.ppt,” Thomas Zoladz
11) “First Stage Final Ballistic Prediction for Crew Launch Vehicle Design and Analysis Cycle Zero”, ATK TR017186
12) “MSC.Nastran Integrated Space Shuttle Vehicle Model,” USA Report SA-AR-01613-2002, Kristen Kendall, November 4, 2002.
13) USA email containing SRB models for use in shuttle derived vehicle studies, “Re SRB Models,” Kristen Kendall, March 10, 2004.
14) “Detailed Modeling of the KSC Mobile Launch Platform,” ED21 report, no date.

15) J. Brunty, "A Transient Response Analysis of the Space Shuttle Vehicle During Liftoff", NASA TM 103505
16) J. Brunty and J. Peck, "X33 Transient Liftoff Analysis", AIAA-2000-158
17) "A Method for Incorporating Changing Structural Characteristics Due to Propellant Mass Usage in a Launch Vehicle Ascent Simulation," NASA/TM—2004–213549, November 2004
18) NASA, Exploration Systems Integrated Collaborative Environment (ICE-Windchill), Path ="CLV - Vehicle Integration / (03) Integrated Design & Analysi... / E) Groups and Panels / 1) AFS Integration Group / PANELS / Loads Struc Dyn Panel/Loads Panel All / Meetings / 2006-04-18/ Copy of CLV Loads Cycle 1a Results/ CLV Loads Cycle 1a Results_Rev1.ppt"
19) NASA, Exploration Systems Integrated Collaborative Environment (ICE-Windchill), Path ="CLV - Vehicle Integration / (03) Integrated Design & Analysi... / E) Groups and Panels / 1) AFS Integration Group / PANELS / Loads Struc Dyn Panel/Loads Panel All / Meetings / 2006-04-18/ CLV Loads Cycle 1a Liftoff Analysis3/ CLV Loads Cycle 1a Liftoff Analysis3.ppt "
20) Abramson, H. N., ed.: The Dynamic Behavior of Liquids in Moving Containers. NASA SP-106, 1966.
21) Martin Marietta Corporation: HYDRO and BEAMER Reference Manual. 1982.
22) Universal Analytics, Inc.: NASTRAN Hydroelastic Modal Studies, Volume 1: Introduction, Theory, and Results. NASA CR-150393, 1977.
23) "Space Shuttle Solid Rocket Booster Design Loads, Pre-launch Through Separation (Book 1)," SE-019-057-2H D, December 2, 2002.
24) NASA, Exploration Systems Integrated Collaborative Environment (ICE-Windchill), Path ="CLV - First Stage / A)Documents / 3)First Stage / DAC-1 Milestone Review / DAC-1 Milestone Review.ppt"
25) NASA, Exploration Systems Integrated Collaborative Environment (ICE-Windchill), Path ="CLV - Vehicle Integration / (03) Integrated Design & Analysi... / E) Groups and Panels / 1) AFS Integration Group / PANELS / Loads Struc Dyn Panel/Loads Panel All / Meetings / 2006-06-20/ CLV Post LC1a Lift Off Overpressure Study_V2-2006-06-20.ppt"

4.0 Vehicle Configuration

The Load Cycle 1a (LC1a) analysis described in this document pertains to the Design Analysis Cycle 1(DAC-1) CLV integrated stack configuration. This configuration consists of a 5.5 meter diameter Upper Stage with a single J2-X, liquid oxygen, liquid hydrogen engine and a 1st Stage Booster (FSB) consisting of a 5 segment solid rocket motor derived from the Shuttle Reusable Solid Rocket Motor. The program specified configuration at the beginning of DAC-1 still contained a 5.5 meter diameter CEV element. However the Aerodynamic and Loads community agreed to assess the 198 inch diameter or "5.0 meter" CEV configuration that was undergoing wind tunnel testing. This configuration was generally expected to be accepted and was approved soon after the beginning of DAC-1. The existing Space Shuttle Program (SSP) Mobile Launch Platform (MLP) was assumed to be the launch pad for the LC1a analysis.

5.0 Loads Analysis Input Parameters

5.1 Reference Geometry and Conventions

All data and analysis results contained in this document are based on the two vehicle configurations illustrated in Figure 5.1-1 and Figure 5.1-2. **The 5.0 meter CEV from Figure 5.1-2 was used for both configurations in place of the 5.5 meter CEV in Figure 5.1-1.**

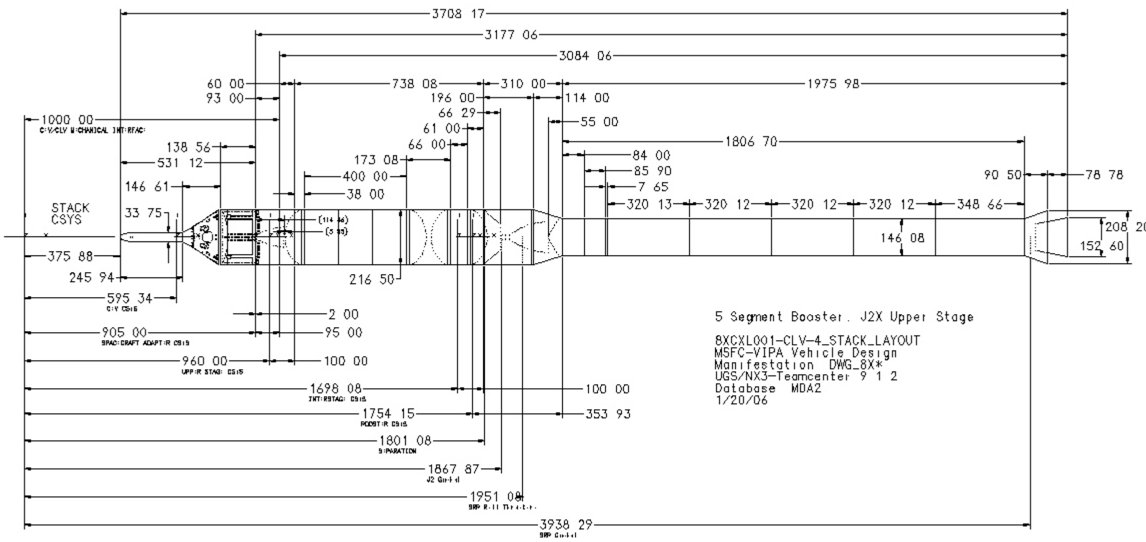

Figure 5.1-1, Reference 5.5 meter Upper Stage CLV configuration

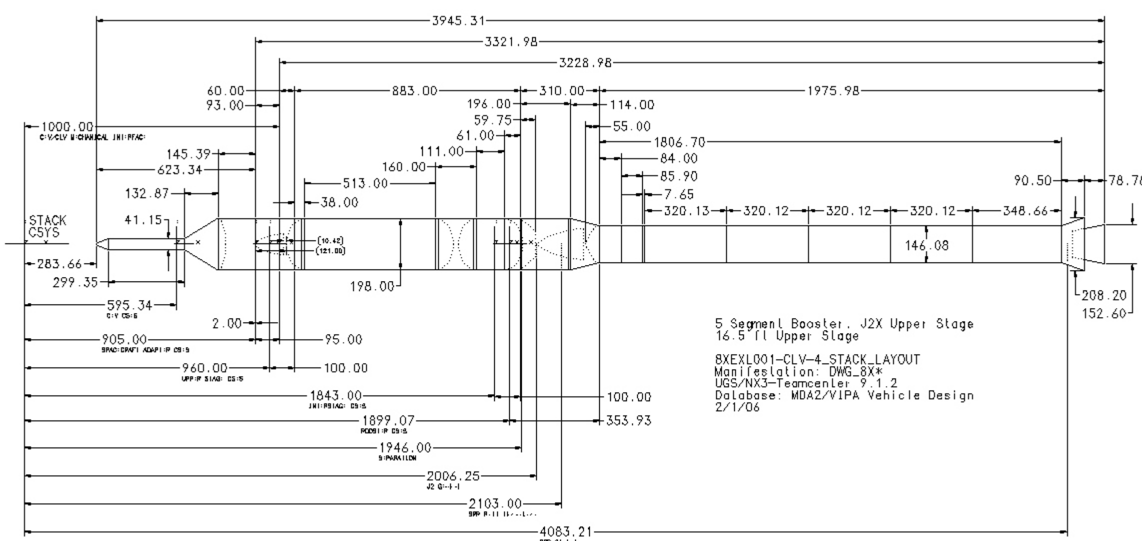

Figure 5.1-2, Reference 5.0 meter Upper Stage CLV configuration

5.1.1 Coordinate Systems

5.1.1.1 System Loads

The System Loads Coordinate system follows the right hand rule. All vehicle stack configurations considered in this analysis use a common System Loads Coordinate system with the FSB to MLP interface at a station of 3765.093. This interface is physically at the center of the spherical bearing supporting the hold-down post, Figure 5.1-3. However due to Upper stage length changes associated with diameter change, the location of element coordinate frames within the system coordinates may change. The coordinate system for each stage is located within the System Loads Coordinate system as indicated in Table 5.1-1, System Loads Coordinate System Origins D55m & D55mR for the D55m and D55mR configurations and in Table 5.1-2, Loads Coordinate System Origins D50m for the D50m configuration. The X coordinate runs in the direction from the nose to the tail. The Z coordinate is positive out the "top" of the vehicle; i.e. pitch up. The Y coordinate is positive out the right hand side of the vehicle.

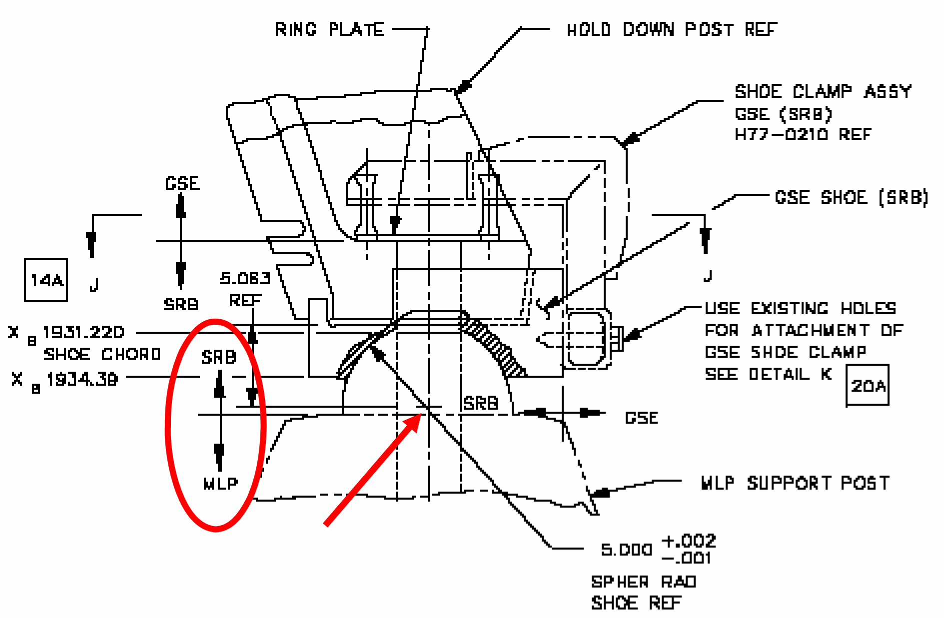

Figure 5.1-3, Booster to Launch Pad Interface

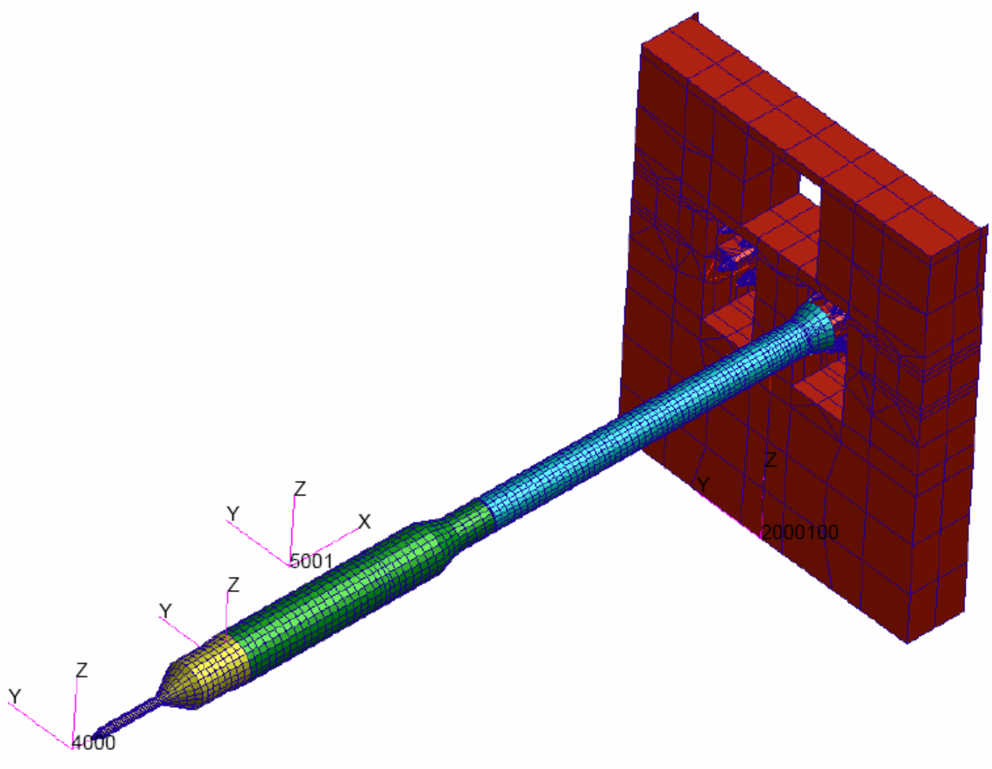

Figure 5.1-4, System Loads Coordinate Systems – D55m & D55mR

Table 5.1-1, System Loads Coordinate System Origins D55m & D55mR

System Loads Coordinate System Origins				
	X	Y	Z	Clocking X
System Loads Coordinate Origin (Coord 0)	0.000	0.000	0.000	0°
Escape/Crew/Service (Coord 4000)	-69.000	-250.500	0.000	0°
Upper Stage (Coord 6000)	707.340	-250.500	0.000	0°
FSB (Coord 5001)	1282.140	0.000	0.000	0°
MLP (Coord 2000100)	3778.270	0.000	-1212.57	0°

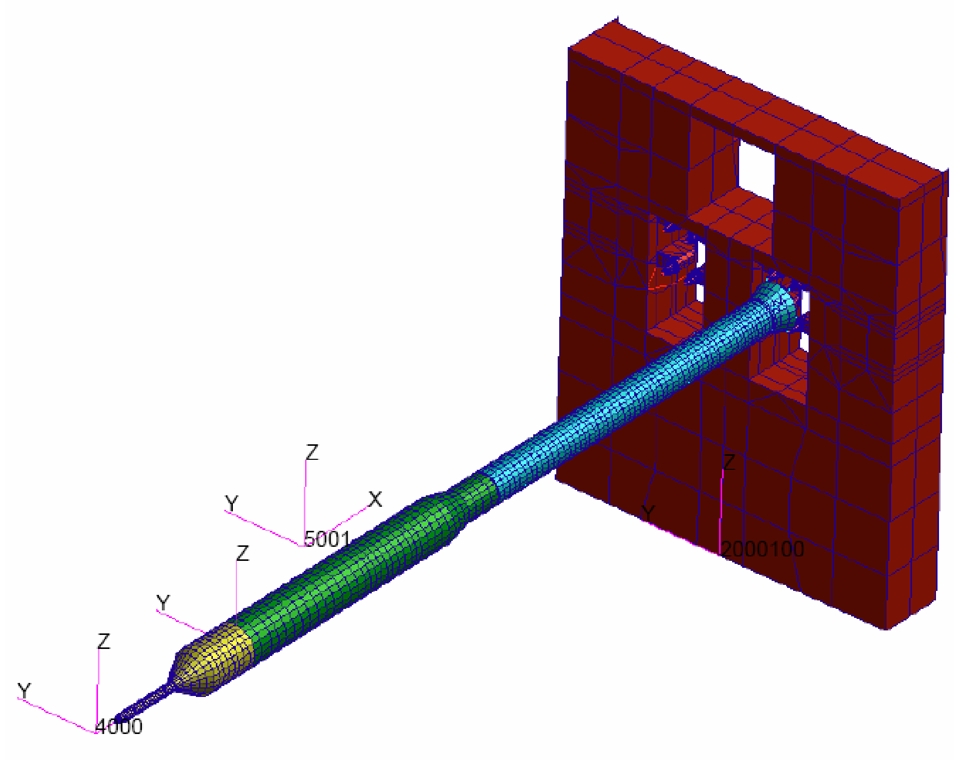

Figure 5.1-5, System Loads Coordinate Systems – D50m

Table 5.1-2, Loads Coordinate System Origins D50m

System Loads Coordinate System Origins				
	X	Y	Z	Clocking X
System Loads Coordinate Origin (Coord 0)	0.000	0.000	0.000	0°
Escape/Crew/Service (Coord 4000)	-246.270	-250.500	0.000	0°
Upper Stage (Coord 6000)	570.070	-250.500	0.000	0°
FSB (Coord 5001)	1282.140	0.000	0.000	0°
MLP (Coord 2000100)	3778.270	0.000	-1212.57	0°

5.1.1.2 Structural Design Coordinate Systems

Coordinate systems used for the structural components are specified in Figure 5.1-1 and Figure 5.1-2. All structural configuration data will be converted to the System Loads Coordinate system prior to use. Unless otherwise noted, all loads results developed for the structural configuration will be in the System Loads Coordinate system. Table 5.1-3, 5.5m Structural Design system within System Loads system and Table 5.1-4, 5.0m Structural Design system within System Loads system indicate the position of the Structural Design Coordinate systems within the System Loads Coordinate system.

Table 5.1-3, 5.5m Structural Design system within System Loads system

5.5m Structural Design system within System Loads system			
	X	Y	Z
Structural Design Coordinate Origin	-247.380	250.050	0.000
CEV	347.960	250.050	0.000
Spacecraft Adapter	657.620	250.050	0.000
Upper Stage	712.620	250.050	0.000
Booster	1506.77	250.050	0.000

Table 5.1-4, 5.0m Structural Design system within System Loads system

5.0m Structural Design system within System Loads system			
	X	Y	Z
Structural Design Coordinate Origin	-392.300	250.050	0.000
CEV	203.040	250.050	0.000
Spacecraft Adapter	512.700	250.050	0.000
Upper Stage	567.700	250.050	0.000
Booster	1506.77	250.050	0.000

5.1.2 Sign Conventions

5.1.2.1 Externally Applied Loads

Externally applied loads are reported and/or applied in the same directions as the System Loads Coordinate system. Moments follow the right hand rule.

5.1.2.2 Section Loads

Axial loads, roll torques, and pitch and yaw shears and bending moments shall be reported for any vehicle station in the sense of the summation of applied loads or applied moments starting at the nose of the vehicle and continuing aft to the reported station.

In this early phase of design many of the structures are modeled using the NASTRAN CBEAM element. Figure 5.1-6 shows the element and element force coordinate system for a CBEAM element. Superimposed on this figure is the System Loads Coordinate system assuming the orientation vector of the CBEAM is [0.0 0.0 1.0]. According to this figure, if the element forces are to be reported in the preferred sense, they will need to be transformed by the transformation matrix in Equation 1. Additionally, the CBEAM element reports all its element forces as reactions rather than applied loads, therefore the transformation must be uniformly multiplied by a factor of -1.0 as shown in Equation 2.

$$\begin{Bmatrix} V_x \\ V_y \\ V_z \\ M_x \\ M_y \\ M_z \end{Bmatrix}_{Stack} = \begin{bmatrix} 1 & 0 & 0 & 0 & 0 & 0 \\ 0 & 0 & -1 & 0 & 0 & 0 \\ 0 & 1 & 0 & 0 & 0 & 0 \\ 0 & 0 & 0 & 1 & 0 & 0 \\ 0 & 0 & 0 & 0 & -1 & 0 \\ 0 & 0 & 0 & 0 & 0 & -1 \end{bmatrix} \begin{Bmatrix} V_x \\ V_1 \\ V_2 \\ M_x \\ M_1 \\ M_2 \end{Bmatrix}_{Element} \quad \text{Eqn. 1}$$

$$\begin{Bmatrix} V_x \\ V_y \\ V_z \\ M_x \\ M_y \\ M_z \end{Bmatrix}_{Stack} = -1.0 \begin{bmatrix} 1 & 0 & 0 & 0 & 0 & 0 \\ 0 & 0 & -1 & 0 & 0 & 0 \\ 0 & 1 & 0 & 0 & 0 & 0 \\ 0 & 0 & 0 & 1 & 0 & 0 \\ 0 & 0 & 0 & 0 & -1 & 0 \\ 0 & 0 & 0 & 0 & 0 & -1 \end{bmatrix} \begin{Bmatrix} V_x \\ V_1 \\ V_2 \\ M_x \\ M_1 \\ M_2 \end{Bmatrix}_{Element} = \begin{bmatrix} -1 & 0 & 0 & 0 & 0 & 0 \\ 0 & 0 & 1 & 0 & 0 & 0 \\ 0 & -1 & 0 & 0 & 0 & 0 \\ 0 & 0 & 0 & -1 & 0 & 0 \\ 0 & 0 & 0 & 0 & 1 & 0 \\ 0 & 0 & 0 & 0 & 0 & 1 \end{bmatrix} \begin{Bmatrix} V_x \\ V_1 \\ V_2 \\ M_x \\ M_1 \\ M_2 \end{Bmatrix}_{Element} \quad \text{Eqn. 2}$$

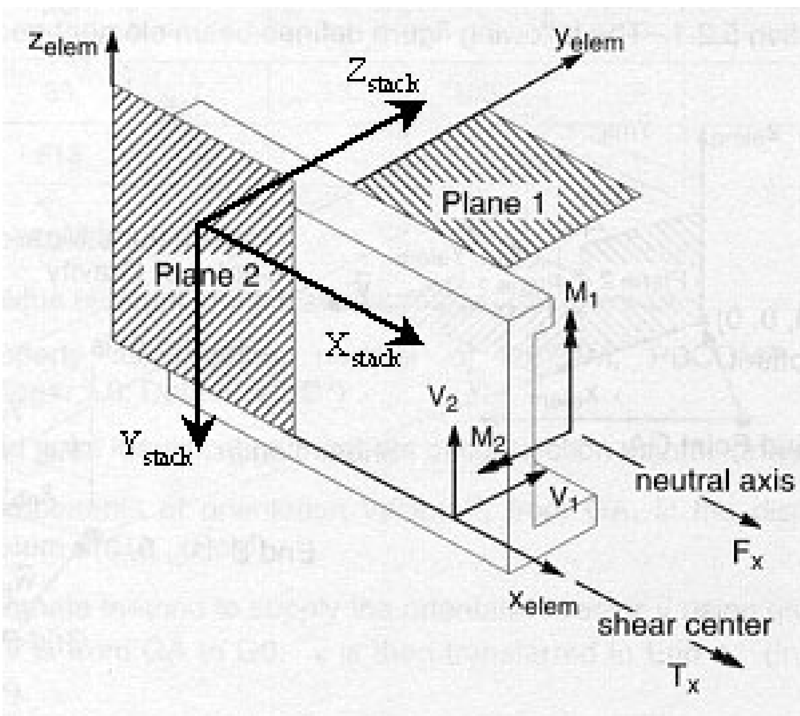

Figure 5.1-6, CBEAM Internal Element Forces and Moments

5.1.2.3 Accelerations

Accelerations are reported and/or applied in the same directions as the System Loads Coordinate system. Rotational accelerations follow the right hand rule.

5.1.2.4 Load Factors

No load factors will be reported within this document. All accelerations will be reported and/or applied as accelerations defined above.

5.2 Transportation & Handling Environments

5.2.1 Rollout

A rollout analysis for the CLV is underway but has not yet been completed. This analysis was out of scope for LC1a.

5.2.2 Ferrying, Jacking, Stacking, & Handling

Analyses for ferrying, jacking, stacking, and handling of the CLV were out of scope for LC1a.

5.3 Pressures

Unless specifically called out, the loads presented in this Loads Databook will not contain pressure relieving effects. Ullage pressure loads are expected to be added in during structural assessments.

Pressure stiffening effects have not yet been considered and were out of scope for LC1a.

5.4 Winds and Natural Environments

The winds and natural environments used for CLV vehicle assessments are specified in NASA-HDBK-1001, Reference 2.

5.4.1 Aloft

Winds aloft are not used directly for loads and dynamics. Rather these winds are used in flight mechanics to establish trajectories and control simulation dispersions used in the loads analysis.

5.4.2 Ground

Ground winds are used to determine loading on the vehicle while it is at the launch site. Currently a ground wind model for KSC is being used from Reference 2. This ground wind model represents peak wind speeds that include wind gust velocities as a static component.

5.4.3 Gusts

Wind gusts models are used to determine transient loading on the vehicle during ascent and at the launch site. Gust wind models for KSC are defined in Reference 2.

5.5 Performance Trajectories

Performance trajectory flight parameters are used to determine loading conditions on the vehicle during ascent. The performance trajectories currently used for the CLV loads analyses are contained in an Excel spreadsheet entitled "Draft-CLV-5_DAC-0_Rev1_-30x100nm_Trajectories_(3-6-2006).xls," Reference 3.

5.6 Control Simulations & Dispersions

Due to phasing of the analyses, control simulation and dispersion data were not used directly in the vehicle loads analysis. However the dispersions documented in a May 11, 2006 AFSIG presentation titled "DAC1Rev2MonteCarloResults (Greg Dukeman).ppt," were used for comparison (Reference 4).

5.7 Mass Properties

Two versions of the 5.5 meter Upper Stage model were created. The first used the Program allocated mass properties contained in Appendix B.1 (Memo1 FSB J2X.doc). The second model used engineering weights from the DAC-0 Upper Stage structural sizing effort contained in Appendix B.2 (DAC0ExitMEL_Prop.xls).

The 5.0 meter Upper Stage configuration did not have an associated mass properties report. See the model description in Section 6.4 for a discussion of how the mass properties were handled.

It was difficult to get mass properties of the CEV so an early estimate was used. This estimate included 13,228 lbs. for the Launch Abort System (LAS); 55140 lbs for the Lunar CEV; and an ISS CEV weighing 5% less.

5.8 Aerodynamic Environments

5.8.1 Steady Aerodynamics

5.8.1.1 5.5 Meter Upper Stage Steady Aerodynamics

An integrated system loads analysis requires distributed aerodynamic forces down the length of the vehicle. At the time this analysis was conducted, the aerodynamic data available from the aerodynamic community was limited to the 6-dof Aerodynamic database designated "CLV5_5.5mU_Aero_R1.0," Reference 5 and a single Mach 1.63 distributed case designated "CLV5m_5mp5US_CNalp_dist2_R1.0", Reference 6.

In order to provide a more complete assessment of the ascent loads environment, the Vehicle Integration Loads team generated a preliminary distributed aerodynamic database using a low order panel code from ZONA technologies, Inc. called ZONAIR. There were a several objectives for assessing a wider range of aerodynamic flight regimes than the typical maximum dynamic pressure case. These objectives are highlighted in Section 7.1.3.1 in Figure 7.1-1. The ZONAIR database was scaled so that the total normal force coefficients and centers-of-pressure matched the 6-dof aerodynamic database. The complete database generation process was documented in a joint Loads and Aerodynamics Panel presentation, Reference 7.

The resulting distributed aerodynamic data used is summarized in Figure 5.8-1. The Vehicle Integration Loads Team typically presents the aerodynamic data as a cumulative distribution down the vehicle that emulates an aerodynamic shear load. Additionally, the figure represents a "per degree" distribution for convenience. The actual database contains distributions individually scaled to the 6-dof database for each angle-of-attack.

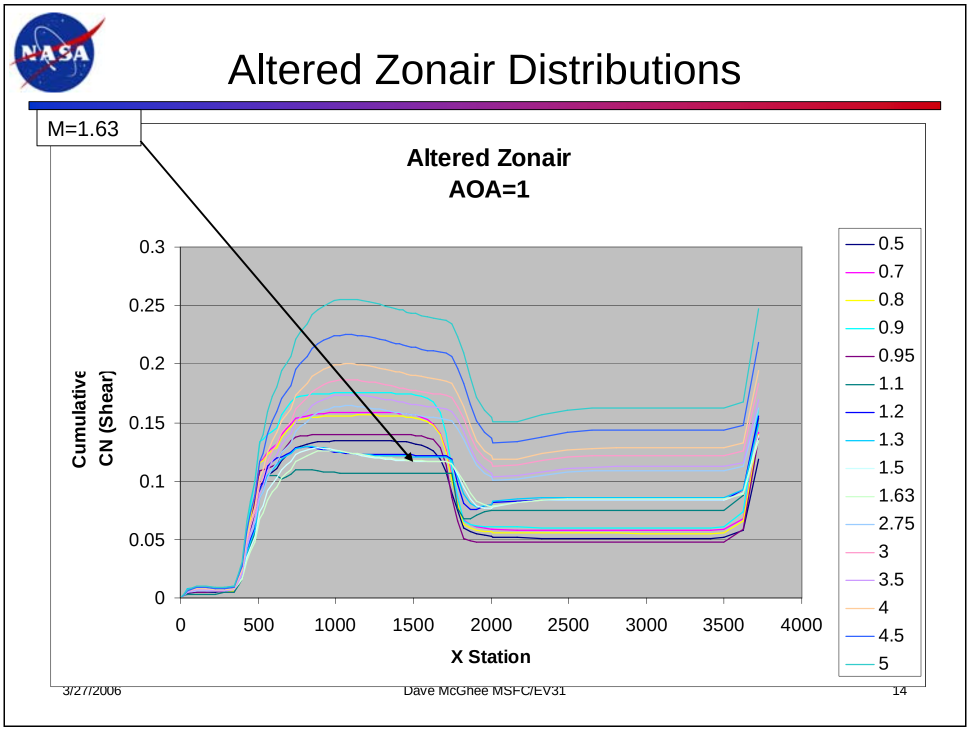

Figure 5.8-1, Ascent Loads Distributed Aerodynamic Database 5.5m Upper Stage

Figure 5.8-2 summarizes a study to verify that the generated distributed database generates reasonable but conservative loads.

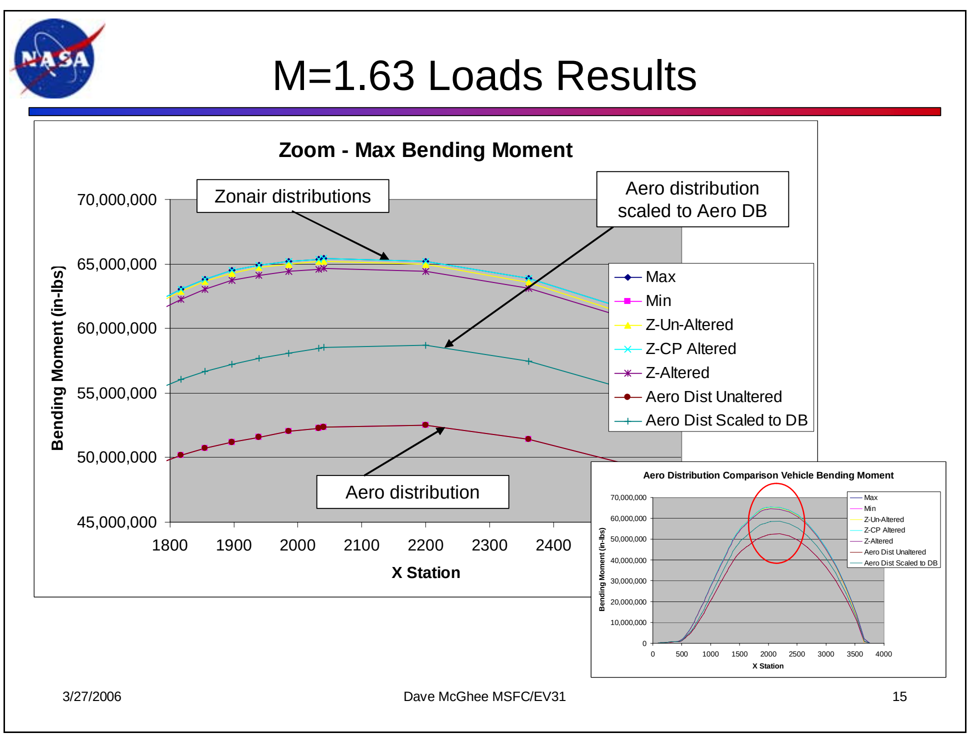

Figure 5.8-2, Sample Loads Result Verification Comparison

Axial drag coefficients were derived from the Aerodynamic community supplied 6-dof aerodynamic database and the Mach 1.63 distributed coefficients. The Mach 1.63 distribution was used as a template and scaled for to match the 6-dof database using the 2 degree angle-of-attack coefficients. The loads analysis considered the drag as a function of Mach number and ignored minor changes due to angle-of-attack changes. Figure 5.8-3 shows the cumulative axial drag coefficient down the vehicle similar to an axial load plot. Figure 5.8-4 shows the drag coefficients used as a function of Mach number and vehicle station.

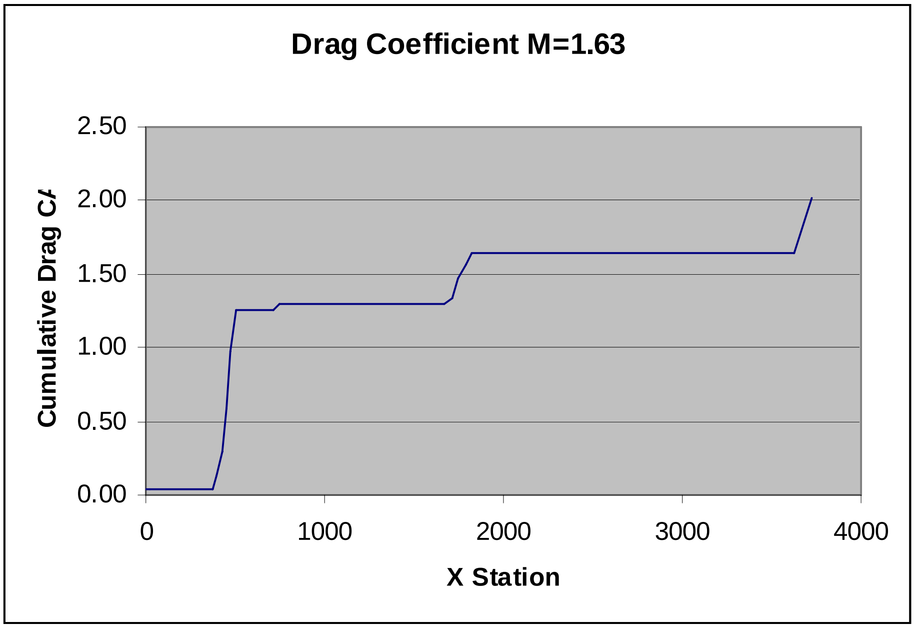

Figure 5.8-3, Ascent Loads Cumulative Distributed Aerodynamic Drag

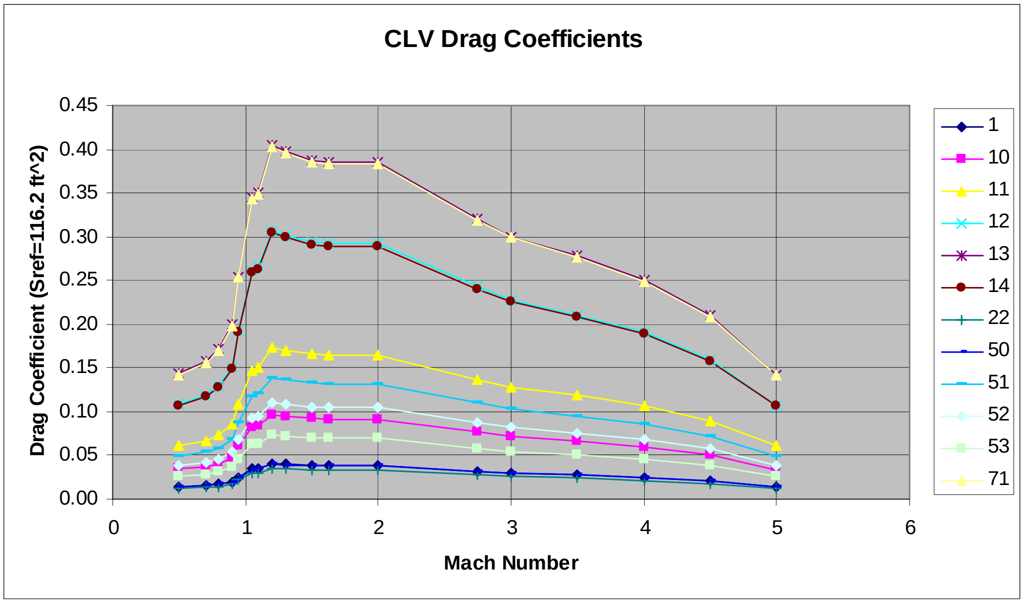

Figure 5.8-4, Aerodynamic Drag as Function of Mach and Station

Additionally, the Base Drag force has not been updated since the ESAS study and is still considered the best available estimate. Figure 5.8-5 shows the Base Drag force used as a function of altitude.

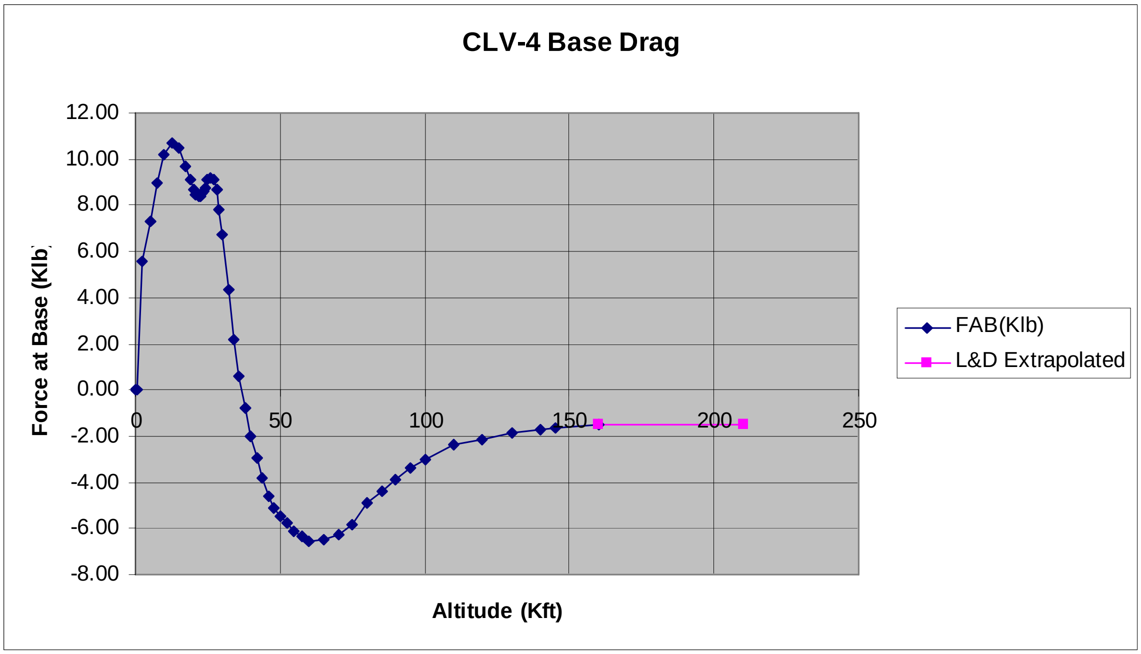

Figure 5.8-5, Aerodynamic Base Drag as Function of Altitude

5.8.1.2 5.0 Meter Upper Stage Steady Aerodynamics

The aero database for the 5.0 meter Upper Stage used the same process. Unfortunately at the time of the analysis the 5.0 meter database from the aerodynamic community was not yet available, in either 6-dof or distributed form. The loads results therefore used the raw, unaltered ZONAIR data. Since then the aerodynamic community has released, for the 5.0 meter Upper Stage, a 6-dof database and a distribution for Mach 1.63. These have not yet been evaluated.

The resulting unaltered ZONAIR distributed aerodynamic data used for the 5.0 meter configuration is summarized in Figure 5.8-6. The Vehicle Integration Loads Team typically presents the aerodynamic data as a cumulative distribution down the vehicle that emulates an aerodynamic shear load.

Drag coefficients used were the same as those used for the 5.5m configuration, Figure 5.8-3 and Figure 5.8-4.

Base drag was also the same as that used for the 5.5m configuration, Figure 5.8-5.

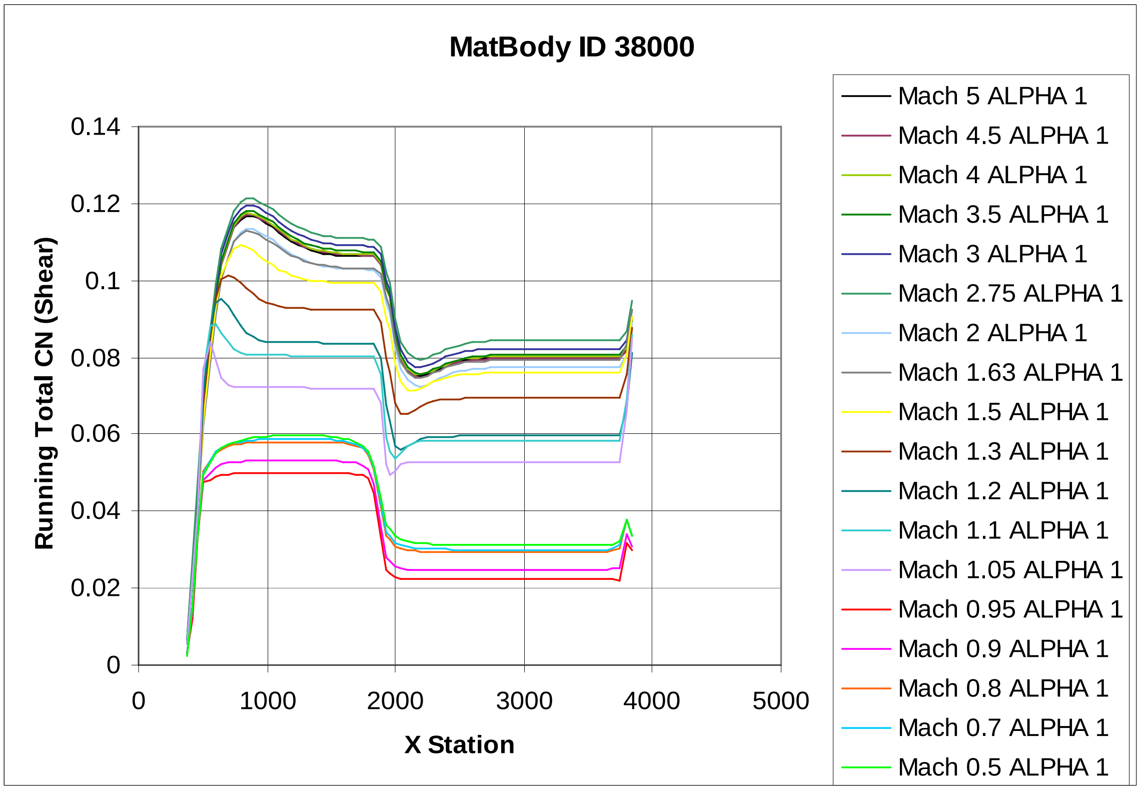

Figure 5.8-6, 5.0m CLV Ascent Loads Distributed Aerodynamic Database 5.0m Upper Stage

5.8.1.3 On-pad Pre-launch Ground Wind Forces

On-pad pre-launch ground winds are based on the peak ground wind model described in NASA-HDBK-1000, Reference 2. Assessments were completed for peak wind speeds using the following wind durations and risk levels:

1) 1 Hour 5% risk
2) 1 Day 5% risk
3) 1 Day 1% risk
4) 10 Day 1% risk

Four cases were assessed using wind incidence from +/- Z and +/- Y directions. The base of the launch vehicle was assumed to be 100 feet above sea level. The vehicle drag coefficient was assumed to be 1.0 for all stations based on Reference 8.

Pre-launch vortex shedding environments have not yet been determined. The 1.5 factor on resulting static wind forces is being used as recommended by NASA-SP-8008, Reference 9.

Several ground wind capability studies were initiated and are discussed in Section 10.2.

5.8.2 Unsteady Aerodynamics

5.8.2.1 Launch Site Vortex Shedding

Pre-launch vortex shedding environments have not yet been determined. The 1.5 factor on resulting static wind forces is being used as recommended by NASA-SP-8008, Reference 9.

5.8.2.2 Acoustics

Acoustic, shock, and vibration environments and criteria have not yet been developed and were out of scope for LC1a.

5.8.2.3 Ascent Buffet

Ascent buffet environments have not yet been developed and were out of scope for LC1a.

5.9 Propulsion

5.9.1 J-2X

Very little data was available at the time loads were being calculated. What data was available was historic information from the J-2 and J-2S programs. The J-2X is currently rated at as 293.7 thousand pounds of thrust at 100% throttle. The trajectories used for ascent analysis, Section 5.5, used 274 thousand pounds of thrust.

5.9.1.1 J-2X Thrust Buildup and Shutdown

Thrust data was taken from historical information for the J-2S. Some information was also found for the J-2, however, the J-2S data was deemed more appropriate. Data for both the J-2 and J-2S were in the form of pictures of thrust curves. Figure 5.9-1 and Figure 5.9-2 are the pictures of these curves. These figures were provided by MSFC/ER41, which is the Structural & Dynamics Analysis Branch of the Propulsion Systems Department.

To use these curves in an analysis, the curves in the pictures were digitized. Figure 5.9-3 is an Excel plot of the digitized J-2S thrust curves. For the analysis, the nominal thrust start transient was modified to start at 0 thrust, and to end and hold at 100% thrust. This was done by linear extrapolation from the last two points of the digitized plot, to the desired value (either 0 or 100). Also contained in Figure 5.9-3 is the start thrust transient used in the trajectory analysis for comparison (provided by MSFC/EV42, which is the Guidance, Navigation and Mission Analysis Branch). The trajectory start transient is considered more benign that the “Modified Nominal” start transient since the latter has a generally steeper slope from 16% to 80%, and thus should excite more dynamics.

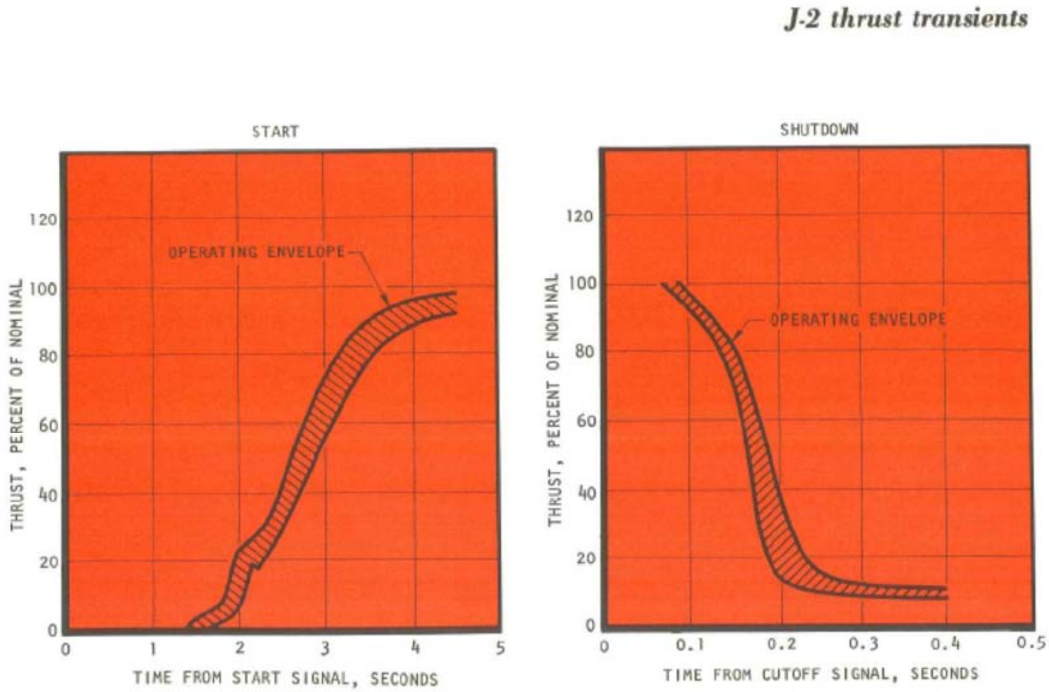

Figure 5.9-1, J-2 transient thrust traces for start and cutoff

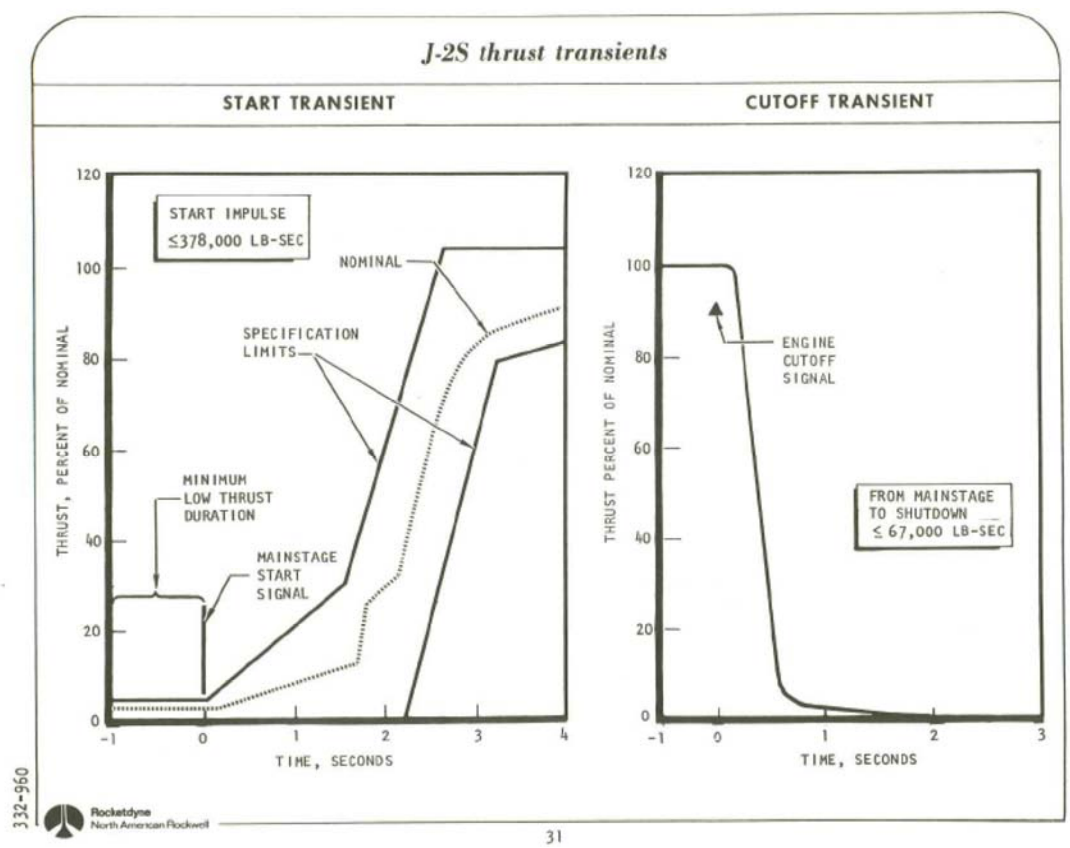

Figure 5.9-2, J-2S transient thrust traces for start and cutoff

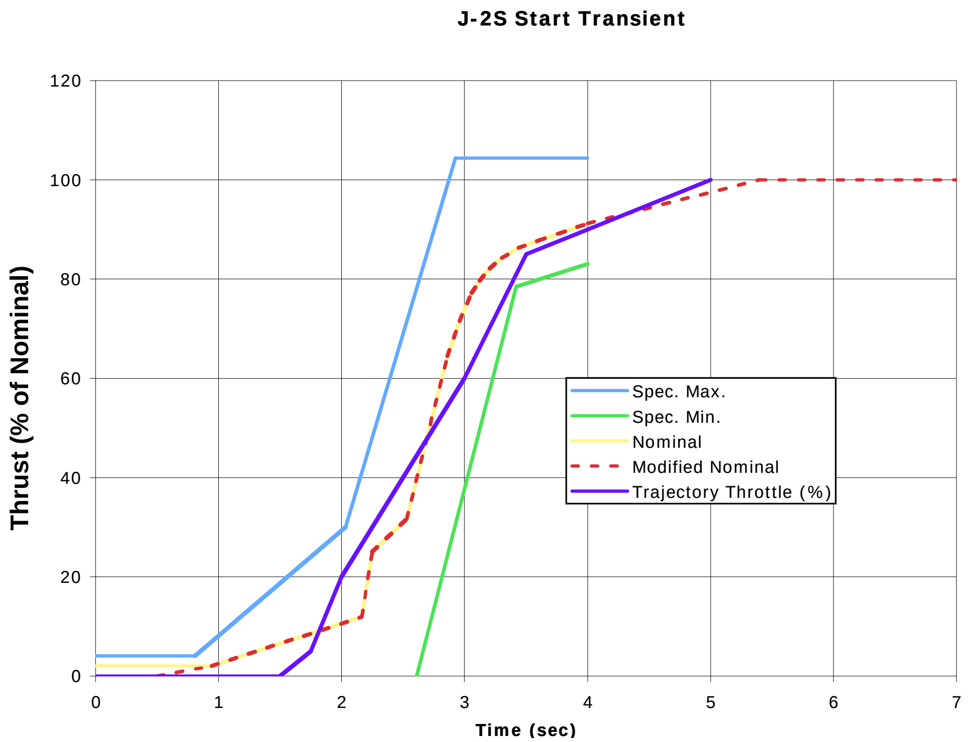

Figure 5.9-3, Digitized J-2S transient start thrust trace

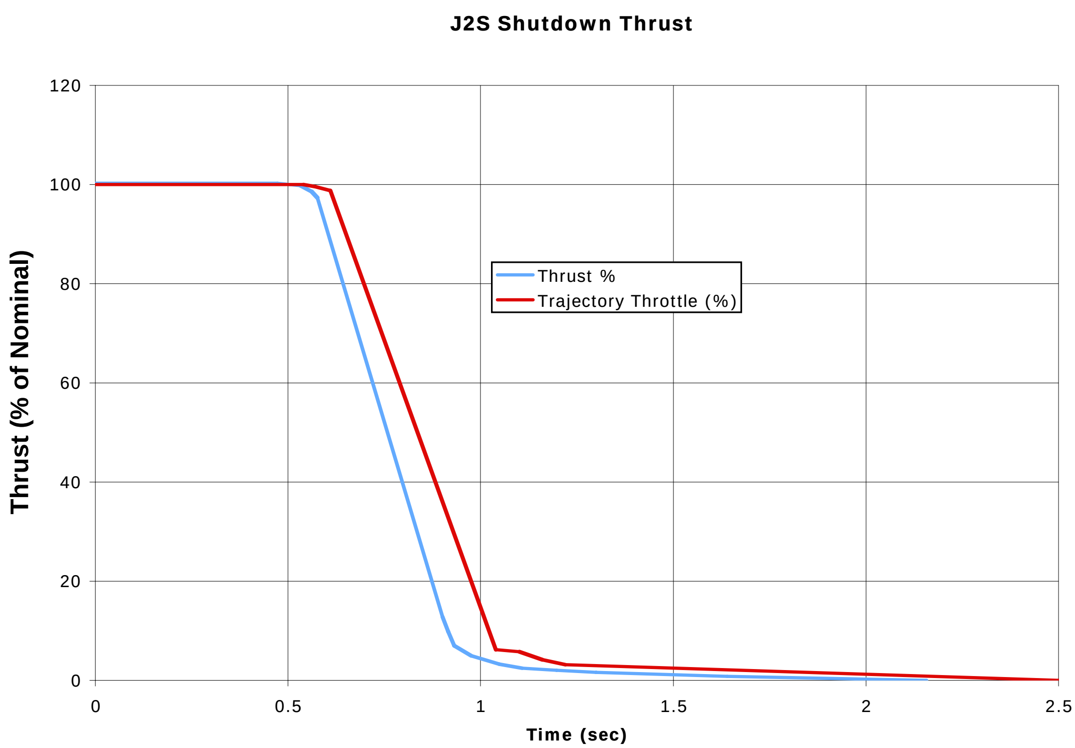

Figure 5.9-4, Digitized J-2S transient cutoff thrust trace

The digitized cutoff transient is shown in Figure 5.9-4. This plot also includes the cutoff transient used in the trajectory analysis (from EV42) for comparison.

5.9.1.2 J-2X Thrust Oscillations

A preliminary assessment of thrust oscillations for the J-2X is available, Reference10. The data is shown in Figure 5.9-5 below. However, no loads analyses were performed using this data. Loads due to thrust oscillations were assumed to be covered by the 1.1 uncertainty factor applied to axial loads.

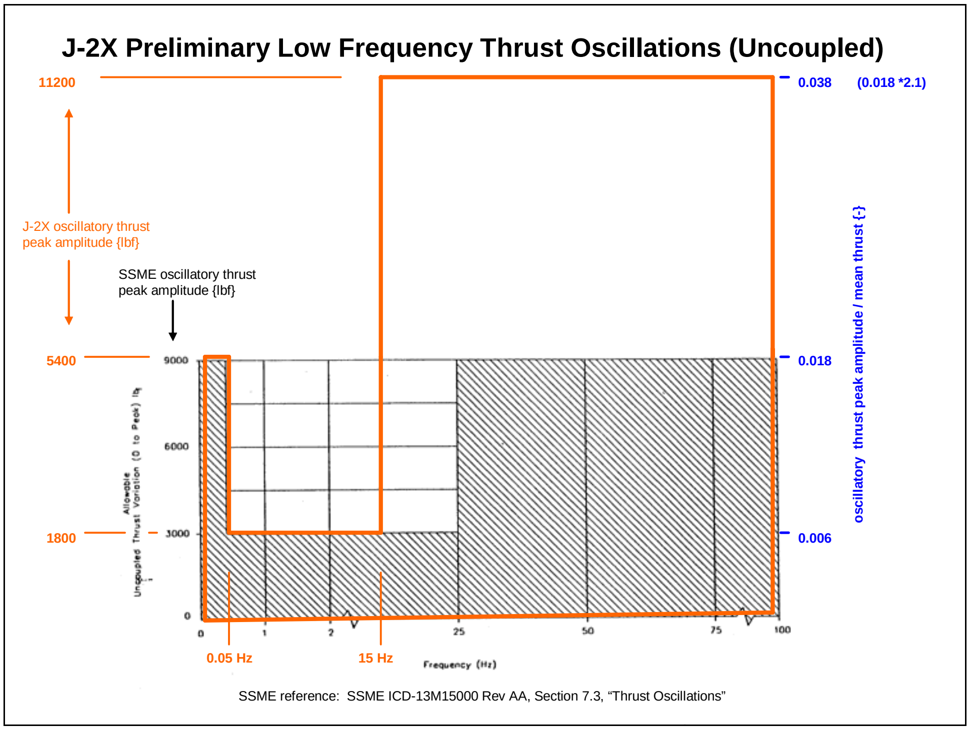

Figure 5.9-5, J-2X Thrust Oscillations

5.9.1.3 J-2X Ignition Overpressure

No J-2X ignition overpressure data was available for inclusion in this document. Assessment of the J-2X ignition overpressure was considered out of scope for LC1a given the thin atmosphere at staging. It will be addressed a future load cycle.

5.9.2 First Stage Booster

5.9.2.1 FSB Thrust Profile

The nominal thrust profile for the first stage booster is based on the ETM3 5-segment motor test. Modifications to the ETM3 thrust trace have been made based on changes planed in propellant loading and other features of the FSB. The thrust trace (ATK designation CLVFSB05306) used for loads analysis is "un-degraded". For further information on the development, see ATK's TR017186, "1st Stage Final Ballistic Prediction for Crew Launch Vehicle Design and Analysis Cycle Zero", Reference 11. Figure 5.9-6 illustrates the CLVFSB05306 vacuum and sea level thrust traces. This thrust trace is developed using a nominal burn rate of 0.337 in/sec. at a mean bulk propellant temperature (MBPT) of 60 degrees F.

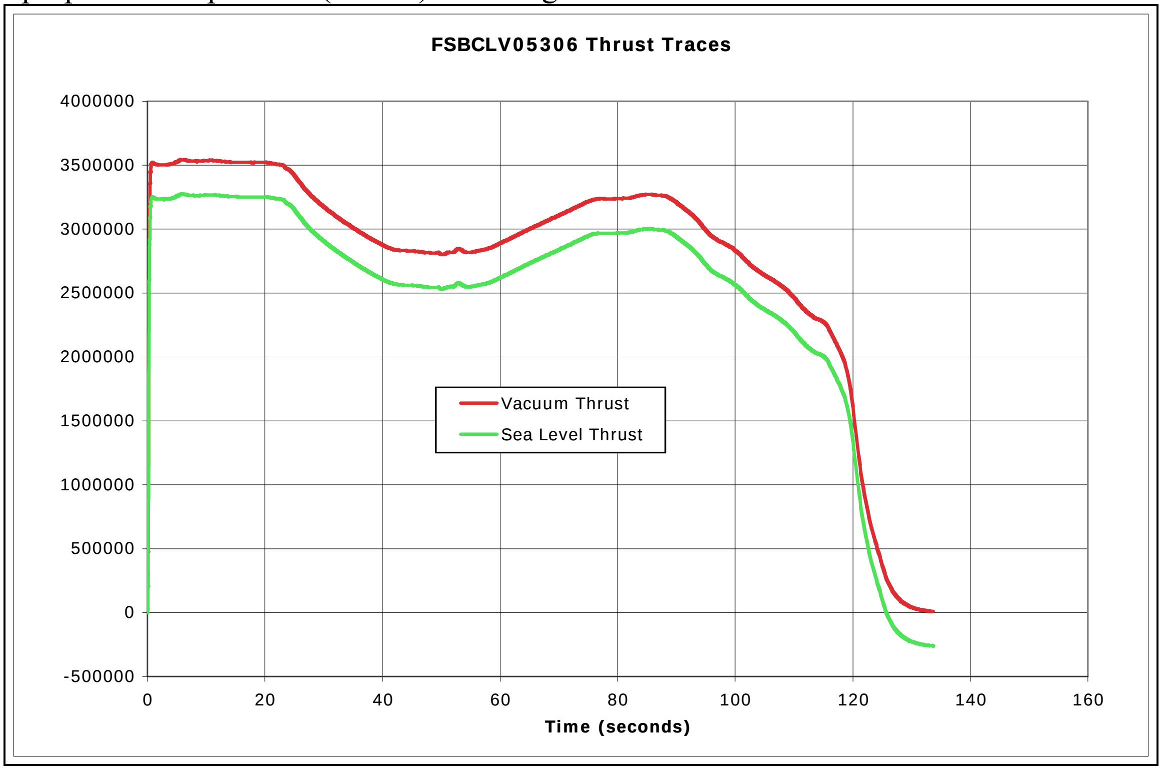

Figure 5.9-6, CLVFSB05306 Vacuum and Sea Level Thrust Force

In Figure 5.9-6, sea level thrust is calculate as the vacuum thrust minus atmospheric pressure at sea level times the nozzle exit plane area. Although this causes the sea level thrust curve to fall below zero as the booster "burns out", this is not a concern since the sea level thrust curve is used only for the first 10 seconds during the liftoff analysis.

5.9.2.2 FSB Thrust Dispersions

Calculation of the thrust dispersions for the first stage booster was a collaborative effort between MSFC/ER22 and ATK. The general approach was to use current SSP data and tools to generate dispersed thrust traces that cover current RSRM dispersions plus a little extra margin to cover unknowns of the FSB. Further details of the dispersion calculations are given in Appendix E.

The resulting dispersion curves are shown in Figure 5.9-7. These curves are labeled as "Early-high-high" to represent an early ignition interval, high pressure rise rate, and high total thrust. While Late-low-low indicates late ignition interval, low pressure rise rate and low total thrust.

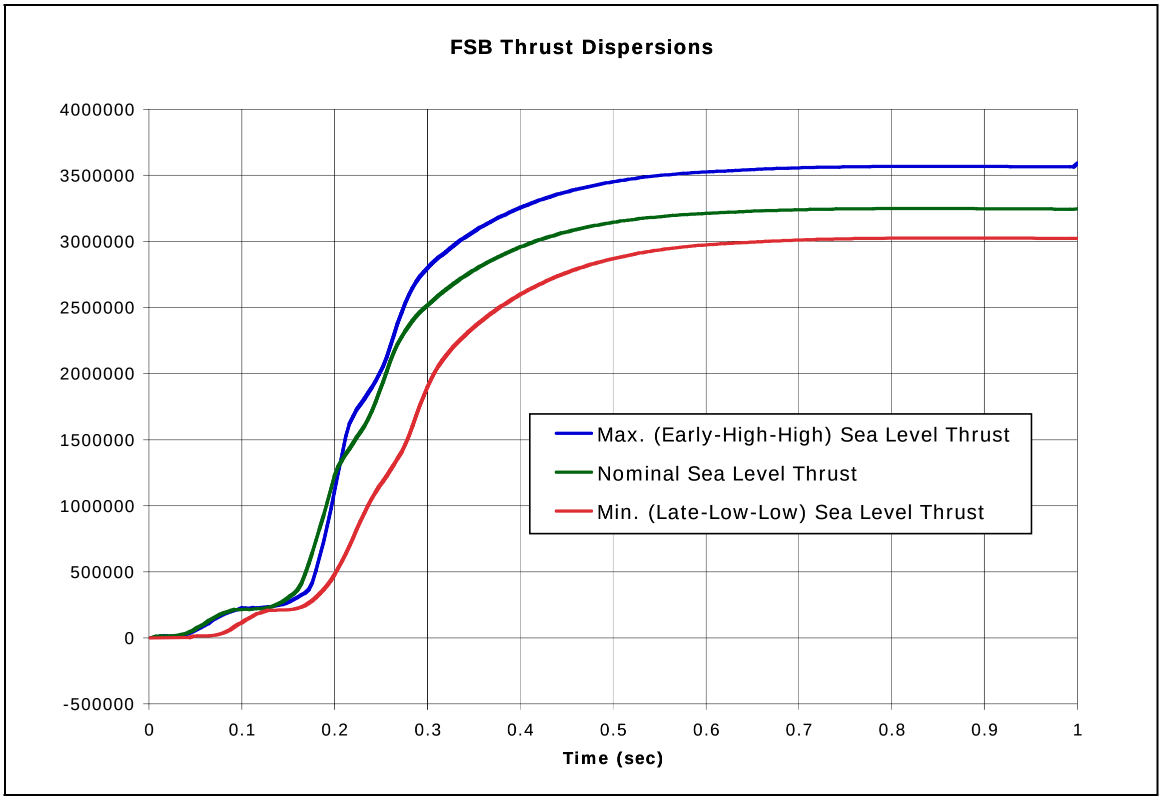

Figure 5.9-7, Build-up portion of FSB thrust traces with dispersions

5.9.2.3 FSB Thrust oscillations

FSB Thrust oscillations were not available in time for this loads analysis, and were accounted for by an uncertainty factor of 1.1 applied to the axial loads.

5.9.2.4 First Stage Booster Ignition Overpressure

Models of the ignition overpressure (IOP) impingement on the CLV were supplied to EV31 by ER42 personnel. See Appendix C for assumptions and details on overpressure calculations.

Four sources of IOP reflection impinging on the vehicle were modeled. These sources included the MLP right hand SRB hole, the MLP left hand SRB hole, the MLP SSME hole and the launch pad flame trench. A diagram of the four IOP reflective sources can be seen in Figure 5.9-8 as red arrows.

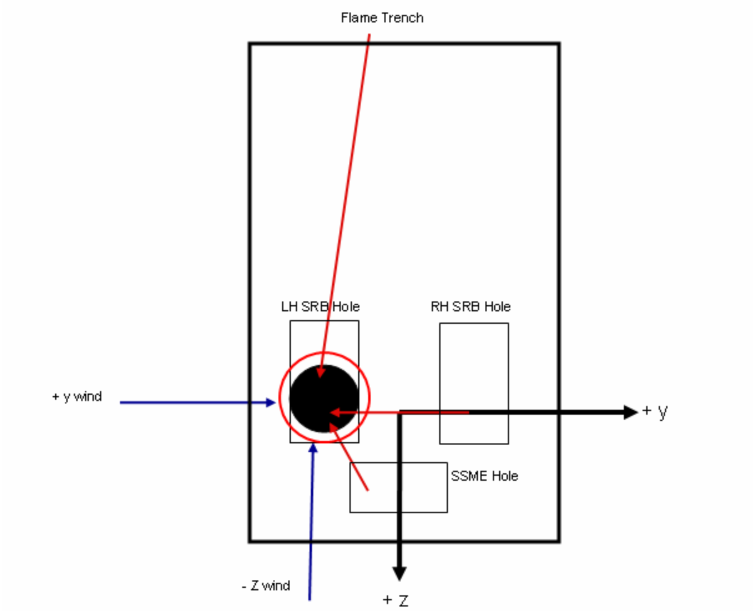

Figure 5.9-8, Overpressure Ignition Sources

For each source, three thrust build up cases were modeled; nominal, early-high-high, and late-low-low (See section 5.9.2.2). These cases coincide with the FSB thrust rise rates which include the nominal CLVFSB05306 case, the maximum rise rate (late ignition rise-low thrust build up-low total thrust) case, and minimum rise rate (early ignition rise-high thrust build up-high total thrust) case.

An example of the ignition overpressure time histories can be seen in Figure 5.9-9. As it can be seen, each station time history has a time delay from the previous station. Thus the overpressure wave impinges on the base of the CLV and travels upward to the CEV.

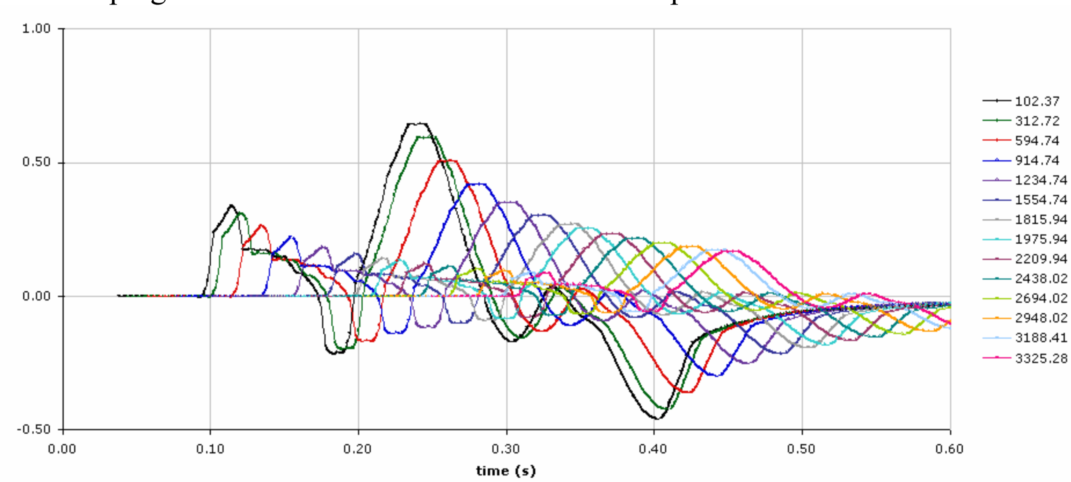

Figure 5.9-9, Ignition Overpressure (asymmetric) From Adjacent SRB Hole Attenuated to 5.5m Body Points

All ignition overpressure time histories were generated for both the 5.0 meter diameter CLV configuration and the 5.5 meter diameter CLV configuration.

Time history tables for the fluctuating pressure were modeled at 14 pre-selected stations axially along the CLV. The pre-selected axial stations along the CLV can be seen in Figure 5.9-10 in yellow.

						Distance from Nose	from previous "Yellow" grid	Distance from Holddown
GRID	4001		31.000	-250.500	0.000	0.000		
GRID	4002		53.865	-250.500	0.000	22.865		
GRID	4003		76.730	-250.500	0.000	22.865		
GRID	4004		136.730	-250.500	0.000	60.000		
GRID	4005		196.730	-250.500	0.000	60.000		
GRID	4006		256.730	-250.500	0.000	60.000		
GRID	4007		316.730	-250.500	0.000	60.000		
GRID	4008		376.080	-250.500	0.000	59.350		
GRID	4009		403.080	-250.500	0.000	27.000		
GRID	4010		430.080	-250.500	0.000	27.000		3325.280
GRID	4011		457.080	-250.500	0.000	27.000		
GRID	4012		484.080	-250.500	0.000	27.000		
GRID	4013		508.950	-250.500	0.000	24.870		
GRID	4014		537.950	-250.500	0.000	29.000		
GRID	4015		566.950	-250.500	0.000	29.000	136.870	3188.410
GRID	4016		595.950	-250.500	0.000	29.000		
GRID	4017		624.950	-250.500	0.000	29.000		
GRID	4018		654.340	-250.500	0.000	29.390		
GRID	4019		685.340	-250.500	0.000	31.000		
GRID	4020		716.340	-250.500	0.000	31.000		
GRID	4021		747.340	-250.500	0.000	31.000		
GRID	6001		747.340	-250.500	0.000	0.000		
GRID	6002		777.340	-250.500	0.000	30.000		
GRID	6003		807.340	-250.500	0.000	30.000	240.390	2948.020
GRID	6004		845.340	-250.500	0.000	38.000		
GRID	6005		881.340	-250.500	0.000	36.000		
GRID	6006		917.340	-250.500	0.000	36.000		
GRID	6007		953.340	-250.500	0.000	36.000		
GRID	6008		989.340	-250.500	0.000	36.000		
GRID	6009		1025.340	-250.500	0.000	36.000		
GRID	6010		1061.340	-250.500	0.000	36.000	254.000	2694.020
GRID	6011		1097.340	-250.500	0.000	36.000		
GRID	6012		1133.340	-250.500	0.000	36.000		
GRID	6013		1169.340	-250.500	0.000	36.000		
GRID	6014		1205.340	-250.500	0.000	36.000		
GRID	6015		1245.340	-250.500	0.000	40.000		
GRID	6016		1281.340	-250.500	0.000	36.000		
GRID	6017		1317.340	-250.500	0.000	36.000	256.000	2438.020
GRID	6018		1353.340	-250.500	0.000	36.000		
GRID	6019		1389.340	-250.500	0.000	36.000		
GRID	6020		1418.420	-250.500	0.000	29.080		
GRID	6021		1442.420	-250.500	0.000	24.000		
GRID	6022		1466.420	-250.500	0.000	24.000		
GRID	6023		1484.420	-250.500	0.000	18.000		
GRID	6024		1514.420	-250.500	0.000	30.000		
GRID	6025		1545.420	-250.500	0.000	31.000	228.080	2209.940
GRID	6026		1584.420	-250.500	0.000	39.000		
GRID	6027		1623.420	-250.500	0.000	39.000		
GRID	6028		1662.420	-250.500	0.000	39.000		
GRID	6029		1701.420	-250.500	0.000	39.000		
GRID	6030		1741.420	-250.500	0.000	40.000		
GRID	6031		1779.420	-250.500	0.000	38.000	234.000	1975.940
GRID	6032		1817.420	-250.500	0.000	38.000		
GRID	6033		1855.420	-250.500	0.000	38.000		
GRID	6034		1897.420	-250.500	0.000	42.000		
GRID	6035		1939.420	-250.500	0.000	42.000	160.000	1815.940
GRID	6036		1986.420	-250.500	0.000	47.000		
GRID	6037		2032.970	-250.500	0.000	46.550		
GRID	706	0	2041.120	-250.500	0.000	8.150		
GRID	707	0	2200.620	-250.500	0.000	159.500	261.200	1554.740
GRID	708	0	2360.620	-250.500	0.000	160.000		
GRID	709	0	2520.620	-250.500	0.000	160.000	320.000	1234.740
GRID	710	0	2680.620	-250.500	0.000	160.000		
GRID	711	0	2840.620	-250.500	0.000	160.000	320.000	914.740
GRID	712	0	3000.620	-250.500	0.000	160.000		
GRID	713	0	3160.620	-250.500	0.000	160.000	320.000	594.740
GRID	714	0	3214.600	-250.500	0.000	53.980		
GRID	715	0	3340.140	-250.500	0.000	125.540		
GRID	716	0	3442.640	-250.500	0.000	102.500	282.020	312.720
GRID	717	0	3526.680	-250.500	0.000	84.040		
GRID	718	0	3652.990	-250.500	0.000	126.310	126.310	102.370
GRID	720	0	3755.360	-250.500	0.000	102.370		

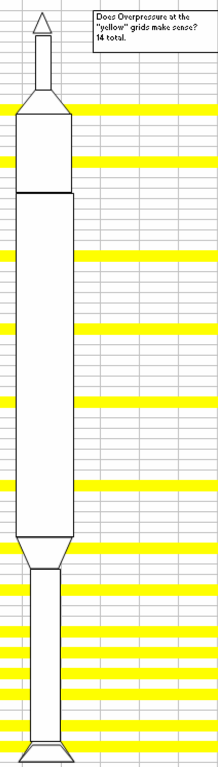

Figure 5.9-10, Ignition Overpressure Modeled Stations (sketch not to scale)

The tabulated fluctuating pressure time histories were applied to the CLV loads model at centerline nodes. Since there are more centerline nodes than modeled ignition overpressure stations in the model, areas of constant pressure were assumed around each station. Half of the nodes above and half of the nodes below each station were excited by the same pressure time histories. For each node, the pressure time histories were transformed into forces through scaling by the projected area around each node.

Projected areas were calculated as the summation of two averaged diameter rectangles; one above and one below each node. An example of a calculated projected area can be seen in Figure 5.9-11.

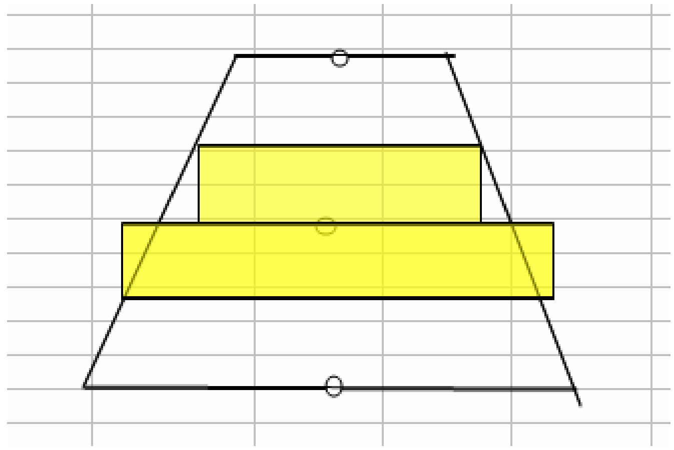

Figure 5.9-11, Calculated Projected Area

The ignition overpressure time histories, scaled by the projected areas, were thus applied to the CLV loads model as forces.

6.0 Structural Models

6.1 Description

The structural models currently in use for the CLV configuration have been derived from existing sources where possible; i.e. the SSP MLP model and RSRB models. For the new structures, simplified beam models were generated to provide a first order load path representation as well as mass and inertia properties and simple beam bending dynamics.

Table 6.1-1, Finite Element Numbering Ranges

Structural Model Element Numbering	
Stack	
Escape/Crew/Service	4000-4999
Spacecraft Adapter	Part of Upper Stage
Upper Stage	6000-6999
1st Stage Fwd Skirt/Recovery/Frustum	Part of Upper Stage
1st Stage FSB	Mixed range 600:2120, 7210:7240, 11089:11096, 106699:666403, 1100751: 1100763, 19131001:19340724
MLP	Primarily 2000000-2634000

6.2 1st Stage Booster (FSB) Model

The FSB model currently in use for the CLV configuration is derived from the Reusable Solid Rocket Booster (RSRB) USA models developed for the Shuttle program. These were provided by USA in support of both Shuttle rollout tests as well as for Shuttle derived vehicle studies, References 12 and 13.

Figure 6.2-1 shows the FSB FEM with stack X stations.

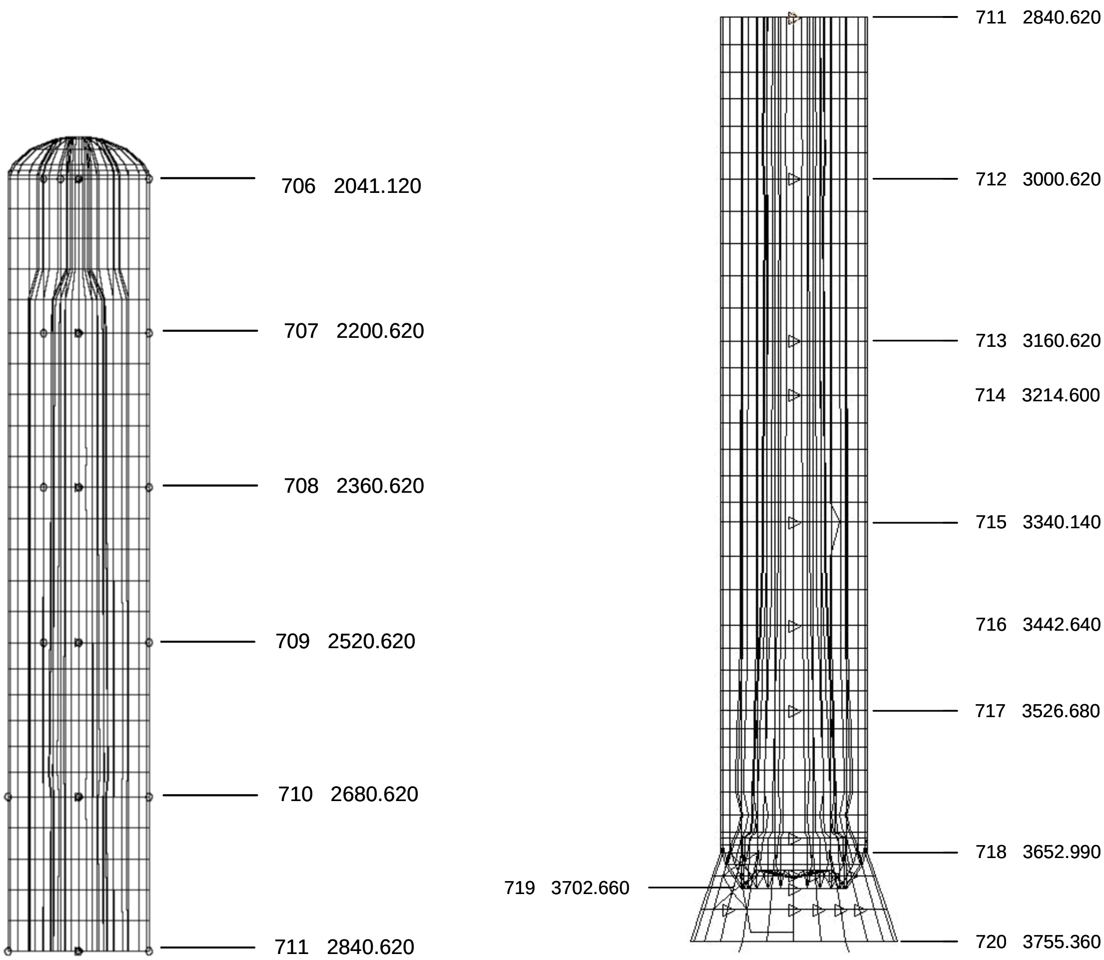

Figure 6.2-1, 1st Stage Booster (FSB) FEM with Stack X Stations

6.2.1 Solid Booster Assumptions and Data Sources

The current model has been derived from the original Shuttle Level II model of the RSRM in three steps.

First the delivered models, References 12 and 13, were assembled for use by the VIPA L&D team. Both the left and right versions of the model were implemented.

Left Hand Model:

	Data Sources and Analysis Assumptions:
	Assumptions:

1.	Left SRB r2b101.bdf came from Level II SRB models delivered by USA for use in shuttle derived vehicle studies.
2.	The delivered r2b101.bdf file contained "include" statements to incorporate the aft and forward skirts. This model was run to generate an inclusive echoed bulkdata file for use in shuttle derived vehicle studies.
3.	The resulting bulkdata was edited with the following changes to generate the model r2b101_modified.bdf:
3a	The ASET cards were commented out.
3b	The ET strut defintion was uncommented for use. These are not the official Level II strut models.
3c	The coordinate system 5001 was added to place the SRB in the Shuttle ET & Stack coordinate system.
4.	The left nozzle model, r2noza.dat, came from the models provided by USA for use in the shuttle rollout tests. This nozzle model is not the official Level II model. The official Level II model is a unique control system model representation.
5.	The following changes were made to allow its use with the main SRB model, generating the model file r2noza_modified.bdf.
5a	Interfacing grids used to run the nozzle model "stand alone" were commented out.
5b	Elements were renumbered in the 666000 range.
5c	The coordinate system 5003 was added to place the nozzle in the Shuttle ET & Stack coordinate system.
6.	The model is constructed in English Mass Units (lbs-sec^2)/in; Inches; Seconds)
7.	The model used is the un-pressurized pre-launch case.

Right Hand Model:

	Data Sources and Analysis Assumptions:
	Assumptions:
1.	The right hand SRB model, r2b101_rh.dat, came from the models provided by USA for use in the shuttle rollout tests.
2.	This model was initially intended to be run only in combination with the Left SRB using its coordinate systems and properties.
3.	The following changes were made to generating the model file r2b101_rh_modified.bdf.
3a	Coordinate systems 5002, 3, 15, and 1 were added to place the SRB in the Shuttle ET & Stack coordinate systems.
3b	The property cards from the left SRB were added to the bottom of the file.
4.	To eliminate numbering conflicts the right hand SRB was then renumbered using the EV31 Excel Macro Offset_Renumber_Bulkdata_V1. The original numbers were offset by 1,000,000.
5.	The Spreadsheet r2b101_rh_renumbered.xls contains the old model, new model, and the number mapping.
6.	The rsulting right hand SRB file is r2b101_rh_modified_renum.bdf.
7.	The right hand SRB nozzle model, rh_nozzle.dat, came from the models provided by USA for use in the shuttle rollout tests.

8.	The following changes were made to allow its use with the main SRB model, generating the model file rh_nozzle_modified.bdf.
8a	Interfacing grids used to run the nozzle model "stand alone" were commented out.
8b	Elements & Grids were renumbered by offsetting by 1,000,000.
8c	The coordinate system 5004 was added to place the nozzle in the Shuttle ET & Stack coordinate system.
9.	The model is constructed in English Mass Units (lbs-sec^2)/in; Inches; Seconds)
10.	The model used is the un-pressurized pre-launch case.

Second, both the right and left hand models were further modified specifically for the VIPA VAC08 analysis cycle; the 60-day Study. This initially required full RSRB versions for a heavy lift concept and versions for the CLV with the forward skirt and nose cone removed.

Full RSRB VAC08 Versions:

	Data Sources and Analysis Assumptions:
	Assumptions:
1.	The SRB models generated for use with VAC08 are derived from the USA SRB models delivered to EV31 for us in both the Shuttle rollout tests and shuttle derived vehicle studies.
2.	The left hand SRB was modified by removing the density from the solid elements representing the propellant to generate the "empty" version, r2b101_Modified_Empty.bdf.
3.	This alteration did not remove the stiffness associated with the solid propellant.
4.	RBE3's were constructed to generate nodes down the centerline of the SRB that would represent the average beam bending characteristics of the SRB. These are contained in the model RBE3s_4seg.bdf.
5.	Additionally, lumped masses can be added to these centerline grids to represent the propellant mass at different burn times.
6.	Aerodynamic loading will also be generated that will be applied to these centerline grids.
7.	The UM option is used for these RBE3's so that the model can be ASET, as needed, to generate a dynamic model that only contains the average beam bending characteristics.
8.	The right hand SRB provided with the USA SRB models was difficult to use.
9.	Instead, a new right hand SRB was mirrored according to the directions in the model documentation provided.
10.	This mirroring was done within an Excel spreadsheet since the mirroring done in Patran is cumbersome and inaccurate. This spreadsheet, Mirror.xls, contains the tracebility from the left hand model to the mirrored right hand model.
11.	This new right hand model, rh_nozzle_modified_Mirrored.bdf, is now accurately mirrored and "consistently" numbered having mirror image grid and element numbers offset by 1,000,000.
12.	The model is constructed in English Mass Units (lbs-sec^2)/in; Inches; Seconds)
13.	The model used is the un-pressurized pre-launch case.
	Recommended Models:
	-
	Left hand:

	r2b101_Modified_Empty.bdf
	r2noza_modified.bdf
	RBE3s_4seg.bdf
	Right Hand:
	r2b101_rh_modified_Empty_Mirrored.bdf
	rh_nozzle_modified_Mirrored.bdf
	RHS_RBE3s_4seg_Mirrored.bdf

No Forward Skirt VAC08 Versions:

	Data Sources and Analysis Assumptions:
	Assumptions:
1.	The SRB models generated for use with the VAC08 Crew Launch Vehicle (CLV) are derived from the USA SRB models delivered to EV31 for us in both the Shuttle rollout tests and shuttle derived vehicle studies.
1.	The CLV SRB models are direct copies of the full VAC08 SRB's with the appropriate nose cone and forward skirt sections commented out..
2.	The model was modified by removing the density from the solid elements representing the propellant to generate the "empty" versions.
3.	This alteration did not remove the stiffness associated with the solid propellant.
4.	RBE3's were constructed to generate nodes down the centerline of the SRB that would represent the average beam bending characteristics of the SRB.
5.	Additionally, lumped masses can be added to these centerline grids to represent the propellant mass at different burn times.
6.	Aerodynamic loading will also be generated that will be applied to these centerline grids.
7.	The UM option is used for these RBE3's so that the model can be ASET, as needed, to generate a dynamic model that only contains the average beam bending characteristics.
12.	The model is constructed in English Mass Units (lbs-sec^2)/in; Inches; Seconds)
13.	The model used is the un-pressurized pre-launch case.
	Recommended Models:
	-
	Left hand:
	r2b101_Modified_Empty_NoFS.bdf
	r2noza_modified.bdf
	RBE3s_4seg_NoFS.bdf
	Right Hand:
	r2b101_rh_modified_Empty_Mirrored_NoFS.bdf
	rh_nozzle_modified_Mirrored.bdf
	RHS_RBE3s_4seg_Mirrored_NoFS.bdf

Finally, the Left hand "No Forward Skirt" version was modified to place it in the correct CLV coordinate frame as well as adding the correct propellant and wind loadings.

Left Hand VAC08 CLV version:

	Data Sources and Analysis Assumptions:
	Assumptions:
1.	These SRB models were generated specifically for use with the VAC08 Crew Launch Vehicle (CLV). They are derived from the USA SRB models delivered to EV31 for us in both the Shuttle rollout tests and shuttle derived vehicle studies. They were further modified for VAC08 use with full SRB versions as well as versions with the nose cone and forward skirt removed.
2.	These models are specific for the VAC08 CLV 4 version.
3.	Compatible propellant loading, wind or aero loading as well as interface and coordinate definition has been developed and applied to the more detailed Level II derived models.
4.	The coordinate systems have been altered such that the SRB (Coord 5001 & 5003) is positioned in the CLV4 Stack coordinate system (Coord 0). This Stack coordinate syste has the +X axis pointing from vehicle nose to tail such that the MLP to SRB interface is at station 3772.743. The SRB to frustrum/forward skirt is at station 2360.62.
5.	The model is constructed in English Mass Units (lbs-sec^2)/in; Inches; Seconds)
6.	The model used is the un-pressurized pre-launch case.
7.	The Ground Wind Load Cases are based on "NLS On-Pad Aerodynamic Database," ED35-114-91, September 12,1991.
8.	The Ground Wind Load Cases assume max wind speeds per "Terrestrial Environment (Climatic) Criteria Handbook for Use in Aerospace Vehicle Development", NASA-HDBK-1001, August 11, 2000.
9.	Wind Loads are applied as equivalent static forces based on standard wind pressure loading on the projected frontal area of the booster.
10.	Vortex-Shedding Loading is accounted for with a 1.5 x factor on the equivalent static wind loads.
11.	Vehicle base is assumed 100 feet above sea level for wind speed calculations.
	Recommended Models:
	-
	Left hand:
	r2b101_Modified_Empty_NoFS_VAC08.bdf
	r2noza_modified_VAC08.bdf
	RBE3s_4seg_NoFS_VAC08.bdf

Left Hand LC1a 5-segment FSB version:

	Data Sources and Analysis Assumptions:
	Assumptions:

1.	This FSB model was generated specifically for use with the Crew Launch Vehicle (CLV). It is derived from the USA SRB models delivered to EV31 for use in both the Shuttle rollout tests and shuttle derived vehicle studies. They were further modified for VAC08 CLV use with versions having the nose cone and forward skirt removed.
2.	These models are specific for the Load Cycle 1A or DAC-0 exit, DAC-1 entry loads analysis..
3.	The forward center segment of the model was copied and renumbered so that it could be reinserted as the center segment of a 5-segment FSB model.
4.	Compatible propellant loading, wind or aero loading as well as interface and coordinate definition has been developed and applied to the more detailed Level II derived models.
5.	The coordinate systems have been altered such that the SRB (Coord 5001 & 5003) is positioned in the D55m Stack coordinate system (Coord 0). This Stack coordinate syste has the +X axis pointing from vehicle nose to tail such that the MLP to SRB interface is at station 3755.360. The SRB to frustrum/forward skirt is at station 2041.120.
6.	The model is constructed in English Mass Units (lbs-sec^2)/in; Inches; Seconds)
7.	The model used is the un-pressurized pre-launch case.
8.	The Ground Wind Load Cases are based on "NLS On-Pad Aerodynamic Database," ED35-114-91, September 12,1991.
9.	The Ground Wind Load Cases assume max wind speeds per “Terrestrial Environment (Climatic) Criteria Handbook for Use in Aerospace Vehicle Development”, NASA-HDBK-1001, August 11, 2000.
10.	Wind Loads are applied as equivalent static forces based on standard wind pressure loading on the projected frontal area of the booster.
11.	Vortex-Shedding Loading is accounted for with a 1.5 x factor on the equivalent static wind loads.
12.	Vehicle base is assumed 100 feet above sea level for wind speed calculations.
	Recommended Models:
	-
	Left hand:
	r2b101_5s_Empty_NoFS_08.bdf
	r2noza_modified_04.bdf
	RBE3s_05_NoFS.bdf
	SRBL_Propellant.bdf
	SRBL_Pre-launch_Winds.bdf

6.2.2 1st Stage Booster (FSB) Model Checks

6.2.2.1 Mass

Table 6.2-1, FSB FEM Mass Properties

FSB Mass Properties			
Weight (lbs.)	X CG (in.)	Y CG (in.)	Z CG (in.)
1,597,259	2869.7	-250.5	0.0

6.2.2.2 Frequencies

Un-pressurized FSB frequencies are shown in Table 6.2-2, FSB Unpressurized Free-Free Frequencies.

Table 6.2-2, FSB Unpressurized Free-Free Frequencies

Mode Number	Frequency (HZ)
1	0.0
2	0.0
3	0.0
4	0.0
5	0.0
6	0.0
7	3.1
8	3.1
9	3.4
10	7.0
11	7.0
12	9.7
13	9.7
14	11.1
15	11.1
16	11.4
17	11.4
18	11.6
19	11.6
20	12.7
21	12.7
22	13.0
23	13.0
24	14.9
25	14.9

6.3 CLV 5.5 Meter Upper Stage Model with 1st Stage Forward Frustum, Recovery Module, and Forward Skirt

The current version of the CLV Upper Stage finite element model is a simplified beam model intended to provide a first order load path representation as well as mass and inertia properties and simple beam bending dynamics. This current version includes the 1st stage forward frustum, recovery module, and forward skirt. The model does not include the Spacecraft Adapter but does include an Instrument Unit ring.

Two versions of the 5.5 meter Upper Stage model were created. The first used the Program allocated mass properties contained in Appendix B.1 (Memo1 FSB J2X.doc). The second used engineering weights from the DAC-0 Upper Stage structural sizing effort contained in Appendix

B.2 (DAC0ExitMEL_Prop.xls). The first model is designated D55m, the second is designated D55mR.

Figure 6.3-1 shows the Upper Stage FEM with stack X stations. This figure is compatible with both models.

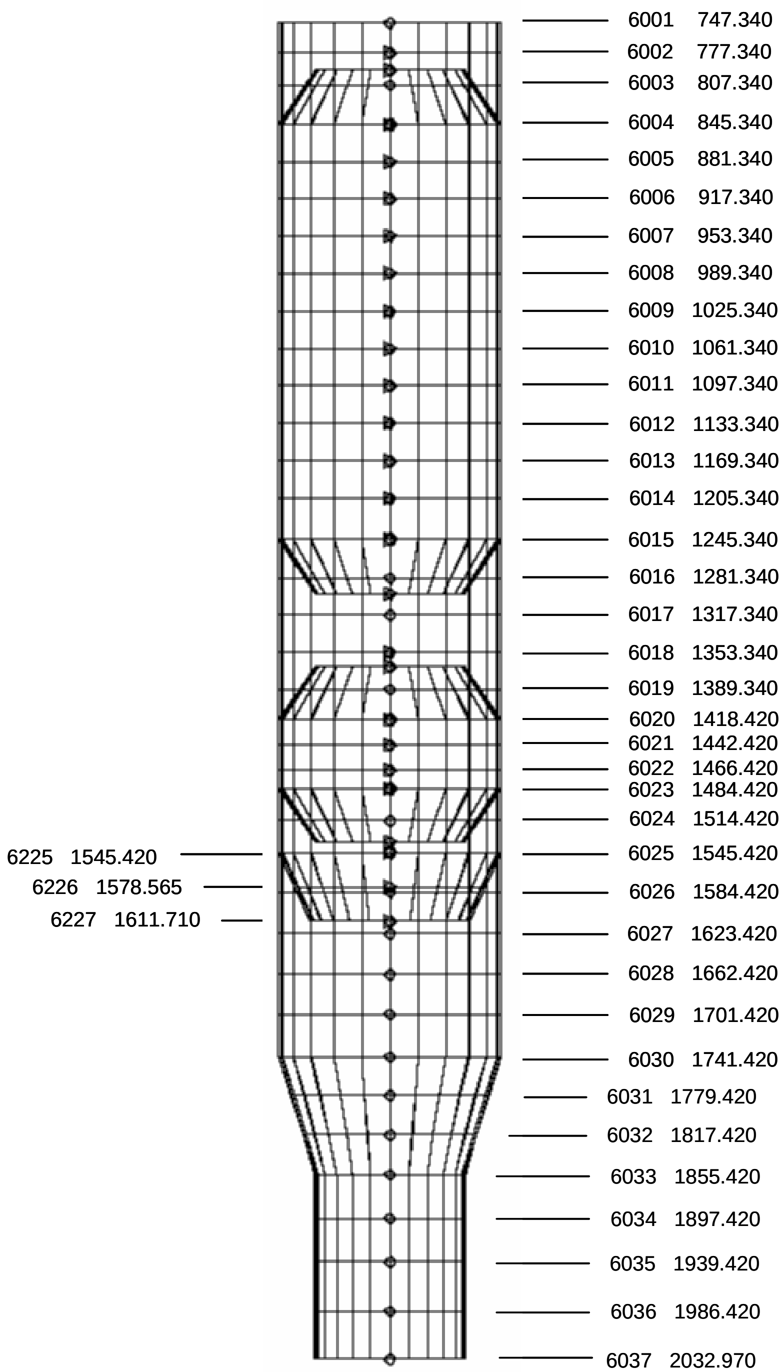

Figure 6.3-1, Upper Stage with 1st Stage Forward Frustum, Recovery Module, and Forward Skirt (D55m & D55mR) with Stack X Stations

6.3.1 CLV Upper Stage D55m Assumptions and Data Sources

	Data Sources and Analysis Assumptions:
	Assumptions:
	Numerous assumptions were made as part of the 5 segment SRM & J-2x CLV 5.5m 2nd Stage model . These assumptions are based on a combination of engineering judgement, the best available design data, and/or historical data.
1.	This model does not contain the spacecraft adapter but does contain an IU ring (Instrument Unit).
2.	The vehicle interstage and 1st stage frustum, recovery module, and forward skirt are included in this model.
3.	The model is constructed in English Mass Units (lbs-sec^2)/in; Inches; Seconds)
4.	The Vehicle Stack coordinate system has the +X axis pointing from vehicle nose to tail such that the MLP to FSB interface is at station 3765.093. The FSB to frustrum/forward skirt is at station 2032.970. The interstage to 1st stage interface is at station 1741.420. The forward edge 2nd Stage is at station 747.340.
5.	The 2nd Stage model is constructed in the 2nd Stage Coordinate System, with the +X-axis pointing from stage nose to tail, with an Origin 3057.753" forward of the MLP to FSB interface or at Vehicle Stack station of 707.340.
6.	The LOX Tank, LH2 Tank, Intertank, and Interstage are currently assumed to be hollow cylindrical sections with an estimated thickness based on the structural mass estimate.
7.	The Thrust structure and SRB forward frustum are currently assumed to be hollow conical sections with an estimated thickness based on the structural mass estimate.
8.	Mass properties for non-structural systems are added as concentrated masses or non-structural mass.
9.	Rigid Elements are used to attach the main structural elements of the 2nd stage booster together.
10.	The Ground Wind Load Cases are based on "NLS On-Pad Aerodynamic Database," ED35-114-91, September 12,1991.
11.	The Ground Wind Load Cases assume max wind speeds per “Terrestrial Environment (Climatic) Criteria Handbook for Use in Aerospace Vehicle Development”, NASA-HDBK-1001, August 11, 2000.
12.	Wind Loads are applied as equivalent static forces based on standard wind pressure loading on the projected frontal area of the booster.
13.	Vortex-Shedding Loading is accounted for with a 1.5 x factor on the equivalent static wind loads.
14.	Vehicle base is assumed 100 feet above sea level for wind speed calculations.
15.	Vehicle mass estimates are DAC-0 "allocated" weights from the below reference.
	Data Sources:
	The primary sources of information used for developing this Excel Workbook, and in turn the NASTRAN Models of the 2nd Stage are summarized below:
1.	5segj2_shortiu_layout_sketch_55m.jpg
2.	Memo1 FSB J2X.doc

6.3.2 CLV Upper Stage D55mR Assumptions and Data Sources

	Data Sources and Analysis Assumptions:
	Assumptions:
	Numerous assumptions were made as part of the 5 segment SRM & J-2x CLV 5.5m 2nd Stage model. These assumptions are based on a combination of engineering judgment, the best available design data, and/or historical data.
1.	This model does not contain the spacecraft adapter but does contain an IU ring (Instrument Unit).
2.	The vehicle interstage and 1st stage frustum, recovery module, and forward skirt are included in this model.
3.	The model is constructed in English Mass Units (lbs-sec^2)/in; Inches; Seconds)
4.	The Vehicle Stack coordinate system has the +X axis pointing from vehicle nose to tail such that the MLP to FSB interface is at station 3765.093. The FSB to frustrum/forward skirt is at station 2032.970. The interstage to 1st stage interface is at station 1741.420. The forward edge 2nd Stage is at station 747.340.
5.	The 2nd Stage model is constructed in the 2nd Stage Coordinate System, with the +X-axis pointing from stage nose to tail, with an Origin 3057.753" forward of the MLP to FSB interface or at Vehicle Stack station of 707.340.
6.	The LOX Tank, LH2 Tank, Intertank, and Interstage are currently assumed to be hollow cylindrical sections with an estimated thickness based on the structural mass estimate.
7.	The Thrust structure and SRB forward frustum are currently assumed to be hollow conical sections with an estimated thickness based on the structural mass estimate.
8.	Mass properties for non-structural systems are added as concentrated masses or non-structural mass.
9.	Rigid Elements are used to attach the main structural elements of the 2nd stage booster together.
10.	The Ground Wind Load Cases are based on "NLS On-Pad Aerodynamic Database," ED35-114-91, September 12,1991.
11.	The Ground Wind Load Cases assume max wind speeds per “Terrestrial Environment (Climatic) Criteria Handbook for Use in Aerospace Vehicle Development”, NASA-HDBK-1001, August 11, 2000.
12.	Wind Loads are applied as equivalent static forces based on standard wind pressure loading on the projected frontal area of the booster.
13.	Vortex-Shedding Loading is accounted for with a 1.5 x factor on the equivalent static wind loads.
14.	Vehicle base is assumed 100 feet above sea level for wind speed calculations.
15.	Vehicle mass estimates are DAC-0 "allocated" weights from the below reference 2. Primary structural weights have been updated based on reference 3 below. Structural thicknesses were modified to provide a minimal amount of NSM to account for the primary structural weight.
	Data Sources:
	The primary sources of information used for developing this Excel Workbook, and in turn the NASTRAN Models of the 2nd Stage are summarized below:
1.	5segj2_shortiu_layout_sketch_55m.jpg

2.	Memo1 FSB J2X.doc
3.	DAC-0 US IPT input Upper Stage 22Feb06.doc

6.3.3 CLV Upper Stage D55m and D55mR Model Checks

6.3.3.1 Mass

Table 6.3-1, CLV 5.5 meter Upper Stage D55m & D55mR Mass Comparison

DAC-0 5.5m Intros Weights of Upper Stage w/ Frustum, Recovery, Fwd Skirt, & IU					
Condition	Mass ($lbs\text{-}sec^2/in$)	Weight (lbs)	X CG (in)	Y CG (in)	Z CG (in)
1st Stage Burn Out	911	351,840	1,421.6	-250.5	0.0
2nd Stage Ignition	823	317,813	1,379.3	-250.5	0.0
2nd Stage Burn Out	85	32,878	1,565.1	-250.5	0.0

DAC-0 5.5mR Resized Weights of Upper Stage w/ Frustum, Recovery, Fwd Skirt, & IU					
Condition	Mass ($lbs\text{-}sec^2/in$)	Weight (lbs)	X CG (in)	Y CG (in)	Z CG (in)
1st Stage Burn Out	941	363,410	1,424.8	-250.5	0.0
2nd Stage Ignition	833	321,485	1,379.1	-250.5	0.0
2nd Stage Burn Out	95	36,550	1,310.7	-250.5	0.0

6.3.3.2 Frequencies

Table 6.3-2, CLV Upper Stage D55m and D55mR Free-Free Frequencies shows the calculated free-free frequencies of the CLV Upper Stage model.

Table 6.3-2, CLV Upper Stage D55m and D55mR Free-Free Frequencies

DAC-0 5.5m Intros Weight Frequencies			
Free-Free Frequencies of US Models			
Mode	**ff-2ndbo**	**ff-2ndign**	**ff-1stbo**
No.	**Fn (Hz)**	**Fn (Hz)**	**Fn (Hz)**
1	0.0	0.0	0.0
2	0.0	0.0	0.0
3	0.0	0.0	0.0
4	0.0	0.0	0.0
5	0.0	0.0	0.0
6	0.0	0.0	0.0
7	30.9	15.6	7.9
8	30.9	15.6	7.9
9	59.0	24.6	20.2
10	59.5	24.6	20.2
11	66.6	28.1	26.0

DAC-0 5.5mR Resized Weight Frequencies			
Free-Free Frequencies of US Models			
Mode	**ff-2ndbo**	**ff-2ndign**	**ff-1stbo**
No.	**Fn (Hz)**	**Fn (Hz)**	**Fn (Hz)**
1	0.0	0.0	0.0
2	0.0	0.0	0.0
3	0.0	0.0	0.0
4	0.0	0.0	0.0
5	0.0	0.0	0.0
6	0.0	0.0	0.0
7	32.7	17.1	9.3
8	32.7	17.1	9.3
9	65.4	27.7	21.6
10	66.6	27.7	21.6
11	66.6	31.3	27.7

12	66.6	46.5	26.0
13	102.6	46.5	28.0
14	102.6	47.5	39.8

12	71.7	38.0	27.7
13	100.8	38.0	31.1
14	100.8	41.6	36.5

6.4 CLV 5.0 Meter Upper Stage Model with 1st Stage Forward Frustum, Recovery Module, and Forward Skirt

The current version of the 5.0 meter CLV Upper Stage finite element model is a simplified beam model intended to provide a first order load path representation as well as mass and inertia properties and simple beam bending dynamics. This current version includes the Forward Frustum and excludes the Spacecraft Adapter. Figure 6.4-1 shows the Upper Stage and Forward Frustum FEM with stack X stations.

The 5.0 meter Upper Stage model is designated D50m.

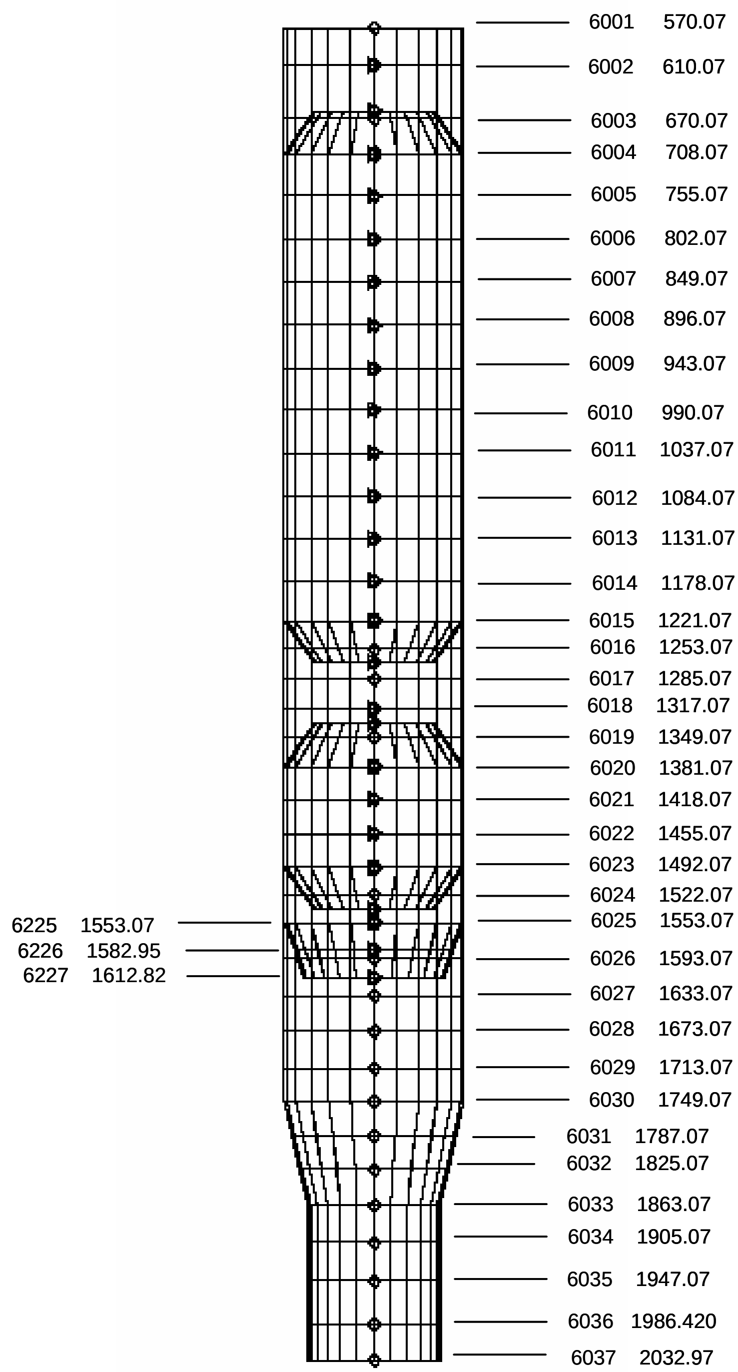

Figure 6.4-1, Upper Stage D50m and Interstage FEM's with Stack X Stations

6.4.1 CLV Upper Stage D50m Assumptions and Data Sources

	Data Sources and Analysis Assumptions:

	Assumptions:
	Numerous assumptions were made as part of the 5 segment FSB & J-2x CLV 5.0m 2nd Stage model . These assumptions are based on a combination of engineering judgement, the best available design data, and/or historical data.
1.	This model does not contain the spacecraft adapter but does contain an IU ring (Instrument Unit).
2.	The vehicle interstage, forward frustum, FSB recovery section, and FSB forward frustum are included in this model.
3.	The model is constructed in English Mass Units (lbs-sec^2)/in; Inches; Seconds)
4.	The Vehicle Stack coordinate system has the +X axis pointing from vehicle nose to tail such that the MLP to SRB interface is at station 3765.093". The FSM to frustrum/forward skirt is at station 1863.07". The forward edge 2nd Stage is at station 570.07".
5.	The 2nd Stage model is constructed in the 2nd Stage Coordinate System, with the +X-axis pointing from stage nose to tail, with an Origin 3195.0229" forward of the MLP to FSB interface or at Vehicle Stack station of 570.07".
6.	The LOX Tank, LH2 Tank, Intertank, and Interstage are currently assumed to be hollow cylindrical sections with an equivalent thickness required to maintain the overall composite cross-sectional area of the skin/stringer/ribs/isogrid.
7.	The Thrust structure, forward frustum, and FSB forward frustum are currently assumed to be hollow conical sections with an equivalent thickness required to maintain the overall composite cross-sectional area of the skin/stringer/ribs/isogrid.
8.	Mass properties for non-structural systems are added as concentrated masses or non-structural mass.
9.	Rigid Elements are used to attach the main structural elements of the 2nd stage together.
10.	The Ground Wind Load Cases are based on "NLS On-Pad Aerodynamic Database," ED35-114-91, September 12,1991.
11.	The Ground Wind Load Cases assume max wind speeds per “Terrestrial Environment (Climatic) Criteria Handbook for Use in Aerospace Vehicle Development”, NASA-HDBK-1001, August 11, 2000.
12.	Wind Loads are applied as equivalent static forces based on standard wind pressure loading on the projected frontal area of the booster.
13.	Vortex-Shedding Loading is accounted for with a 1.5 x factor on the equivalent static wind loads.
14.	Vehicle base is assumed 100 feet above sea level for wind speed calculations.
15.	Since there was no data available for the mass properties of the 5.0m diameter CEV/CLV, this models mass properties were scaled off of the 5.5m model which had much better definition with respect to mass properties. Each 5.0m component mass was left equal to the mass of each respective 5.5m component. The linear non-structural masses were all left the same in both models. The structural masses changed with diameter and component length changes, wall thicknesses were also left the same in both models.
	Data Sources:
	The primary sources of information used for developing this Excel Workbook, and in turn the NASTRAN Models of the 2nd Stage are summarized below:
1.	5.0m intros schematic diagram.
2.	Memo1 FSB J2X.doc

6.4.2 CLV Upper Stage D50m Model Checks

6.4.2.1 Mass

There were no INTROS mass properties supplied for the 5.0m/CLV Upper Stage model. Since there was no data given for the mass properties of the 5.0m/CLV diameter CEV/CLV, the models mass properties were scaled off of the 5.5m/CLV model which had much better definition with respect to mass properties. Each 5.0m/CLV component mass was left equal to the mass of each respective 5.5m/CLV component. The linear non-structural masses were all left the same in both models. The structural masses changed with diameter and component length changes, wall thicknesses were also left the same in both models. The mass properties of the FEM are shown below in Table 6.4-1, CLV 5.0 meter Upper Stage D50m Mass. All consumables are considered to be included in the 2nd Stage Ignition case.

Table 6.4-1, CLV 5.0 meter Upper Stage D50m Mass

DAC-0 5.0m Weights of Upper Stage w/ Frustum, Recovery, Fwd Skirt, & IU					
Condition	Mass ($lbs\text{-}sec^2/in$)	Weight (lbs)	X CG (in)	Y CG (in)	Z CG (in)
1st Stage Burn Out	915	353,272	1,393.7	-250.5	0.0
2nd Stage Ignition	829	320,069	1,349.6	-250.5	0.0
2nd Stage Burn Out	91	35,134	1,242.5	-250.5	0.0

6.4.2.2 Frequencies

Table 6.4-2, CLV Upper Stage D50m Free-Free Frequencies shows the calculated free-free frequencies of the 5.0m/CLV Upper Stage model.

Table 6.4-2, CLV Upper Stage D50m Free-Free Frequencies

DAC-0 5.0m Frequencies			
Free-Free Frequencies of US Models			
Mode	ff-2ndbo	ff-2ndign	ff-1stbo
No.	Fn (Hz)	Fn (Hz)	Fn (Hz)
1	0.0	0.0	0.0
2	0.0	0.0	0.0
3	0.0	0.0	0.0
4	0.0	0.0	0.0
5	0.0	0.0	0.0
6	0.0	0.0	0.0
7	21.6	11.3	6.30
8	21.6	11.3	6.30
9	49.6	20.6	15.7
10	50.0	20.6	15.7
11	50.6	26.2	22.2
12	50.6	38.9	22.2
13	83.1	38.9	26.0

14	83.1	42.5	38.7

6.5 CLV J2-X System Model

The J2-X system model has not yet been incorporated into the CLV system model. It is currently modeled as a lumped mass of 5100 pounds.

6.6 CEV Spacecraft with Spacecraft Adapter

The current version of the CEV Spacecraft finite element model is a simplified beam model intended to provide a first order load path representation as well as mass and inertia properties and simple beam bending dynamics. The model reflects the “5.0 meter” diameter CEV which actually measures 198 inches. Two versions of the CEV model were constructed; one for the 5.5 meter Upper Stage and one for the 5.0 meter Upper Stage. The only difference was in the Spacecraft adapter. Figure 6.6-1 shows the CEV and Spacecraft Adapter models used with the D55m, D55mR, and D50m models, with axial stations in the System Loads Coordinate system (Section 5.1.1).

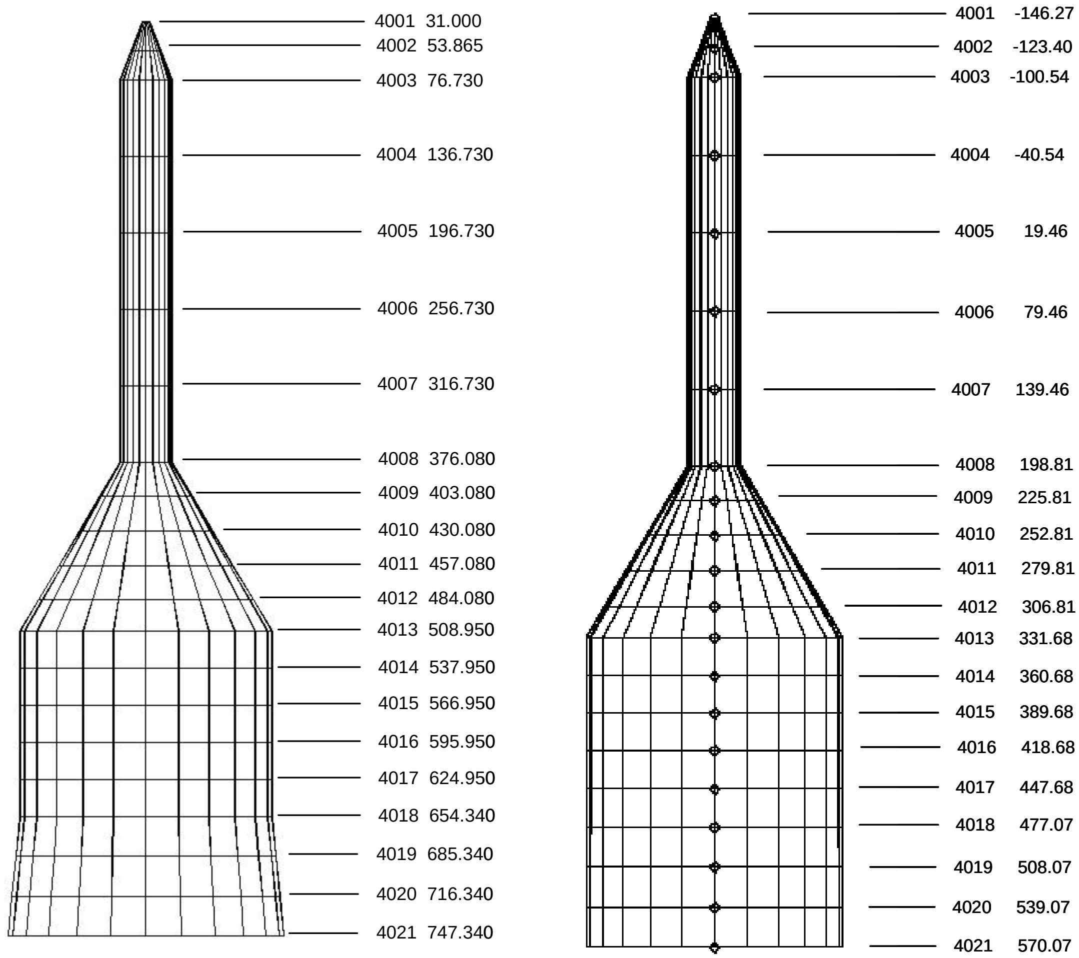

Figure 6.6-1, CEV D55m, D55mR, and D50m FEM Model Stations with Spacecraft Adapter

6.6.1 CEV Spacecraft Assumptions and Data Sources

Data Sources and Analysis Assumptions:

	Assumptions:
	Numerous assumptions were made as part of the 5.0m CEV spacecraft model for the 5.5m CEV/CLV. These assumptions are based on a combination of engineering judgment, the best available design data, and/or historical data.
1.	This model includes the Escape tower, Crew capsule, Service module, and Spacecraft Adapter.
2.	The model is constructed in English Mass Units (lbs-sec^2)/in; Inches; Seconds)
3.	The Vehicle Stack coordinate system has the +X axis pointing from vehicle nose to tail such that the MLP to SRB interface is at station 3765.093. The Service module to spacecraft adapter is at station 654.340. The aft edge of the spacecraft adapter is at station 747.340.
4.	The Model is constructed in the Local EscCrewServ Coordinate System, with the +X-axis pointing from nose to tail, with an Origin 3834.093" in front of the MLP to SRB interface. (Note that the Local EscCrewServ Coordinate System is at Stack Coordinate station -69.000.)
6.	Mass properties for non-structural systems are added as concentrated masses or non-structural mass.
7.	Rigid Elements are used to attach the main structural elements of the payload to the rest of the launch vehicle (to allow for recovery of internal connection forces).
8.	The Ground Wind Load Cases are based on "NLS On-Pad Aerodynamic Database," ED35-114-91, September 12,1991.
9.	The Ground Wind Load Cases assume max wind speeds per “Terrestrial Environment (Climatic) Criteria Handbook for Use in Aerospace Vehicle Development”, NASA-HDBK-1001, August 11, 2000.
10.	Wind Loads are applied as equivalent static forces based on standard wind pressure loading on the projected frontal area of the CEV.
11.	Vortex-Shedding Loading is accounted for with a 1.5 x factor on the equivalent static wind loads.
12.	Vehicle base is assumed 100 feet above sea level for wind speed calculations.
13.	Mass properties from reference 3 were used for the Lunar mission as being the best available CEV masses. The ISS mission mass for the CEV minus LAS mass was estimated as being 95% of the CEV minus LAS Lunar mass.
	Data Sources:
	The primary sources of information used for developing this Excel Workbook, and in turn the NASTRAN Models of the CEV spacecraft are summarized below:
1.	5segj2_shortiu_layout_sketch1_50m.jpg
2.	5segj2_shortiu_layout_sketch_55m.jpg
3.	USDAC-0_ADFT.xls

6.6.2

6.6.3 CEV Spacecraft Model Checks

6.6.3.1 Mass

Table 6.6-1, CEV Spacecraft Mass Properties shows the model weight of the CEV model including the Launch Abort System, and Spacecraft Adapter. It was difficult to get mass properties of the CEV so an early estimate was used. This estimate included 13,228 lbs. for the LAS; 55140 lbs for the Lunar CEV; and an ISS CEV weighing 5% less. The same mass was used for the D55m, D55mR, and D50m versions.

Table 6.6-1, CEV Spacecraft Mass Properties

Escape / Crew / Service / Adapter Mass					
Condition	Mass (lbs-sec^2/in)	Weight (lbs)	X CG (in)	Y CG (in)	Z CG (in)
Lunar	177	68,284	497.0	-250.5	0.0
ISS	169	65,418	493.8	-250.5	0.0

6.6.3.2 Frequencies

Table 6.6-2, CEV Spacecraft Free-Free Frequencies

Free-Free Frequencies of CEV Spacecraft for 5.5m Upper Stage		
Mode No.	ISS Fn (Hz)	Lunar Fn (Hz)
1	0.0	0.0
2	0.0	0.0
3	0.0	0.0
4	0.0	0.0
5	0.0	0.0
6	0.0	0.0
7	8.8	8.7
8	8.8	8.7
9	31.6	31.4
10	31.6	31.4
11	56.8	56.5
12	65.8	65.4
13	65.8	65.4

Free-Free Frequencies of CEV Spacecraft for 5.0m Upper Stage		
Mode No.	ISS Fn (Hz)	Lunar Fn (Hz)
1	0.0	0.0
2	0.0	0.0
3	0.0	0.0
4	0.0	0.0
5	0.0	0.0
6	0.0	0.0
7	8.8	8.7
8	8.8	8.7
9	31.6	31.4
10	31.6	31.4
11	56.8	56.5
12	65.8	65.3
13	65.8	65.3

6.7 MLP Model

The mobile launch platform (MLP) model was constructed by John Townsend of MSFC/EV31 and recently updated for the MLP rollout tests currently being conducted. It is documented in

Reference 14. Figure 6.7-1 shows this model and Figure 6.7-2 shows a detail of the hold-down posts.

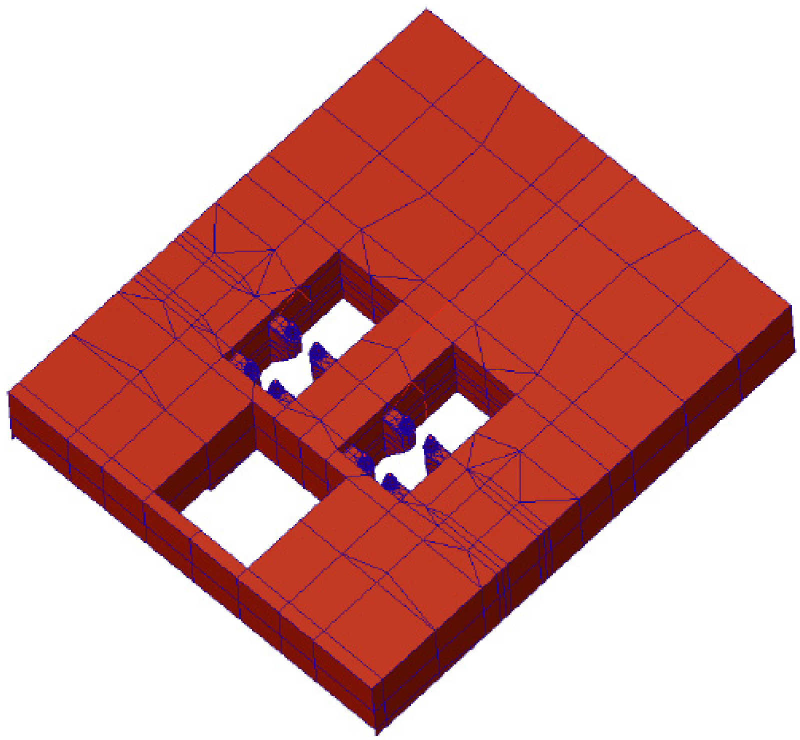

Figure 6.7-1, Mobile Launch Platform FEM

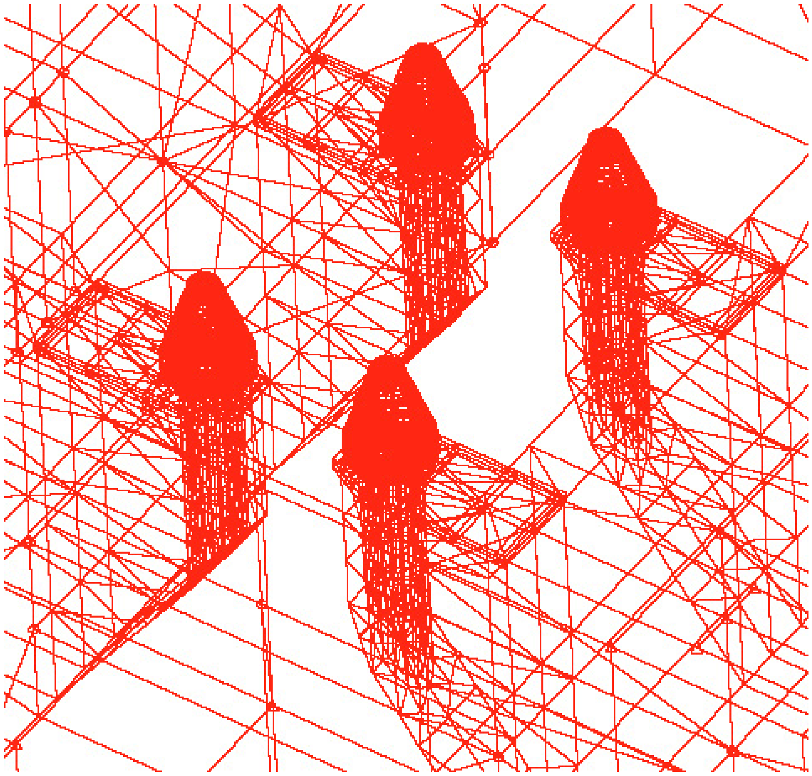

Figure 6.7-2, Detail Showing Hold-Down Posts

6.8 Stage Stack Model

Three stack models were constructed; D55m stack using the allocated mass Upper Stage, D55mR stack using the Engineering weight Upper Stage, and D50m stack using the 5 meter Upper Stage. All three stacks had ISS and Lunar weight CEV versions, resulting in a total of six stack configurations. Figure 6.8-1 shows an illustration of the D55m or D55mR FEM of the integrated vehicle stack. Figure 6.8-2 shows an illustration of the D50m FEM of the integrated vehicle stack.

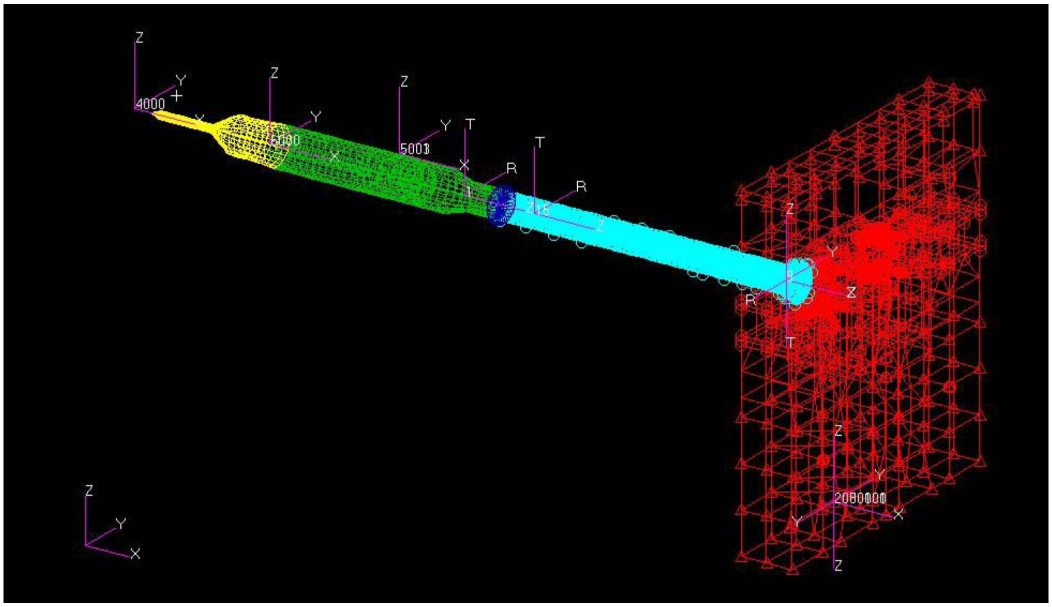

Figure 6.8-1, CLV D55m or D55mR Integrated to MLP Stack FEM

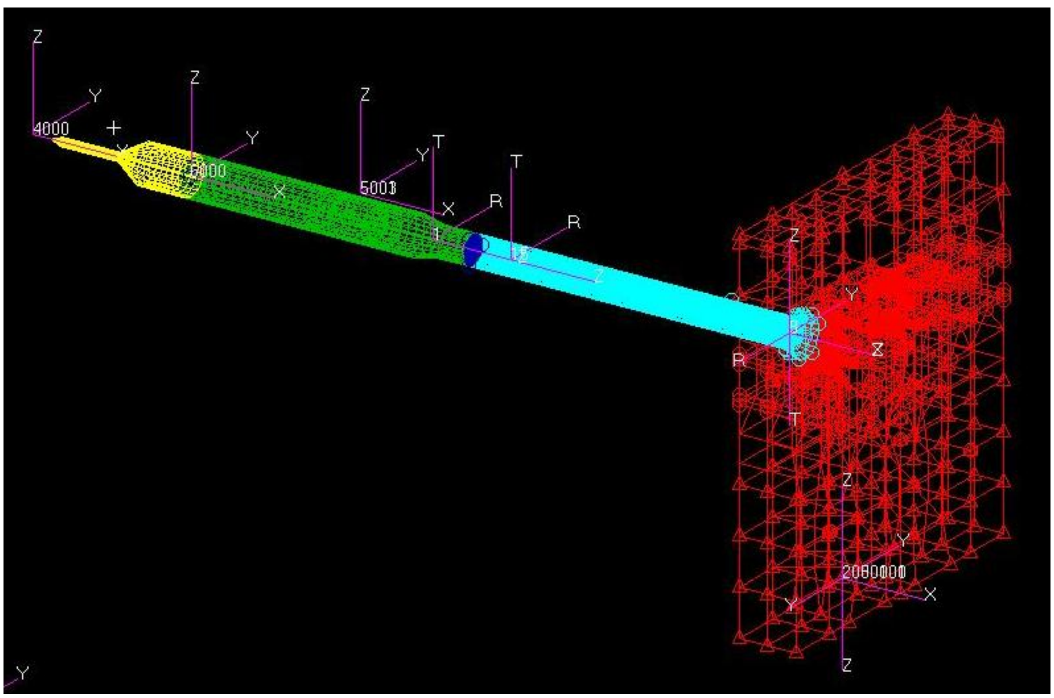

Figure 6.8-2, CLV D50m Integrated to MLP Stack FEM

6.8.1 Stack Assumptions and Data Sources

6.8.1.1 D55m and D55mR Stack Assumptions and Data Sources

<u>Data Sources and Analysis Assumptions:</u>

Assumptions:

Numerous assumptions were made as part of the 5 segment FSB, J2-X CLV Integrated Stack model . These assumptions are based on a combination of engineering judgement, the best available design data, and/or historical data.

1. The Integrated Stack model is intended to be the simple assembly of the various CLV elements.
2. The model is constructed in English Mass Units (lbs-sec^2)/in; Inches; Seconds)
3. The Vehicle Stack coordinate system has the +X axis pointing from vehicle nose to tail such that the MLP to SRB interface is at station 3765.093. The FSB to forward skirt is at station 2032.970. The forward edge 2nd Stage is at station 747.340.
4. Rigid Elements or stif springs are used to attach the main CLV structural elements together.
5. The Ground Wind Load Cases are based on "NLS On-Pad Aerodynamic Database," ED35-114-91, September 12,1991.
6. The Ground Wind Load Cases assume max wind speeds per “Terrestrial Environment (Climatic) Criteria Handbook for Use in Aerospace Vehicle Development”, NASA-HDBK-1001, August 11, 2000.
7. Wind Loads are applied as equivalent static forces based on standard wind pressure loading on the projected frontal area of the CLV.
8. Vortex-Shedding Loading is accounted for with a 1.5 x factor on the equivalent static wind loads.
9. Vehicle base is assumed 100 feet above sea level for wind speed calculations.

Data Sources:

The primary sources of information used for developing this Excel Workbook, and in turn the NASTRAN Models of the Integrated Stack are summarized below:
5segj2_shortiu_layout_sketch_55m.jpg

6.8.1.2 D50m Stack Assumptions and Data Sources

Data Sources and Analysis Assumptions:

Assumptions:

Numerous assumptions were made as part of the 5 segment FSB, J2-X CLV Integrated Stack model . These assumptions are based on a combination of engineering judgement, the best available design data, and/or historical data

1. The Integrated Stack model is intended to be the simple assembly of the various CLV elements.
2. The model is constructed in English Mass Units (lbs-sec^2)/in; Inches; Seconds)
3. The Vehicle Stack coordinate system has the +X axis pointing from vehicle nose to tail such that the MLP to FSB interface is at station 3765.093. The FSM to frustrum/forward skirt is at station 2032.970. The forward edge 2nd Stage is at station 570.070.
4. Rigid Elements or stiff springs are used to attach the main CLV structural elements together.
5. The Ground Wind Load Cases are based on "NLS On-Pad Aerodynamic Database," ED35-114-91, September 12,1991.
6. The Ground Wind Load Cases assume max wind speeds per “Terrestrial Environment (Climatic) Criteria Handbook for Use in Aerospace Vehicle Development”, NASA-HDBK-1001, August 11, 2000.

7. Wind Loads are applied as equivalent static forces based on standard wind pressure loading on the projected frontal area of the CLV.
8. Vortex-Shedding Loading is accounted for with a 1.5 x factor on the equivalent static wind loads.
9. Vehicle base is assumed 100 feet above sea level for wind speed calculations.

Data Sources:

The primary sources of information used for developing this Excel Workbook, and in turn the NASTRAN Models of the Integrated Stack are summarized below:

6.8.2 Stack Model Checks

6.8.2.1 Mass

The mass properties of the assembled stack components for three CLV configurations are shown below in Table 6.8-1, CLV Stack Weights (Lunar Weight CEV). This table reflects the Lunar weight CEV only.

Table 6.8-1, CLV Stack Weights (Lunar Weight CEV)

DAC-0 5.5m Intros Weights of Stack Configurations

Condition	Mass ($lbs\text{-}sec^2/in$)	Weight (lbs)	X CG (in)	Y CG (in)	Z CG (in)
Free-Free Empty	4,487	1,732,448	2,725.8	-250.5	0.0
On Pad Empty	4,487	1,732,448	2,725.8	-250.5	0.0
On Pad GLOW	5,225	2,017,383	2,536.9	-250.5	0.0
Free-Free GLOW	5,225	2,017,383	2,536.9	-250.5	0.0
1st Stage Burn Out	1,509	582,477	1,772.8	-250.6	0.1
2nd Stage Ignition	1,000	386,097	1,223.2	-250.5	0.0
2nd Stage Burn Out	228	87,934	842.8	-250.5	0.0

DAC-0 5.5m Resized Weights of Stack Configurations

Condition	Mass ($lbs\text{-}sec^2/in$)	Weight (lbs)	X CG (in)	Y CG (in)	Z CG (in)
Free-Free Empty	4,517	1,744,017	2,717.9	-250.5	0.0
On Pad Empty	4,517	1,744,017	2,717.9	-250.5	0.0
On Pad GLOW	5,255	2,028,952	2,531.1	-250.5	0.0
Free-Free GLOW	5,255	2,028,952	2,531.1	-250.5	0.0
1st Stage Burn Out	1,539	594,046	1,767.9	-250.6	0.1
2nd Stage Ignition	1,010	389,769	1,224.6	-250.5	0.0
2nd Stage Burn Out	237	91,606	863.8	-250.5	0.0

DAC-0 5.0m Weights of Stack Configurations (2)

Condition	Mass (lbs-sec/in) ($lbs\text{-}sec^2/in$)	Weight (lbs)	X CG (in)	Y CG (in)	Z CG (in)
Free-Free Empty	4,483	1,730,893	2,720.2	-250.5	0.0
On Pad Empty	28,141	10,864,905	3,726.4	-39.9	-159.3

On Pad GLOW	28,879	11,149,839	3,666.0	-45.3	-155.3
Free-Free GLOW	5,221	2,015,828	2,528.3	-250.5	0.0
1st Stage Burn Out	1,505	580,922	1,741.0	-250.6	0.1
2nd Stage Ignition	999	385,528	1,174.2	-250.5	0.0
2nd Stage Burn Out	226	87,365	732.9	-250.5	0.0

(2) 5.5m Intros, Contant NSM/in, Constant thickness, varied Length & Diameter

Table 6.8-2, CLV Stack Weights Compared to Allocated Mass Properties shows a comparison of CLV stack weights to the allocated mass properties of Appendix B.1.

Table 6.8-2, CLV Stack Weights Compared to Allocated Mass Properties

	Memo1 FSB J2X.doc		55m	55mR	50m
Full Stack ISS		N/A	2014710	2026279	2016018
Full Stack Lunar		2011548	2017467	2029036	2018775
LAS	13228		13228	13228	13228
CEV ISS	N/A		52383	52383	52383
CEV Lunar	55140		55140	55140	55140
1st & 2nd Stages		1943180	1949099	1960668	1950407
1st Stage motor & aft skirt		1591048	1597259	1597259	1597259
1st stage motor & aft skirt struct	191195		162352	162352	162352
1st Stage Propellant & Residuals	1399853		1434906	1434906	1434906
Upper Stage and Fwd 1st Stage		352132	351840	363410	353148
1st Stage Flight hardware		33255	34027	42008	33042
Fwd Frustum	24185		24185	24185	23670
Interstage	9070		9842	17823	9372
Upper Stage Gross (317261)		318877	317813	321401	320106
Propellant		284561	284935	284935	284935
Main Propellant	279980				
Residuals & reserves (Main Prop)	4581				
US [Burnout]		34316	32878	36466	35171
Propellants (Other)	1946				
Residuals & reserves (Other)	825				
Growth	3449				
US Dry Mass	28096				

6.8.2.2 Frequencies

Table 6.8-3, CLV Stack Frequencies (Lunar Weight CEV)

DAC-0 5.5m Intros Weight Frequencies

Free-Free Frequencies of Stack Models						On-Pad Frequencies	
Mode	FF-empty	ff-glow	ff-2ndbo	ff-2ndign	ff-1stbo	Empty	GLOW
No.	Fn (Hz)	Fn (Hz)	Fn (Hz)	Fn (Hz)	Fn (Hz)	Fn (Hz)	Fn (Hz)
1st	0.98	0.96	14.98	4.96	1.34	0.23	0.18

DAC-0 5.5m Resized Weight Frequencies

Free-Free Frequencies of Stack Models						On-Pad Frequencies	
Mode	FF-empty	ff-glow	ff-2ndbo	ff-2ndign	ff-1stbo	Empty	GLOW
No.	Fn (Hz)	Fn (Hz)	Fn (Hz)	Fn (Hz)	Fn (Hz)	Fn (Hz)	Fn (Hz)
1st	1.04	1.02	14.80	4.94	1.48	0.23	0.18

DAC-0 5.0m Frequencies (2)

Free-Free Frequencies of Stack Models						On-Pad Frequencies	
Mode	FF-empty	ff-glow	ff-2ndbo	ff-2ndign	ff-1stbo	Empty	GLOW
No.	Fn (Hz)	Fn (Hz)	Fn (Hz)	Fn (Hz)	Fn (Hz)	Fn (Hz)	Fn (Hz)
1st	0.86	0.83	11.10	4.41	1.09	0.23	0.17

(2) 5.5m Intros, Contant NSM/in, Constant thickness, varied Length & Diameter

7.0 Analysis and Design Loads Conditions

Load cases are under development for analyzing the flight regimes over which the CLV is expected to fly and determining the designing cases. A short description of the assumptions made for each flight regime is given in Section 7.1.

7.1 Flight Regimes

7.1.1 Pre-Launch Winds

Table 7.1-1 describes the currently assessed pre-launch wind cases. These assessments assume the CLV stack is alone on MLP attached to the left hand SRB posts. Ground wind models and assumptions made for this analysis are discussed in Section 5.4.2. These identified cases are believed to represent the worst case static wind loads with an allowance for vortex shedding.

Forcing functions were created for each of these load cases. Shear and bending moments for the vehicle were calculated from these applied loads. These forces were also applied to the various stack FEM models (D55m, D55mR, D50m) attached to the MLP model to recover hold-down post reactions.

Additional load cases will be developed as dynamic wind environments are defined. These would include wind turbulence caused by the presence of other structures on the launch pad.

These cases and assumptions will change as warranted by the developing design.

Table 7.1-1, Pre-Launch Wind Conditions

SUBCASE ID	STRUCTURAL CONFIGURATION	PROPELLANT LOADING	GRAVITY	WIND INCIDENCE	EXPOSURE TIME	RISK LEVEL	KSC WIND @ 18 meters (kts)	KSC WIND @ 18 meters (m/s)
7.1.1-1	Full Stack on MLP, no tower support	Dry	Yes	None	None	None	0.0	0.0
7.1.1-2	Full Stack on MLP, no tower support	Dry	Yes	Top (-Z)	1 Hour	5%	34.4	17.7
7.1.1-3	Full Stack on MLP, no tower support	Dry	Yes	Top (-Z)	1 Day	1%	47.0	24.2
7.1.1-4	Full Stack on MLP, no tower support	Dry	Yes	Top (-Z)	1 Day	5%	37.5	19.3
7.1.1-5	Full Stack on MLP, no tower support	Dry	Yes	Top (-Z)	10 Day	1%	57.5	29.6
7.1.1-6	Full Stack on MLP, no tower support	GLOW	Yes	None	None	None	0.0	0.0
7.1.1-7	Full Stack on MLP, no tower support	GLOW	Yes	Top (-Z)	1 Hour	5%	34.4	17.7
7.1.1-8	Full Stack on MLP, no tower support	GLOW	Yes	Top (-Z)	1 Day	1%	47.0	24.2
7.1.1-9	Full Stack on MLP, no tower support	GLOW	Yes	Top (-Z)	1 Day	5%	37.5	19.3
7.1.1-10	Full Stack on MLP, no tower support	GLOW	Yes	Top (-Z)	10 Day	1%	57.5	29.6
7.1.1-11	Full Stack on MLP, no tower support	Dry	Yes	None	None	None	0.0	0.0
7.1.1-12	Full Stack on MLP, no tower support	Dry	Yes	Bottom (+Z)	1 Hour	5%	34.4	17.7
7.1.1-13	Full Stack on MLP, no tower support	Dry	Yes	Bottom (+Z)	1 Day	1%	47.0	24.2
7.1.1-14	Full Stack on MLP, no tower support	Dry	Yes	Bottom (+Z)	1 Day	5%	37.5	19.3
7.1.1-15	Full Stack on MLP, no tower support	Dry	Yes	Bottom (+Z)	10 Day	1%	57.5	29.6
7.1.1-16	Full Stack on MLP, no tower support	GLOW	Yes	None	None	None	0.0	0.0
7.1.1-17	Full Stack on MLP, no tower support	GLOW	Yes	Bottom (+Z)	1 Hour	5%	34.4	17.7
7.1.1-18	Full Stack on MLP, no tower support	GLOW	Yes	Bottom (+Z)	1 Day	1%	47.0	24.2
7.1.1-19	Full Stack on MLP, no tower support	GLOW	Yes	Bottom (+Z)	1 Day	5%	37.5	19.3
7.1.1-20	Full Stack on MLP, no tower support	GLOW	Yes	Bottom (+Z)	10 Day	1%	57.5	29.6
7.1.1-21	Full Stack on MLP, no tower support	Dry	Yes	None	None	None	0.0	0.0
7.1.1-22	Full Stack on MLP, no tower support	Dry	Yes	Right (-Y)	1 Hour	5%	34.4	17.7
7.1.1-23	Full Stack on MLP, no	Dry	Yes	Right (-Y)	1 Day	1%	47.0	24.2

	tower support							
7.1.1-24	Full Stack on MLP, no tower support	Dry	Yes	Right (-Y)	1 Day	5%	37.5	19.3
7.1.1-25	Full Stack on MLP, no tower support	Dry	Yes	Right (-Y)	10 Day	1%	57.5	29.6
7.1.1-26	Full Stack on MLP, no tower support	GLOW	Yes	None	None	None	0.0	0.0
7.1.1-27	Full Stack on MLP, no tower support	GLOW	Yes	Right (-Y)	1 Hour	5%	34.4	17.7
7.1.1-28	Full Stack on MLP, no tower support	GLOW	Yes	Right (-Y)	1 Day	1%	47.0	24.2
7.1.1-29	Full Stack on MLP, no tower support	GLOW	Yes	Right (-Y)	1 Day	5%	37.5	19.3
7.1.1-30	Full Stack on MLP, no tower support	GLOW	Yes	Right (-Y)	10 Day	1%	57.5	29.6
7.1.1-31	Full Stack on MLP, no tower support	Dry	Yes	None	None	None	0.0	0.0
7.1.1-32	Full Stack on MLP, no tower support	Dry	Yes	Left (+Y)	1 Hour	5%	34.4	17.7
7.1.1-33	Full Stack on MLP, no tower support	Dry	Yes	Left (+Y)	1 Day	1%	47.0	24.2
7.1.1-34	Full Stack on MLP, no tower support	Dry	Yes	Left (+Y)	1 Day	5%	37.5	19.3
7.1.1-35	Full Stack on MLP, no tower support	Dry	Yes	Left (+Y)	10 Day	1%	57.5	29.6
7.1.1-36	Full Stack on MLP, no tower support	GLOW	Yes	None	None	None	0.0	0.0
7.1.1-37	Full Stack on MLP, no tower support	GLOW	Yes	Left (+Y)	1 Hour	5%	34.4	17.7
7.1.1-38	Full Stack on MLP, no tower support	GLOW	Yes	Left (+Y)	1 Day	1%	47.0	24.2
7.1.1-39	Full Stack on MLP, no tower support	GLOW	Yes	Left (+Y)	1 Day	5%	37.5	19.3
7.1.1-40	Full Stack on MLP, no tower support	GLOW	Yes	Left (+Y)	10 Day	1%	57.5	29.6

7.1.2 Liftoff Transient

The CLV Liftoff event was assessed using a linear transient analysis with interface forces calculated to maintain vehicle/launch pad compatibility until the time of release. The details of the theory of this analysis can be found in Reference 15. Reference 16 gives an overview of applying this theory to the X33 launch vehicle. Details on the finite element models used in this analysis can be found in Section 6.0.

For the liftoff analysis, both the vehicles and pad models were reduced into a set of uncoupled equations of motion, with displacement, velocity and acceleration compatibility enforced at the FSB/MLP hold-down posts locations. Modes up to 50 Hz were kept for each. A modal damping of 0.5 % was assumed for the analysis. Modal acceleration method was used for data recovery. An uncertainty factor of 1.5 was added to the dynamic portion of the responses.

7.1.2.1 LC1a Liftoff Transient

A number of parameters and combinations of those parameters dictate the magnitude of the loads associated with a vehicle liftoff transient. For the LC1a cycle, a limited number of these parameters were combined in order to obtain a first cut load set for the event. These parameters include wind direction, vehicle configuration, and thrust rise rate.

Two wind incidence directions were chosen; the top wind (-z) and left side wind (+y). Both wind cases consisted of 1 Hour winds at a 5% risk level as documented in Section 7.1.1. Due to vehicle symmetry, reciprocal wind incidence directions were not investigated. An uncertainty factor of 1.5 was multiplied to the results to account for wind induced oscillation.

Four vehicle configurations were analyzed for LC1a. Details of the four configurations can be found in Section 6.8. These include the allocated mass CLV (D55m) with a lunar CEV, the allocated mass CLV with an ISS CEV, the engineering mass CLV (D55mR) with a lunar CEV, the engineering mass CLV with an ISS CEV. All configurations used the same FSB model.

All load cases for LC1a assume the nominal CLVFSB05306 thrust rise rate except two, LO00049 and LO00050. These two cases were chosen in lieu of a full set of dispersed cases to speed the completion of the liftoff analysis and thereby meet DAC deadlines. At the time of this decision, there was no clear "worst case" from the existing results, so LO0001 was chosen, somewhat arbitrarily, as the parameter set to use for dispersions. This resulted in dispersed cases consisting of a top wind load case combined with a minimum FSB thrust rise rate (late ignition, low thrust rise rate, low total thrust) and a maximum thrust rise rate (early ignition, high thrust rise rate-high total thrust) for the allocated mass CLV with a lunar CEV. Further explanation of the FSB thrust time histories can be found in Section 5.9.2.

In addition to thrust dispersions, overpressure data also, was not available early enough to be included in the EV31-06-006 memo. To account for the lack of overpressure, an uncertainty factor of 1.5 was applied to the lateral loads from the liftoff analysis.

The total number of liftoff transient load cases for LC1a with the two wind incidence directions and four vehicle configurations, plus the two thrust rise rate cases was ten. A table of the Liftoff LC1a load cases can be seen in Table 7.1-2.

Table 7.1-2, LC1a Liftoff Load Cases

LOAD CASE	WIND	THRUST	OP	CLV	CEV
LO0001	TOP (+z)	NOMINAL	NO	5.5m / Eng. Mass	LUNAR
LO0002	SIDE (+y)	NOMINAL	NO	5.5m / Eng. Mass	LUNAR
LO0003	TOP (+z)	NOMINAL	NO	5.5m / Alloc. Mass	LUNAR
LO0004	SIDE (+y)	NOMINAL	NO	5.5m / Alloc. Mass	LUNAR
LO0005	TOP (+z)	NOMINAL	NO	5.0m / Alloc. Mass	LUNAR
LO0006	SIDE (+y)	NOMINAL	NO	5.0m / Alloc. Mass	LUNAR
LO0025	TOP (+z)	NOMINAL	NO	5.5m / Eng. Mass	ISS
LO0026	SIDE (+y)	NOMINAL	NO	5.5m / Eng. Mass	ISS
LO0027	TOP (+z)	NOMINAL	NO	5.5m / Alloc. Mass	ISS
LO0028	SIDE (+y)	NOMINAL	NO	5.5m / Alloc. Mass	ISS
LO0029	TOP (+z)	NOMINAL	NO	5.0m / Alloc. Mass	ISS
LO0030	SIDE (+y)	NOMINAL	NO	5.0m / Alloc. Mass	ISS
LO0049	TOP (+z)	MIN RISE RATE	NO	5.5m / Alloc. Mass	LUNAR
LO0050	TOP (+z)	MAX RISE RATE	NO	5.5m / Alloc. Mass	LUNAR

The absolute maximum section loads and accelerations at each vehicle station from the LC1a liftoff transient analyses can be found in Section 8.2.3.

7.1.3 Ascent

7.1.3.1 Quasi-Static with Static Aero-elastic

Currently ascent loads for the launch vehicle have been calculated in a quasi-static sense. Static aero-elastic effects have not been calculated.

At the start of the LC1a analysis 6-dof control simulations had not yet been constructed (Section 5.6). The analysis was based on the 3-dof flight performance trajectory (Section 5.5) using a uniform 7 degree dispersion to account for the expected flight parameter dispersions. The 7 degrees was applied in the pitch plane only due to the symmetry of the vehicle and is assumed to envelope the RSS of angle-of-attack (α) and sideslip (ß) dispersions. Aerodynamic coefficients were still in development at the start of the LC1a analysis. An engineering based aerodynamic coefficient database was constructed as described in Section 5.8.

A simulation was run calculating the quasi-static loads for each point in the trajectory. Forces were calculated at each time to trim the vehicle to null rotational accelerations; no load relief was assumed. The vehicle mass was adjusted at each time using the methodology described in Reference 17. The resulting element forces and section loads from this analysis were then searched for maxima and minima. These results are discussed in Section 8.0.

There were a several objectives for assessing a wider range of aerodynamic flight regimes than the typical maximum dynamic pressure case. These objectives are highlighted in Figure 7.1-1.

Ascent Loads Objectives

- Cover as much of the Ascent flight regime as possible
- Provide reasonable, but conservative loads to reduce risk of large load increases after SRR
- Traditional high load areas include
  - Max Q, Max G, Max thrust, etc.
  - Are there any surprises?
- Be responsive and anticipatory to still changing configuration
- Remain as close to Aero Database as feasible
  - CA, CN, CM tables provided to Trajectories
  - Distributed aero provided to Loads

Figure 7.1-1, Ascent Loads Objectives

Figures Figure 7.1-2, Figure 7.1-3, and Figure 7.1-4 from the LC1a results presentation to the CLV Loads Panel, Reference 18, illustrate additional parameters, assumptions, and objectives for the ascent load cases.

Flight Regime Coverage

- Very early flight
  - Characteristics
    - 0psf > Q > 250psf
    - High a's
    - Ground winds
  - Current analysis coverage minimal
    - Assume no aero
    - Primarily looking for max axial load conditions
    - Lack of fidelity puts structure associated with or near engine gimbal at risk from dynamic gimballing
      - Assume covered within uncertainty factors
- Early flight
  - Characteristics
    - 200psf > Q > 300psf
    - Trajectory a's low (0°)
    - Ascent wind environments available
    - Low Mach number < 0.5
  - Current analysis coverage minimal
    - Assume no aero
    - Primarily looking for max axial load conditions
    - Low mach numbers hard to predict
      - Traditionally a low aero loading environment
        - » This vehicle may not be traditional?
      - Assume covered within uncertainty factors

4/18/2006 Dave McGhee MSFC/EV31 12

Analysis Results Only – Not for Design – Design Loads Published Post Uncertainty Factor Approval

Figure 7.1-2, LC1a Flight Regime Coverage

Flight Regime Coverage (cont.)

- 1st Stage Ascent flight
  - Characteristics
    - Max Q occurs in this region (300psf > 800 psf > 100psf > 15psf)
    - 0.5 > Mach > 6.0 (0.5 > 1.5-2.0 > 5.0 > 6.0)
    - Trajectory a's mainly low (0° > 0° > 0° > 12°)
    - Ascent wind environments available
    - 6-dof dispersed flight envelopes typically largest
  - Current analysis coverage
    - *Aero*
      - *3-dof aero database: CLV5_5.5mU_Aero_R1.0.doc*
      - *Mach 1.63 drag and normal force vehicle distributions:*
        - » *CLV5m_5mp5US_CAF_dist2_R1.0*
        - » *CLV5m_5mp5US_CNalp_dist2_R1.0*
      - *3-dof aero database for 5.0 meter Upper Stage just received (not evaluated)*
    - 6-dof flight envelopes unavailable
    - Using 3-dof Trajectories with an assumed 7°a dispersion
      - Traditional "robust" estimate for Max Q region (carried over from ESAS)
      - Early 6-dof estimates w/ Vector Wind model indicate 6°a dispersion
        - » Based on biasing trajectory to "mean monthly" winds
    - At Max-Q primarily looking for max bending load conditions
    - Over whole regime, looking for worst axial & bending combinations
    - Quasi-static analysis puts structure at risk from aeroelastics and dynamic loading
      - Assume covered within uncertainty factors
      - Developing STEL, Gust, and buffet analyses

4/18/2006 Dave McGhee MSFC/EV31 13

Analysis Results Only – Not for Design – Design Loads Published Post Uncertainty Factor Approval

Figure 7.1-3, LC1a Flight Regime Coverage

Flight Regime Coverage (cont.)

- Late 1st Stage Ascent flight
  - Characteristics
    - Q in this region (100psf > 15psf)
    - 5.0 > Mach > 6.0 (5.0 > 6.0)
    - Trajectory a's increasing (0° > 12°)
  - Current analysis coverage minimal
    - Assume no aero
    - Primarily looking for max axial load conditions
    - Higher a's, some Q
      - Traditionally a low aero loading environment
        - » This vehicle may not be traditional?
      - Assume covered within uncertainty factors
- 2nd Stage Ascent flight
  - Characteristics
    - Q < 15psf (15psf > 0psf)
    - Mach > 6.0 (6.0 > 7.5 > 20+)
    - Trajectory a's increasing (12° > 25° > 12°)
  - Current analysis coverage
    - Assume no aero
    - Primarily looking for max axial load conditions
    - Need to assess thrust vector maneuver loads
      - Thrust vector profiles in 3-dof, 6-dof?

4/18/2006 Dave McGhee MSFC/EV31 14

Analysis Results Only – Not for Design – Design Loads Published Post Uncertainty Factor Approval

Figure 7.1-4, LC1a Flight Regime Coverage

Additional load cases will be developed as the dynamic and statistical nature of these forcing functions and events are better defined.

These cases and assumptions will change as warranted by the developing design.

7.1.3.2 Gust Transient

Gust transient analyses are under development and out of scope for this load cycle.

7.1.3.3 Buffet

Buffet analyses are under development and out of scope for this load cycle.

7.1.3.4 2nd Stage Ignition and Shutdown Transients

Loads for the upper stage engine ignition and cutoff were performed. The primary purpose of this analysis was to gauge the degree to which the dynamics of the upper stage could be excited by these two events. For this reason, only nominal ignition and cutoff thrust traces were used (see Section 5.9.1.1). Also, no aerodynamic, thrust offset or hydrodynamic effects where considered. The dynamic pressures in this flight regime are less than 50 psf. This was a simple transient analysis, beginning from steady state conditions, and excited by the J-2X thrust traces described in Section 5.9.1.1. Table 7.1-3, Load cases for upper stage transient loads analysis lists the 12 load cases calculated for the upper stage transient loads.

Table 7.1-3, Load cases for upper stage transient loads analysis

LOAD CASE	THRUST	CLV	CEV
SST001	START	5.5m / Eng. Mass	ISS
SST002	SHUTDOWN	5.5m / Eng. Mass	ISS
SST003	START	5.5m / Alloc. Mass	ISS
SST004	SHUTDOWN	5.5m / Alloc. Mass	ISS
SST005	START	5.0m / Alloc. Mass	ISS
SST006	SHUTDOWN	5.0m / Alloc. Mass	ISS
SST007	START	5.5m / Eng. Mass	LUNAR
SST008	SHUTDOWN	5.5m / Eng. Mass	LUNAR
SST009	START	5.5m / Alloc. Mass	LUNAR
SST010	SHUTDOWN	5.5m / Alloc. Mass	LUNAR
SST011	START	5.0m / Alloc. Mass	LUNAR
SST012	SHUTDOWN	5.0m / Alloc. Mass	LUNAR

The models used for the upper stage transient analyses were based on the D55m, D55mR, and the D50m CLV models described in Sections 6.3 and 6.4, and on the CEV models described in Section 6.6. The CLV models were modified by removing the interstage, and all other aft components. Also, CEV models for the shutdown cases did not include the LAS. Propellant loading was adjusted as appropriate to match either the start, or shutdown condition. Thrust forces were applied in the axial direction only, and 293,750 lbf was used as the 100% thrust value for the J-2X (Section 5.9.1.1).

The max-min data from each start load case was tabulated across all start load cases to form a composite max-min table for the J-2X start event. Similarly, searching across all of the shutdown load cases generated a composite max-min table of the shutdown event. Because of the way the loads were applied, only the axial element forces were significant. The results of these tabulations are shown in Section 8.3.

8.0 System Analysis Results

A complete presentation of Load Cycle 1a analysis results was given to the CLV Loads Panel, the CLV Ascent Flight Systems Integration Group, as well as several well respected members of the launch vehicle loads community that are now retired from NASA. This presentation has been placed in References 18 and 19.

8.1 Flight Parameters

The LC1a analysis yielded the ascent flight parameter results shown in Table 8.1-1, Ascent 1st Stage Flight Parameters. The Max Q+ case highlighted with a red box was the primary driver for in-flight vehicle bending moments. This is several seconds after the traditional Max Q driver and is believed to be the result of the Mach 2 aerodynamic load distribution. This led the Vehicle Integration Loads Team to request additional Mach numbers for the follow on aerodynamic distributed load cases. Table 8.1-2, Ascent 2nd Stage Flight Parameters shows the 2nd stage flight parameters which are benign compared to 1st stage flight.

Static aero-elastic (STEL), gust transients and buffet flight assessments are underway but have not yet been completed. Rotational acceleration rates are currently assumed zero as the vehicle is assumed to be trimmed during ascent flight. Dynamic effects must be completed to determine the impact of these accelerations. These assessments were out of scope for LC1a.

Due to the low fidelity of the models and forcing functions, no significant dynamic effects were observed from the second stage ignition transient (see section 7.1.3.4). The second Stage ignition transient studies used a nominal thrust of 293.7K lbs.

Table 8.1-1, Ascent 1st Stage Flight Parameters

	psf		deg.			seconds	lbs.
	Q	Mach	Dispersed Alpha	G's Axial	G's Latera	Time	Thrust
Max Q	793	1.5-1.6	7	1.9-2.0	0.12	57-60	2.75-2.80M
Max Q+	650-760	2.0-2.5	7	2.2-2.7	0.15	66-75	2.95-3.18M
Max Thrust/G	400-450	3.2-3.5	7	3.1-3.3	0.10	85-92	3.1-3.25M
Transonic	650-725	0.9-1.1	7	1.7	0.08	39-45	2.70-2.68M

Table 8.1-2, Ascent 2nd Stage Flight Parameters

	psf		deg.			seconds	lbs.
	Q	Mach	Dispersed Alpha	G's Axial	G's Lateral	Time	Thrust
2nd Stage Ignition+	8	6.3	0	0.7	0	136	274K
LAS Separation	0	NA	0	0.7-0.8	0	166	274K
2nd Stage Burnout	0	NA	0	3.0	0	592	274K

8.2 Section Loads

The loads results reported in this section contain margins within some of the input parameters but do not reflect uncertainty factors applied to the results. **These results reflect the analysis but are not recommended for design. See Section 9.0 for recommended design loads.**

8.2.1 Ascent Results

Section load results from the ascent loads analysis are shown in Figure 8.2-1 through Figure 8.2-4. All loads are presented without the effect of internal compartment or tank pressures. Pressure effects should be added during structural assessments. The line loads were calculated on a time consistent basis and the maximum and minimum results tabulated. There is effectively little difference between the time consistent envelopes and those calculated from the maximum and minimum axial load and bending moment calculations. Flight parameter results are discussed in Section 8.1.

Axial loads were evaluated for 2nd stage flight including quasi-static loads and ignition and shutdown transients. Lateral loads were not assessed due both to the lack of fidelity of lateral disturbance forces at this time as well as the very low dynamic pressures during this flight regime. Figure 8.2-5 shows the resulting loads illustrating that all the 2nd stage flight loads are benign compared to 1st stage flight.

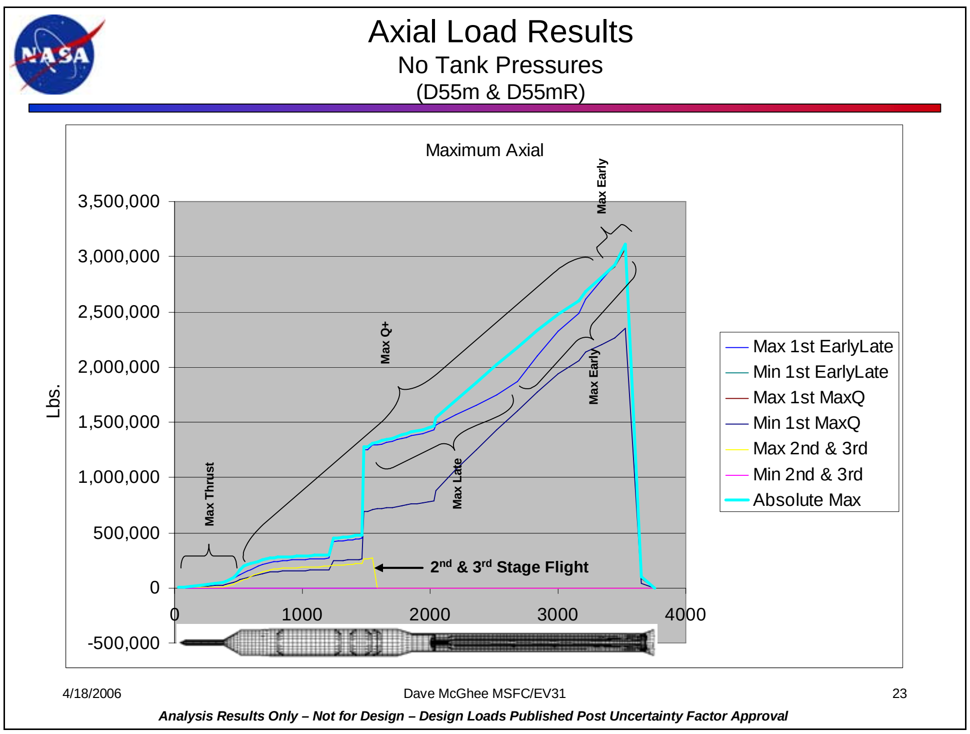

Figure 8.2-1, Ascent Axial Loads

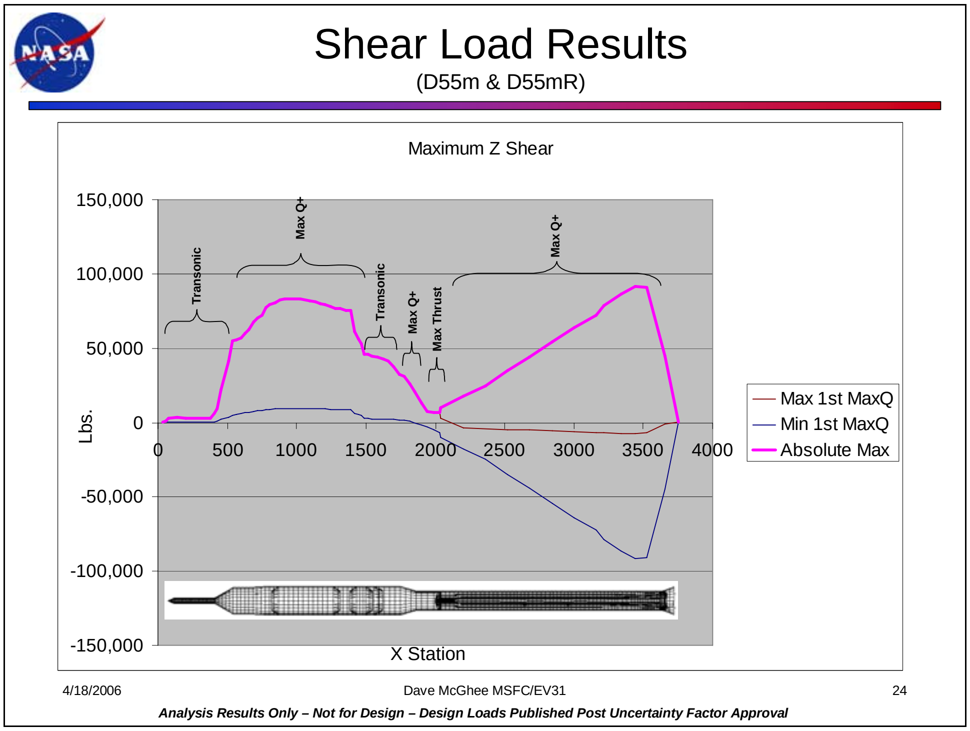

Figure 8.2-2, Ascent Shear Loads

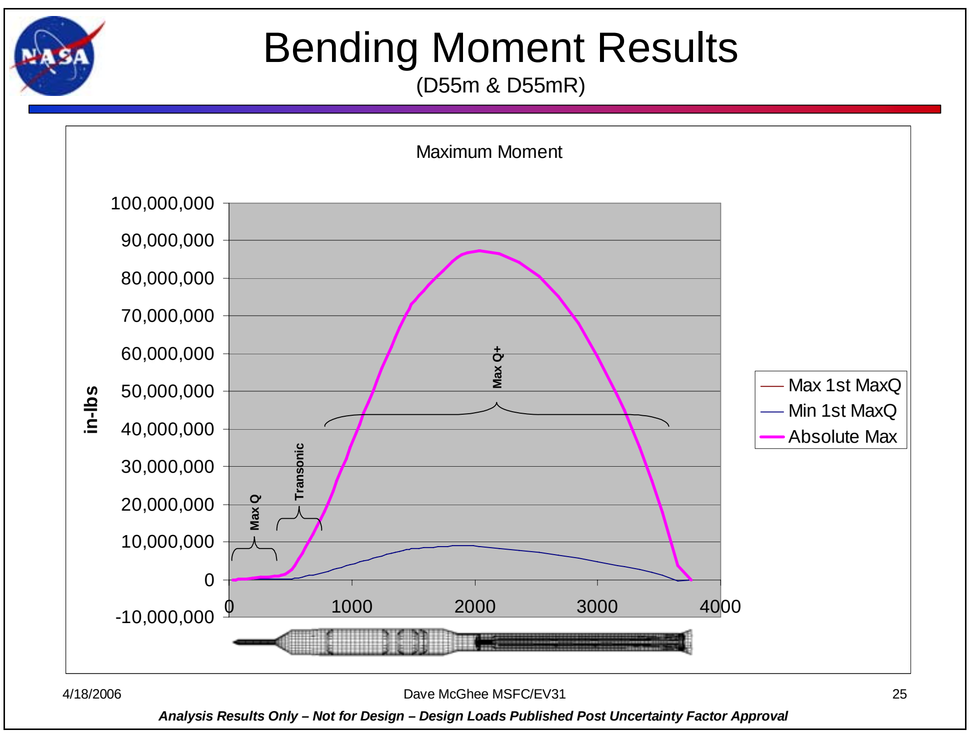

Figure 8.2-3, Ascent Bending Moments

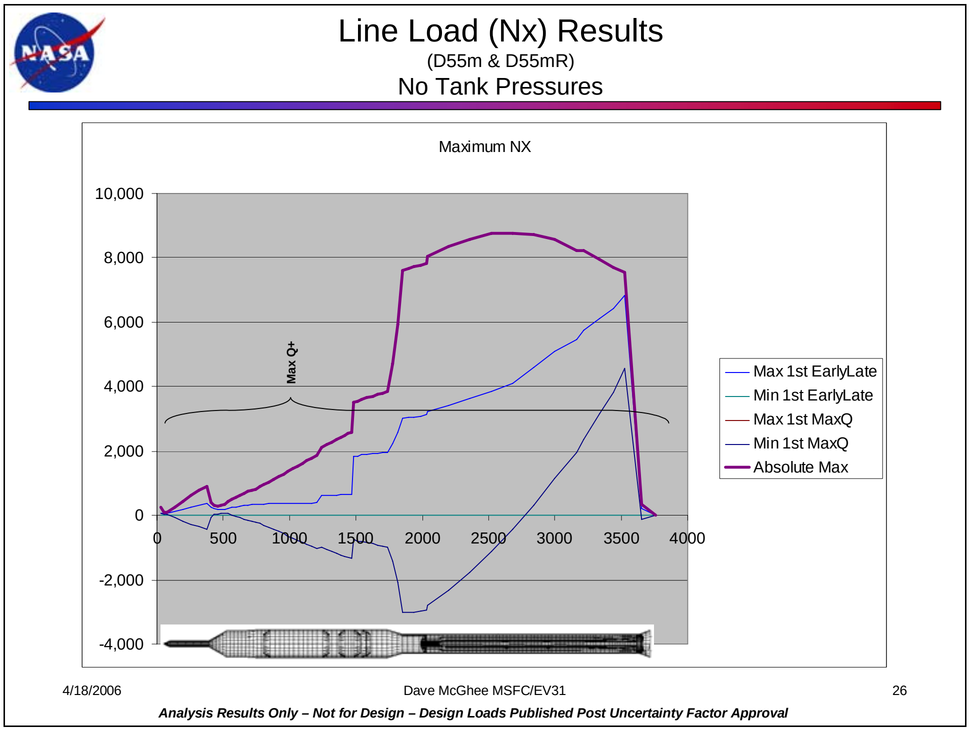

Figure 8.2-4, Ascent Line Loads

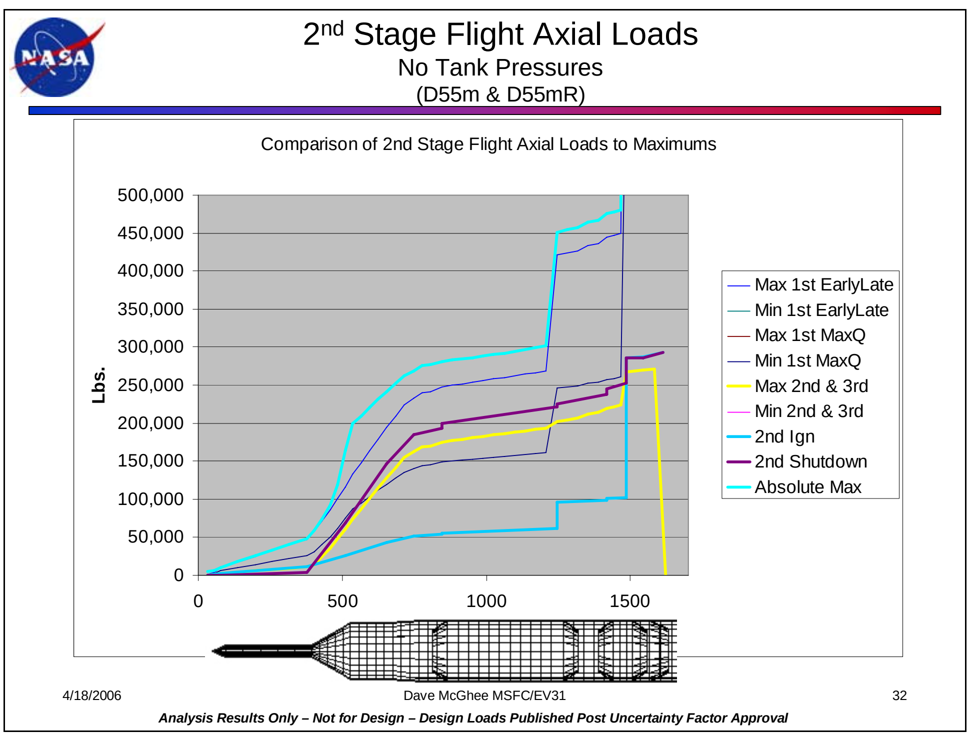

Figure 8.2-5, 2nd Stage Flight Loads

After the recommended design loads data for the original ESAS concept study were release it was realized that an error was made in not correctly combining bending moments in the pitch and yaw planes. Therefore a 40% bending moment increase was expected. During this analysis cycle this large increase did not appear. The best explanation available for this is the CEV diameter reduction from 5.5 meters to 5.0 meters and its effect on aerodynamic loads. Figure 8.2-6 illustrates this effect by looking at a comparison of the cumulative aerodynamic normal force coefficients. It can be seen that the ESAS aerodynamic coefficients peaked substantially higher and farther forward on the vehicle than the current LC1a coefficients. This will generally increase the total aerodynamic load as well as increase the vehicle bending moments.

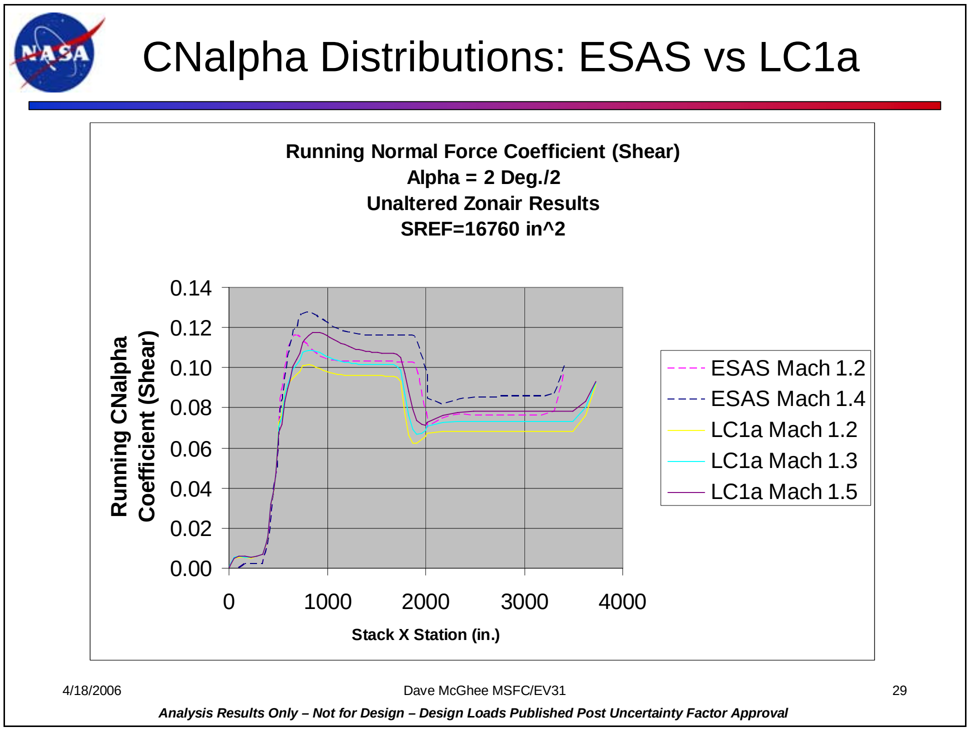

Figure 8.2-6, Comparison of Aerodynamic Loads for ESAS and LC1a

In summary, the Max Q+ loading condition during 1st stage flight is the primary vehicle loads driver. No noticeable difference in loads was noticed for the allocated weights (D55m) vehicle versus the engineering weights (D55mR) vehicle.

8.2.2 Pre-launch Results

Figure 8.2-7 shows the resultant vehicle bending moments of the LC1a pre-launch wind analysis. Figure 8.2-8 shows the resultant hold down post loads and Table 8.2-1, Launch Abort System Tip deflections shows the resulting tip deflections of the most forward point on the Launch Abort System.

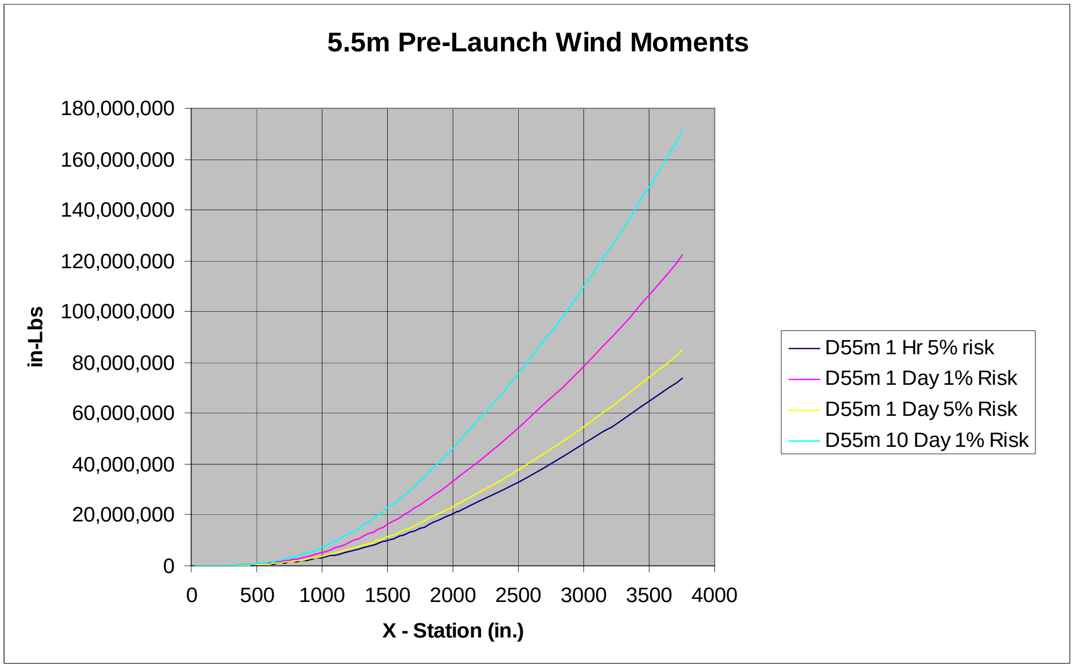

Figure 8.2-7, Vehicle Pre-launch Bending Moments

Holddown Post Load Indicator		
Load	Indicator(KIPS)	55m
Maximum F(X)	1591.49	1340.3
Minimum F(X)	-706.67	-402.7
+ Post Compression		- Post Tension

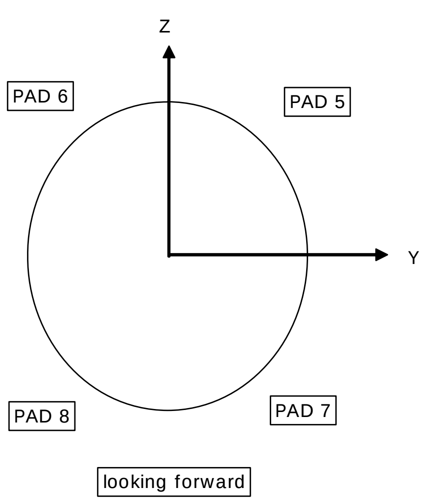

D55m			
		Max*	Min*
PAD 5	X	390,462	-1,340,286
	Y	56,657	-239,806
	Z	180,965	-502,736
PAD 6	X	402,674	-1,327,021
	Y	235,962	-59,021
	Z	187,484	-501,223
PAD 7	X	344,225	-1,267,260
	Y	48,957	-245,319
	Z	475,036	-164,016
PAD 8	X	331,390	-1,281,148
	Y	247,923	-45,353
	Z	484,690	-160,199

* Load as Applied to Vehicle

Figure 8.2-8, Pre-launch Hold-down Post Results

Table 8.2-1, Launch Abort System Tip deflections

Wind	Max Tip Deflection (inches)			
		X	Y	Z
Gravity Only	D55m_Dry	1	2	1
	D55m_GLOW	1	2	1
1Hr 5% Risk	D55m_Dry	2	27	19
	D55m_GLOW	2	27	19
1Day 1%Risk	D55m_Dry	2	43	31
	D55m_GLOW	2	43	31
1Day 5%Risk	D55m_Dry	2	31	22
	D55m_GLOW	2	31	22
10 Day 1% Risk	D55m_Dry	2	60	43
	D55m_GLOW	2	60	43

It can be seen that the hold down forces are nearing the Shuttle documented capabilities for the 10 day wind loading. Additionally, the vehicle tip deflections are growing quite large.

8.2.3 Liftoff Results

The absolute maximum section loads and accelerations at each vehicle station from the LC1a liftoff transient analyses as described in Section 7.1.2 are seen in Figure 8.2-9 thru Figure 8.2-16. These section loads are considered “raw” analysis results however they do contain a dynamic uncertainty factor (DUF) of 1.5. The DUF is applied only to the dynamic portion of the modal responses. Other uncertainty factors are added to the loads in Section 9.0. The legend labels for Figure 8.2-9 thru Figure 8.2-16 are described in Table 8.2-2, Description of legend for Figures 8.2.3-1 through 8.2.3-8.

Table 8.2-2, Description of legend for Figures 8.2.3-1 through 8.2.3-8

55RLUN	5.5 METER VEHICLE, REVISED MASS, LUNAR CEV
55RLUN DISP	5.5 METER VEHICLE, REVISED MASS, LUNAR CEV, DISPERSED THRUST
55RISS	5.5 METER VEHICLE, ALLOCATED MASS, ISS CEV
55LUN	5.5 METER VEHICLE, ALLOCATED MASS, LUNAR CEV
55ISS	5.5 METER VEHICLE, ALLOCATED MASS, ISS CEV

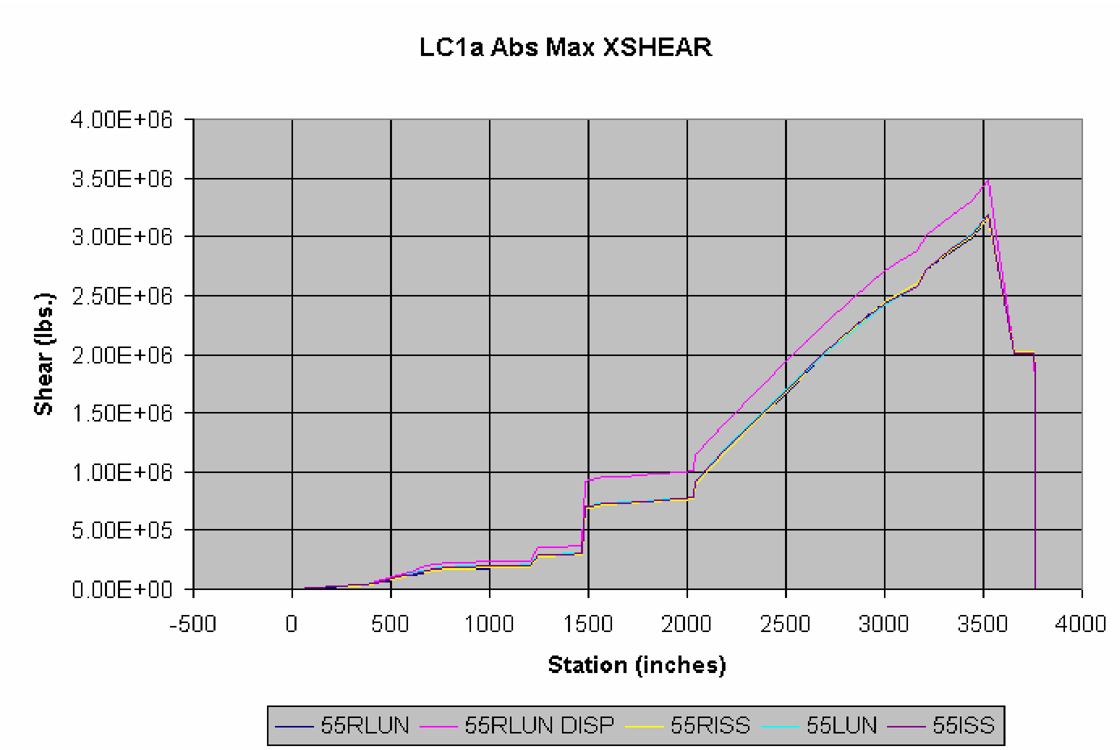

Figure 8.2-9, Liftoff Axial Load

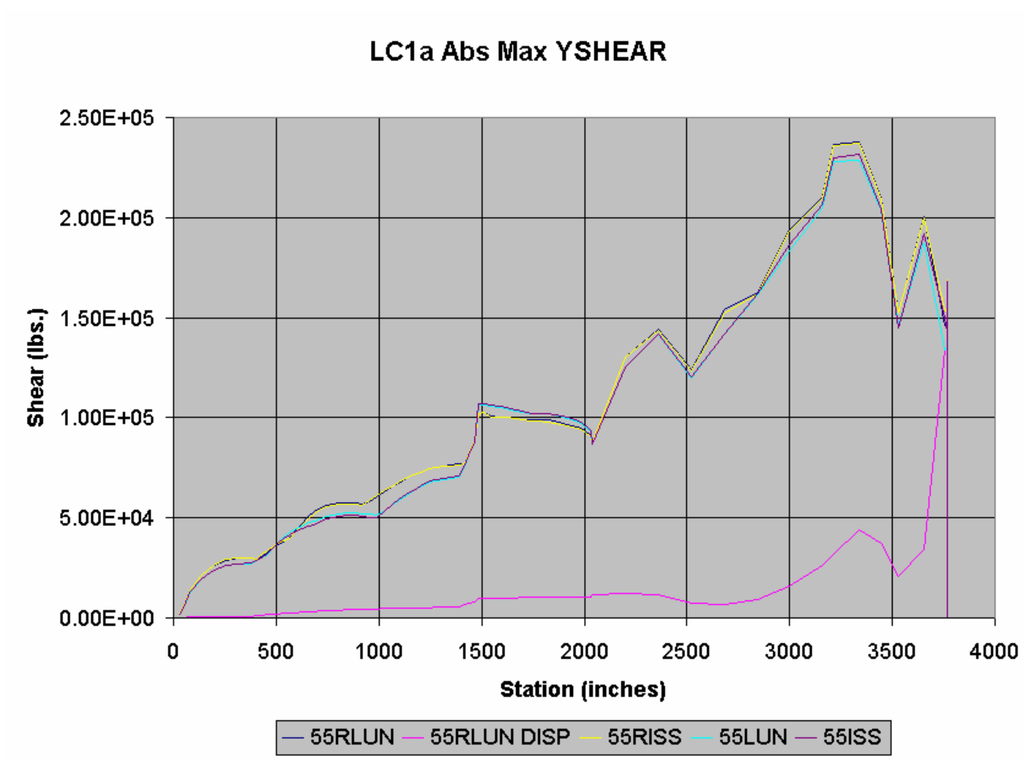

Figure 8.2-10, Liftoff Y-Shear

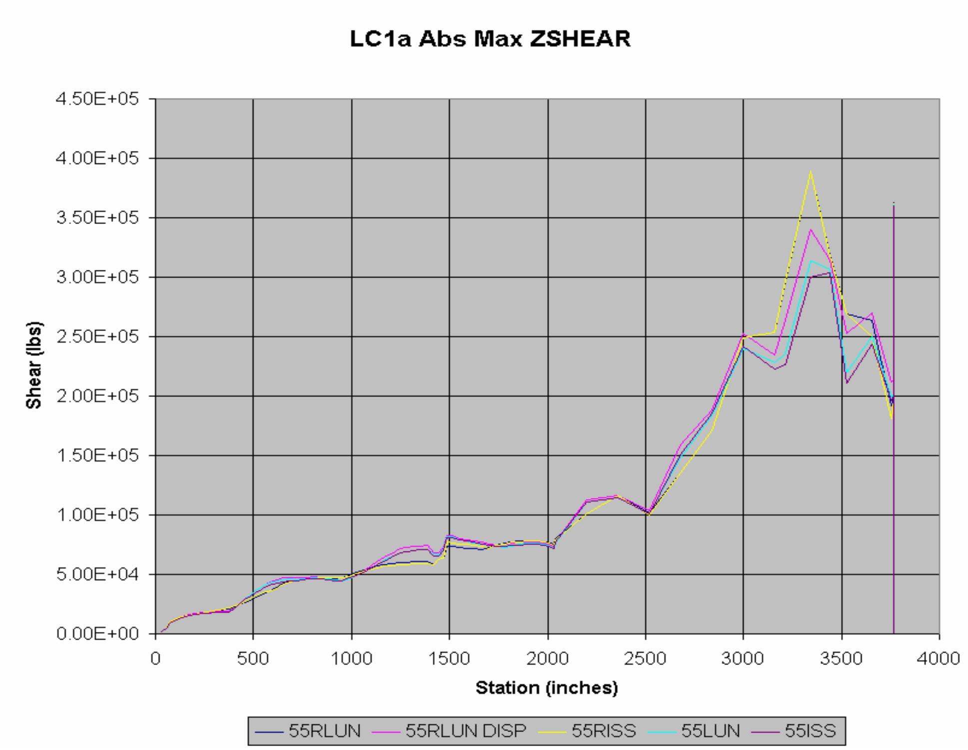

Figure 8.2-11, Liftoff Z-Shear

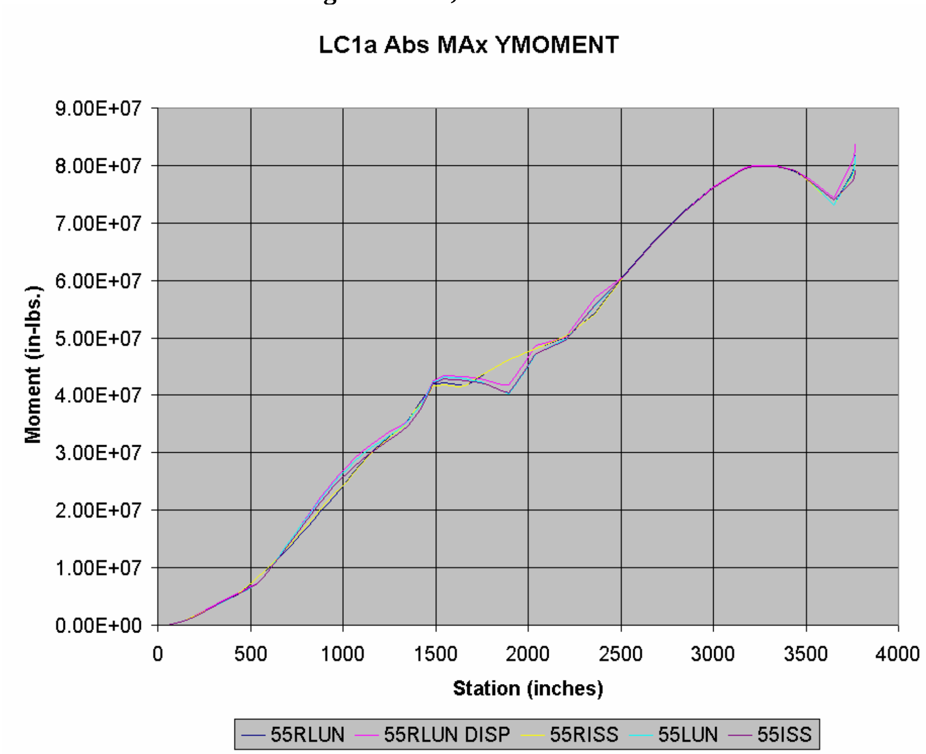

Figure 8.2-12, Liftoff Y-Moment

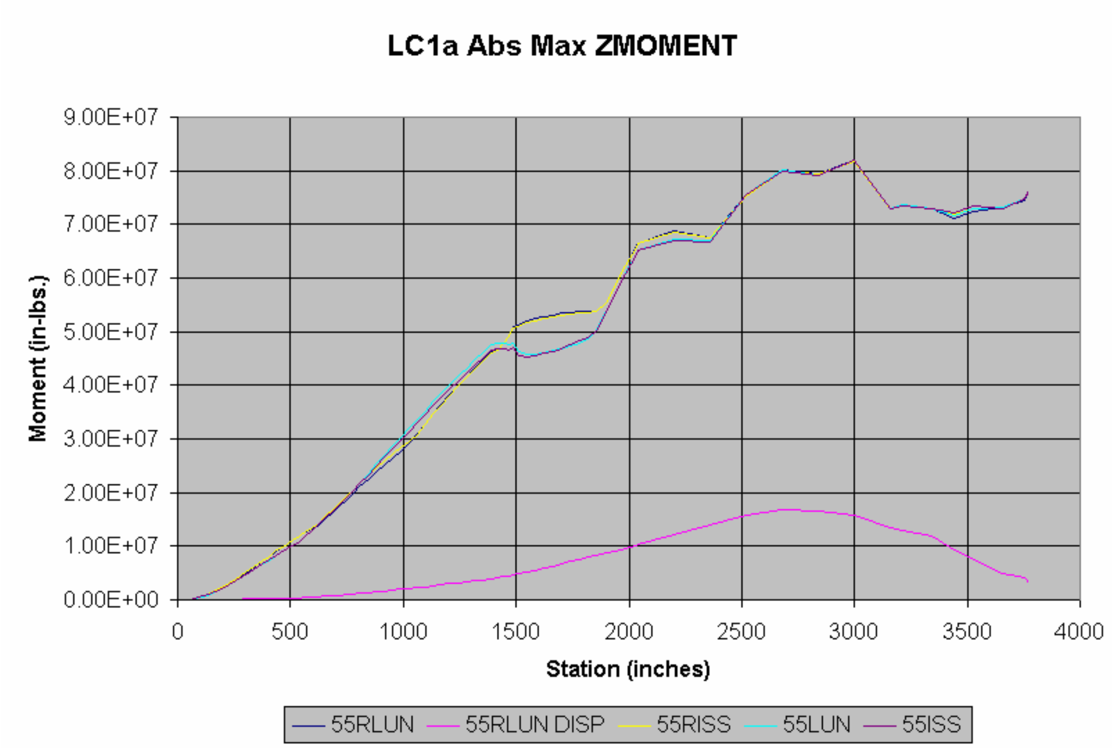

Figure 8.2-13, Liftoff Z-Moment

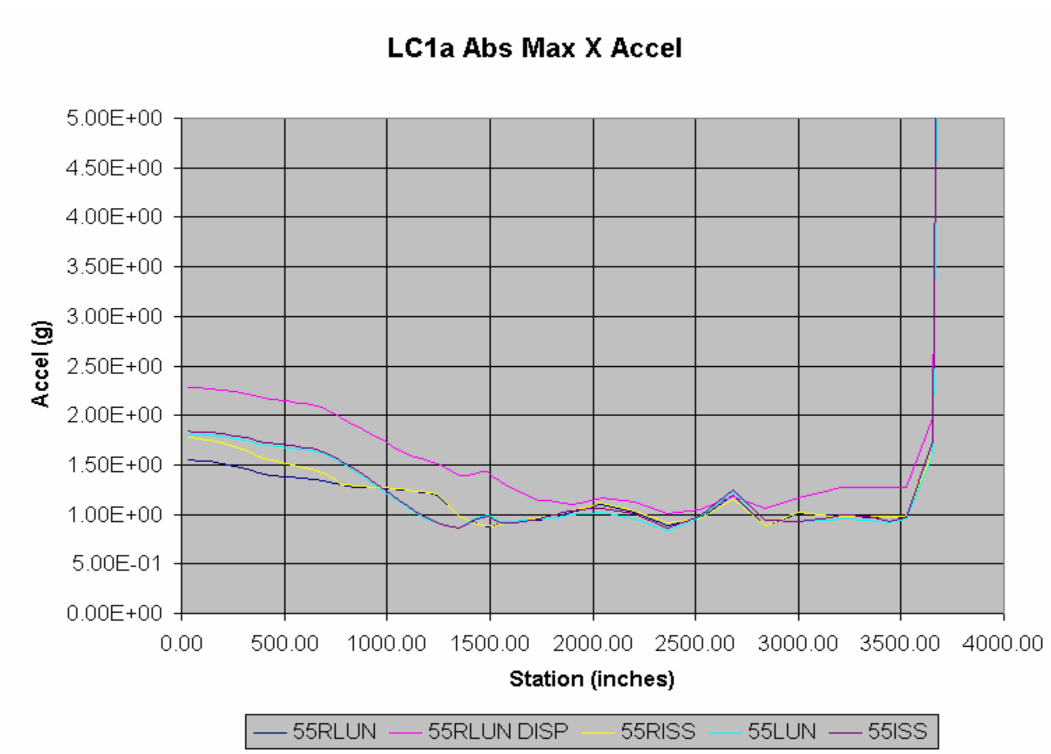

Figure 8.2-14, Liftoff X-Accelerations

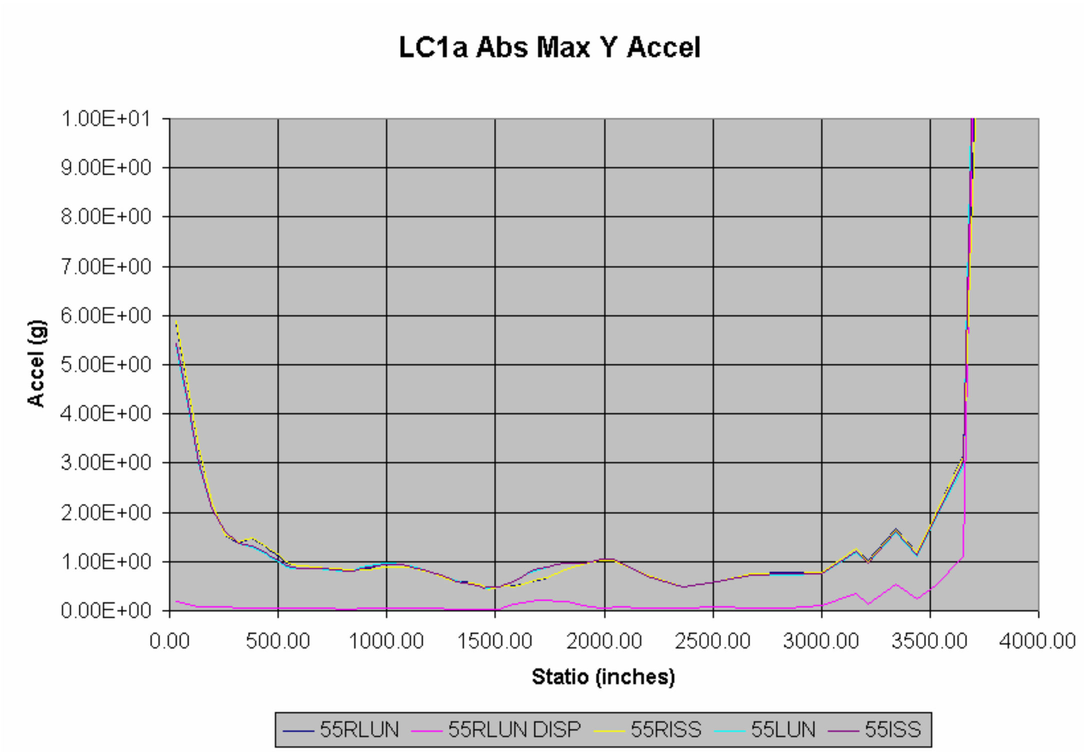

Figure 8.2-15, Liftoff Y-Accelerations

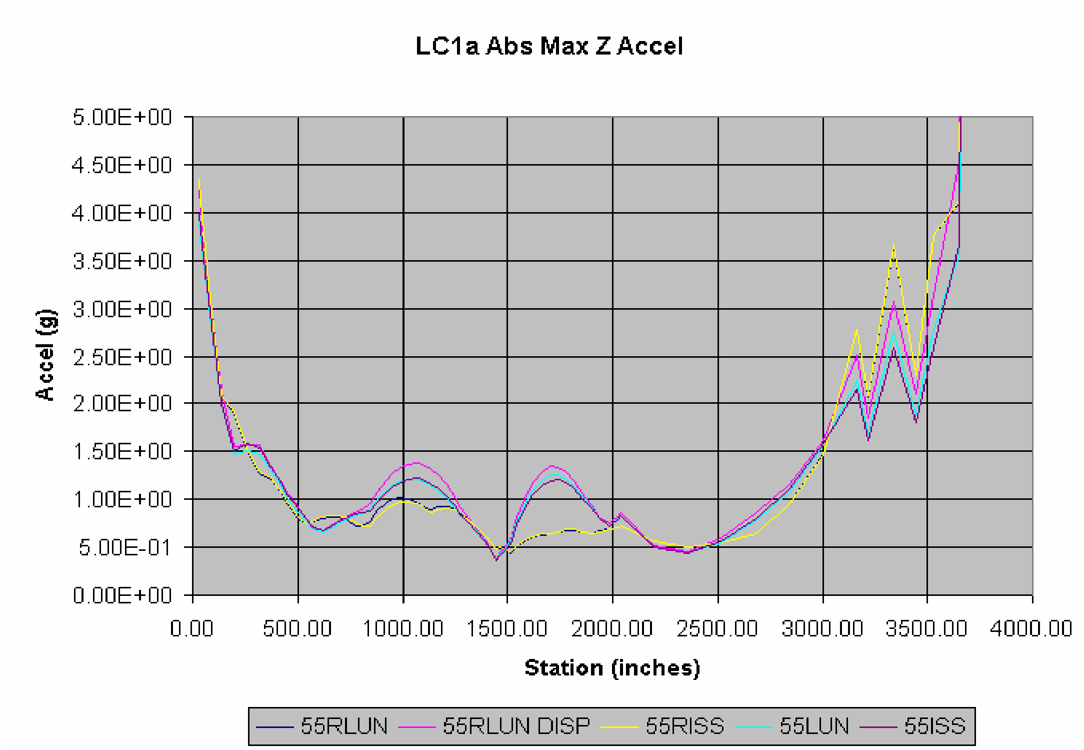

Figure 8.2-16, Liftoff Z-Accelerations

8.2.4 Overall Results

Section load results from the Loads Cycle 1a analysis are shown in Figure 8.2-17 through Figure 8.2-20.

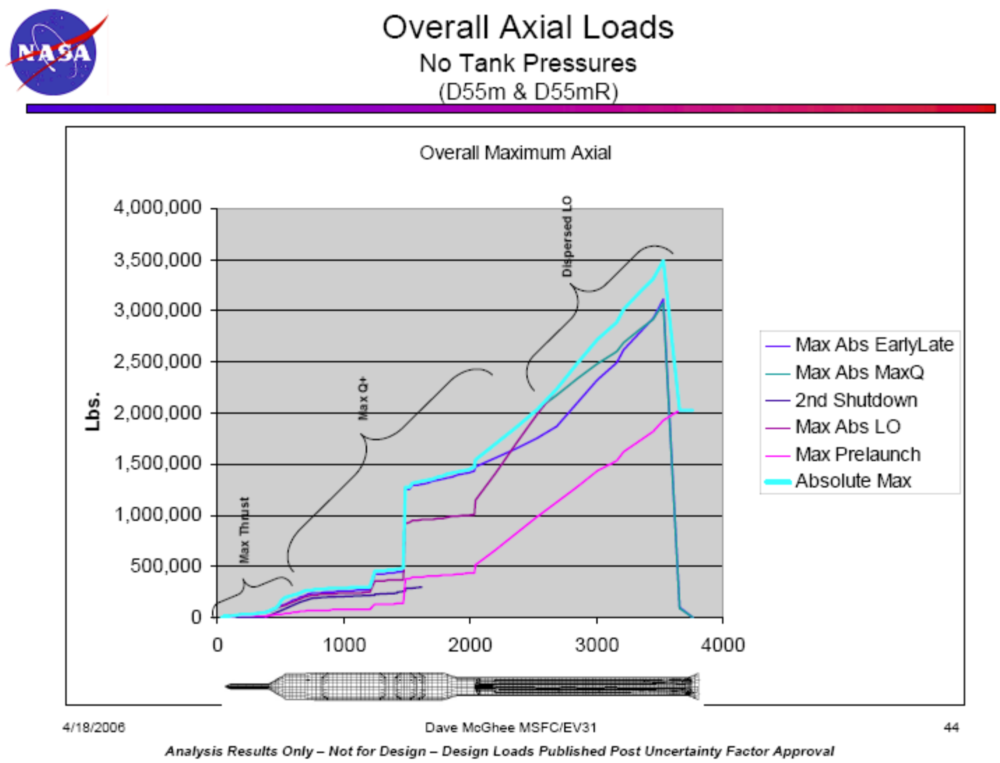

Figure 8.2-17, Load Cycle 1a Resulting Axial Loads

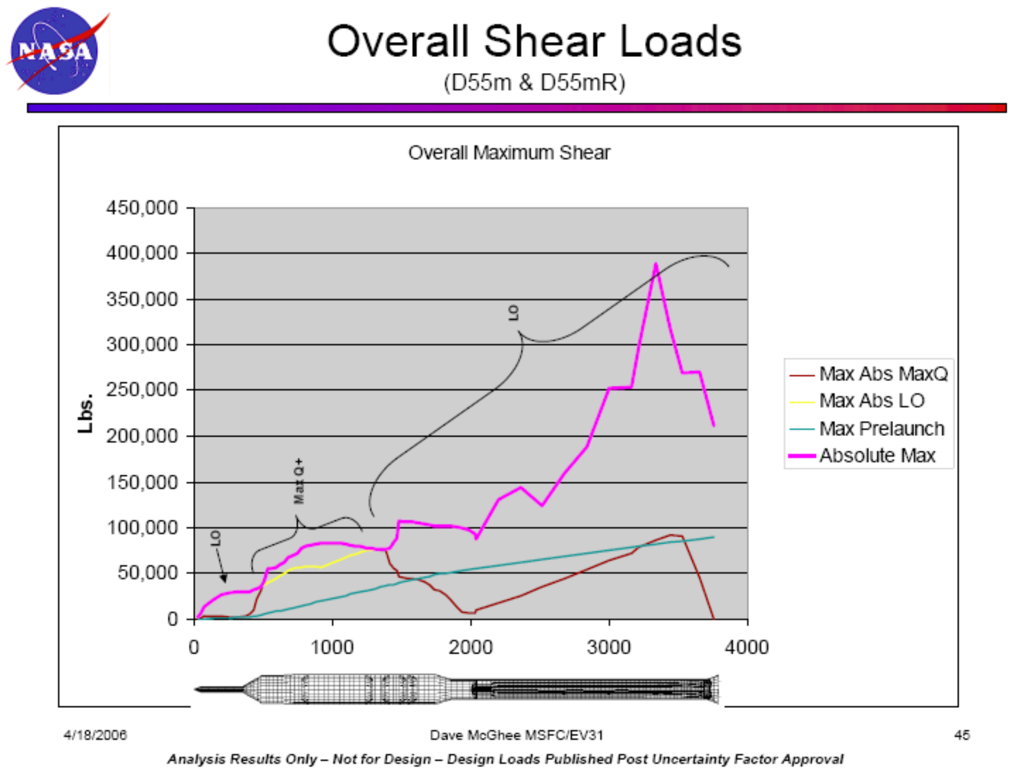

Figure 8.2-18, Load Cycle 1a Resulting Shear Loads

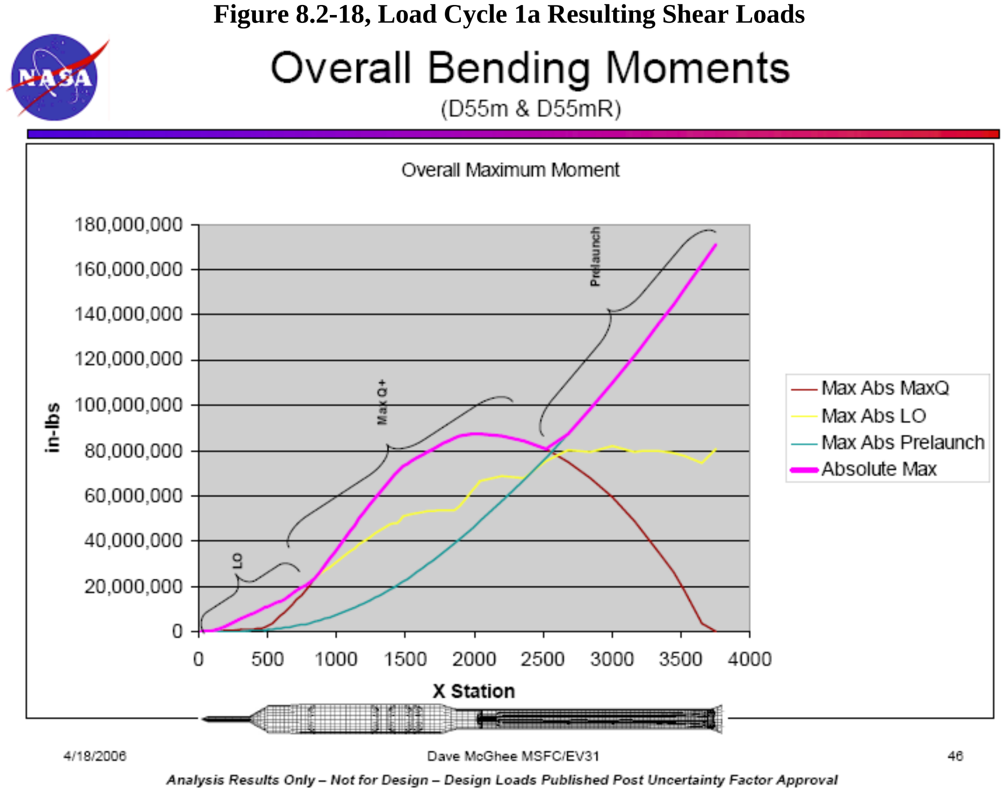

Figure 8.2-19, Load Cycle 1a Resulting Bending Moments

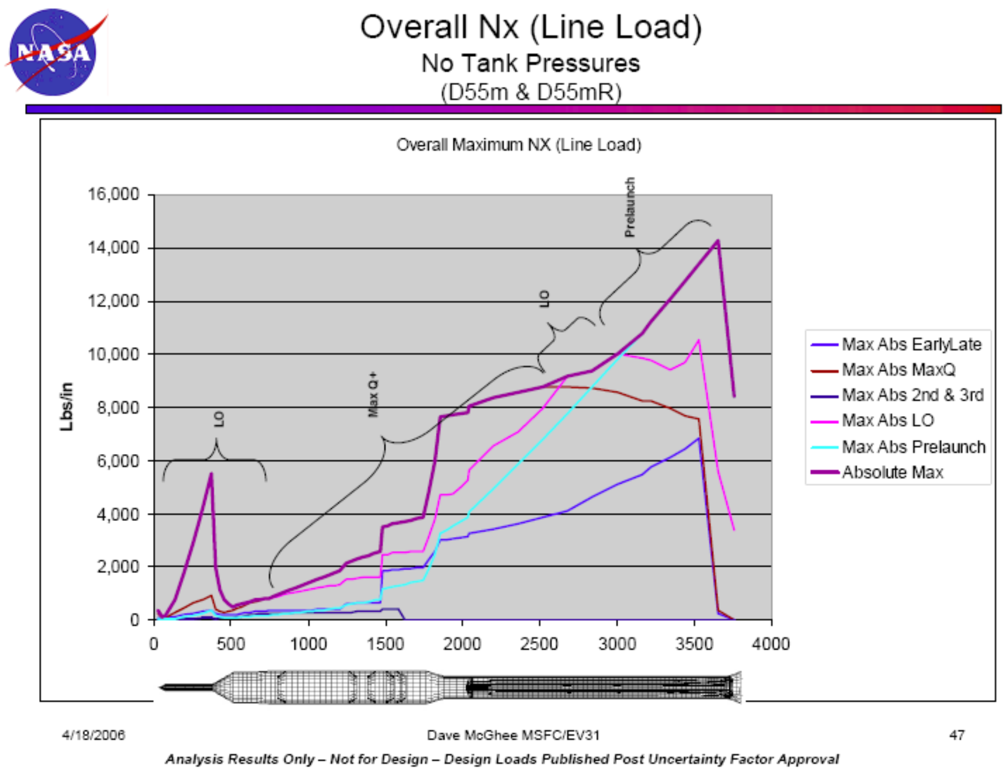

Figure 8.2-20, Load Cycle 1a Resulting Line Loads

8.3 Second Stage Ignition and Cutoff Results

The axial loads resulting from the second stage ignition and cutoff analysis are plotted in Figure 8.3-1. This is raw analysis data, and does not include any uncertainty factors. It was found that the upper stage did not respond dynamically to any significant degree to either the start or shutdown transients. For this reason, and because the max G produced by the J-2X did not exceed the max G from the first stage flight phase, these loads do not influence the vehicle design.

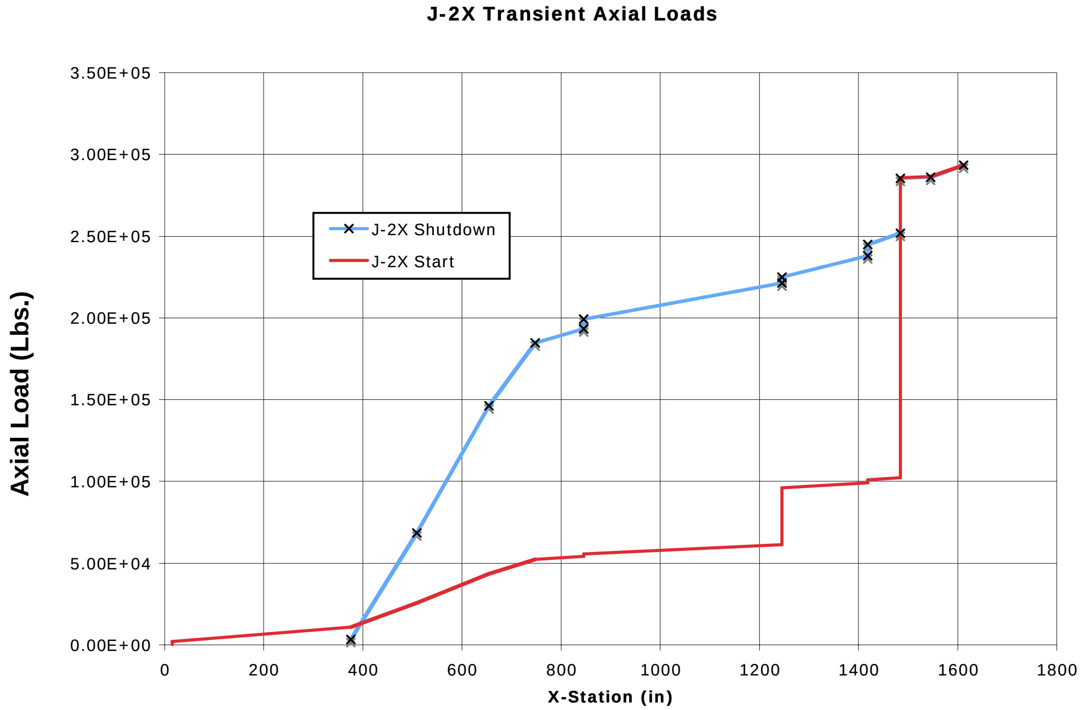

Figure 8.3-1, J-2X Transient Axial Loads

8.4 Mode and Frequency Data

8.4.1 Structural Flex-Modes

Current estimates of the CLV structural flex modes were provided for assessment with the flight control system. A Guyan reduction was performed on the structural models described in Section 6.0 to reduce them to a series of centerline points. Mass normalized modes were then calculated below 25 Hz for several configurations. The mass properties, modal frequencies, mode shape deflection data, and station coordinates of the centerline points were then provided. This data is included in the Vehicle Integration Loads Team database located on the ICE Windchill server, Reference 1.

8.4.1.1 D55m Flex-Mode Summary

Table 8.4-1, CLV D55m Configuration Flex-Mode Weights shows the vehicle weights for various configurations. Table 8.4-2, CLV D55m Flex-mode Frequencies < 25Hz shows the calculated frequencies. Table 8.4-3 shows the centerline stations at which mode shape deflections are reported. For reference the FSB gimbal is located at station 3690.910.

Table 8.4-1, CLV D55m Configuration Flex-Mode Weights

DAC-0 5.5m Intros Weights of Stack Configurations

Condition	Mass (lbs-sec/in)	Weight (lbs)	X CG (in)	Y CG (in)	Z CG (in)
Free-Free Empty	4,487	1,732,448	2,725.8	-250.5	0.0
On Pad Empty	4,487	1,732,448	2,725.8	-250.5	0.0

On Pad GLOW	5,225	2,017,383	2,536.9	-250.5	0.0
Free-Free GLOW	5,225	2,017,383	2,536.9	-250.5	0.0
1st Stage Burn Out	1,509	582,477	1,772.8	-250.6	0.1
2nd Stage Ignition	1,000	386,097	1,223.2	-250.5	0.0
2nd Stage Burn Out	228	87,934	842.8	-250.5	0.0

Table 8.4-2, CLV D55m Flex-mode Frequencies < 25Hz

DAC-0 5.5m Intros Weight Frequencies < 25 Hz

Free-Free Frequencies of Stack Models						On-Pad Frequencies	
Mode No.	**FF-empty Fn (Hz)**	**ff-glow Fn (Hz)**	**ff-2ndbo Fn (Hz)**	**ff-2ndign Fn (Hz)**	**ff-1stbo Fn (Hz)**	**Empty Fn (Hz)**	**GLOW Fn (Hz)**
1	0.00	0.00	0.00	0.00	0.00	0.23	0.18
2	0.00	0.00	0.00	0.00	0.00	0.29	0.22
3	0.00	0.00	0.00	0.00	0.00	0.84	0.82
4	0.00	0.00	0.00	0.00	0.00	0.92	0.91
5	0.00	0.00	0.00	0.00	0.00	2.54	1.99
6	0.00	0.00	0.00	0.00	0.00	2.80	2.12
7	0.98	0.96	15.02	4.96	1.34	3.89	3.56
8	0.98	0.96	15.02	4.96	1.34	4.73	3.68
9	3.15	2.26		9.31	4.02	4.83	3.93
10	3.15	2.26		9.31	4.02	5.95	5.41
11	4.97	4.32		15.91	5.53	6.25	5.45
12	4.97	4.32		18.49	5.53	7.73	6.57
13	6.97	5.54		18.49	9.69	8.27	7.03
14	6.97	5.54			9.70	9.14	7.79
15	9.21	8.23			12.42	9.40	8.72
16	9.21	8.24			12.42	9.84	9.39
17	10.71	8.24			12.64	10.10	9.64
18	11.04	10.73			15.30	10.90	10.58
19	11.04	10.73			17.72	11.22	10.94
20	11.99	11.21			20.68	11.54	11.15
21	12.00	11.21			20.70	12.93	11.29
22	13.47	11.99			23.99	13.43	11.52
23	13.47	12.00			24.01	13.47	12.68
24	15.30	13.54				13.83	13.48
25	15.94	13.54				18.06	13.53
26	18.06	15.30				18.06	13.84
27	18.06	15.49				18.73	17.19
28	22.85	18.16				21.14	18.74
29	22.87	21.21				23.78	21.14
30		21.21				24.48	21.22
31		22.85				25.00	21.22

32		22.87					24.33
33		24.49					24.47
34		24.49					24.68
35							24.80

Table 8.4-3, CLV D55m & 55mR Centerline Stations

		X	Y	Z
GRID	4001	31.000	-250.500	0.000
GRID	4002	53.865	-250.500	0.000
GRID	4003	76.730	-250.500	0.000
GRID	4004	136.730	-250.500	0.000
GRID	4005	196.730	-250.500	0.000
GRID	4006	256.730	-250.500	0.000
GRID	4007	316.730	-250.500	0.000
GRID	4008	376.080	-250.500	0.000
GRID	4009	403.080	-250.500	0.000
GRID	4010	430.080	-250.500	0.000
GRID	4011	457.080	-250.500	0.000
GRID	4012	484.080	-250.500	0.000
GRID	4013	508.950	-250.500	0.000
GRID	4014	537.950	-250.500	0.000
GRID	4015	566.950	-250.500	0.000
GRID	4016	595.950	-250.500	0.000
GRID	4017	624.950	-250.500	0.000
GRID	4018	654.340	-250.500	0.000
GRID	4019	685.340	-250.500	0.000
GRID	4020	716.340	-250.500	0.000
GRID	4021	747.340	-250.500	0.000
GRID	6002	777.340	-250.500	0.000
GRID	6003	807.340	-250.500	0.000
GRID	6004	845.340	-250.500	0.000
GRID	6005	881.340	-250.500	0.000
GRID	6006	917.340	-250.500	0.000
GRID	6007	953.340	-250.500	0.000
GRID	6008	989.340	-250.500	0.000
GRID	6009	1025.340	-250.500	0.000
GRID	6010	1061.340	-250.500	0.000
GRID	6011	1097.340	-250.500	0.000
GRID	6012	1133.340	-250.500	0.000
GRID	6013	1169.340	-250.500	0.000
GRID	6014	1205.340	-250.500	0.000
GRID	6015	1245.340	-250.500	0.000
GRID	6016	1281.340	-250.500	0.000
GRID	6017	1317.340	-250.500	0.000
GRID	6018	1353.340	-250.500	0.000
GRID	6019	1389.340	-250.500	0.000
GRID	6020	1418.420	-250.500	0.000

GRID	6021	1442.420	-250.500	0.000
GRID	6022	1466.420	-250.500	0.000
GRID	6023	1484.420	-250.500	0.000
GRID	6024	1514.420	-250.500	0.000
GRID	6025	1545.420	-250.500	0.000
GRID	6026	1584.420	-250.500	0.000
GRID	6027	1623.420	-250.500	0.000
GRID	6028	1662.420	-250.500	0.000
GRID	6029	1701.420	-250.500	0.000
GRID	6030	1741.420	-250.500	0.000
GRID	6031	1779.420	-250.500	0.000
GRID	6032	1817.420	-250.500	0.000
GRID	6033	1855.420	-250.500	0.000
GRID	6034	1897.420	-250.500	0.000
GRID	6035	1939.420	-250.500	0.000
GRID	6036	1986.420	-250.500	0.000
GRID	6037	2032.970	-250.500	0.000
GRID	706	2041.120	-250.500	0.000
GRID	707	2200.620	-250.500	0.000
GRID	708	2360.620	-250.500	0.000
GRID	709	2520.620	-250.500	0.000
GRID	710	2680.620	-250.500	0.000
GRID	711	2840.620	-250.500	0.000
GRID	712	3000.620	-250.500	0.000
GRID	713	3160.620	-250.500	0.000
GRID	714	3214.600	-250.500	0.000
GRID	715	3340.140	-250.500	0.000
GRID	716	3442.640	-250.500	0.000
GRID	717	3526.680	-250.500	0.000
GRID	718	3652.990	-250.500	0.000
GRID	720	3755.360	-250.500	0.000

8.4.1.2 D55mR Flex-Mode Summary

Table 8.4-4, CLV D55mR Configuration Weights shows the vehicle weights for various configurations. Table 8.4-5, CLV D55mR Flex-mode Frequencies < 25Hz shows the calculated frequencies. The centerline stations at which mode shape deflections are reported are the same as in Table 8.4-3. For reference the FSB gimbal is located at station 3690.910.

Table 8.4-4, CLV D55mR Configuration Weights

DAC-0 5.5m Resized Weights of Stack Configurations

Condition	Mass (lbs-sec^2/in)	Weight (lbs)	X CG (in)	Y CG (in)	Z CG (in)
Free-Free Empty	4,517	1,744,017	2,717.9	-250.5	0.0
On Pad Empty	4,517	1,744,017	2,717.9	-250.5	0.0
On Pad GLOW	5,255	2,028,952	2,531.1	-250.5	0.0

Free-Free GLOW	5,255	2,028,952	2,531.1	-250.5	0.0
1st Stage Burn Out	1,539	594,046	1,767.9	-250.6	0.1
2nd Stage Ignition	1,010	389,769	1,224.6	-250.5	0.0
2nd Stage Burn Out	237	91,606	863.8	-250.5	0.0

Table 8.4-5, CLV D55mR Flex-mode Frequencies < 25Hz

DAC-0 5.5m Resized Weight Frequencies < 25 Hz

Free-Free Frequencies of Stack Models						On-Pad Frequencies	
Mode No.	**FF-empty Fn (Hz)**	**ff-glow Fn (Hz)**	**ff-2ndbo Fn (Hz)**	**ff-2ndign Fn (Hz)**	**ff-1stbo Fn (Hz)**	**Empty Fn (Hz)**	**GLOW Fn (Hz)**
1	0.00	0.00	0.00	0.00	0.00	0.23	0.18
2	0.00	0.00	0.00	0.00	0.00	0.29	0.22
3	0.00	0.00	0.00	0.00	0.00	0.88	0.86
4	0.00	0.00	0.00	0.00	0.00	0.97	0.95
5	0.00	0.00	0.00	0.00	0.00	2.60	2.13
6	0.00	0.00	0.00	0.00	0.00	2.86	2.27
7	1.04	1.02	14.84	4.94	1.48	3.88	3.57
8	1.04	1.02	14.84	4.94	1.48	4.69	3.77
9	3.20	2.42		9.58	4.12	4.79	4.00
10	3.20	2.42		9.58	4.12	5.98	5.48
11	4.95	4.39		16.71	5.66	6.29	5.54
12	4.95	4.39		19.53	5.67	7.74	6.65
13	7.00	5.66		19.53	9.90	8.28	7.11
14	7.00	5.66			9.91	8.86	8.24
15	9.23	8.31			13.05	9.18	8.84
16	9.23	8.32			13.05	9.98	8.91
17	11.04	9.17			13.98	10.20	9.69
18	11.05	10.83			15.55	10.93	10.67
19	11.40	10.84			19.06	11.22	11.09
20	11.99	11.47			20.91	11.56	11.42
21	12.00	11.47			20.93	13.47	11.48
22	13.53	11.99			24.48	13.53	11.56
23	13.53	12.00			24.50	13.62	13.30
24	15.55	13.81				13.88	13.70
25	16.24	13.81				17.94	13.81
26	17.94	15.55				17.94	13.93
27	17.94	15.91				18.73	18.20
28	22.85	19.44				22.48	18.76
29	22.87	21.41				23.71	21.41
30		21.41				24.51	21.42
31		22.86					22.48
32		22.88					24.47

33		24.84					24.82
34		24.84					24.92

8.5 POGO

The current set of structural flex-modes described in Section 8.4 is the best available structural data for use in a POGO stability analysis.

8.6 Slosh

8.6.1 Introduction

Sloshing is defined as the oscillations of the free surface of a liquid in a partially filled tank or container. These oscillations are the result of motions of the vehicle. Sloshing of propellants is a potential source of disturbance that may affect the stability and structural integrity of space vehicles.

The dynamic response of a vehicle to liquid sloshing can be calculated if an equivalent mechanical system is used to represent the liquid dynamics. Such dynamical systems are composed of fixed masses and oscillating masses connected to the tank by springs or pendulums, and dashpots. Mechanical models have been derived for several common tank geometries Reference 20. The models are designed so that they have the same resultant pressure force, moment, damping, and frequency as the actual systems.

The mechanical model of a tank is shown in Figure 8.6-1, where m_1 is the oscillating (slosh) mass, m_0 is the fixed mass, k is the spring stiffness, c is the dashpot damping, h_1 is the distance from the liquid free surface to the slosh mass, and h_0 is the distance from the liquid free surface to the fixed mass.

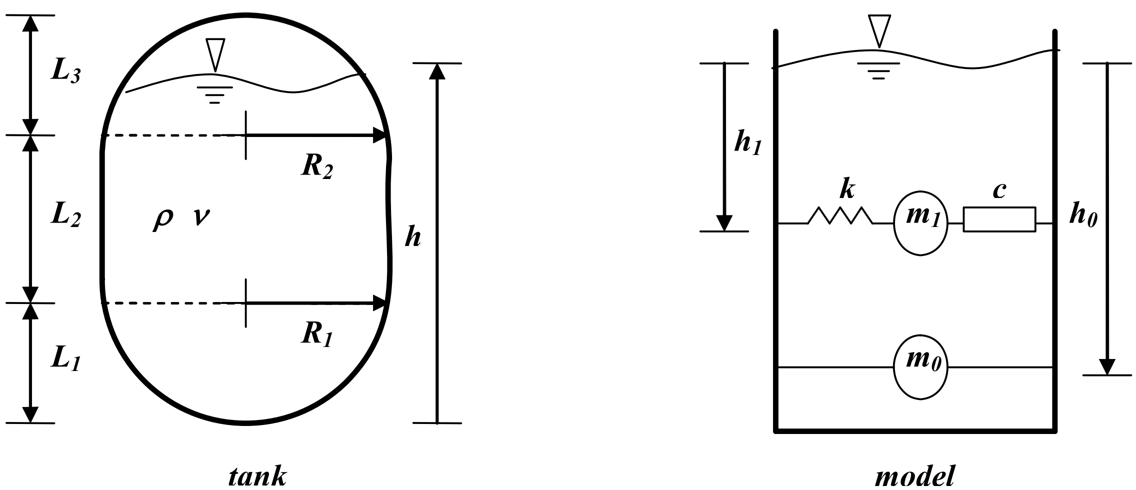

Figure 8.6-1, Tank with sloshing propellant, and equivalent spring-mass mechanical model of the system

8.6.2 Slosh analysis and the HYDRO program series

The HYDRO program series, written in FORTRAN, was developed to be used for both, hydroelastic and slosh analyses. Details about the formulation and analysis used in the HYDRO program series can be found in References 21 and 22.

From the program series, computer codes TANK, HYDRO, and SLOSH were used to perform the slosh analyses and to obtain the parameters of the mechanical models of the liquid oxygen (LOX) and the liquid hydrogen (LH2) tanks of the Crew Launch Vehicle (CLV).

The tank physical parameters used as input to the HYDRO program series to generate the slosh analysis are summarized in Table 8.6-1, Tank characteristics for both configurations (radius R = 108.25 in., and radius R = 99.0 in.), used as input to HYDRO and to calculate the damping ratio, and can be referenced to Figure 8.6-1, where L_1 is the length of the lower dome, L_2 is the length of the frustum, L_3 is the length of the upper dome, R_1 is the radius of the lower end of the frustum, R_2 is the radius of the upper end of the frustum, and ρ is the density of the liquid. In both tables it is also listed the value of the kinematic viscosity ν, required to calculate the smooth-wall damping using formulas from the references. The variable h in Figure 8.6-1 is the fluid level above the bottom of the lower dome. Total length of the tank may be defined as $L = L_1 + L_2 + L_3$.

Table 8.6-1, Tank characteristics for both configurations (radius R = 108.25 in., and radius R = 99.0 in.), used as input to HYDRO and to calculate the damping ratio

tank	L_1 (in.)	L_2 (in)	L_3 (in.)	R_1=R_2 (in.)	ρ (lb·s^2/in.^{4})	ν (in.^{2}/s)
LOX	76.54	66.0	76.54	108.25	$1.068*10^{-4}$	$2.393*10^{-4}$
LH2	76.54	400.0	76.54	108.25	$6.625*10^{-6}$	$4.140*10^{-4}$
LOX	70.0	111.0	70.0	99.0	$1.068*10^{-4}$	$2.393*10^{-4}$
LH2	70.0	513.0	70.0	99.0	$6.625*10^{-6}$	$4.140*10^{-4}$

8.6.3 Calculation of smooth-wall damping

The computer code HYDRO does not generate a value for the parameter of smooth-wall damping for the mechanical model, so it is necessary to calculate this parameter from equations.

The magnitude of liquid damping in smooth-wall tanks has been determined for several configurations, Reference 20. In tanks of various geometries without baffles, this parameter may be described by a semi-empirical equation of the form
(see E.14):

$$\zeta = C\, \nu^{0.5}\, R^{-0.75}\, g^{-0.25}$$

where ζ is the damping ratio, R is the tank radius, g is the longitudinal acceleration (for these cases, the acceleration of gravity = 386.088 in./s^2), and C is a numerical coefficient that takes on different values depending upon tank geometry and fluid level h. For a cylindrical tank with a spherical bottom (center of sphere inside the tank):

$C = (4.98/2\pi)*C_1$

where C_1 : ≈ 1, for $h/R \geq 1$
$\approx R/h$, for $0 < h/R < 1$

The values of the damping ratio for fluid heights in the areas of the domes were extrapolated from E.15. A scaling parameter was used to apply to that test data (see D.12):

$\zeta = \zeta_{test} \, (R_{test} / R)^{0.75}$

8.6.4 Slosh analysis results

The numerical results obtained from the HYDRO program series and the smooth-wall damping coefficient formulas are summarized in Table 8.6-2 and Table 8.6-3 for the liquid oxygen (LOX) and liquid hydrogen (LH2) tanks with R = 108.25 in., respectively.

For the LOX tank, the variation of the slosh, fixed and total (slosh plus fixed) masses with respect to fluid level is shown in Figure 8.6-2, and the variation of the frequency with respect to fluid level is shown in Figure 8.6-3.

For the LH2 tank, the variation of the masses with respect to fluid level is shown in Figure 8.6-4, and the variation of the frequency with respect to fluid level is shown in Figure 8.6-5.

Table 8.6-2, CLV5 LOX tank (R = 108.25 in.) slosh analysis results

fluid level h (in.)	frequency f (Hz)	slosh mass m_1 (lb·s²/in.)	fixed mass m_0 (lb·s²/in.)	stiffness k (lb/in.)	h_1 (in.)	h_0 (in.)	damping ratio ζ
0	-	0	0	-	-	-	0.0020
19.14	0.272	16.8	0.839	49.0	12.5	-113.5	0.0015
38.27	0.292	56.7	6.81	190.5	25.6	-88.8	0.0006
57.40	0.315	103.6	23.0	407.1	38.8	-60.9	0.0004
76.54	0.346	141.6	54.0	669.5	51.8	-32.8	0.0003
83.14	0.359	152.3	70.2	775.2	56.5	-23.6	0.0001
89.74	0.370	161.5	87.9	872.3	60.9	-15.2	0.0001
96.34	0.379	170.0	106.4	966.0	65.0	-7.58	0.0001
102.94	0.385	175.3	128.0	1028.1	69.4	-0.0398	0.0001
109.54	0.392	181.1	149.1	1097.1	73.1	6.74	0.0001
116.14	0.396	184.8	172.5	1141.4	77.0	13.4	0.0001
122.74	0.400	188.8	195.4	1190.9	80.3	19.6	0.0001
129.34	0.402	191.1	220.0	1220.4	83.6	25.6	0.0001
135.94	0.405	193.8	244.2	1255.3	86.5	31.3	0.0001
142.54	0.407	195.2	269.7	1273.8	89.3	36.9	0.0003
161.68	0.427	189.1	351.5	1362.5	97.2	53.1	0.0003
180.81	0.475	147.4	459.5	1312.2	107.0	70.2	0.0002
193.27	0.533	102.4	536.5	1146.6	113.6	82.3	0.0005
199.94	0.582	73.8	577.4	987.1	117.0	89.1	0.0010
219.08	-	0	660.7	-	-	109.5	0.0020

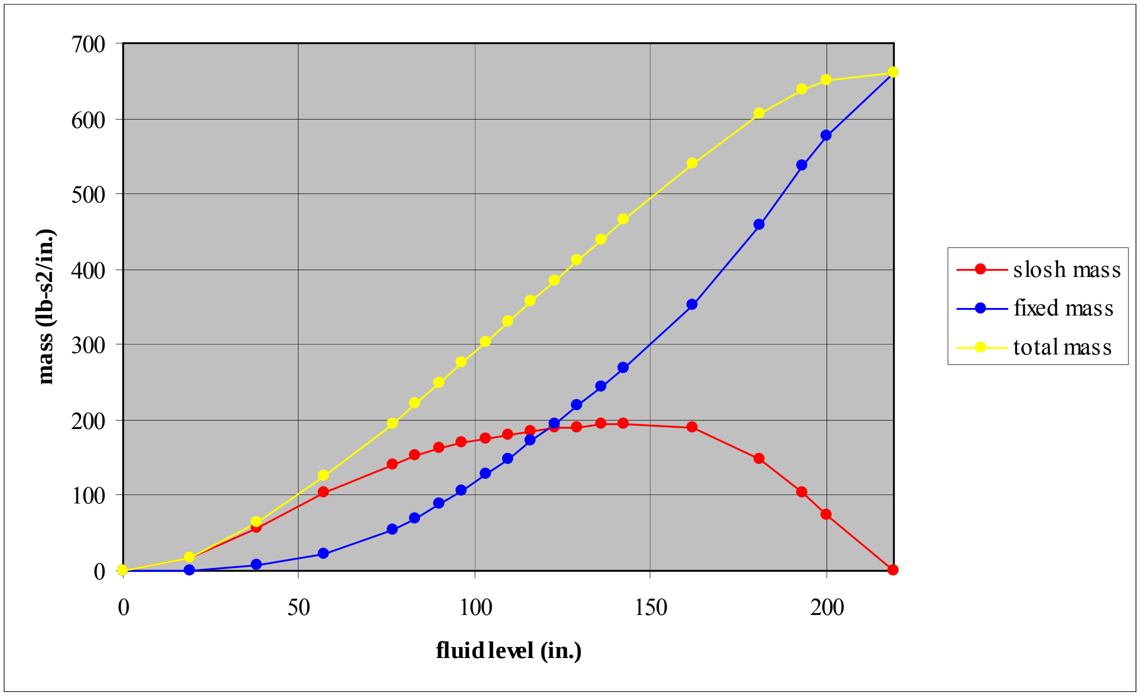

Figure 8.6-2, CLV5 LOX (R = 108.25 in.) variation of mass with respect to liquid height

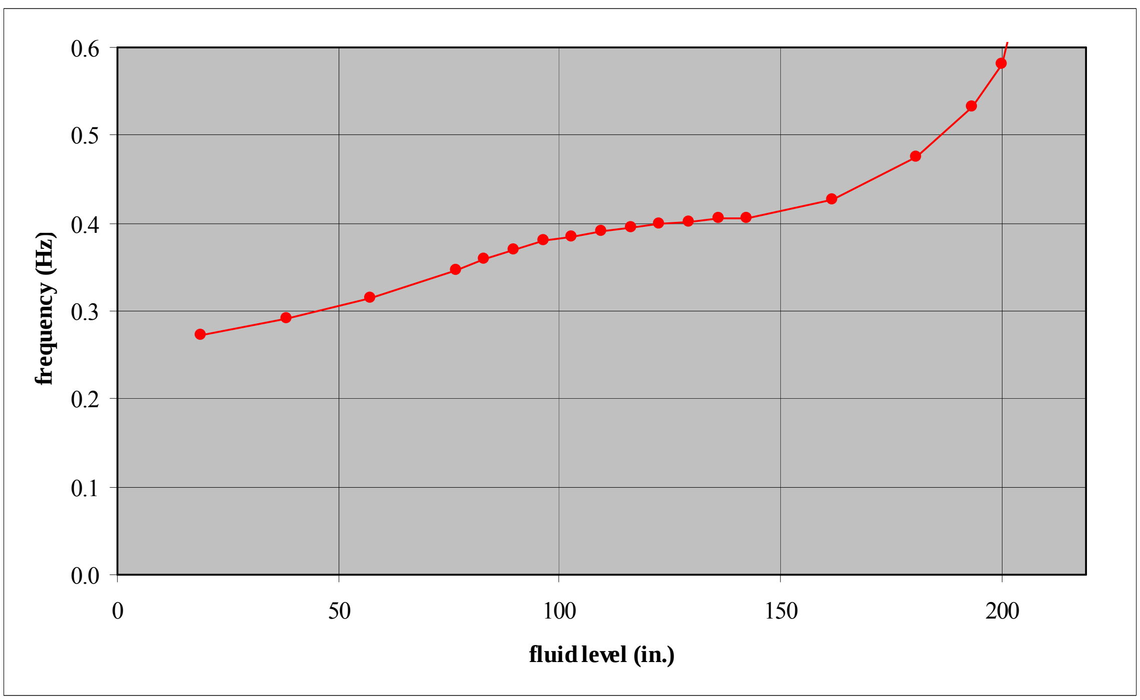

Figure 8.6-3, CLV5 LOX (R = 108.25 in.) variation of frequency with respect to liquid height

Table 8.6-3, CLV5 LH2 tank (R = 108.25 in.) slosh analysis results

fluid level h (in.)	frequency f (Hz)	slosh mass m_1 (lb·s^2/in.)	fixed mass m_0 (lb·s^2/in.)	stiffness k (lb/in.)	h_1 (in.)	h_0 (in.)	damping ratio ζ
0	-	0	0	-	-	-	0.0020
19.14	0.272	1.03	0.0514	3.00	12.5	-113.5	0.0015
38.27	0.292	3.47	0.417	11.7	25.6	-88.8	0.0006
57.40	0.315	6.34	1.41	24.9	38.8	-60.9	0.0004
76.54	0.346	8.67	3.30	41.0	51.8	-32.8	0.0003
116.54	0.396	11.3	10.6	70.1	77.2	13.8	0.0001
156.54	0.409	12.1	19.8	80.3	94.4	48.2	0.0001
196.54	0.413	12.3	29.6	83.2	104.5	77.3	0.0001
236.54	0.414	12.4	39.5	84.0	110.1	103.5	0.0001
276.54	0.414	12.4	49.5	84.2	113.1	127.9	0.0001
316.54	0.414	12.4	59.5	84.2	114.6	151.1	0.0001
356.54	0.414	12.4	69.5	84.2	115.4	173.5	0.0001
396.54	0.414	12.4	78.5	84.2	115.8	195.4	0.0001
436.54	0.414	12.4	88.4	84.2	116.0	216.9	0.0001
476.54	0.415	12.4	98.3	84.3	116.1	238.1	0.0003
495.68	0.431	11.8	103.6	86.3	117.9	247.4	0.0003
514.81	0.478	9.13	110.2	82.2	123.4	255.2	0.0002
521.74	0.506	7.70	113.2	77.8	125.8	258.1	0.0003
533.94	0.587	4.62	117.4	62.9	129.8	263.7	0.0010
553.08	-	0	122.4	-	-	276.5	0.0020

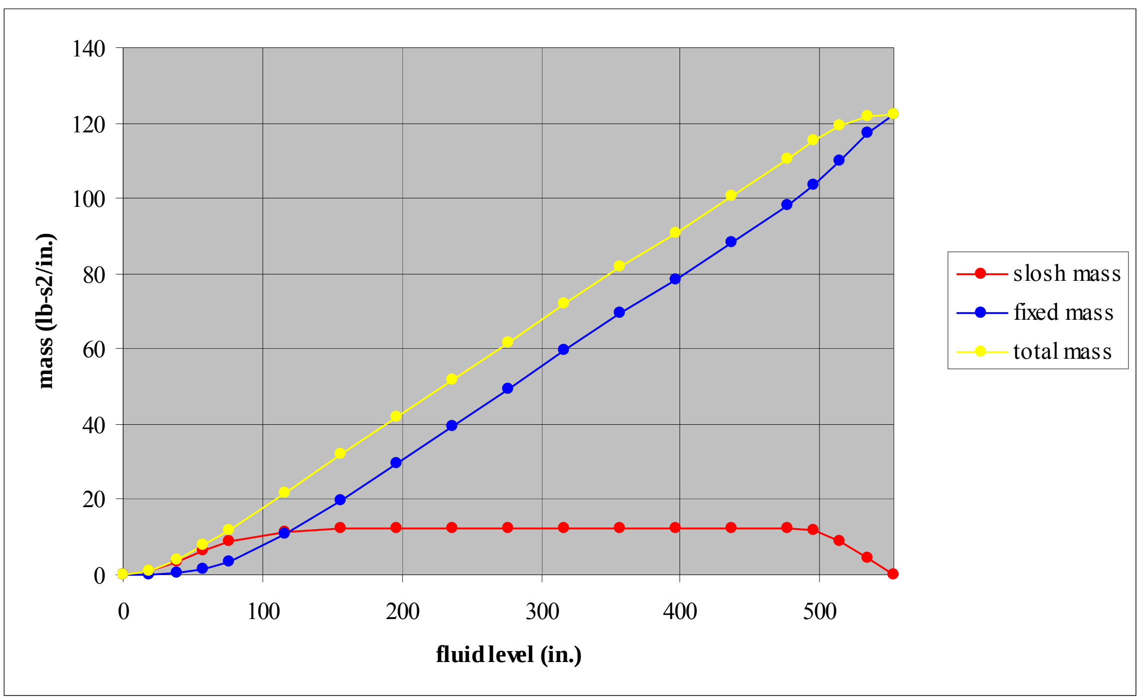

Figure 8.6-4, CLV5 LH2 (R = 108.25 in.) variation of mass with respect to liquid height

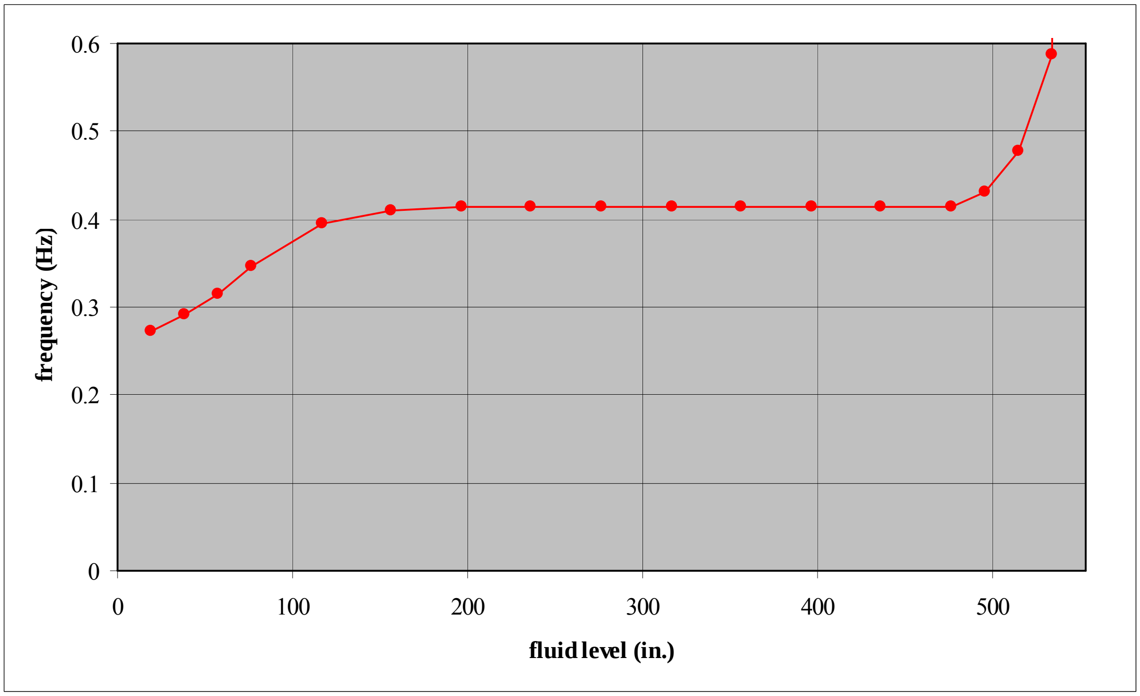

Figure 8.6-5, CLV5 LH2 (R = 108.25 in.) variation of frequency with respect to liquid height

The corresponding results for the tanks with R = 99.0 in. are shown in Table 8.6-4, CLV5 LOX tank (R = 99.0 in.) slosh analysis resultsand Table 8.6-5, CLV5 LH2 tank (R = 99.0 in.) slosh analysis results, and in Figure 8.6-6 to Figure 8.6-9.

Table 8.6-4, CLV5 LOX tank (R = 99.0 in.) slosh analysis results

fluid level h (in.)	frequency f (Hz)	slosh mass m_1 (lb·s²/in.)	fixed mass m_0 (lb·s²/in.)	stiffness k (lb/in.)	h_1 (in.)	h_0 (in.)	damping ratio ζ
0	-	0	0	-	-	-	0.0020
17.5	0.284	12.7	0.635	40.6	11.4	-103.8	0.0016
35.0	0.305	43.0	5.16	157.7	23.5	-81.2	0.0006
52.5	0.330	78.5	17.4	337.2	35.5	-55.7	0.0004
70.0	0.362	107.3	40.9	554.5	47.4	-30.0	0.0003
81.1	0.385	121.3	64.4	709.8	55.1	-15.1	0.0001
92.2	0.401	131.3	91.9	832.0	62.3	-2.12	0.0001
103.3	0.411	138.3	122.4	923.7	68.8	9.41	0.0001
114.4	0.418	143.2	155.0	990.0	74.6	19.9	0.0001
125.5	0.424	147.2	188.6	1044.8	79.6	29.6	0.0001
136.6	0.427	149.4	223.9	1075.8	84.0	38.8	0.0001
147.7	0.429	150.8	260.0	1096.8	87.7	47.5	0.0001
158.8	0.431	151.8	296.5	1110.9	90.0	55.9	0.0001
169.9	0.431	152.5	333.4	1120.3	93.6	63.8	0.0001
181.0	0.432	152.9	370.5	1126.5	95.8	71.6	0.0003
198.5	0.451	145.7	434.9	1167.6	99.9	83.4	0.0003
216.0	0.499	112.5	518.4	1103.8	106.8	95.4	0.0002
233.5	0.609	56.1	608.4	821.7	113.9	109.1	0.0011

251.0	-	0	671.9	-	112.3	125.5	0.0020

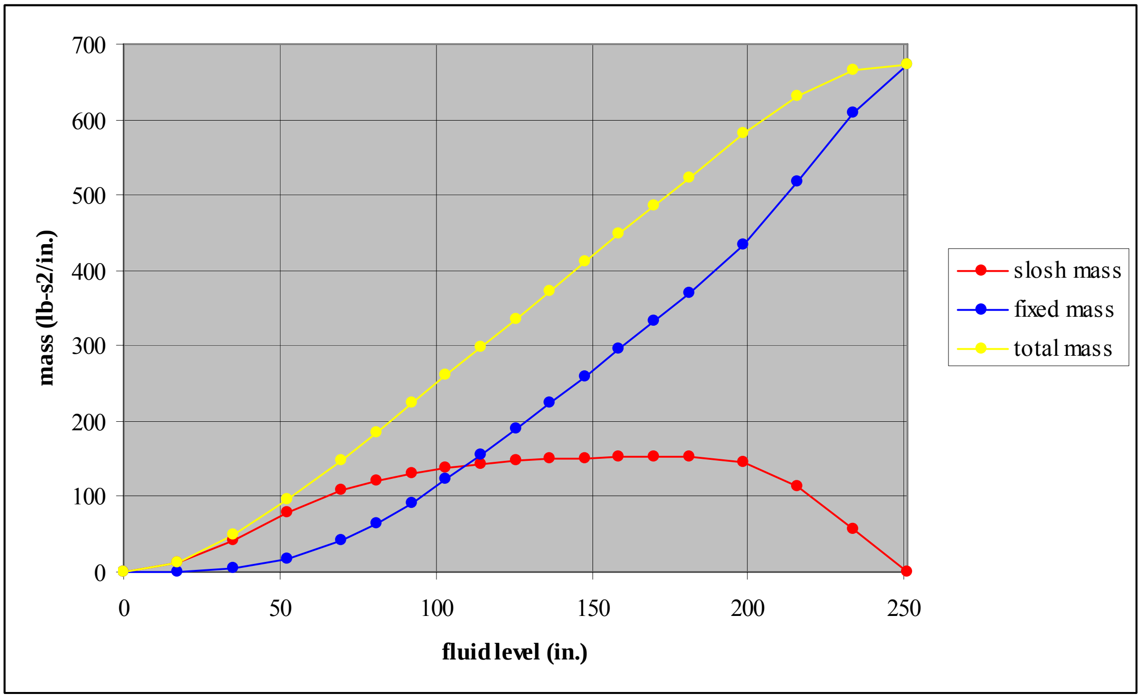

Figure 8.6-6, CLV5 LOX (R = 99.0 in.) variation of mass with respect to liquid height

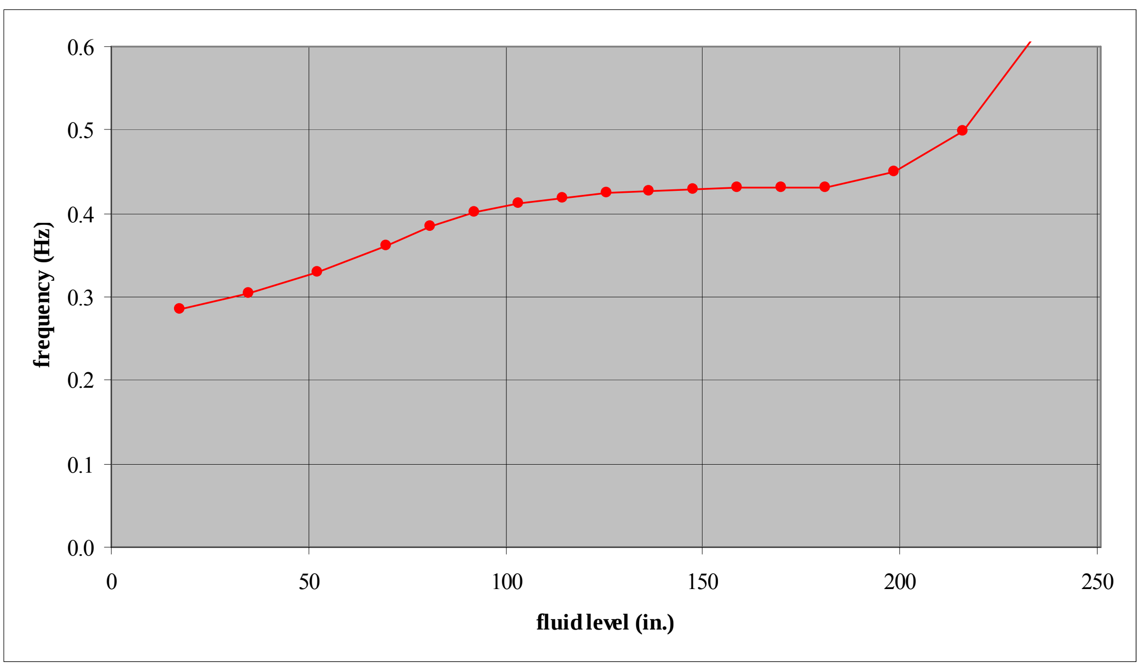

Figure 8.6-7, CLV5 LOX (R = 99.0 in.) variation of frequency with respect to liquid height

Table 8.6-5, CLV5 LH2 tank (R = 99.0 in.) slosh analysis results

fluid level h (in.)	frequency f (Hz)	slosh mass m_1 (lb·s²/in.)	fixed mass m_0 (lb·s²/in.)	stiffness k (lb/in.)	h_1 (in.)	h_0 (in.)	damping ratio ζ
0	-	0	0	-	-	-	0.0020
17.5	0.284	0.773	0.0386	2.47	11.4	-103.8	0.0016
35.0	0.305	2.61	0.314	9.59	23.5	-81.2	0.0006
52.5	0.330	4.77	1.06	20.5	35.5	-55.7	0.0004
70.0	0.362	6.52	2.49	33.7	47.4	-30.0	0.0003
121.3	0.422	8.86	10.7	62.4	77.8	26.0	0.0001
172.6	0.431	9.28	20.8	68.3	94.2	65.7	0.0001
223.9	0.433	9.35	31.3	69.3	101.4	99.4	0.0001
275.2	0.433	9.35	41.8	69.2	104.4	130.0	0.0001
326.5	0.433	9.35	52.4	69.3	105.5	158.9	0.0001
377.8	0.433	9.36	63.0	69.4	106.0	186.9	0.0001
429.1	0.433	9.36	73.5	69.4	106.2	214.2	0.0001
480.4	0.433	9.36	84.1	69.4	106.3	241.1	0.0001
531.7	0.433	9.36	94.7	69.4	106.3	267.7	0.0001
583.0	0.433	9.36	105.3	69.5	106.3	294.2	0.0003
600.5	0.451	8.87	109.3	71.1	107.9	302.4	0.0003
618.0	0.499	6.88	114.4	67.7	112.9	308.9	0.0002
635.5	0.614	3.48	119.8	51.8	118.7	315.7	0.0011
653.0	-	0	123.7	-	116.9	326.5	0.0020

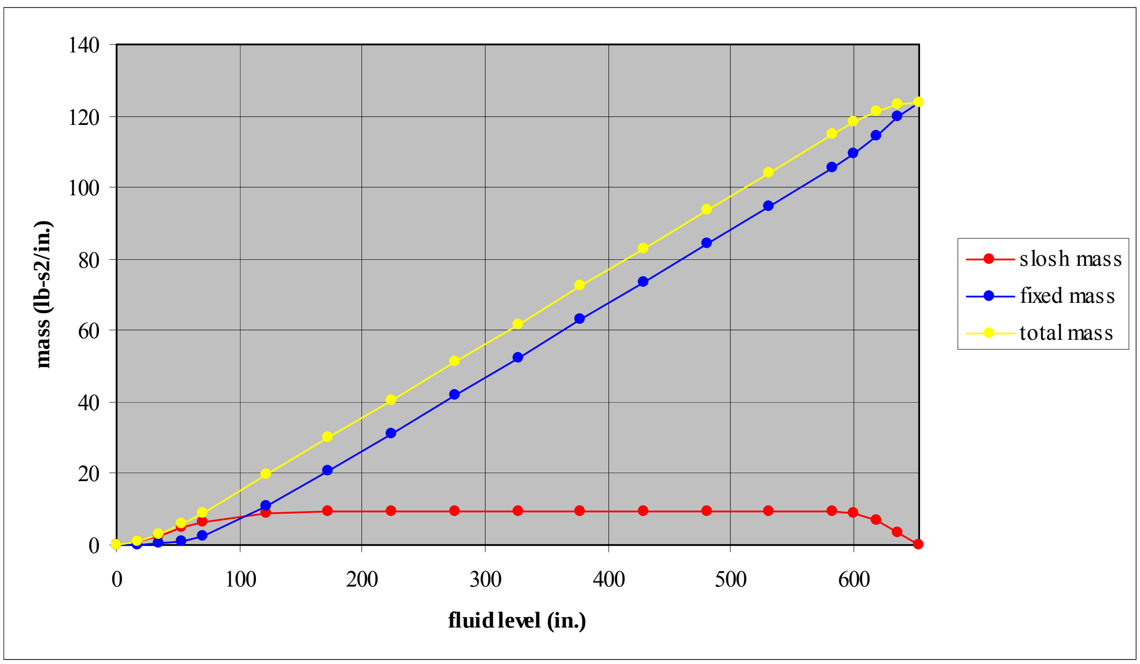

Figure 8.6-8, CLV5 LH2 (R = 99.0 in.) variation of mass with respect to liquid height

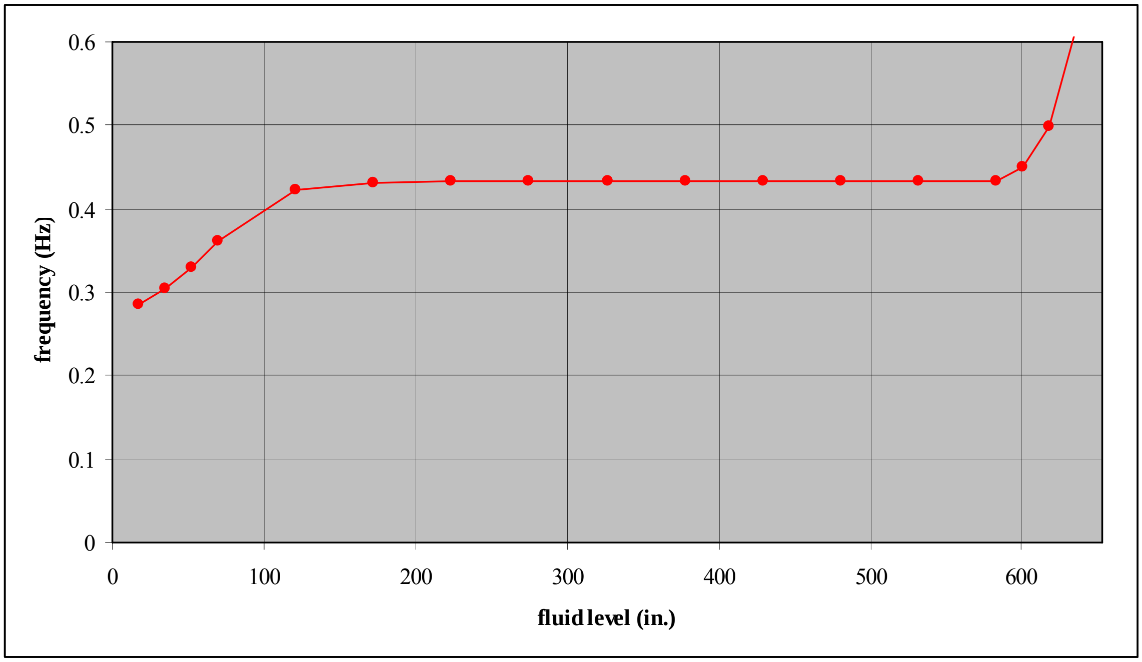

Figure 8.6-9, CLV5 LH2 (R = 99.0 in.) variation of frequency with respect to liquid height

9.0 Limit Loads for Design

9.1 Design Uncertainty Factors

When the results of LC1a were presented to the CLV Loads Panel recommendations for design uncertainty factors were made. The Loads Panel increased two of the recommendations. These modified recommendations were used to derive the recommended design loads presented in this section.

For axial loads an uncertainty factor of 1.1 was recommended and approved. The following are cited as rationale for this factor:

1) Axial loads are primarily static
2) Liftoff dynamics were already covered by a 1.5 uncertainty factor
3) Thrust oscillations are assumed to be covered by the 1.1

For the ascent flight regime an uncertainty factor of 1.5 was recommended and approved for lateral loads. The following is cited as rationale for this factor:

1) Aeroelastic effects such as static aeroelastics (STEL), gust, and buffet have not been evaluated.

For the liftoff an uncertainty factor of 1.1 was recommended but raised to 1.5 for lateral loads. The following are cited as rationale for this factor:

1) Liftoff dynamics were already covered by a 1.5 uncertainty factor.
2) Ignition overpressure had not yet been evaluated.

3) The issue of launch pad design and ignition overpressure sources have not yet been defined (e.g. coverage of SSME and right hand RSRB holes on the MLP).

For the pre-launch bending moments an uncertainty factor of 1.0 was recommended but raised to 1.25 for lateral loads. The following are cited as rationale for this factor

1) Peak wind speed includes gust static component.
2) A 1.5 factor already included for the wind induced oscillation phenomenon.
3) Dynamic gust component assumed covered by the additional 1.25 uncertainty factor.

Figure 9.1-1 shows the results of the DAC-1 Rev 2 3-dof dispersion analysis, Reference 4, for the ascent flight envelope along with circles representing the LC1a analysis. Note that the analysis assumption of 7 degree dispersion appears to be a reasonable estimate at this stage of development. Note too that the ascent uncertainty factor is used to cover STEL, gust, and buffet effects that are not evaluated as part of the GN&C simulation represented in this figure.

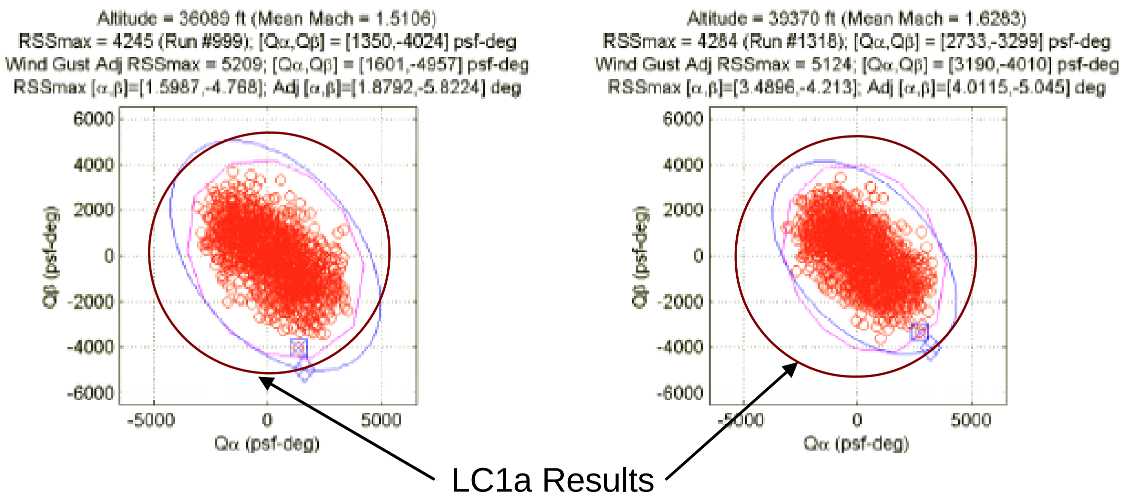

Figure 9.1-1, Ascent Flight Envelope Dispersions

Figure 9.1-2 shows DAC-1 Rev 2 3-dof dispersion analysis, Reference 4, axial acceleration dispersions along with a line representing the LC1a result. Additionally a line representing the design value obtained by applying the axial load uncertainty factor to the LC1a result is shown. The figure indicates the 1.1 factor is reasonable compared to the 3-dof dispersions.

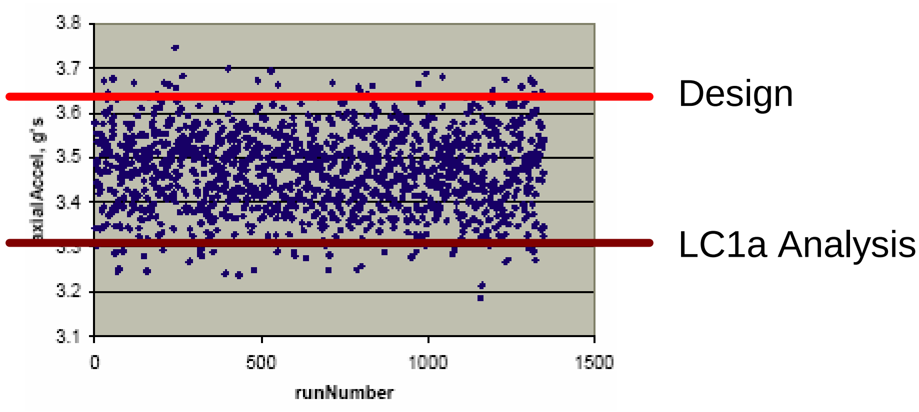

Figure 9.1-2, Ascent Maximum Axial Acceleration Dispersions

9.2 Element System Design Loads

Presented here are the recommended Element design loads. These design loads have been determined by the integrated system level loads analysis (Section 8.0) and contain additional uncertainty factors to account for current uncertainties in the structure and environments (Section 9.1). Design loads are only presented for the 5.5 meter Upper Stage configuration. Results for the 5.0 meter Upper Stage are discussed in Section 10.1. These loads should be used in conjunction with any other loads determined necessary at the element level as derived from the Element's independent operation and documented in the Element's individual Loads Databook.

The flight parameter design values in Table 9.2-1, Ascent 1st Stage Flight Design Parameters are currently the most appropriate for use in design activities of the CLV Elements for ascent 1st stage flight. The flight parameter design values in Table 9.2-2, Ascent 2nd Stage Flight Design Parameters are currently the most appropriate for use in current design activities of the CLV Elements for ascent 2nd stage flight. Liftoff acceleration levels are tabulated with the Element loads.

Table 9.2-1, Ascent 1st Stage Flight Design Parameters

	psf		deg.			seconds	lbs.
	Q	**Mach**	**Dispersed Alpha**	**G's Axial**	**G's Lateral**	**Time**	**Thrust**
Max Q	793	1.5-1.6	7	2.2	0.18	57-60	2.75-2.80M
Max Q+	650-760	2.0-2.5	7	3	0.23	66-75	2.95-3.18M
Max Thrust/G	400-450	3.2-3.5	7	3.6	0.15	85-92	3.1-3.25M
Transonic	650-725	0.9-1.1	7	1.9	0.12	39-45	2.70-2.68M

Table 9.2-2, Ascent 2nd Stage Flight Design Parameters

	psf		deg.			seconds	lbs.
	Q	**Mach**	**Dispersed Alpha**	**G's Axial**	**G's Lateral**	**Time**	**Thrust**
2nd Stage Ignition+	8	6.3	0	0.8	0	136	274K
LAS Separation	0	NA	0	0.9	0	166	274K
2nd Stage Burnout	0	NA	0	3.3	0	592	274K

Unless noted in the following sections, the coordinate system definitions are detailed in Section 5.1.1 and sign conventions are detailed in Section 5.1.2.

9.2.1 CLV 1st Stage

All loads presented here follow the coordinate definitions and sign conventions described in Section 5.1. These loads are intended to encompass the response of the Element structure to the environments and inputs described in Section 5.0. The loads presented here only represent loads for nominal and dispersed integrated operation (e.g. pre-launch, liftoff, and ascent flight) using the load cases described in Section 7.0. Structural models used to predict the response to the defined environments and design criteria are described in Section 6.0. Figure 9.2-1 shows the 1st Stage FEM with stack X stations.

No loads are applicable for abort or abort trajectories.

The flight parameter design values in Table 9.2-1, Ascent 1st Stage Flight Design Parameters are currently the most appropriate for use in current design activities of the 1st Stage.

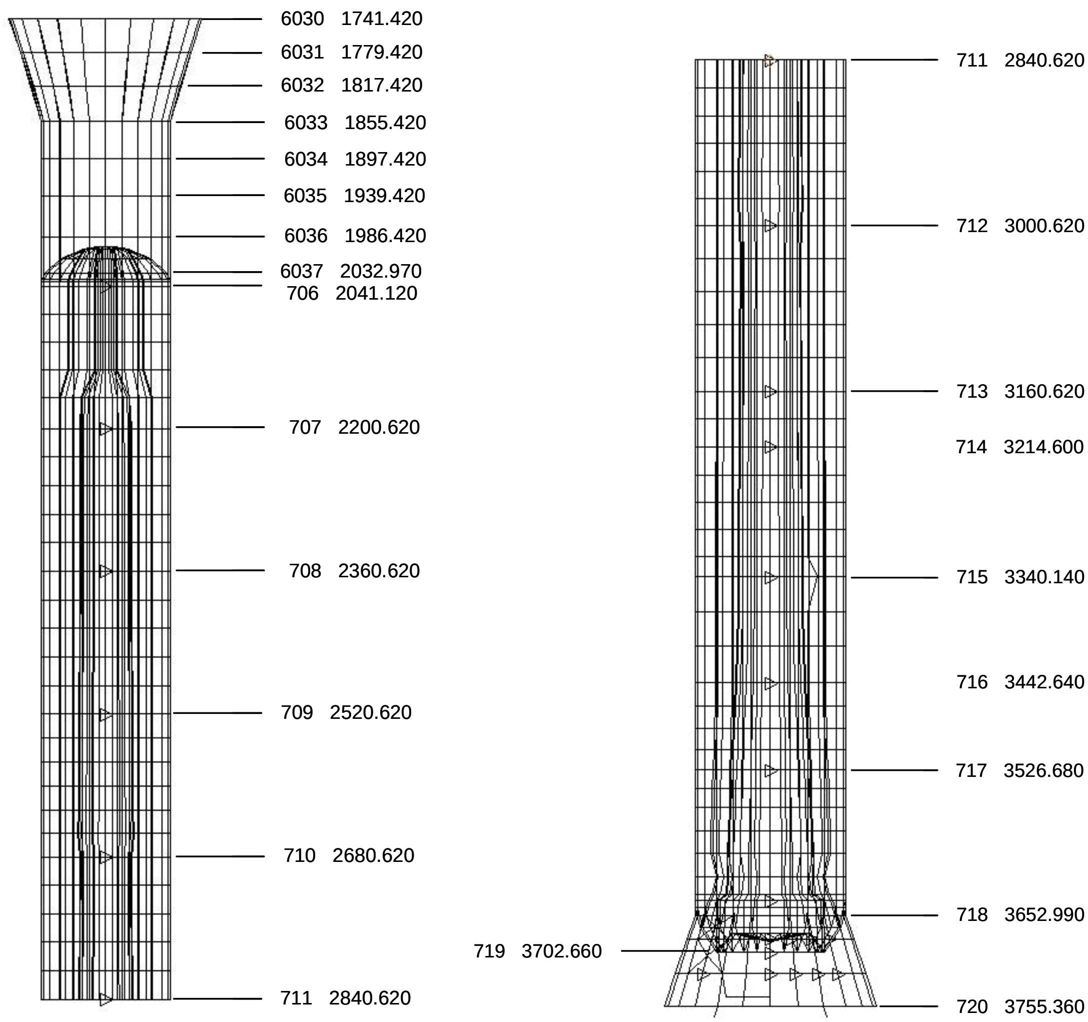

Figure 9.2-1, Solid Booster with Forward Frustum FEM Model and Stack X Stations

Figure 9.2-2 through Figure 9.2-4 show section design loads for the 1st Stage. These curves are envelopes of the loads resulting from all assessed load cases. These results reflect the system

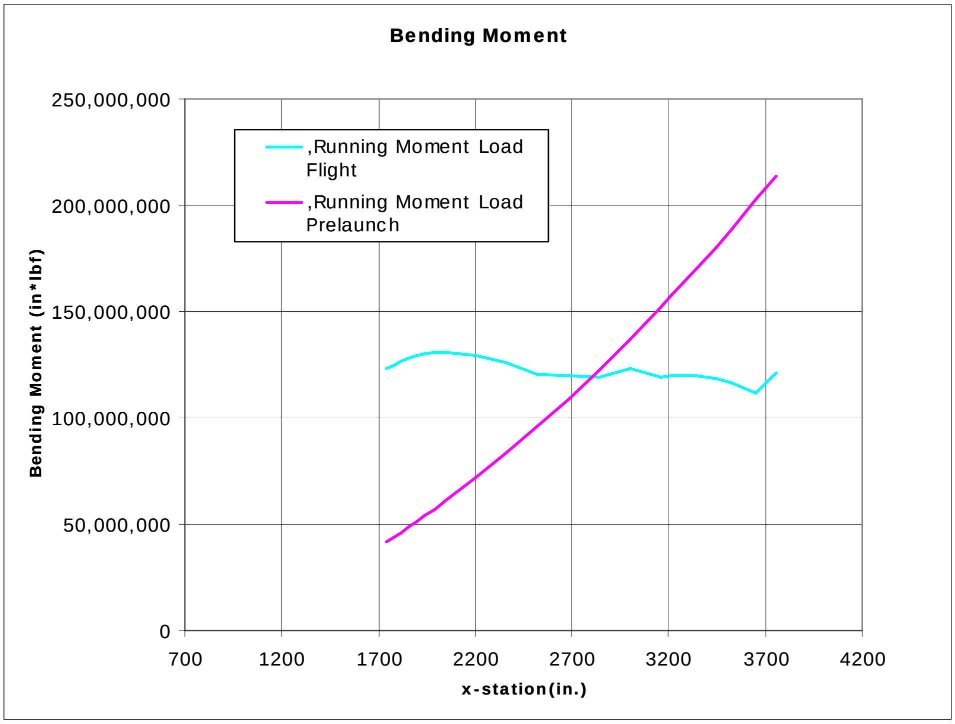

Figure 9.2-2, Recommended 1st Stage Design Moment

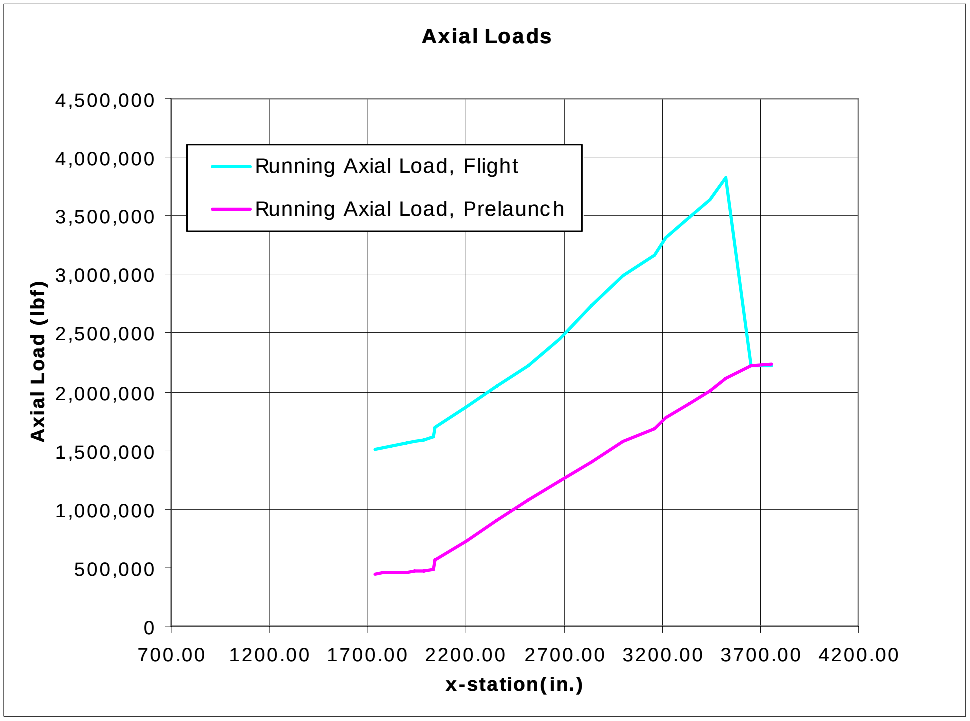

Figure 9.2-3, Recommended 1st Stage Design Axial Load

response loads with appropriate uncertainty factors. Internal pressure is not reflected in the axial load plot.

Figure 9.2-4, Recommended 1st Stage Design Shear

Table 9.2-3 contains the Design Section loads data shown in Figures 9.2.1-2 through 9.2.1-4.

Table 9.2-3, Recommended 1st Stage Section Loads

		PRELAUNCH			FLIGHT		
Interface	X-Station (in)	Moment (in-lb)	Shear (lb)	Axial (lb)	Moment (in-lb)	Shear (lb)	Axial (lb)
Interstage/Frustum	1741.420	41,492,032	60,325	450,283	123,150,123	153,450	1,508,756
x-stat 1779.420	1779.420	43,784,371	61,743	454,010	124,955,306	153,300	1,524,613
x-stat 1817.420	1817.420	46,130,591	62,980	457,513	126,680,059	153,150	1,538,971
Frustum/recovery	1855.420	48,523,816	64,048	461,064	128,151,061	152,550	1,552,523
x-stat 1897.420	1897.420	51,213,816	65,224	464,766	129,449,269	151,350	1,564,623
recovery/Fwd Skirt	1939.420	53,953,227	66,396	468,689	130,268,312	149,295	1,577,442
x-stat 1986.420	1986.420	57,073,859	67,703	472,812	130,766,222	146,520	1,590,917
Fwd skirt/attach ring	2032.970	60,225,445	68,992	480,540	130,971,053	140,355	1,616,176
x-stat 2041.120	2041.120	60,787,733	68,992	563,781	131,018,469	131,160	1,696,908
x-stat 2200.620	2200.620	71,792,030	73,327	732,554	129,776,529	195,450	1,869,249
x-stat 2360.620	2360.620	83,524,356	77,611	901,492	126,261,134	216,000	2,042,355
x-stat 2520.620	2520.620	95,942,074	81,827	1,074,328	120,837,644	185,700	2,229,407
x-stat 2680.620	2680.620	109,034,383	85,972	1,239,495	120,150,000	239,250	2,456,300
x-stat 2840.620	2840.620	122,789,942	90,043	1,406,217	119,070,000	282,600	2,730,200
x-stat 3000.620	3000.620	137,196,805	94,035	1,571,364	123,000,000	379,350	2,987,600
x-stat 3160.620	3160.620	152,242,337	97,942	1,688,716	119,175,000	380,250	3,169,100
x-stat 3214.600	3214.600	157,529,265	99,251	1,782,742	119,970,000	445,950	3,312,100
x-stat 3340.140	3340.140	169,989,199	102,238	1,905,727	119,970,000	584,100	3,495,800
x-stat 3442.640	3442.640	180,468,564	104,637	2,004,255	118,650,000	477,900	3,639,900
x-stat 3526.680	3526.680	189,262,267	106,577	2,115,644	116,280,000	403,800	3,832,400
x-stat 3652.990	3652.990	202,723,984	109,426	2,222,703	111,540,000	404,850	2,219,800
SRB aft end	3755.360	213,994,222	112,365	2,231,848	121,230,000	317,850	2,227,500

Table 9.2-4, 1st Stage Design Transient Accelerations (G's) from Liftoff contains the maximum absolute design transient accelerations, in G's, from the liftoff analysis including the recommended design uncertainty factors. Given the fidelity of the current analysis these should be considered as +/- values.

Table 9.2-4, 1st Stage Design Transient Accelerations (G's) from Liftoff

X Station (in)	X Abs Max	Y Abs Max	Z Abs Max
1741.420	1.3	1.3	2.0
1779.420	1.2	1.4	1.9
1817.420	1.2	1.4	1.8
1855.420	1.2	1.5	1.6
1897.420	1.2	1.5	1.4
1939.420	1.2	1.5	1.2
1986.420	1.3	1.6	1.1
2032.970	1.3	1.6	1.2
2041.120	1.3	1.6	1.3
2200.620	1.2	1.1	0.9
2360.620	1.1	0.7	0.8
2520.620	1.1	0.9	0.9
2680.620	1.4	1.1	1.3
2840.620	1.2	1.2	1.7

3000.620	1.3	1.2	2.4
3160.620	1.4	1.9	4.2
3214.600	1.4	1.5	3.1
3340.140	1.4	2.5	5.5
3442.640	1.4	1.8	3.5
3526.680	1.4	3.0	5.6
3652.990	2.2	4.8	6.8
3755.360	26.2	34.7	45.9
3765.090	100.0	742.7	318.5
3765.090	144.9	503.6	305.7
3765.090	88.3	383.0	314.1
3765.090	135.4	386.0	354.9

The hold-down interface loads between the CLV and the MLP are shown in Table 9.2-5, FSB/MLP Hold-down Forces. The indicator loads are from the Space Shuttle SRB Loads Databook, Reference 23. These loads were recovered from the current pre-launch wind and liftoff cases. Rollout has not been considered yet.

Table 9.2-5, FSB/MLP Hold-down Forces

Hold-down Post Load Indicator*		
Load	Indicator(KIPS)	55m
Maximum F(X)	1591.49	1547.6
Minimum F(X)	-706.67	-610.0
+ Post Compression		- Post Tension

* Includes 1.25 on wind

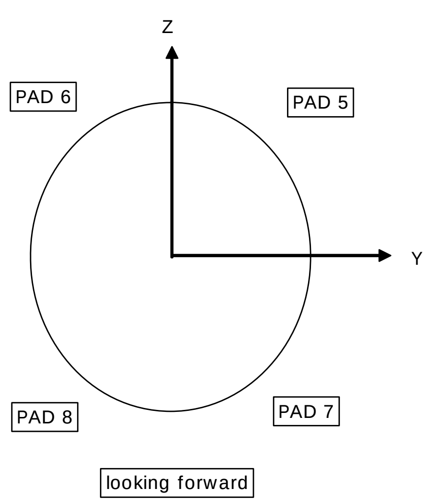

D55m**			
		Max*	Min*
PAD 5	X	597,746	-1,547,570
	Y	92,276	-275,425
	Z	263,349	-585,121
PAD 6	X	609,958	-1,534,305
	Y	271,426	-94,485
	Z	270,517	-584,256
PAD 7	X	536,732	-1,459,768
	Y	84,237	-280,599
	Z	551,891	-240,871
PAD 8	X	523,897	-1,473,656
	Y	283,048	-80,478
	Z	562,194	-237,703

* Load as Applied to Vehicle
** Includes 1.25 on wind

9.2.2 CLV Upper Stage

All loads presented here follow the coordinate definitions and sign conventions described in Section 5.1. These loads are intended to encompass the response of the Element structure to the environments and inputs described in Section 5.0. The loads presented here only represent loads for nominal and dispersed integrated operation (e.g. pre-launch, liftoff, and ascent flight) using the load cases described in Section 7.0. Structural models used to predict the response to the defined environments and design criteria are described in Section 6.0. Figure 9.2-5 shows the Upper Stage FEM with stack X stations.

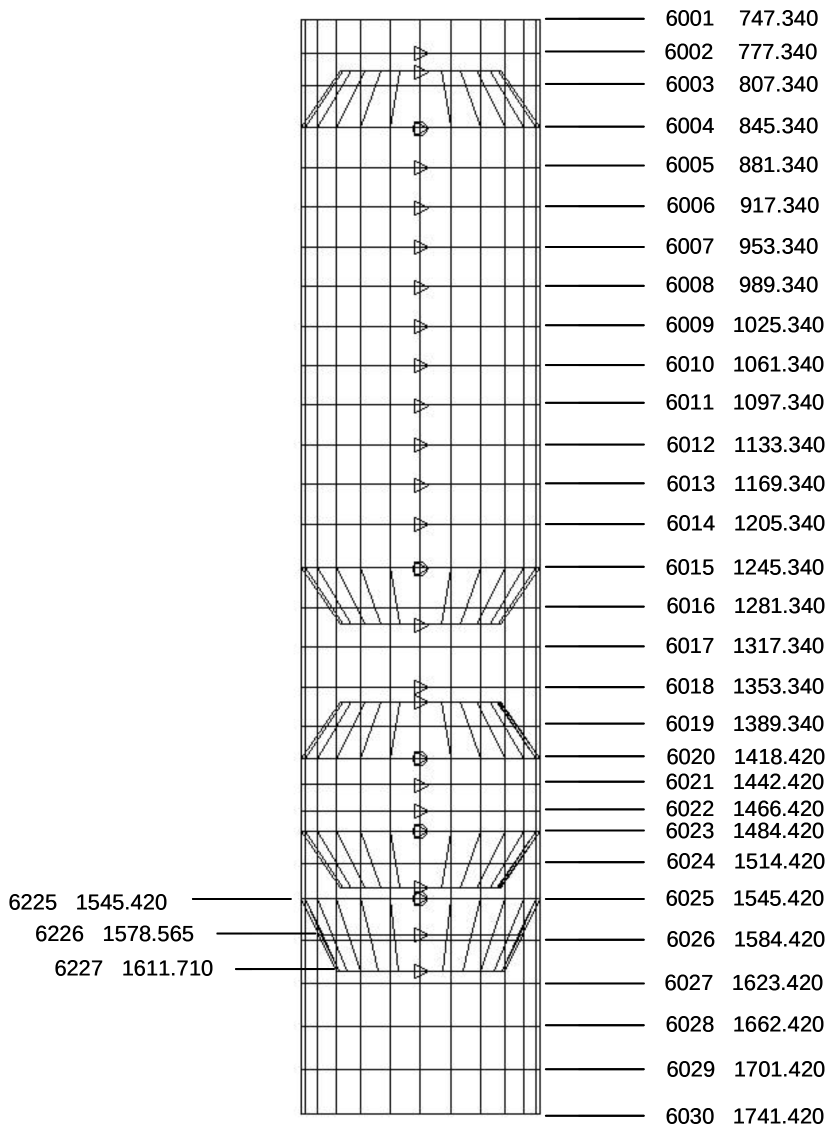

Figure 9.2-5, Upper Stage and Spacecraft Adapter FEM with Stack X Stations

No loads are applicable for abort or abort trajectories.

The flight parameter design values in Table 9.2-1, Ascent 1st Stage Flight Design Parameters and Table 9.2-2, Ascent 2nd Stage Flight Design Parameters are currently the most appropriate for use in current design activities of the Upper Stage.

Figure 9.2-6 through Figure 9.2-8 show section design loads for the Upper Stage. These curves are envelopes of the loads resulting from all assessed load cases. These results reflect the system response loads with appropriate uncertainty factors. Internal pressure is not reflected in the axial load plot.

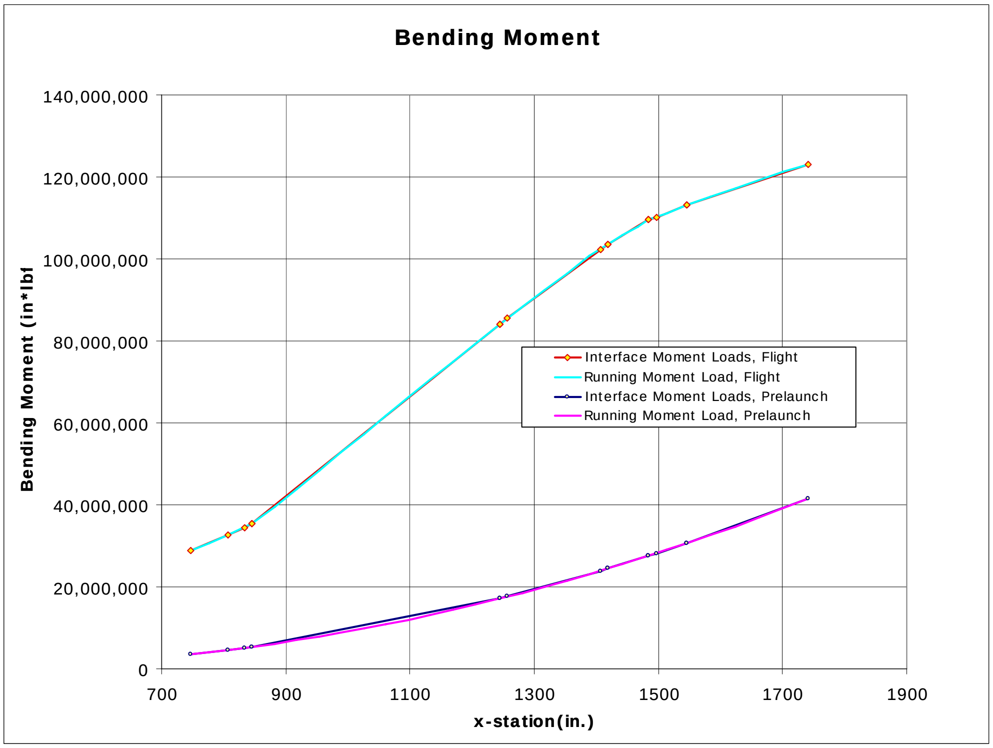

Figure 9.2-6, Recommended Upper Stage Design Moments

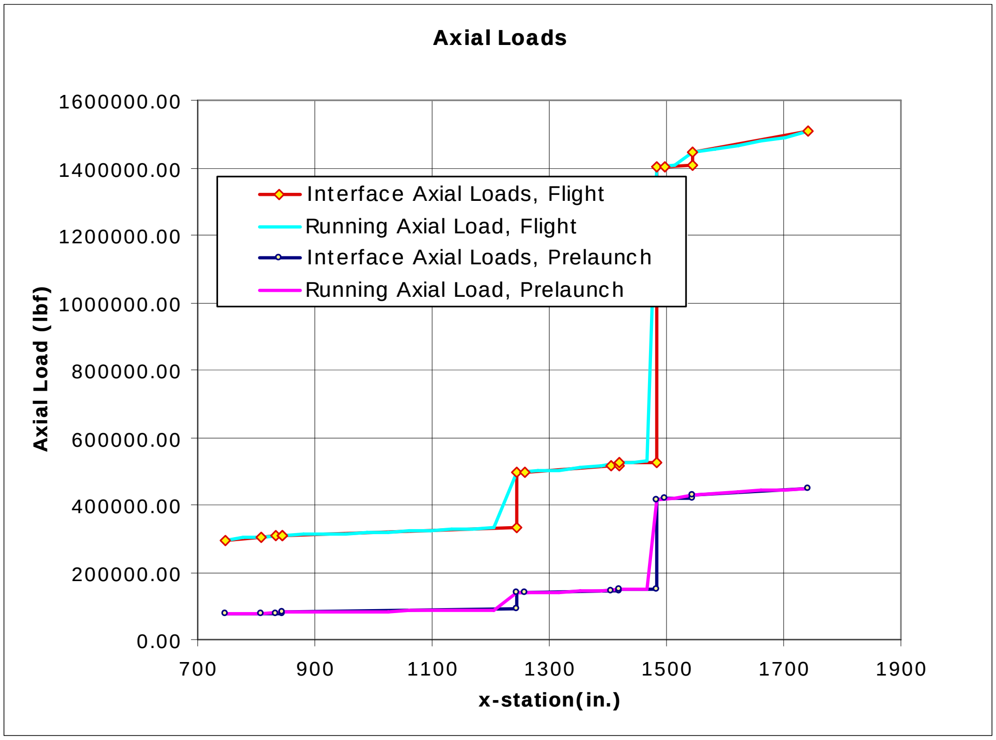

Figure 9.2-7, Recommended Upper Stage Design Axial Loads

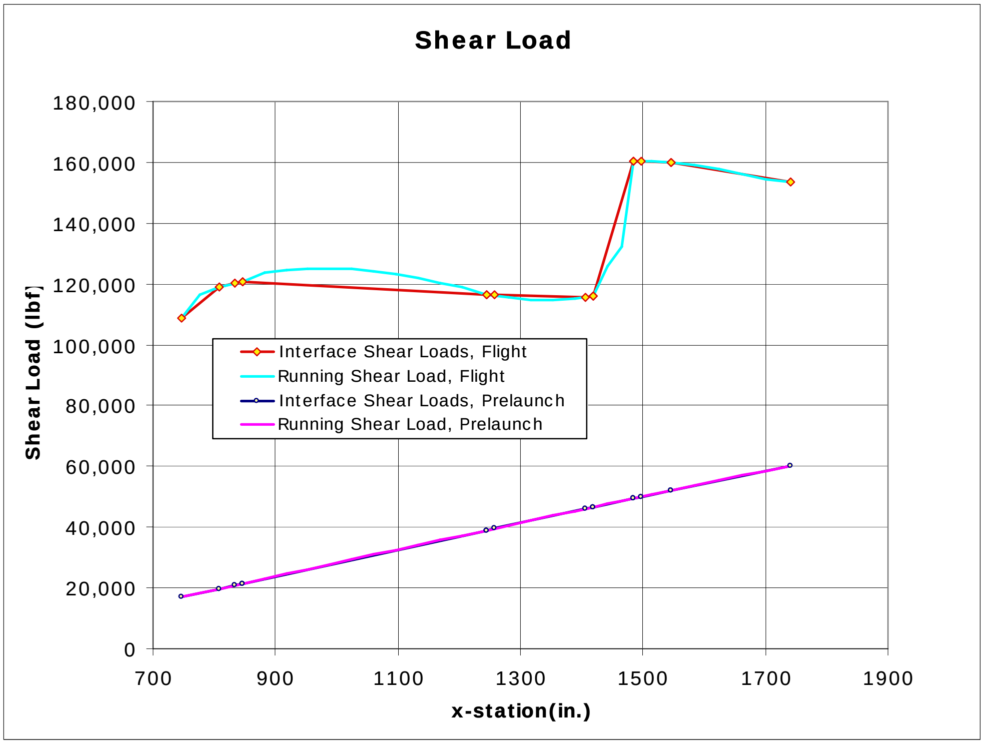

Figure 9.2-8, Recommended Upper Stage Design Shear Loads

Table 9.2-6, Recommended CLV Upper Stage Section Loads

		PRELAUNCH			FLIGHT		
Interface	X-Station (in)	Moment (in-lb)	Shear (lb)	Axial (lb)	Moment (in-lb)	Shear (lb)	Axial (lb)
CEV Adaptor/IU	747.34	3619954.47	16912.72	75495.71	28935000.00	108800.95	295141.99
IU/fwd skirt	807.34	4675276.87	19614.22	78334.87	32715000.00	119085.44	304876.44
fwd skirt/fwd LH2 ring	833.34	5185246.59	20781.12	79012.36	34500789.47	120331.99	306250.29
fwd LH2 ring/LH2 CYL (above)	845.34	5420617.23	21319.69	79325.05	35325000.00	120907.33	306884.38
fwd LH2 ring/LH2 CYL(below)	845.34	5420617.23	21319.69	80261.33	35325000.00	120907.33	309422.72
LH2 CYL/aft LH2 ring (above)	1245.34	17182808.62	39026.82	89448.53	84130959.88	116602.78	334433.81
LH2 CYL/aft LH2 ring (below)	1245.34	17182808.62	39026.82	139355.50	84130959.88	116602.78	495641.99
aft LH2 ring/intertank	1257.34	17651130.44	39550.47	139726.04	85526274.46	116257.61	496843.04
intertank/fwd LOX ring	1406.42	23914944.47	46025.56	145477.61	102331848.81	115660.98	515482.32
fwd LOX ring/LOX CYL (above)	1418.42	24458391.97	46544.25	145837.48	103510071.85	115890.00	516648.95
fwd LOX ring/LOX CYL (below)	1418.42	24458391.97	46544.25	147915.06	103510071.85	115890.00	523379.34
LOX CYL/aft LOX ring (above)	1484.42	27592416.85	49388.06	149938.94	109526279.17	160500.00	523787.23
LOX CYL/aft LOX ring (below)	1484.42	27592416.85	49388.06	416462.44	109526279.17	160500.00	1402125.79
aft LOX ring/Thrust Structure	1496.42	28185073.60	49903.19	416882.51	110212016.24	160380.00	1403529.17
Thrust Structure/Interstage (above)	1545.42	30645011.12	52003.62	418597.78	113095338.93	159900.00	1409259.64
Thrust Structure/Interstage (below)	1545.42	30645011.12	52003.62	430697.92	113095338.93	159900.00	1445161.64
Interstage/Frustum	1741.42	41492031.60	60324.72	450282.81	123150122.61	153450.00	1508756.35

Extrapolated Data
Interpolated Data

In Table 9.2-6 some data was either extrapolated, or interpolated from the "Design" worksheets. This was done for two reasons. First, the Upper Stage models did not have grids at the location for the tank "Y ring" flanges. And second, because the loads were extracted at the grids (as opposed to element stations), the axial plots from the "Design" worksheets will not exhibit the correct discontinuities at the model branches (i.e. tank dome, and thrust cone intersections). All extrapolation and interpolation was linear.

Table 9.2-7, Upper Stage Design Transient Accelerations (G’s) from Liftoff contains the maximum absolute design transient accelerations, in G’s, from the liftoff analysis including the recommended design uncertainty factors. Given the fidelity of the current analysis these should be considered as +/- values.

Table 9.2-7, Upper Stage Design Transient Accelerations (G’s) from Liftoff

X Station (in)	X Abs Max	Y Abs Max	Z Abs Max
747.340	2.2	1.3	1.2
777.340	2.2	1.3	1.3
807.340	2.1	1.3	1.3
845.340	2.1	1.3	1.4
881.340	2.0	1.3	1.6
917.340	2.0	1.4	1.8
953.340	2.0	1.4	1.9
989.340	1.9	1.4	2.0
1025.340	1.9	1.4	2.0
1061.340	1.8	1.4	2.1
1097.340	1.8	1.4	2.0
1133.340	1.7	1.3	2.0
1169.340	1.7	1.3	1.9

1205.340	1.7	1.2	1.7
1245.340	1.7	1.1	1.6
1281.340	1.6	1.0	1.4
1317.340	1.6	0.9	1.2
1353.340	1.5	0.9	1.1
1389.340	1.5	0.8	0.9
1418.420	1.5	0.8	0.8
1442.420	1.6	0.7	0.7
1466.420	1.6	0.7	0.7
1484.420	1.6	0.7	0.7
1514.420	1.5	0.7	0.9
1545.420	1.5	0.8	1.2
1584.420	1.4	0.9	1.5
1623.420	1.4	1.1	1.8
1662.420	1.3	1.2	1.9
1701.420	1.3	1.3	2.0
1741.420	1.3	1.3	2.0

9.2.3 CLV J-2X

LC1a modeled the J-2X as a simple lumped mass.

The flight parameter design values in Table 9.2-1, Ascent 1st Stage Flight Design Parameters and Table 9.2-2, Ascent 2nd Stage Flight Design Parameters are currently the most appropriate for use in current design activities of the J-2X.

Maximum absolute design transient accelerations, in G's, were recovered from the liftoff analysis along the axis of the vehicle. The values in the vicinity of the J-2X, including the recommended design uncertainty factors are 1.5 G's in the X direction, 1.1 G's in the Y direction, and 1.8 G's in the Z direction. Given the fidelity of the current analysis these should be considered as +/- values.

9.2.4 CEV Spacecraft with LAS and Spacecraft Adapter

All loads presented here follow the coordinate definitions and sign conventions described in Section 5.1. These loads are intended to encompass the response of the Element structure to the environments and inputs described in Section 5.0. The loads presented here only represent loads for nominal and dispersed integrated operation (e.g. pre-launch, liftoff, and ascent flight) using the load cases described in Section 7.0. Structural models used to predict the response to the defined environments and design criteria are described in Section 6.0. Figure 9.2-9 shows the CEV Spacecraft with LAS and Spacecraft Adapter FEM with stack X stations.

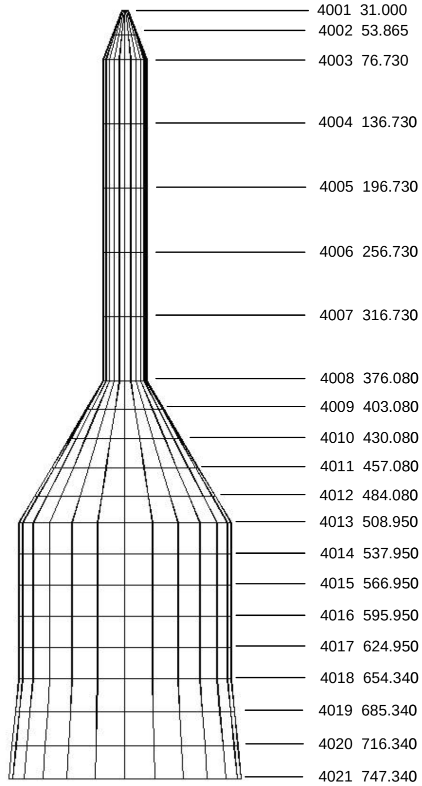

Figure 9.2-9, CEV FEM Model with Stack X Stations

No loads are applicable for abort or abort trajectories.

The flight parameter design values in Table 9.2-1, Ascent 1st Stage Flight Design Parameters and Table 9.2-2, Ascent 2nd Stage Flight Design Parameters are currently the most appropriate for use in current design activities of the Upper Stage.

Figure 9.2-10 through Figure 9.2-12 show section design loads for the CEV. These curves are envelopes of the loads resulting from all assessed load cases. These results reflect the system response loads with appropriate uncertainty factors. Internal pressure is not reflected in the axial load plot.

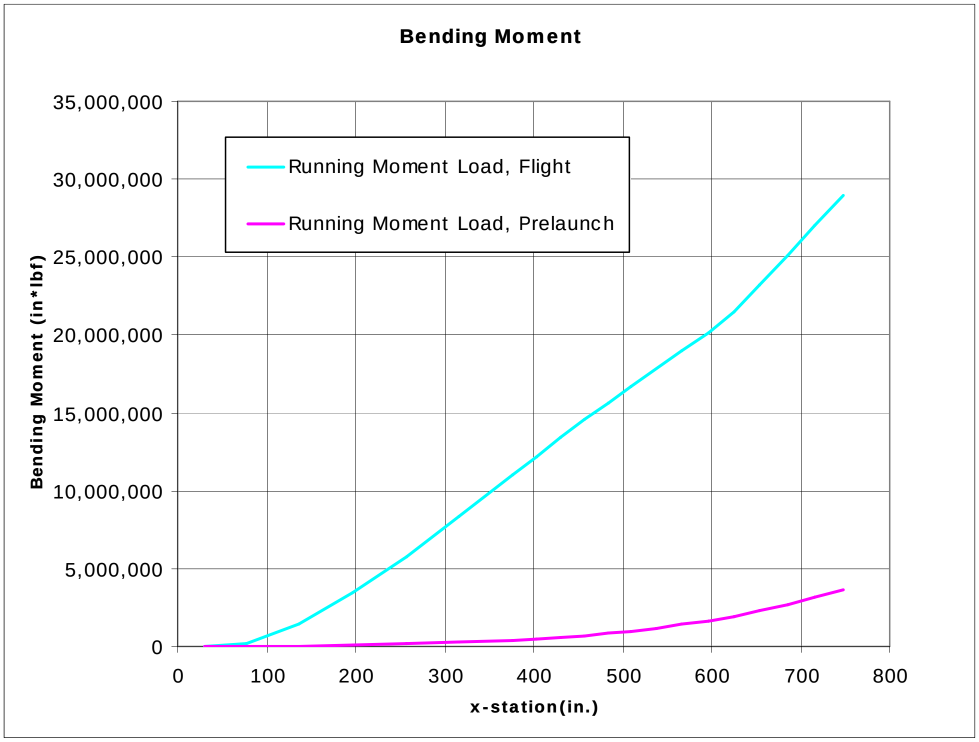

Figure 9.2-10, Recommended CEV Design Bending Moment

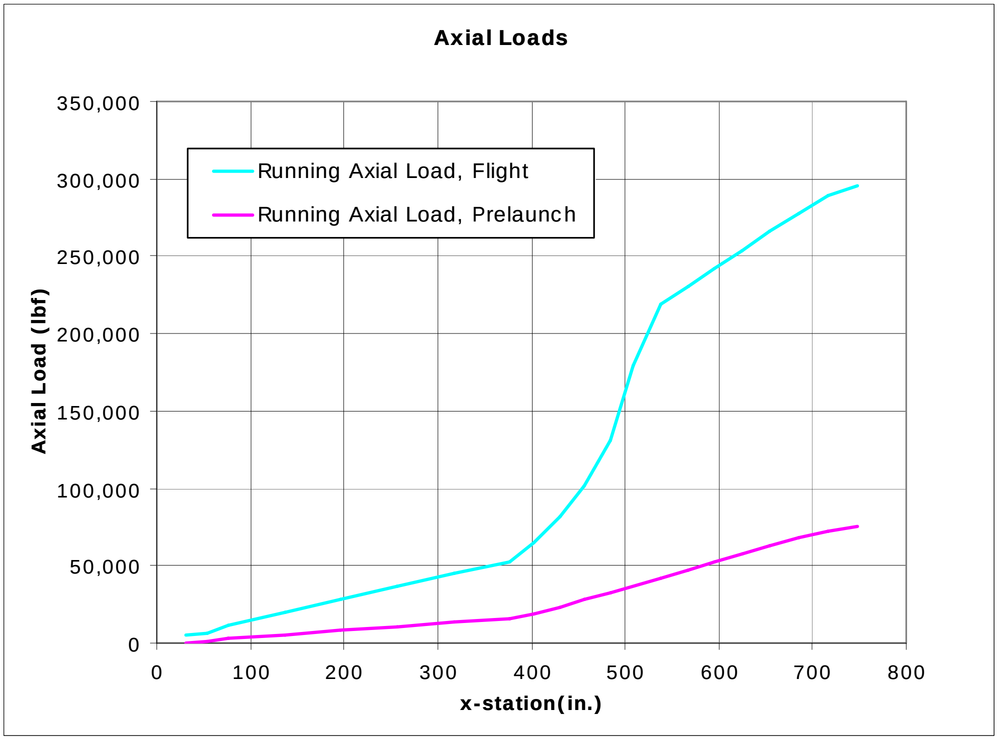

Figure 9.2-11, Recommended CEV Design Axial Load

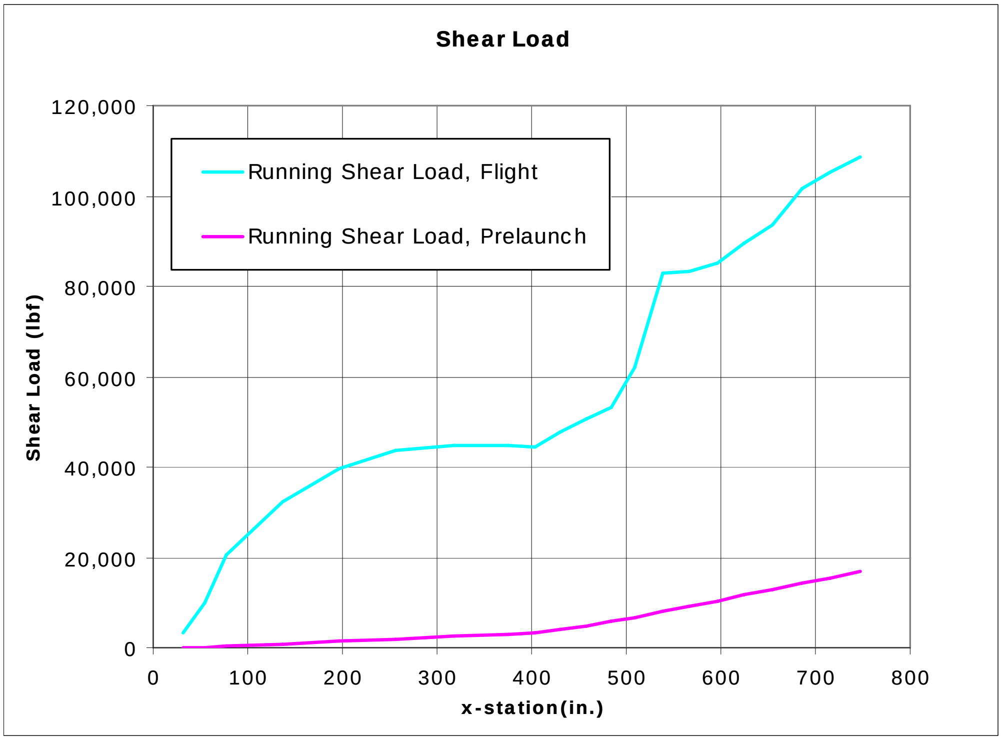

Figure 9.2-12, Recommended CEV Design Shear Load

Table 9.2-8 contains the Design Section loads data shown in Figure 9.2-10, Figure 9.2-11, and Figure 9.2-12.

Table 9.2-8, Recommended CEV Design Section Loads

		PRELAUNCH			FLIGHT		
Interface	X-Station (in)	Moment (in-lb)	Shear (lb)	Axial (lb)	Moment (in-lb)	Shear (lb)	Axial (lb)
LAS Tip	31.000	0	0	420	12416	3257	4778
	53.865	0	117	1319	62220	9801	6763
LAS diameter	76.730	2670	320	3073	226950	20505	11383
	136.730	21895	853	5630	1476750	32190	19798
	196.730	73078	1384	8186	3420000	39615	28243
	256.730	156119	1913	10743	5793000	43605	36717
	316.730	270919	2441	13286	8386500	44895	45162
LAS / CEV	376.080	415787	2961	15623	11019000	44850	52793
	403.080	495736	3380	19286	12217500	44355	64889
	430.080	587008	3982	23574	13390500	47610	81777
	457.080	694518	4765	28016	14539500	50655	101921
	484.080	823171	5729	32425	15660000	53385	131211
CEV / SM	508.950	965650	6770	37128	16680000	61960	179497
	537.950	1161982	7982	42214	17835000	82839	219528
	566.950	1393464	9192	47301	18990000	83394	230947
	595.950	1660037	10400	52387	20115000	85314	242402
	624.950	1961642	11606	57508	21435000	89717	254114
SM / SPA	654.340	2302748	12826	62716	23235000	93515	266024
	685.340	2700365	14151	67717	25140000	101682	277461
	716.340	3139046	15513	72643	27045000	105421	288727
SPA / Upr Stg	747.340	3619954	16913	75496	28935000	108801	295142

Table 9.2-9 contains the maximum absolute design transient accelerations, in G's, from the liftoff analysis including the recommended design uncertainty factors. Given the fidelity of the current analysis these should be considered as +/- values.

Table 9.2-9, CEV Design Transient Accelerations (G's) from Liftoff

X Station (in)	X Abs Max	Y Abs Max	Z Abs Max
31.000	2.5	8.8	6.5
53.870	2.5	7.9	5.7
76.730	2.5	7.1	4.9
136.730	2.5	5.0	3.2
196.730	2.5	3.3	2.9
256.730	2.5	2.4	2.4
316.730	2.4	2.1	2.4
376.080	2.4	2.2	2.0
403.080	2.4	2.1	1.9
430.080	2.4	2.0	1.7
457.080	2.4	1.9	1.6
484.080	2.4	1.8	1.5
508.950	2.4	1.7	1.3
537.950	2.4	1.5	1.2
566.950	2.3	1.4	1.2
595.950	2.3	1.4	1.2
624.950	2.3	1.4	1.2
654.340	2.3	1.3	1.2
685.340	2.3	1.3	1.2
716.340	2.3	1.3	1.2
747.340	2.2	1.3	1.2

9.2.5 Launch Management System

9.2.5.1 Hold-Down Forces

The hold-down interface loads between the CLV and the MLP are shown in Table 9.2-5, FSB/MLP Hold-down Forces. The indicator loads are from the Space Shuttle SRB Loads Databook, Reference 23. These loads were recovered from the current pre-launch wind and liftoff cases. Rollout has not been considered yet.

9.2.5.2 On-pad Vehicle Tip Deflections

The maximum tip deflections from the pre-launch analysis are shown in Table 9.2-10, On-Pad Vehicle Tip deflections. These tip deflections do not include uncertainty factors.

Table 9.2-10, On-Pad Vehicle Tip deflections

Wind	Max Tip Deflection (inches)			
		X	Y	Z
Gravity Only	D55m_Dry	1	2	1
	D55m_GLOW	1	2	1
1Hr 5% Risk	D55m_Dry	2	27	19
	D55m_GLOW	2	27	19
1Day 1%Risk	D55m_Dry	2	43	31
	D55m_GLOW	2	43	31
1Day 5%Risk	D55m_Dry	2	31	22
	D55m_GLOW	2	31	22
10 Day 1% Risk	D55m_Dry	2	60	43
	D55m_GLOW	2	60	43

10.0 Trade Studies

10.1 5.0 Meter Upper Stage

An integral part of the Load Cycle 1A analysis was the simultaneous assessment of the 5.0 meter Upper Stage configuration. None of the results from the 5.0 meter configuration assessment have been incorporated in the Section 9 recommended design loads. The results of the 5.0 meter assessments are presented here for future use. **These results reflect the analysis results but are not recommended for design.** As a result of the simultaneous assessment, all of the assumptions, models, and inputs to the 5.0 meter assessment are documented in the previous sections alongside those of the 5.5 meter configurations. This was deemed the most appropriate method for easy comparison of each input.

10.1.1 5.0 Meter Structural Flex-Mode Summary

Current estimates of the D50m structural flex modes were provided for assessment with the flight control system. A Guyan reduction was performed on the structural models described in Section 6.0 to reduce them to a series of centerline points. Mass normalized modes were then calculated below 25 Hz for several configurations. The mass properties, modal frequencies, mode shape deflection data, and station coordinates of the centerline points were then provided. This data is included in the Vehicle Integration Loads Team database located on the ICE Windchill server, Reference 1.

Table 10.1-1, 5.0m CLV ISS Weights and Table 10.1-2, 5.0m CLV LUNAR Weights show the vehicle weights for various configurations for both the ISS and LUNAR vehicle masses. Table 10.1-3, 5.0m CLV ISS weight Flex-mode Frequencies < 25Hz and Table 10.1-4, 5.0m CLV LUNAR weight Flex-mode Frequencies < 25Hz show the calculated frequencies for those configurations. Table 10.1-5, 5.0m CLV Centerline Stations shows the centerline stations at which mode shape deflections are reported. For reference the FSB gimbal is located at station 3690.910.

Table 10.1-1, 5.0m CLV ISS Weights

DAC-0 5.0m ISS Weights of Stack Configurations

Condition	Mass (lbs-sec/in)	Weight (lbs)	X CG (in)	Y CG (in)	Z CG (in)
Free-Free Empty	4,483	1,730,893	2,720.2	-250.5	0.0
On Pad Empty	28,141	10,864,905	3,726.4	-39.9	-159.3
On Pad GLOW	28,879	11,149,839	3,666.0	-45.3	-155.3
Free-Free GLOW	5,221	2,015,828	2,528.3	-250.5	0.0
1st Stage Burn Out	1,505	580,922	1,741.0	-250.6	0.1
2nd Stage Ignition	999	385,528	1,174.2	-250.5	0.0
2nd Stage Burn Out	226	87,365	732.9	-250.5	0.0

Table 10.1-2, 5.0m CLV LUNAR Weights

DAC-0 5.0m Lunar Weights of Stack Configurations

Condition	Mass (lbs-sec/in)	Weight (lbs)	X CG (in)	Y CG (in)	Z CG (in)
Free-Free Empty	4,491	1,733,758	2,716.3	-250.5	0.0
On Pad Empty	28,148	10,867,769	3,725.6	-40.0	-159.3
On Pad GLOW	28,886	11,152,704	3,665.2	-45.3	-155.2
Free-Free GLOW	5,229	2,018,693	2,525.3	-250.5	0.0
1st Stage Burn Out	1,512	583,787	1,734.4	-250.6	0.1
2nd Stage Ignition	1,006	388,393	1,168.5	-250.5	0.0
2nd Stage Burn Out	234	90,229	722.1	-250.5	0.0

Table 10.1-3, 5.0m CLV ISS weight Flex-mode Frequencies < 25Hz

DAC-0 5.0m ISS Weight Frequencies < 25hz

Free-Free Frequencies of Stack Models						On-Pad Frequencies	
Mode No.	FF-empty Fn (Hz)	ff-glow Fn (Hz)	ff-2ndbo Fn (Hz)	ff-2ndign Fn (Hz)	ff-1stbo Fn (Hz)	Empty Fn (Hz)	GLOW Fn (Hz)
1	0.00	0.00	0.00	0.00	0.00	0.23	0.17
2	0.00	0.00	0.00	0.00	0.00	0.28	0.21
3	0.00	0.00	0.00	0.00	0.00	0.74	0.73
4	0.00	0.00	0.00	0.00	0.00	0.82	0.80
5	0.00	0.00	0.00	0.00	0.00	2.40	1.73
6	0.00	0.00	0.00	0.00	0.00	2.65	1.86
7	0.86	0.83	11.11	4.41	1.09	3.89	3.49
8	0.86	0.83	11.11	4.41	1.09	4.46	3.56
9	2.98	1.99		7.42	3.68	4.57	3.75
10	2.98	1.99		7.42	3.68	5.80	5.11
11	4.74	4.13		14.12	5.24	6.07	5.16
12	4.74	4.13		14.52	5.24	7.42	6.47
13	6.63	5.25		14.52	8.38	7.85	6.91
14	6.63	5.25		22.64	8.38	8.84	7.63
15	8.79	7.98		22.64	11.30	9.39	8.47
16	8.79	7.98			11.31	9.51	8.90
17	10.03	7.99			11.85	9.87	9.26
18	10.95	9.25			14.35	10.78	9.39
19	10.96	9.25			16.46	11.18	9.89
20	11.99	10.97			17.76	11.51	10.78
21	12.00	10.97			17.77	12.43	11.19
22	12.70	11.99			22.19	12.69	11.50
23	12.70	12.00			22.20	12.70	12.37
24	14.35	13.19			24.98	13.79	13.16
25	15.66	13.19			25.00	16.14	13.18
26	16.15	14.35				16.15	13.81
27	16.15	14.44				18.72	15.74
28	22.83	17.43				19.37	17.70
29	22.85	17.70				23.63	17.70
30	23.99	17.70				23.90	18.73
31	23.99	22.66				23.96	19.37
32		22.66				24.64	22.71
33		22.91					22.71
34		22.93					24.49
35							24.70

Table 10.1-4, 5.0m CLV LUNAR weight Flex-mode Frequencies < 25Hz

DAC-0 5.0m LUNAR Weight Frequencies < 25hz

Free-Free Frequencies of Stack Models						On-Pad Frequencies	
Mode No.	FF-empty Fn (Hz)	ff-glow Fn (Hz)	ff-2ndbo Fn (Hz)	ff-2ndign Fn (Hz)	ff-1stbo Fn (Hz)	Empty Fn (Hz)	GLOW Fn (Hz)
1	0.00	0.00	0.00	0.00	0.00	0.23	0.17
2	0.00	0.00	0.00	0.00	0.00	0.28	0.21
3	0.00	0.00	0.00	0.00	0.00	0.74	0.72
4	0.00	0.00	0.00	0.00	0.00	0.82	0.79
5	0.00	0.00	0.00	0.00	0.00	2.40	1.73
6	0.00	0.00	0.00	0.00	0.00	2.65	1.86
7	0.85	0.83	11.02	4.41	1.08	3.89	3.48
8	0.85	0.83	11.02	4.41	1.08	4.46	3.55
9	2.98	1.99		7.37	3.68	4.57	3.75
10	2.98	1.99		7.37	3.68	5.80	5.09
11	4.72	4.13		13.92	5.22	6.07	5.14
12	4.72	4.13		14.48	5.22	7.42	6.46
13	6.61	5.23		14.48	8.35	7.85	6.90
14	6.61	5.23		22.53	8.35	8.84	7.60
15	8.78	7.94		22.53	11.28	9.39	8.45
16	8.78	7.97			11.29	9.51	8.87
17	9.88	7.97			11.73	9.87	9.24
18	10.95	9.22			14.35	10.78	9.39
19	10.95	9.22			16.38	11.18	9.89
20	11.99	10.97			17.72	11.51	10.78
21	12.00	10.97			17.73	12.43	11.19
22	12.67	11.99			22.12	12.69	11.50
23	12.67	12.00			22.13	12.70	12.31
24	14.35	13.18			24.95	13.79	13.16
25	15.64	13.19			24.97	16.14	13.18
26	16.08	14.31				16.15	13.80
27	16.08	14.35				18.72	15.62
28	22.83	17.40				19.37	17.66
29	22.85	17.66				23.63	17.66
30	23.96	17.66				23.90	18.73
31	23.96	22.59				23.96	19.37
32		22.59				24.64	22.63
33		22.89					22.63
34		22.91					24.49
35							24.70

Table 10.1-5, 5.0m CLV Centerline Stations

		X	Y	Z
GRID	4001	-146.2700	-250.5000	0.0000
GRID	4002	-123.4050	-250.5000	0.0000
GRID	4003	-100.5400	-250.5000	0.0000
GRID	4004	-40.5400	-250.5000	0.0000

GRID	4005	19.4600	-250.5000	0.0000
GRID	4006	79.4600	-250.5000	0.0000
GRID	4007	139.4600	-250.5000	0.0000
GRID	4008	198.8100	-250.5000	0.0000
GRID	4009	225.8100	-250.5000	0.0000
GRID	4010	252.8100	-250.5000	0.0000
GRID	4011	279.8100	-250.5000	0.0000
GRID	4012	306.8100	-250.5000	0.0000
GRID	4013	331.6800	-250.5000	0.0000
GRID	4014	360.6800	-250.5000	0.0000
GRID	4015	389.6800	-250.5000	0.0000
GRID	4016	418.6800	-250.5000	0.0000
GRID	4017	447.6800	-250.5000	0.0000
GRID	4018	477.0700	-250.5000	0.0000
GRID	4019	508.0700	-250.5000	0.0000
GRID	4020	539.0700	-250.5000	0.0000
GRID	4021	570.0700	-250.5000	0.0000
GRID	6002	610.0700	-250.5000	0.0000
GRID	6003	670.0700	-250.5000	0.0000
GRID	6004	708.0700	-250.5000	0.0000
GRID	6005	755.0700	-250.5000	0.0000
GRID	6006	802.0700	-250.5000	0.0000
GRID	6007	849.0700	-250.5000	0.0000
GRID	6008	896.0700	-250.5000	0.0000
GRID	6009	943.0700	-250.5000	0.0000
GRID	6010	990.0700	-250.5000	0.0000
GRID	6011	1037.0700	-250.5000	0.0000
GRID	6012	1084.0700	-250.5000	0.0000
GRID	6013	1131.0700	-250.5000	0.0000
GRID	6014	1178.0700	-250.5000	0.0000
GRID	6015	1221.0700	-250.5000	0.0000
GRID	6016	1253.0700	-250.5000	0.0000
GRID	6017	1285.0700	-250.5000	0.0000
GRID	6018	1317.0700	-250.5000	0.0000
GRID	6019	1349.0700	-250.5000	0.0000
GRID	6020	1381.0700	-250.5000	0.0000
GRID	6021	1418.0700	-250.5000	0.0000
GRID	6022	1455.0700	-250.5000	0.0000
GRID	6023	1492.0700	-250.5000	0.0000
GRID	6024	1522.0700	-250.5000	0.0000
GRID	6025	1553.0700	-250.5000	0.0000
GRID	6026	1673.0700	-250.5000	0.0000
GRID	6027	1713.0700	-250.5000	0.0000
GRID	6028	1749.0700	-250.5000	0.0000
GRID	6029	1787.0700	-250.5000	0.0000
GRID	6030	1825.0700	-250.5000	0.0000

GRID	6031	1863.0700	-250.5000	0.0000
GRID	6032	1905.0700	-250.5000	0.0000
GRID	6033	1947.0700	-250.5000	0.0000
GRID	6034	1994.0700	-250.5000	0.0000
GRID	6035	2032.9700	-250.5000	0.0000
GRID	6036	2041.1200	-250.5000	0.0000
GRID	6037	2200.6200	-250.5000	0.0000
GRID	706	2360.6200	-250.5000	0.0000
GRID	707	2520.6200	-250.5000	0.0000
GRID	708	2680.6200	-250.5000	0.0000
GRID	709	2840.6200	-250.5000	0.0000
GRID	710	3000.6200	-250.5000	0.0000
GRID	711	3160.6200	-250.5000	0.0000
GRID	712	3214.6000	-250.5000	0.0000
GRID	713	3340.1400	-250.5000	0.0000
GRID	714	3442.6400	-250.5000	0.0000
GRID	715	3526.6800	-250.5000	0.0000
GRID	716	3652.9900	-250.5000	0.0000
GRID	717	3755.3600	-250.5000	0.0000

10.1.2 5.0 Meter Upper Stage Pre-launch Results

Figure 10.1-1 through Figure 10.1-4 show comparisons of the 5.0 meter vs. 5.5 meter results. Figure 10.1-1 indicates little if any difference in axial load results. Axial load is primarily driven by the large propellant weights.

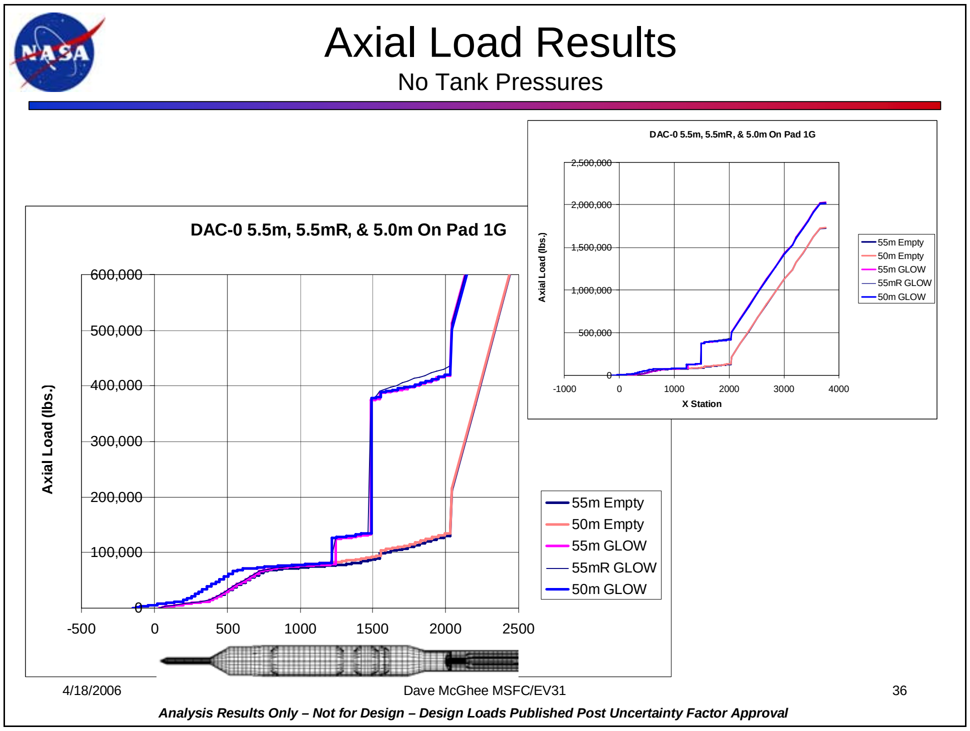

Figure 10.1-1, Pre-launch Axial Load Comparison

Figure 10.1-2 and Figure 10.1-3 indicate the higher on-pad bending moments and therefore hold-down post loads, produced by the 5.0 meter vehicle. While the 5.0 meter vehicle is narrower it is

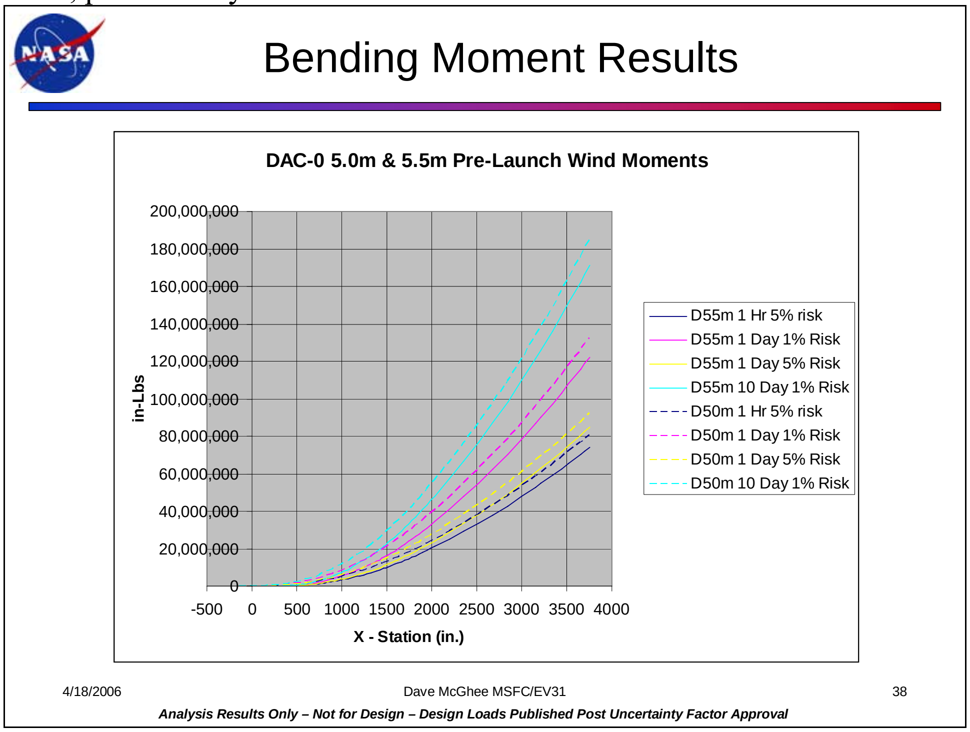

Figure 10.1-2, Pre-launch Bending Moment Comparison

Holddown Post Loads

Holddown Post Load Indicator				
Load	Indicator(KIPS)	Overall	55m	50m
Maximum F(X)	1591.49	1408.2	1340.3	1408.2
Minimum F(X)	-706.67	-469.2	-402.7	-469.2
	+ Post Compression		- Post Tension	

D55m			
		Max*	Min*
PAD 5	X	390,462	-1,340,286
	Y	56,657	-239,806
	Z	180,965	-502,736
PAD 6	X	402,674	-1,327,021
	Y	235,962	-59,021
	Z	187,484	-501,223
PAD 7	X	344,225	-1,267,260
	Y	48,957	-245,319
	Z	475,036	-164,016
PAD 8	X	331,390	-1,281,148
	Y	247,923	-45,353
	Z	484,690	-160,199

* Load as Applied to Vehicle

D50m			
		Max*	Min*
PAD 5	X	456,972	-1,408,177
	Y	68,637	-252,006
	Z	207,946	-530,187
PAD 6	X	469,199	-1,394,907
	Y	248,089	-70,933
	Z	214,684	-528,889
PAD 7	X	405,820	-1,330,218
	Y	60,815	-257,407
	Z	500,633	-189,152
PAD 8	X	392,970	-1,344,110
	Y	259,940	-57,136
	Z	510,506	-185,541

* Load as Applied to Vehicle

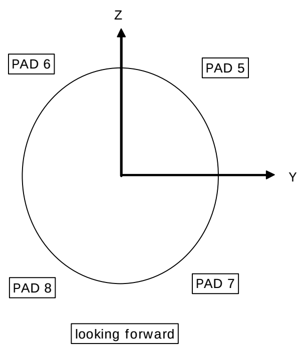

4/18/2006 Dave McGhee MSFC/EV31 39

Analysis Results Only – Not for Design – Design Loads Published Post Uncertainty Factor Approval

Figure 10.1-3, Hold-Down Post Load Comparison

longer and therefore increases bending moment. Additionally the wind speeds are a function of height above the surface. Finally, Figure 10.1-4 shows the accompanying increase in tip deflections.

Maximum On-Pad Tip Deflections

Wind	Max Tip Deflection (inches)			
		X	Y	Z
Gravity Only	D55m_Dry	1	2	1
	D55m_GLOW	1	2	1
	D50m_Dry	1	2	1
	D50m_GLOW	1	2	1
1Hr 5% Risk	D55m_Dry	2	27	19
	D55m_GLOW	2	27	19
	D50m_Dry	2	32	24
	D50m_GLOW	2	32	24
1Day 1%Risk	D55m_Dry	2	43	31
	D55m_GLOW	2	43	31
	D50m_Dry	2	52	38
	D50m_GLOW	2	52	38

Wind	Max Tip Deflection (inches)			
		X	Y	Z
1Day 5%Risk	D55m_Dry	2	31	22
	D55m_GLOW	2	31	22
	D50m_Dry	2	37	27
	D50m_GLOW	2	37	27
10 Day 1% Risk	D55m_Dry	2	60	43
	D55m_GLOW	2	60	43
	D50m_Dry	2	72	53
	D50m_GLOW	2	72	53

4/18/2006 Dave McGhee MSFC/EV31 40

Analysis Results Only – Not for Design – Design Loads Published Post Uncertainty Factor Approval

Figure 10.1-4, Vehicle Tip Deflection Comparison

10.1.3 5.0 Meter Upper Stage Ascent Results

Figure 10.1-5 and Figure 10.1-6 illustrate the expected increase in bending loads for the 5.0 meter vehicle. Note the comparison was made to the 5.5 meter "unaltered" ZONAIR data. This is because at the time of the analysis there was no wind tunnel data available for the 5.0 meter configuration to anchor or scale the ZONAIR data to. See Section 5.8.1.2 for a discussion of this.

It can bee seen from Figure 10.1-6 that the aerodynamic shear load is lower in the Upper Stage region but is shifted forward due to the increased length. The dotted line is an approximate attempt to compare equivalent loads for equivalent sections of the vehicle. As a result of this forward aerodynamic loading shift, Figure 10.1-5 shows the corresponding increase in bending moments for the majority of the vehicle.

An assessment scaling the aerodynamic loads to the now existent 5.0 meter database remains to be conducted.

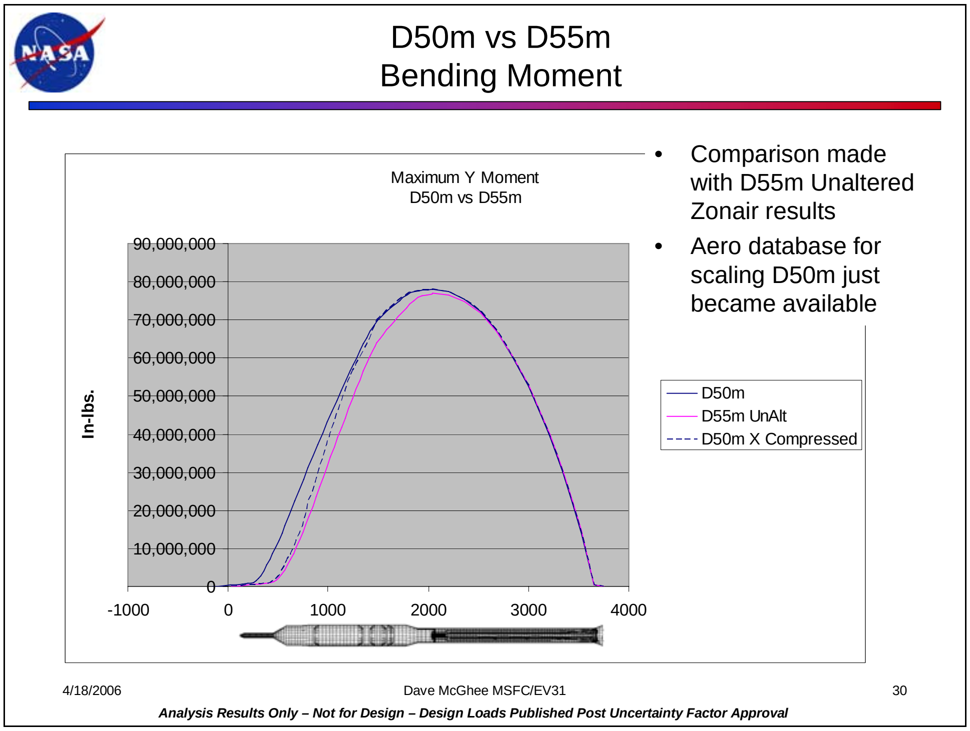

Figure 10.1-5, Ascent Bending Moment Comparison

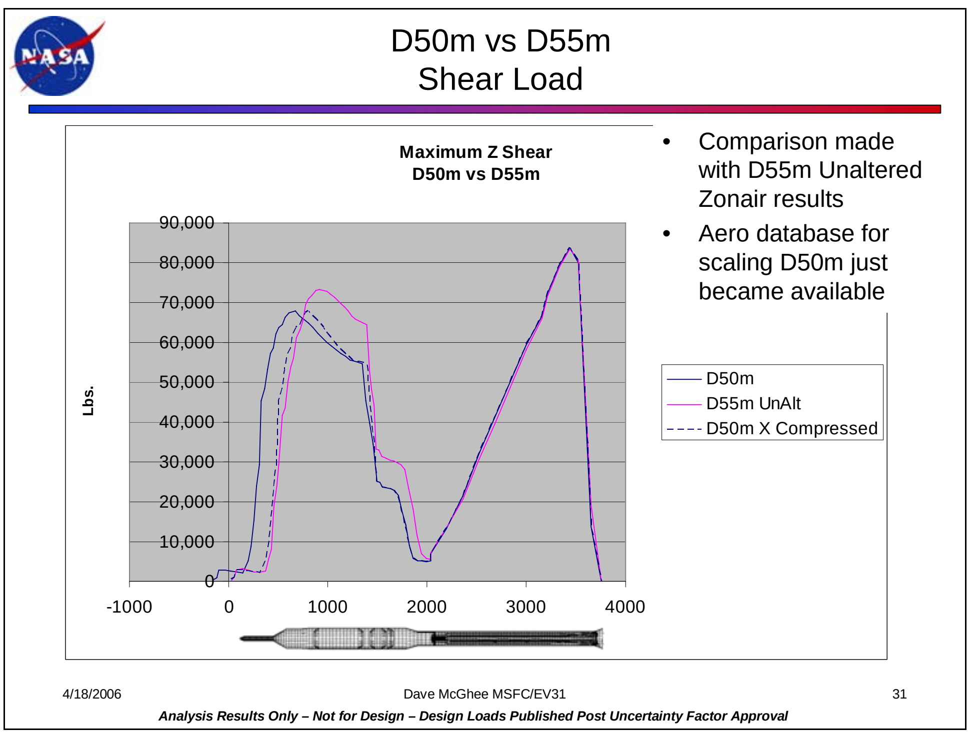

Figure 10.1-6, Ascent Shear Load Comparison

10.1.4 5.0 Meter Upper Stage Liftoff Results

As described in Section 7.1.2, transient liftoff loads analyses were performed on multiple configurations of the CLV. Two of the configurations included were the 5.0 meter Upper Stage with Lunar CEV and the 5.0 meter Upper Stage with the ISS CEV. Though the results of these analyses were not included in the LC1a design loads, they were used as part of the 5.0 Meter Upper Stage trade study.

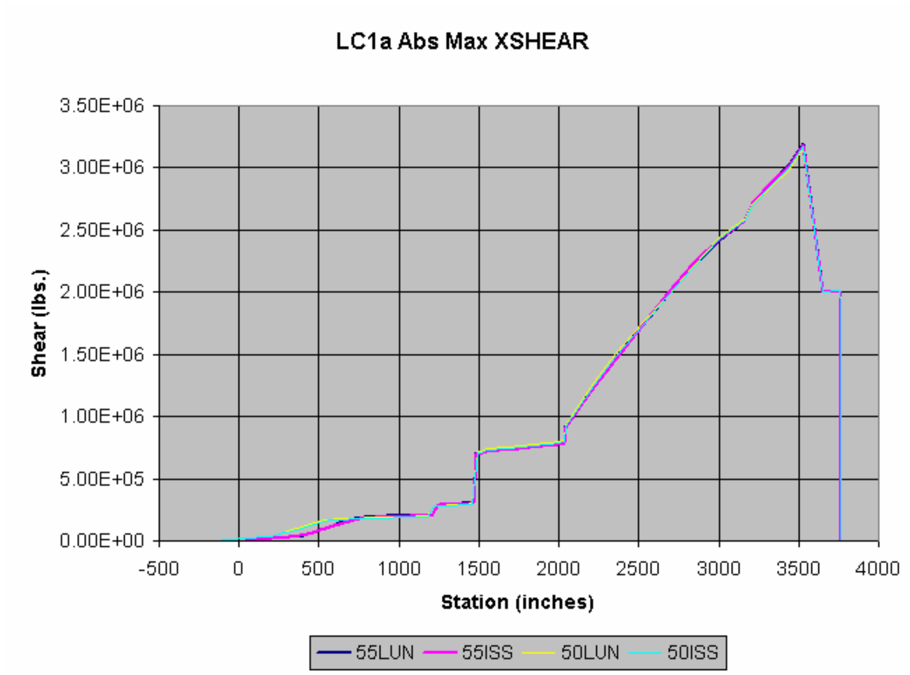

Figure 10.1-7, Liftoff Axial Load Compare

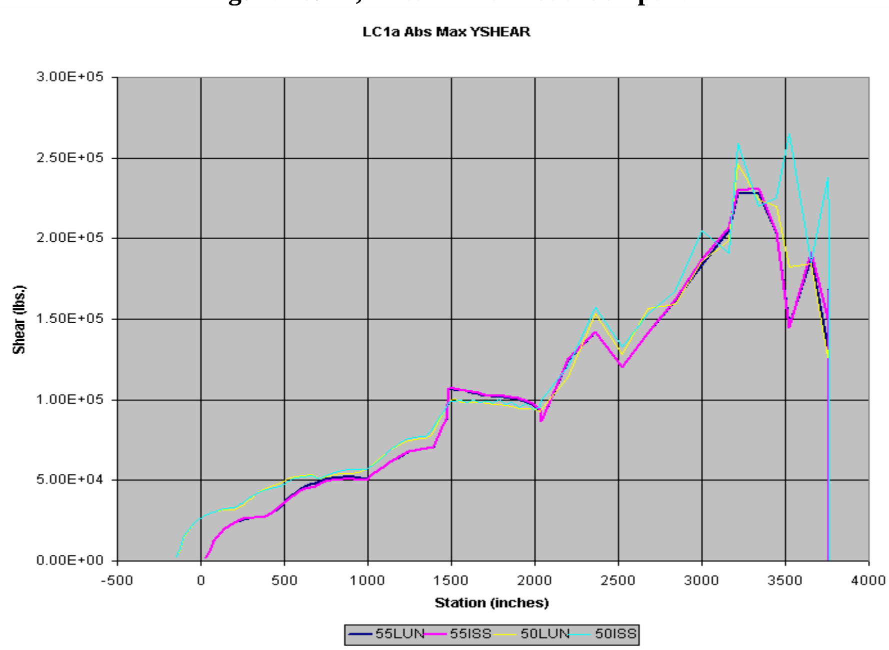

Figure 10.1-8, Liftoff Y-Shear Compare

The absolute maximum section loads and accelerations at each vehicle station from the 5.0 Meter Upper Stage were compared to the LC1a liftoff transient analysis results for the 5.5 Meter Allocated Mass Upper Stage. The comparisons can be seen in Figure 10.1-7 thru Figure 10.1-14.

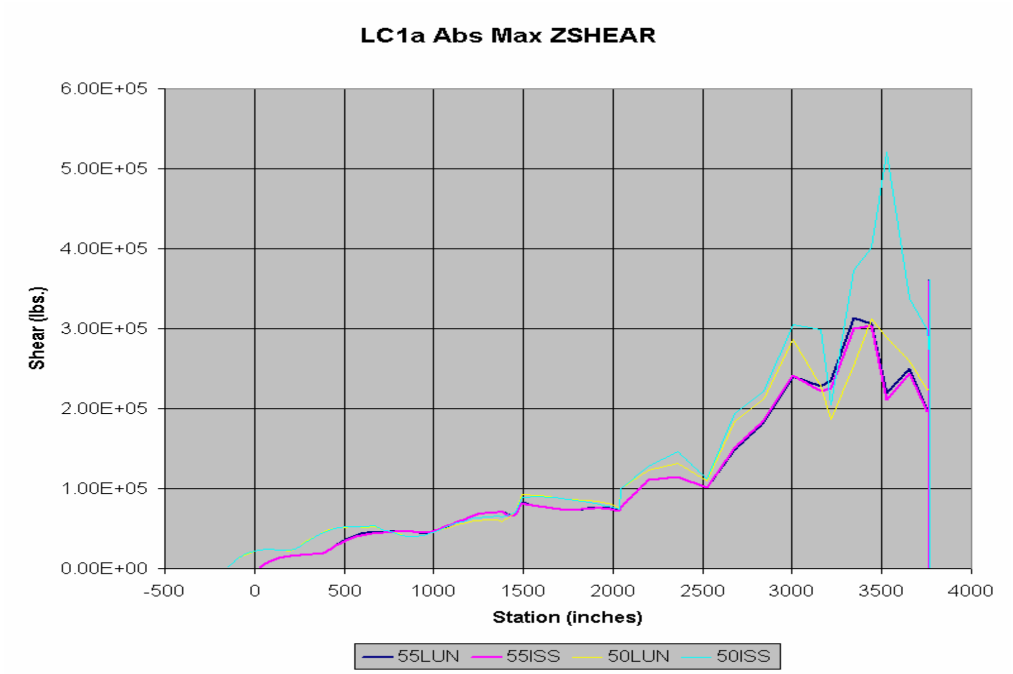

Figure 10.1-9, Liftoff Z-Shear Compare

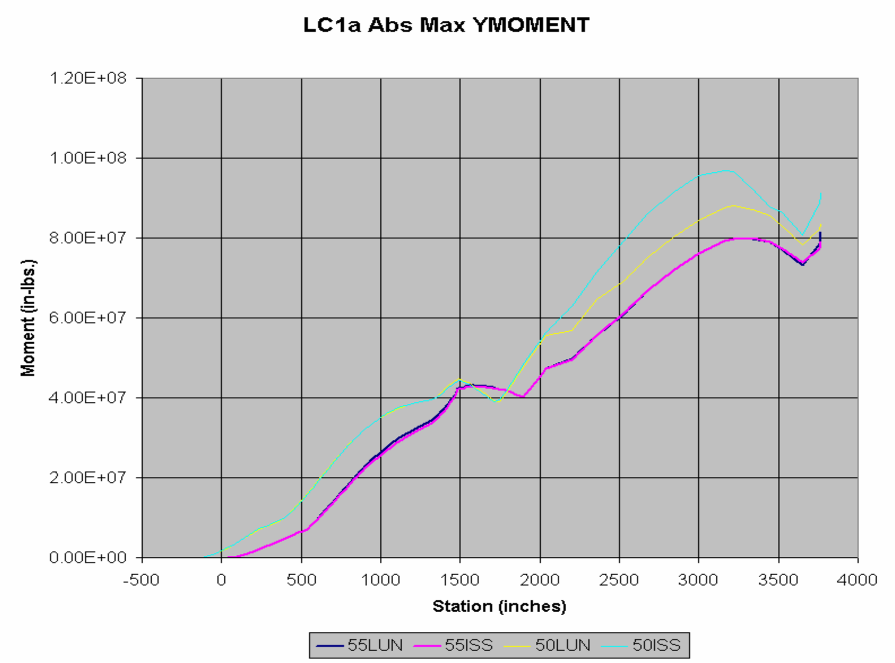

Figure 10.1-10, Liftoff Y-Moment Compare

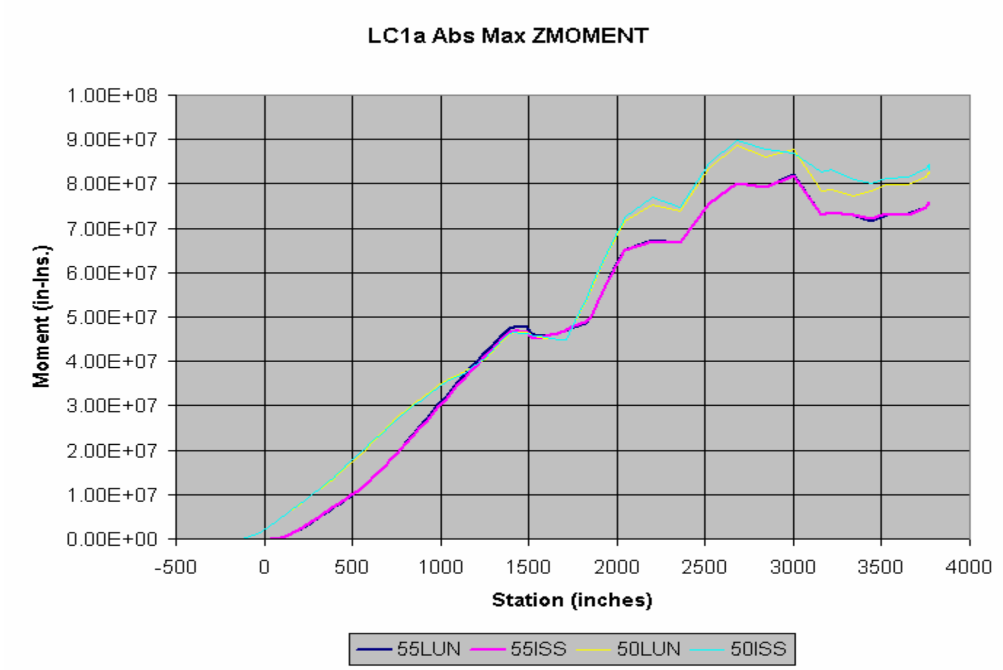

Figure 10.1-11, Liftoff Z-Moment Compare

As seen in Figure 10.1-7, there is very little difference between the 5.5 meter and 5.0 meter upper stage axial loads. Figure 10.1-8 through Figure 10.1-11 reveal that over the aft end of the vehicle, the 5.0 meter has significantly higher shear and moments than the 5.5 meter upper stage configuration.

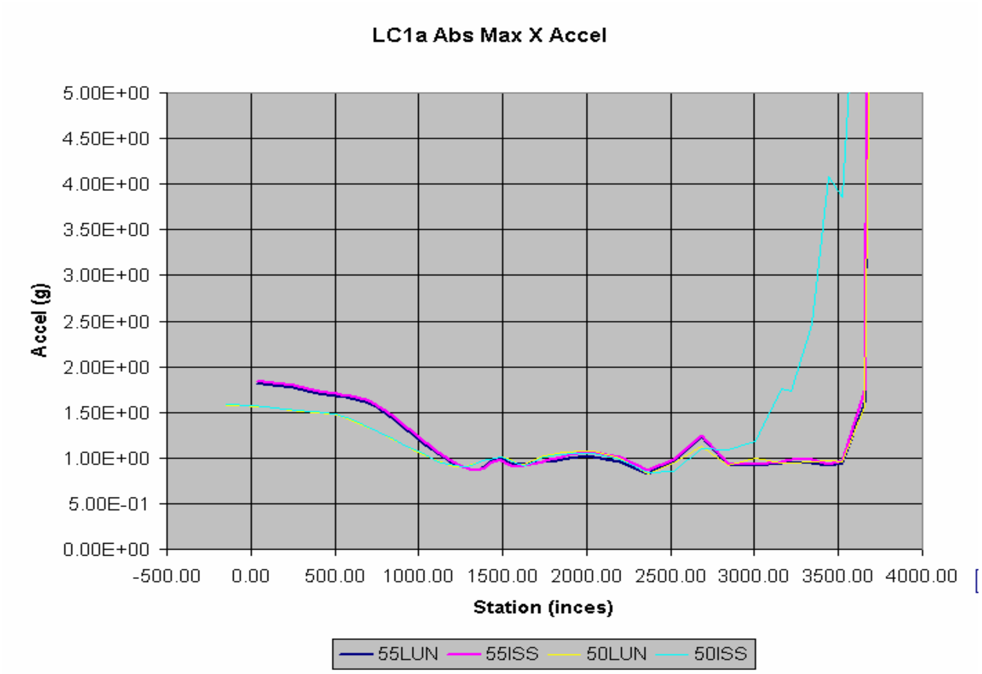

Figure 10.1-12, Liftoff X-Acceleration Compare

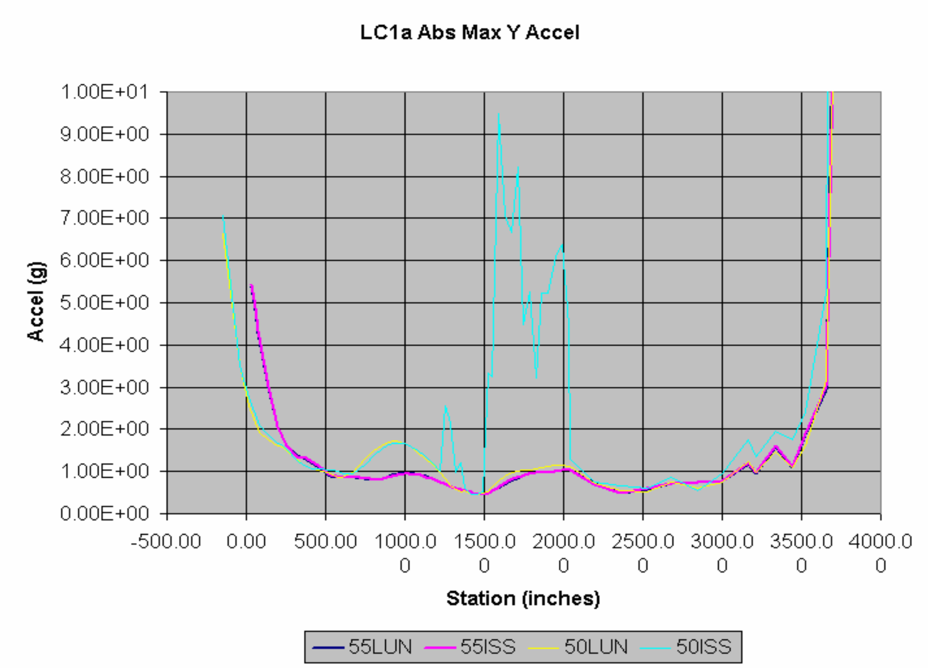

Figure 10.1-13, Liftoff Y-Acceleration Compare

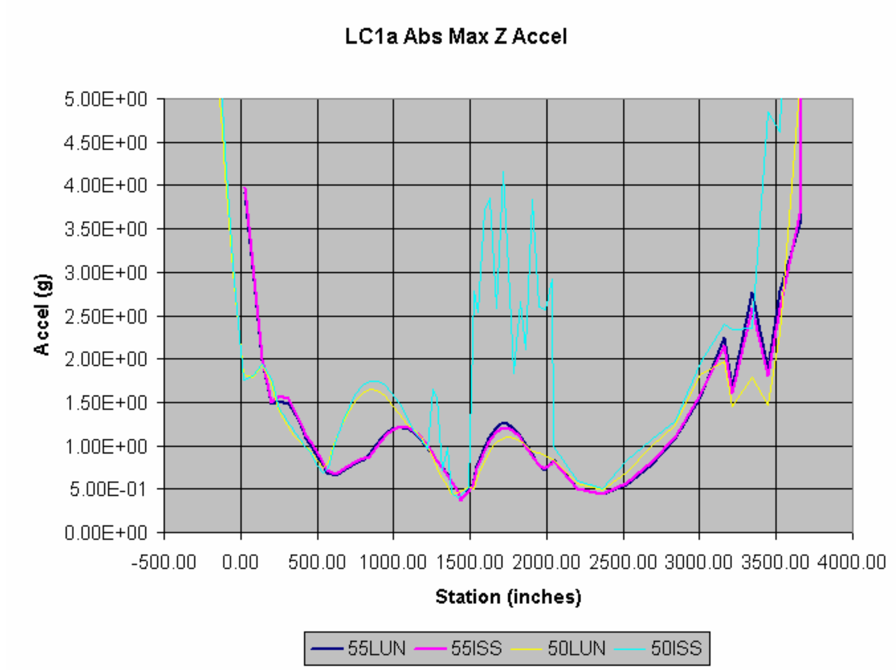

Figure 10.1-14, Liftoff Z-Acceleration Compare

Figure 10.1-12 through Figure 10.1-14 also show, though to a lesser extent, this trend in the acceleration response of the vehicle. It should be noted that for the 5.0 meter upper stage, large lateral accelerations were calculated around the LOX tank and Inter-stage. An explanation for these high responses has not yet been found and thus the results are considered questionable.

10.2 Ground Wind Capability

10.2.1 Aft Skirt Balanced Load Sets

With the possibility that there could be negative margins associated with some of the on pad wind load conditions, it was determined that ATK/USA should conduct an Aft-Skirt Capability Assessment to ensure proper margins. Therefore an Aft-Skirt Pre-launch wind Loads Assessment needed to be developed for this Aft-Skirt Capability Assessment. The Aft-Skirt Pre-launch wind Loads Assessment enabled the development of a balanced load set, so that ATK/USA could perform their Capability Assessment.

10.2.1.1 Aft-Skirt Pre-launch wind Loads Assessment Assumptions

First, the on-pad winds loads were assessed for the LC-1a vehicle configuration. The wind velocity profile imposed on this model was derived with respect to Reference 2. Pad stay times of 10, 30, 60 and 90 days with a 1% risk were assessed for this analysis. The wind directions that were applied to the model were from the north (negative y) and from the east (negative z).

The calculated wind loads are based on Reference 8. These wind loads were applied to the model as equivalent static forces based on the standard wind pressure loading on the projected frontal area of the booster. Vortex shedding was accounted for as a 1.5 multiplier on the equivalent static wind loads. There was a 1.1 uncertainty factor added to the axial loads on the vehicle, and an uncertainty factor of 1.25 added to the lateral loads. The vehicle base is assumed to be 100 feet above sea level for wind speed calculations.

The model used was identical to the one utilized in the LC1a efforts, that being the revised mass model CLV with the 5.0m CEV and the 5.5m Upper Stage. There is assumed to be no tower support, and there are also no internal pressure effects in the model. The Stack is modeled in a dry configuration also.

10.2.1.2 Aft-Skirt Pre-launch wind Loads Assessment Procedures

The procedures used to derive the on-pad wind loads in this case are the same as those for the LC1a effort as described above.

The efforts to derive a case consistent hold-down post load set were as follows. First, the wind loads over the aft skirt were removed from the load set. It was assumed that their deletion would have little overall affect on the applicability of the solution. That gave the resolved loads at the top of the aft skirt. The hold-down post loads were then extracted.

10.2.1.3 Aft-Skirt Pre-launch wind Loads Assessment Results

The results for the 10, 30, 60 and 90 day 1% risk wind cases are shown below in Figure 10.2-1.

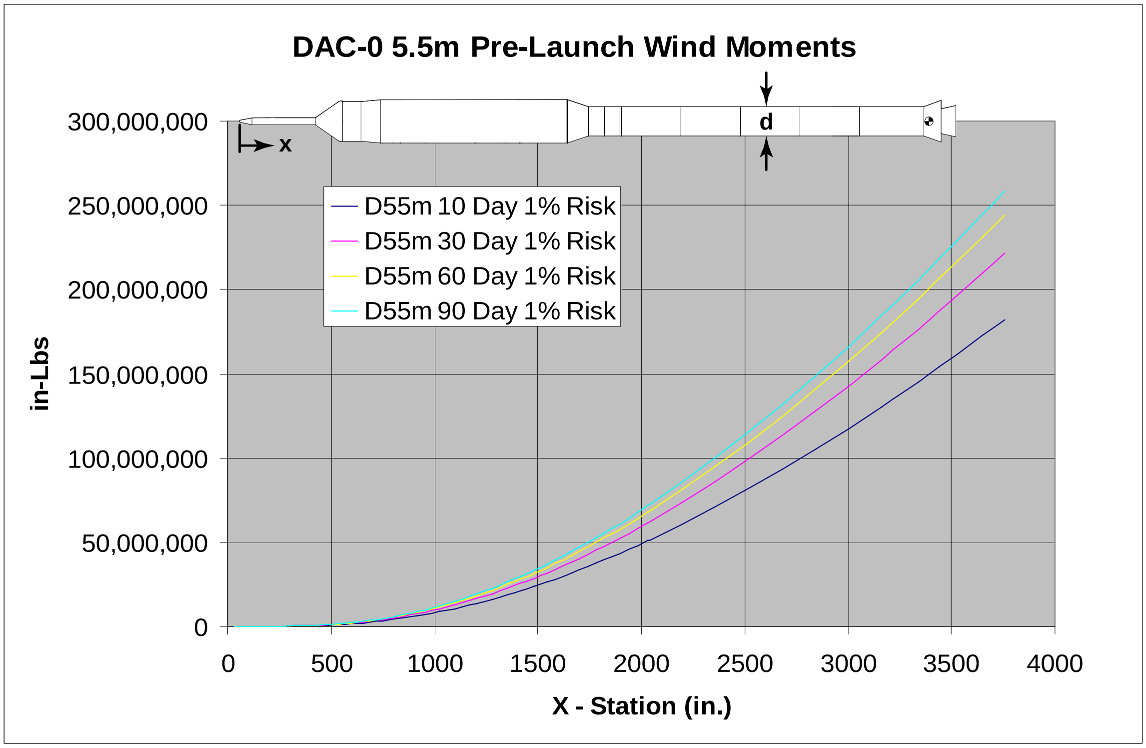

Figure 10.2-1, Moments induced by 10, 30, 60 and 90 Day winds with 1% risk

10.2.1.4 Reported Case Consistent Hold-Down Post Loads

The case consistent hold-down post loads as reported to ATK/USA are shown in Table 10.2-1:

Table 10.2-1, Aft Skirt Balanced Load Set

CALCULATED LOADS RESOLVED TO TOP OF AFT SKIRT, NODE #718

	SHEAR	(LONG AND SHORT SIDES)		
DAYS	**10**	**30**	**60**	**90**
SHEAR(LBF)	**89793.24**	**109515.70**	**120891.00**	**127947.37**

	MOMENTS	(LONG AND SHORT SIDES)		
DAYS	**10**	**30**	**60**	**90**
MOMENT(IN*LBF)	**172826962.40**	**210090663.78**	**231555848.95**	**244862642.59**

	MOMENT ARM FROM CP TO AFT SKIRT INTERFACE			
DAYS	**10**	**30**	**60**	**90**
MOMENT ARM(IN.)	**1799.58**	**1792.21**	**1788.80**	**1786.90**

	AXIAL	(VEHICLE WT. ABOVE AFT SKIRT)		

DAYS	10	30	60	90
LOAD(LBF)	1735704.36	1735704.36	1735704.36	1735704.36

10.2.1.5 Aft-Skirt Pre-launch wind Loads Assessment Conclusions

Lastly, it was determined that the maximum wind load case was not orthogonal to the launch vehicle and MLP, the maximum load case actually is oriented at approximately 30 degrees from the easterly (negative y) wind direction towards post #7. A follow on set of case consistent hold-down post loads is being developed to address this issue.

10.2.2 USA Aft Skirt Assessment Summary

It was determined that the aft skirt needed to be evaluated for structural acceptability against the CLV loads environment. ATK/USA conducted a capability assessment of the Aft Skirt. The results of this assessment were presented to 1st Stage Engineering Review Board, Reference 24. The SRB Aft Skirts critical loads are experienced by the Shuttle during pre-launch thrust build-up of the Space Shuttle Main Engine (SSME). The SSME generated bending loads occur about the Major axis of the aft skirt foot pad pattern, Figure 10.2-2.

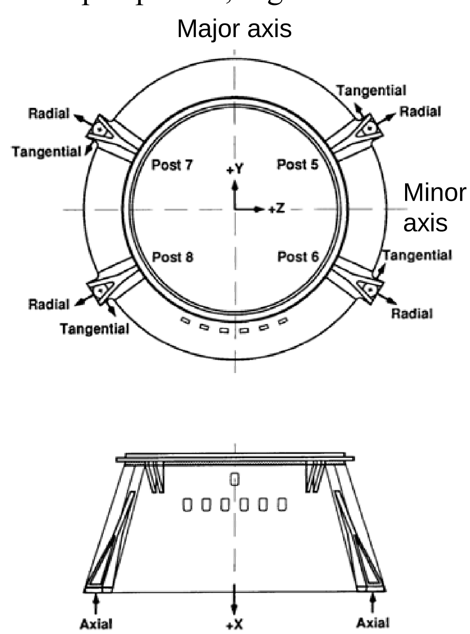

Figure 10.2-2, Left SRB to MLP post attachment drawing

For the CLV, the long exposure on-pad wind loads are considered to be the critical load case. The CLV is significantly taller than Shuttle, and the wind generated loads can cause bending about any direction, including the Minor axis of the skirt foot pad pattern. These conditions will have a significant impact to the magnitude of the foot pad loads for CLV.

The LC1a loads received included loads at the skirt hold down post. They included a gravity factor of 1.1 and a vortex shedding factor of 1.5. The loads were provided as an enveloping set of maximum and minimum values that resulted from wind load application in each of the four orthogonal directions. They were not a set of self-consistent balanced loads across all 4 posts. The loads provided were based on a 10-day 1% risk pad stay.

USA backed out a simplified wind condition that produced an axial compressive load on a post so that it matched the maximum compressive load provided by the LC1a loads data. That simplified wind condition was then applied at every 15° azimuth around the vehicle to find the highest axial compressive post load and the high axial tensile post load. Results were then compared to the STS load requirements below in Figure 10.2-3

CLV DAC-1 Load at a Worst Case Wind Direction

Maximum F(X) =1,624.19 kips on Post 6				
LH SRB	Post 5	Post 6	Post 7	Post 8
F(X)	-124.59	1624.19	-605.91	990.84
F(R)	-83.80	550.62	-160.81	409.03
F(T)	-210.50	-85.89	72.44	223.95

STS Load Requirement

SRB Maximum Compression Load Fx = 1591.49 kips				
Load	Post 1/5	Post 2/6	Post 3/7	Post 4/8
F(X)	-642.92	-403.84	1266.13	1591.49
F(R)	-63.02	20.45	308.97	411.59
F(T)	-153.97	271.26	-188.55	188.73

SRB Maximum Tension Load Fx = -706.67 kips				
Load	Post 1/5	Post 2/6	Post 3/7	Post 4/8
F(X)	-706.67	-365.78	1326.67	152.44
F(R)	-94.2	40.88	328.87	390.05
F(T)	-151.61	271.68	-188.14	188.55

Figure 10.2-3, CLV DAC-1 vs. STS Hold-down post load comparison

The following areas below were considered to be the most critical portions of the aft skirt to analyzed for the CLV pre-launch wind load conditions stated above, the letters by each area are also shown in Figure 10.2-4 and Figure 10.2-5:

a. Hold-down Post Forging
b. Hold-down Post Longitudinal Welds
c. Forward Ring/Skin Circumferential Welds
d. Hold-down Assembly
e. Kick Ring Flange/RSRM
f. Kick Ring/Forward Ring Fasteners

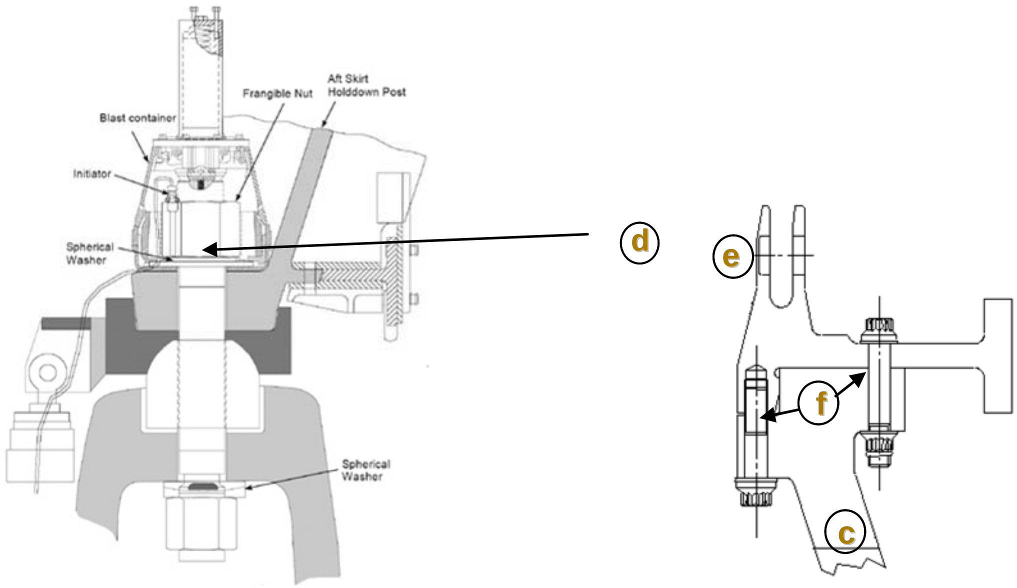

Figure 10.2-4, Left SRB Hold-Down assembly (Left) and Kick Ring assembly (Right)

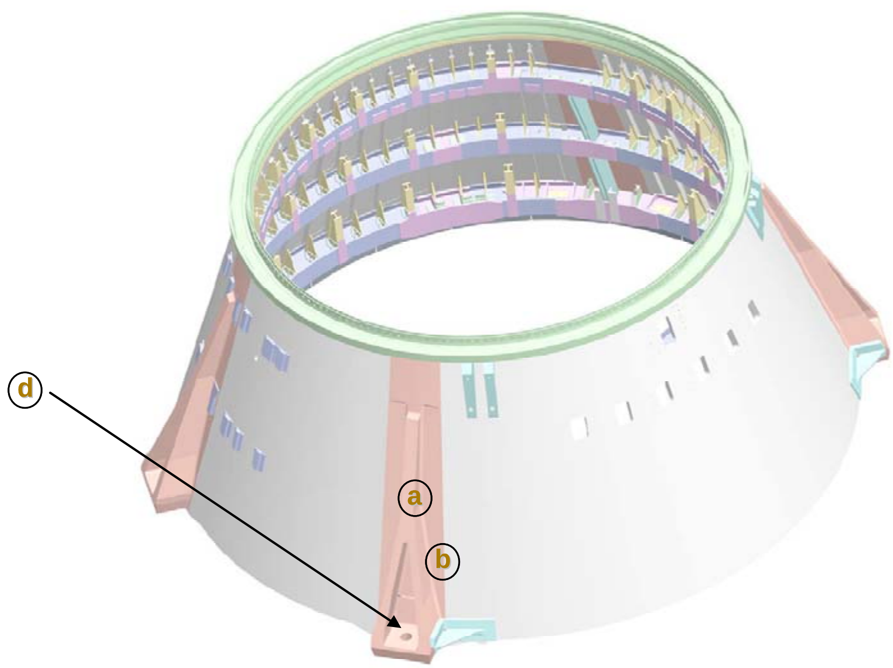

Figure 10.2-5, Left SRB Aft Skirt

Table 10.2-2, Left SRB Aft Skirt Critical area

	DAC-1 Load F.O.S.	STS F.O.S.
Holddown Post Forging	1.65	1.68
Holddown Post Longitudinal Welds	1.58 (unbrkt side)	1.50 (unbrkt side)
	2.03 (brkt side)	1.60 (brkt side)
Fwd Ring/Skin Circumferential Welds	3.30	3.00
Holddown Stud	1.75	1.68
Frangible Nut	2.14	2.02
Kick Ring Flange	3.42	2.33
Kick Ring/Fwd Ring Fastener	1.55	1.61

A comparison of the calculated factors of safety (FOS) for the aft skirt critical areas are shown in Table 10.2-2, Left SRB Aft Skirt Critical area. This table gives a comparison of the DAC-1 versus STS FOS's. Preliminary strength assessment confirms that the Aft Skirt as designed configuration meets the minimum factor of safety requirement of 1.4. This effort does not yet include a fracture assessment.

Future efforts will include an updated wind load assessment generated by MSFC that includes the new balanced load cases. This future assessment should examine multiple duration pad stay times, applied at various wind orientations to maximize post loads. It is also imperative to ensure that all dynamic wind effects (i.e., vortex shedding) have been fully captured. Specific structure unique defects would also require individual detailed strength and fracture assessments. There is also the need to assess the impact of any changes to the MLP stiffness on the loads imparted to the aft skirt.

10.2.3 180 Day On-Pad Upper Stage Wind Load Assessment

The Space Shuttle SRB post load attachment to the MLP required that the post arrangement be asymmetric to enable the structure to resist the SSME thrust buildup loads as shown in Figure 10.2-6.

In addition to the asymmetry of the MLP attachment points, the CLV is a much taller launch vehicle than the Space Shuttle. The increased height of the vehicle as well as the smaller attachment footprint to the MLP gives a much higher base bending moment for the CLV as opposed to the Space Shuttle.

The ability to resist the SSME thrust buildup load was the driver in the design of the post arrangement for the STS, this enabled extended pad stay times up to approximately 180 days in length. Conversely for the CLV, the on-pad wind stay time, even for such short durations as 10 days, are approaching the load capabilities of the 1st Stage Aft Skirt, Section 10.2.2.

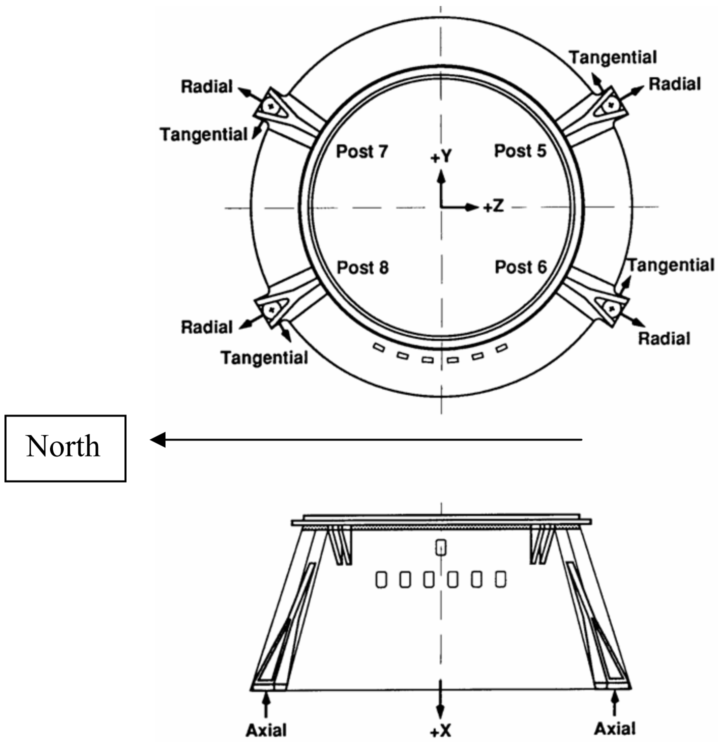

Figure 10.2-6, Left SRB to MLP post attachment drawing

Figure 10.2-7 shows the design bending moment derived for the CLV DAC-1 configuration from the LC1a efforts. As one can see that at the bottom of the vehicle, near x station number 3700, the on-pad wind loads drive the design in that region. But it is less clear how a 180 day wind load drives the Upper stage design.

Therefore, first objective of this Assessment was to determine the impact to bending moments on CLV Upper Stage for 180 day ground winds conditions. The second objective was to compare these 180 day on-pad wind loads to the LC1a Design loads to ensure that the 180 day wind loads were indeed enveloped by the design loads.

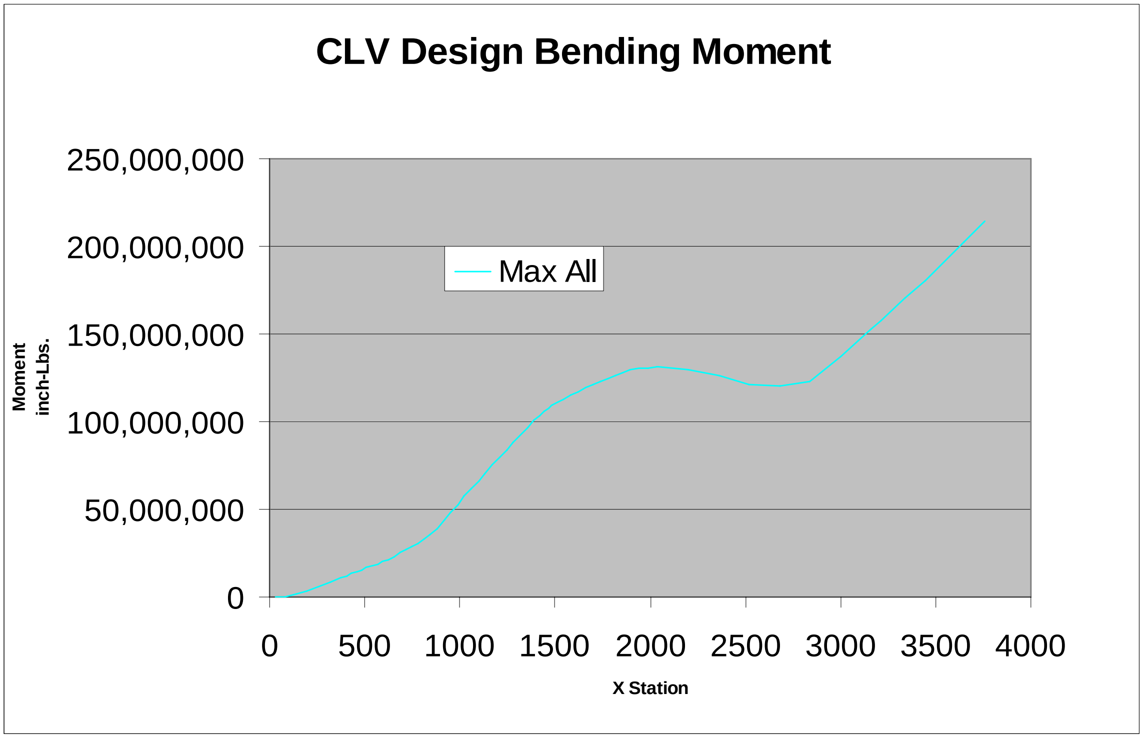

Figure 10.2-7, Ascent design bending moment

10.2.3.1 180 Day On-Pad Upper Stage Wind Load Assessment Assumptions

Firstly, the on-pad winds loads were assessed for the LC1a vehicle configuration. The wind loads imposed on this model were derived with respect to Reference 2. A pad stay time of 180 days with a 1% risk was assumed for the on-pad wind analysis.

The ground wind load cases are also based on Reference 8. The wind loads were applied to the model as equivalent static forces based on the standard wind pressure loading on the projected frontal area of the booster. There was a 1.1 uncertainty factor added to the axial loads on the vehicle, and vortex shedding was accounted for as a 1.5 multiplier on the equivalent static wind loads. The vehicle base is assumed to be 100 feet above sea level for wind speed calculations.

The model used was the D55mR revised mass model CLV with the 5.0m CEV and the 5.5m Upper Stage. There is assumed to be no tower support. There is also assumed to be no internal pressure effects in the model. The Stack is modeled in a dry configuration also.

10.2.3.2 LC1a 180 Day On-Pad Upper Stage Wind Load Assessment Procedures

The procedures used to derive the on-pad wind loads in this case are the same as those for the LC1a effort.

10.2.3.3 LC1a 180 Day On-Pad Upper Stage Wind Load Assessment Results

For a 180 day 1% risk wind case we saw approximately a 61% increase over 10 day 1% wind case in calculated bending moments at the base of the vehicle, as shown in Figure 10.2-8.

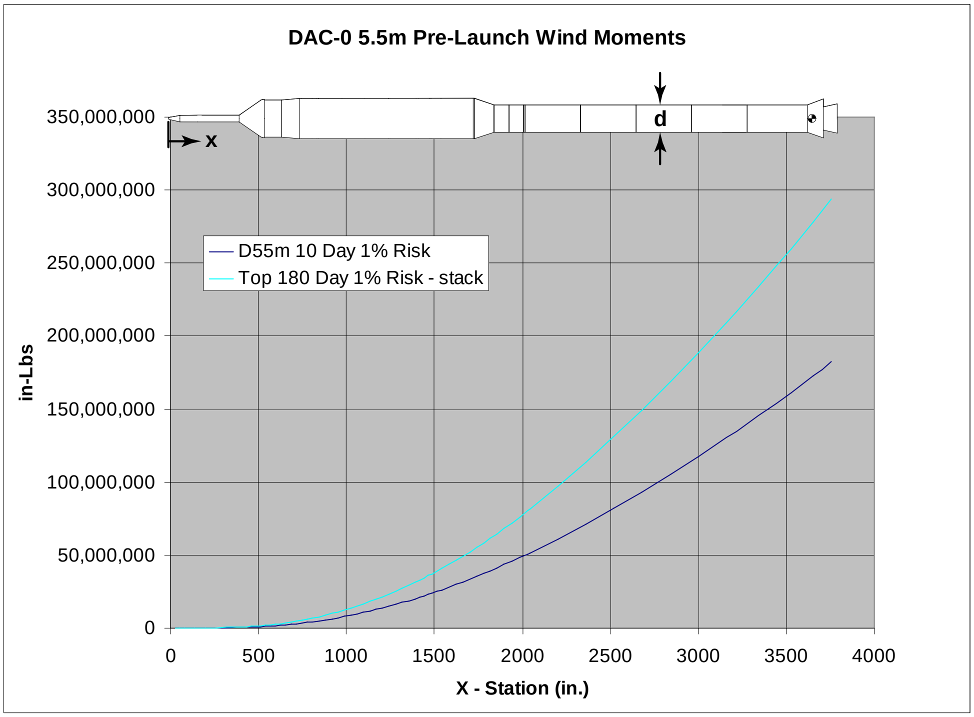

Figure 10.2-8, Comparison of Moments, 180 day 1% winds versus 10 day 1% winds

Figure 10.2-9 shows the LC1a design loads, Section 9.0 and the design loads combined with the estimated design 180 day Ground Winds. We can see that the Ground winds do not dominate the load on the vehicle until well below the upper stage/1st Stage interface.

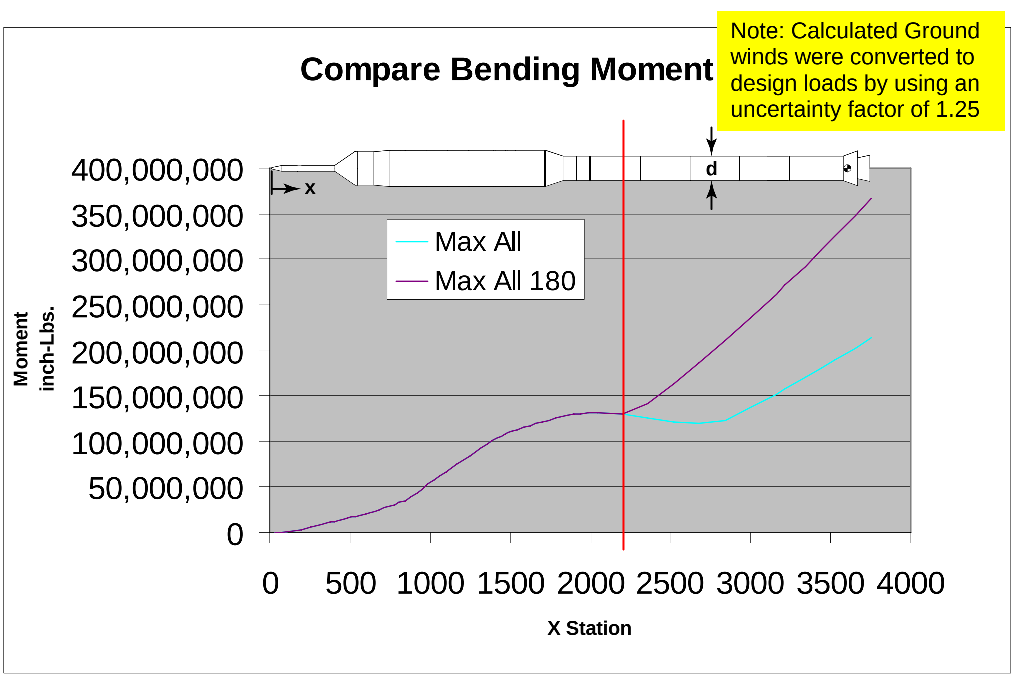

Figure 10.2-9, Comparison of Moments, 180 day 1% winds versus 10 day 1% winds

10.2.4 Conclusions and Forward Work

Upper Stage design bending moments are not exceeded by 180 day Pre-Launch winds, though a full structural assessment would be needed to verify that the 180 day wind moments, combined with the un-pressurized tank condition (pre-launch), do not affect Upper Stage sizing.

The effect of additional vehicle support to protect 1st Stage has not been assessed. But from the large increase in on-pad bending moments, it is likely that additional on-pad struts will be required for pad stay times longer than a 10 Day stay. The effect of the altered loads and load paths would also need to be assessed for on-pad bracing.

10.3 Upper Stage Nested Tank Study

Currently a large amount of the work in the CLV program is being directed towards decreasing the mass of the vehicle. In the case of the Nested Tanks study, it was thought that the shortening of the inter-tank structure would reduce the overall bending moments imposed on the launch vehicle, which would then allow the structure to be sized smaller and therefore be lighter in weight.

To ensure the maximum wet to dry mass fraction in the Apollo program, the inter-tank structure between the two fuel tanks of the S-II second stage and the S-IVB third stage used a common bulkhead that was constructed from the top of the LOX tank and bottom of the LH2 tank. It consisted of two aluminum sheets separated by a honeycomb structure made of phenol. This had to insulate against the 70 °C (125 °F) temperature difference between the two tanks, and is thought to have saved approximately 3.6 metric tons in weight in the S-II stage alone.

Due to a lack of confidence in the maturity level of the technology needed to inspect the bonded aluminum face sheets to the honeycomb structure, a nested tank concept was envisioned that would allow inspections of the tank dome exteriors and would also shorten the overall vehicle length, it would also allow the application of enough insulation for the liquid hydrogen tank dome to preclude fuel boil-off.

The CLV Nested Tank studies were done to investigate the sensitivities that length reductions in the inter-tank structure have on maximum CLV loading conditions, both on-pad and ascent loads were examined. There were two studies completed, referred as NT1 and NT2. The first study, NT1, was a quick look study that modified the current ascent aerodynamics database and then used those “shortened” loads on the current CLV model. The second Nested Tank study, NT2, consisted of reusing the “shortened aerodynamics from NT1, as well as creating a new reduced finite element beam model of the proper length.

10.3.1 Nest Tank Study 1, NT1

The premise of the quick look NT1 study was to determine the loads imposed on a launch vehicle with a nested tank Upper Stage in the timeliest manner possible. The turnaround time needed for this study precluded any changes to the ascent simulation model, which were not in and of themselves difficult, but the associated simulation bookkeeping can sometimes become the most difficult part of developing a new model. It was assumed that the aerodynamic load on the vehicle was the primary driver of bending loads during the ascent regime, therefore the inertial loads imposed by the unmodified model could be assumed to be negligible in comparison. The model used for this study was the Lunar Stack Configuration, the 5.0m CEV and a 5.5m Upper stage with revised masses, D55mR.

Firstly, the on-pad winds loads were assessed. For this potion of the NT1 analysis a new wind profile was created to represent the wind loads imposed on the shortened vehicle. A pad stay time of 10 days with a 1% risk was assumed for the on-pad wind analysis. F.

For the on-pad wind loads portion of the NT1 study, approximately a 7% reduction in wind moments at the base of the vehicle was seen, as shown in Figure 10.3-1.

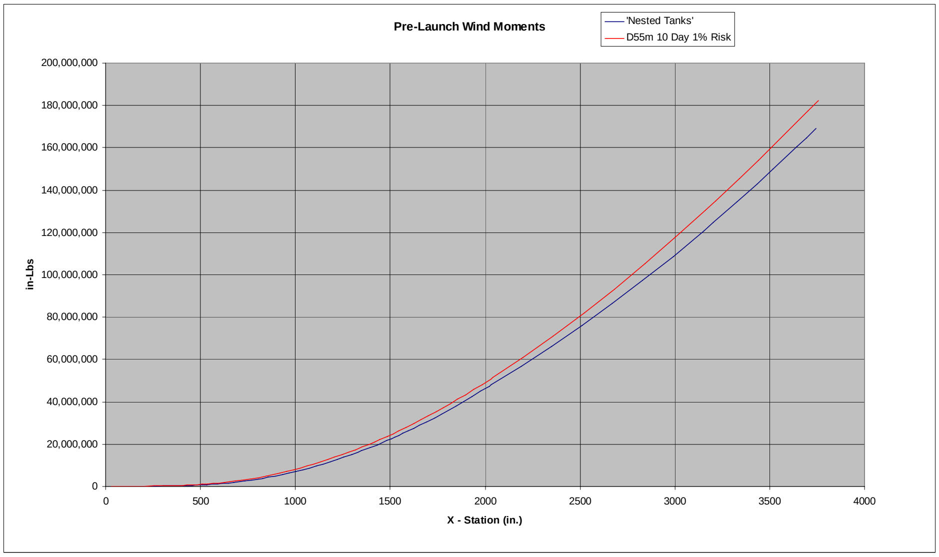

Figure 10.3-1, NT1 vs. LC-1a CLV on-pad wind load comparison

For the ascent portion of NT1, the current aerodynamic database was simply modified by shortening it 50 inches. Approximately 50” of Normal Force coefficients (CN) near the nested tank area were “clipped” to produce an aerodynamic load that a shorter vehicle would experience, Figure 10.3-2 shows vertical lines that represent the portion of the vehicle where the CN values were removed to simulate a shorter vehicle length. All other factors were unchanged for the ascent simulation.

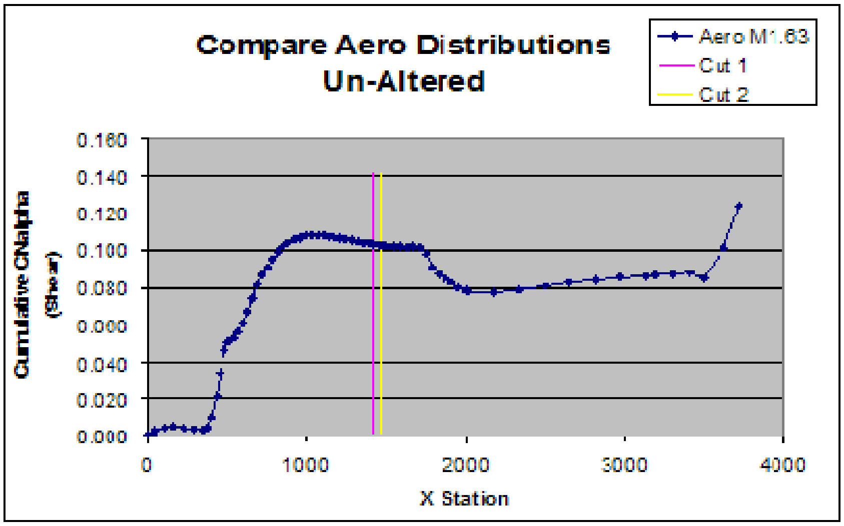

Figure 10.3-2, Chart showing area from which CN values were clipped

This shortened aero distribution was remapped to the existing vehicle model. The ascent simulation was run in the same manner as was done in LC1a, and an approximately 16% reduction was seen in bending moments between the Nested Tank and the LC-1a loads.

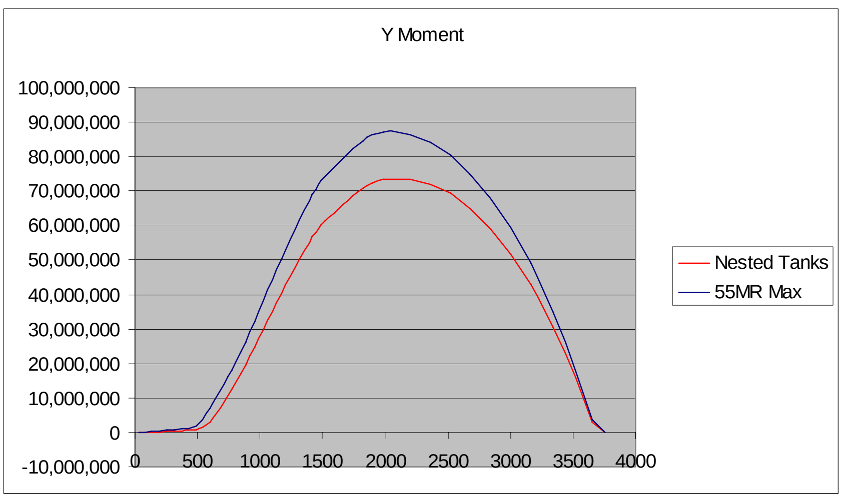

Figure 10.3-3, Ascent bending moment comparison, Nested tank to LC-1a

10.3.2 Nested Tank Study 2, NT2

The intent of NT2 was to build on the NT1 study, to refine the analysis by building a new model to be used in the ascent simulations, this involved more work than NT1 so therefore more time was allotted for the analysis.

Shown below, in Figure 10.3-4, is a comparison of the LC-1a model, top figure, versus the NT2 model, bottom figure. The NT2 model was shortened by 60 inches overall, 43 inches of which were eliminated from the inter-tank region. To nest the tanks, the aft LH2 tank dome was inverted with respect to the LC-1a configuration. This also necessitated changing the manner in which the propellant was modeled in the upper stage as well. To keep the same volume of fluid in the LH2 tank, with the inverted dome, the LH2 cylinder length was increased to 471.33 inches. Since these are just beam models, and the nested tank configuration has some fairly heavy ring frames at the base of the LH2 tank, the mass of the reconfigured model did not match the target mass for the stage. But as was mentioned earlier in the NT1 study, the inertial loads are considered to be secondary to the aerodynamic loads. Lastly, there was a needed coordinate transform for the NT2 model because of its shortened length. This also made it necessary to modify the coordinate system of the 5.0m CEV as well.

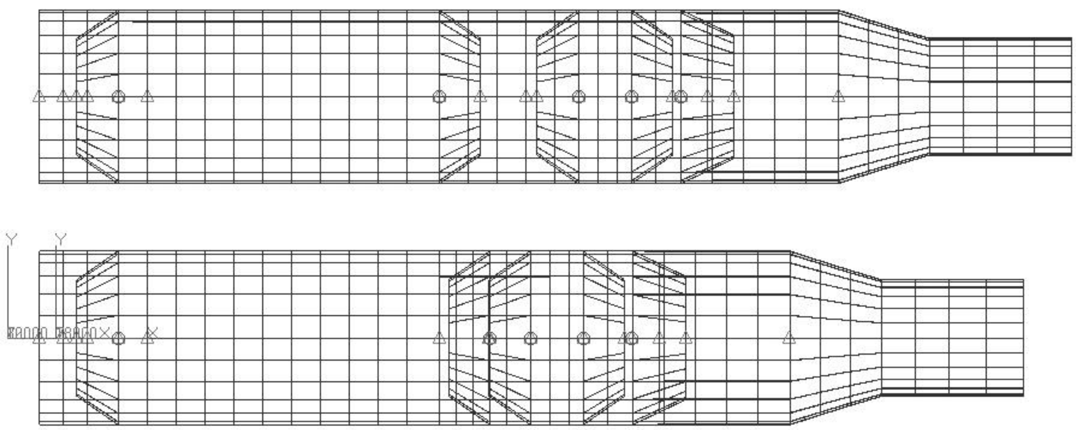

Figure 10.3-4, D55mR vs. NT2 model differences

As in the NT1 study, an on-pad wind load assessment was performed first, in exactly the same manner. For the 10 day 1% risk winds, an approximately 7% reduction in bending moment at the base of the vehicle was seen, as shown in Figure 10.3-5. This was approximately the same on-pad bending moments as the NT1 study produced.

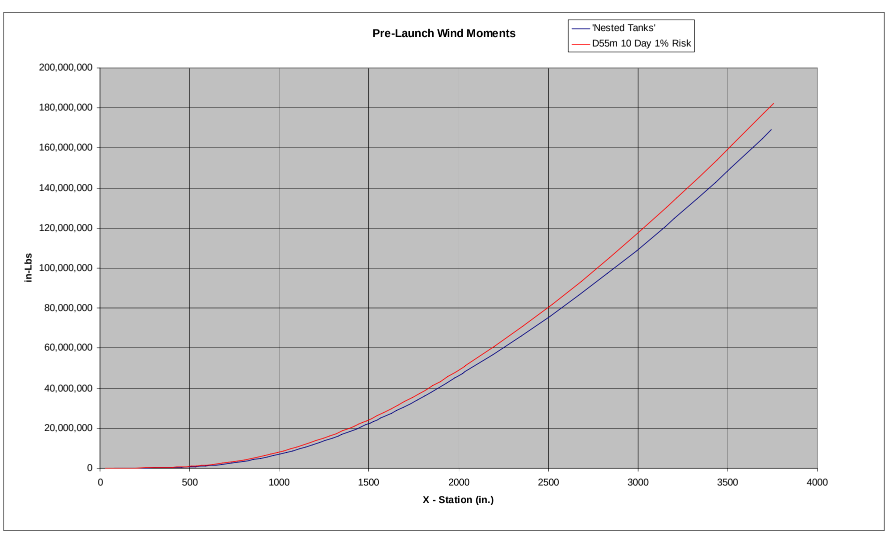

Figure 10.3-5, NT2 vs. LC-1a CLV on-pad wind load comparison

Once the ascent simulation was complete, an approximately 8% reduction was seen in the bending moment for the Nested Tank configuration, as compared to the current LC-1a configuration.

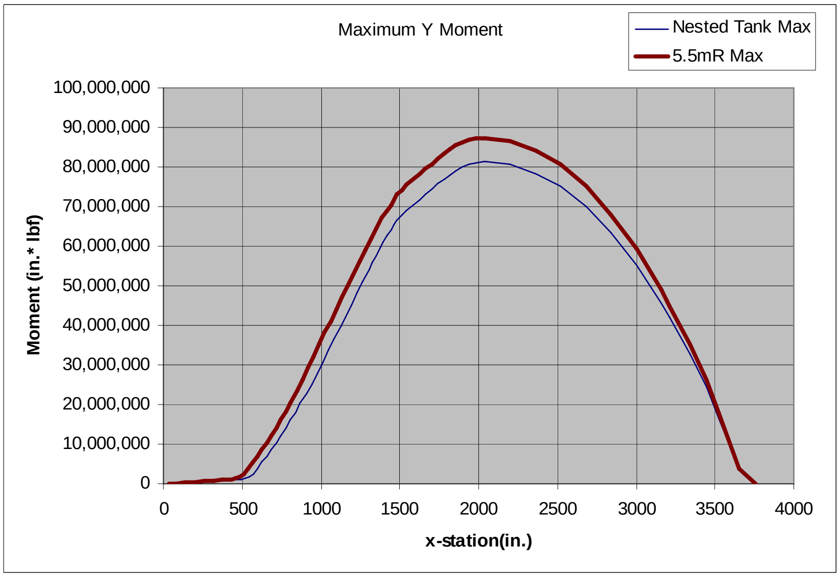

Figure 10.3-6, Ascent bending moment comparison, NT2 to LC-1a

10.4 Integrated CEV / CLV Stack Frequency Assessment

At the request of the CEV Program, the Vehicle Integration Loads Team conducted an assessment of stack frequencies integrating two CEV configurations under study.

A 3D FEM model of the Crew Exploration Vehicle Lunar configuration stack consisting of the Command Module, the Service Module and the Launch Abort System was received from JSC-CEV in May 2006. A summary of the models delivered is contained in a file named "CEV_FEM_DAC2_summary.doc" contained in Appendix D. The set of bulk data files had two assembly options - one with the regular Launch Abort System tower and another with a Launch Abort System tower modified with a bi-conic structural adapter to accommodate an APAS-LIDS adapter combination mounted atop the CM. Both assemblies were built and integrated with the remaining sections of the LC-1a D55mR FEM; the Upper Stage all-beam model and the FSB 3D model. Additionally, these two stacks were compared to the lunar configuration of the LC-1a D55mR FEM featuring an all-beam CEV model. Figure 10.4-1 shows all three stack configurations. Table 10.4-1, Free-free Mode Frequency Comparisons for Several CEV /CLV Integrated Stacks compares results from Free-Free runs of the stacks with frequencies matched by mode shape. In general, the stack with the Upper Stage all-beam model shows higher frequencies than those using the 3D CEV models. The frequencies for the stack featuring the biconic LAS configuration are barely higher than those for the regular LAS configuration, showing not much stiffness improvement offered by the selected biconic LAS geometry. There were some modeling issues noted with the delivered CEV models, particularly the (weak) support structure for the Service Module tanks. However, the lower stack modes do not appear to be significantly affected. Improved iterations of these models should nonetheless give better results.

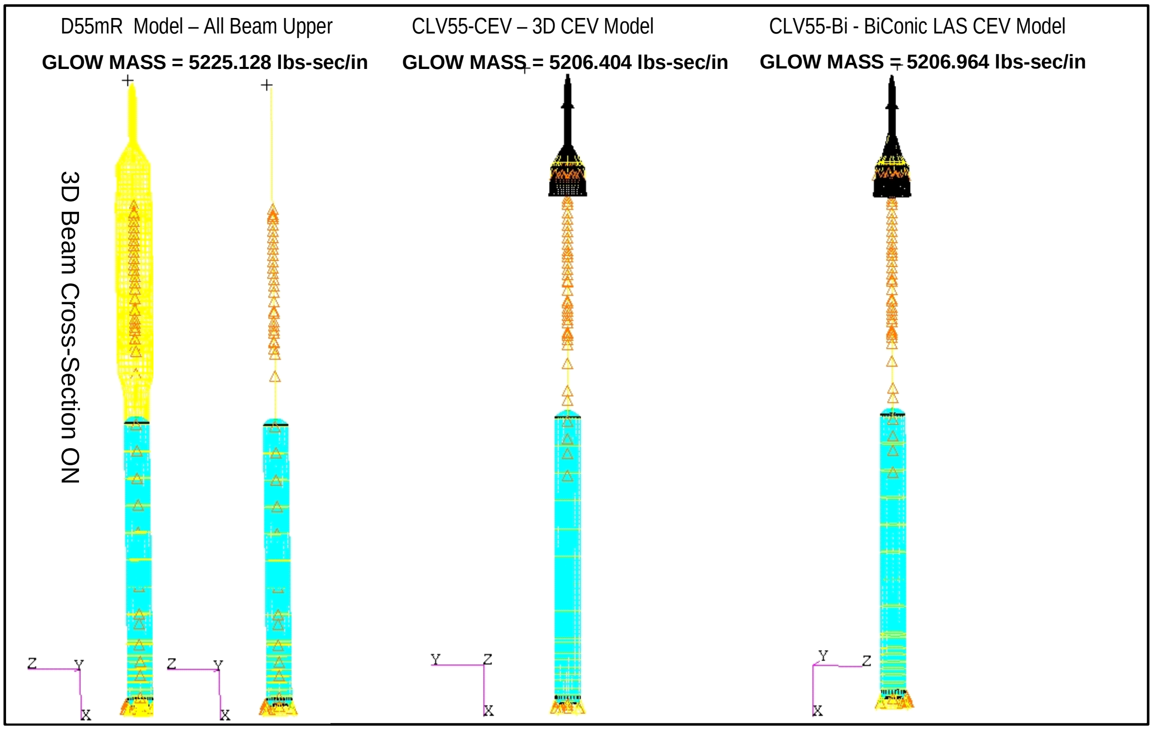

Figure 10.4-1, Stack Configurations with beam and 3D CEV models

Table 10.4-1, Free-free Mode Frequency Comparisons for Several CEV /CLV Integrated Stacks

D55mR All Beam Upper		CLV55-CEV 3D CEV Model		CLV55-BiConic Biconic LAS CEV Model		Mode Shape
Mode #	Frequency (Hz)	Mode #	Frequency (Hz)	Mode #	Frequency (Hz)	Description
7	1.0	7	1.0	7	1.0	1st Bending
8	1.0	8	1.0	8	1.0	1st Bending
9	2.4	9	2.2	9	2.3	2nd Bending
10	2.4	10	2.2	10	2.3	2nd Bending
11	4.4	11	3.2	12	3.8	3rd Bending
12	4.4	12	3.2	13	3.8	3rd Bending
13	5.7	14	4.6	14	4.7	4th Bending
14	5.7	15	4.6	15	4.7	4th Bending

10.5 Liftoff Transient Overpressure Sensitivity Study

The intent of the Overpressure Sensitivity Study was to 1) verify that the 1.5 "overpressure uncertainty factor" on the LC1a Liftoff Transient loads was conservative and 2) to investigate the relative effects of the different overpressure configuration had on the vehicle section loads.

To investigate these questions, only one vehicle configuration was used, the Allocated Mass CLV with a Lunar CEV. This was deemed acceptable since the sensitivity to the overpressures should be similar for the other vehicle configurations, and it greatly reduced the number of load cases required.

10.5.1 Parameters for Overpressure Sensitivity Study

Three parameters were varied for the study. These were four incident wind directions (top wind (+/-z) and left side wind (+/-y)), three SRB thrust rise rates (a maximum, minimum and nominal) and four over pressure cases.

The four wind cases consisted of 1 Hour winds at a 5% risk level as documented in the Section 7.1.1. A 1.5 scale factor was multiplied to the results to account for Wind Induced Oscillation. Four wind cases were included to investigate the interplay between the different wind directions and the directional overpressure forcing functions. This is in contrast to the original liftoff analysis, were the models and forcing functions were primarily symmetric, and therefore, two wind directions were judged to be adequate.

The SRB thrust forces include the nominal CLVFSB05306 case, the maximum case (late ignition, low thrust rise rate-low total thrust), and minimum case (early ignition, high thrust rise rate-high total thrust) as described in 5.9.2. Each of the three SRB thrust traces had corresponding overpressure time histories.

The overpressure cases consisted of different combinations of overpressure waves from the various overpressure sources. These sources are illustrated in figure 5.9-8, and are the right SRB hole (RSRB), the SSME hole (SSME), the left SRB hole (LSRB, which is the symmetric overpressure) and the flame trench (FT). Table 10.5-1 gives a basic description of the four different cases used in the sensitivity study.

Table 10.5-1, Overpressure Cases

Case	Description	OP Sources	Legend
1	No overpressure	none	55LUN
2	All overpressure sources	LSRB, RSRB, SSME, FT	55LUN OP
3	Overpressure from flame trench only	FT	55LUN FT OP
4	All overpressure except symmetric	RSRB, SSME, FT	55LUN OP w/o SYM

The first case, no overpressure, corresponds roughly to using water suppression. Cases 2) and 3) represent the effect of having the right SRB and SSME holes covered or not. And case 4) was included to determine if any axial load may be expected from the symmetric overpressure wave. Further information on the FSB ignition overpressure can be found in section 5.9.2.4.

10.5.2 Load Cases

Investigating the three parameters using a full factorial design (all possible combinations), results in 48 load cases. These are shown in Table 10.5-2. The colored rows indicate those cases that were run in LC1a.

Table 10.5-2, Liftoff Overpressure Sensitivity Study Load Cases

LOAD CASE	WIND	THRUST	OP
LO0052	SIDE (+y)	MAX RISE RATE	NO
LO0004	SIDE (+y)	NOMINAL	NO
LO0051	SIDE (+y)	MIN RISE RATE	NO
LO0050	TOP (-z)	MAX RISE RATE	NO
LO0003	TOP (-z)	NOMINAL	NO
LO0049	TOP (-z)	MIN RISE RATE	NO
LO0077	SIDE (-y)	MAX RISE RATE	NO
LO0078	SIDE (-y)	NOMINAL	NO
LO0079	SIDE (-y)	MIN RISE RATE	NO
LO0080	TOP (+z)	MAX RISE RATE	NO
LO0081	TOP (+z)	NOMINAL	NO
LO0082	TOP (+z)	MIN RISE RATE	NO
LO0016	SIDE (+y)	MAX RISE RATE	YES
LO0010	SIDE (+y)	NOMINAL	YES
LO0022	SIDE (+y)	MIN RISE RATE	YES
LO0015	TOP (-z)	MAX RISE RATE	YES
LO0009	TOP (-z)	NOMINAL	YES
LO0021	TOP (-z)	MIN RISE RATE	YES
LO0059	SIDE (-y)	MAX RISE RATE	YES
LO0060	SIDE (-y)	NOMINAL	YES
LO0061	SIDE (-y)	MIN RISE RATE	YES
LO0062	TOP (+z)	MAX RISE RATE	YES
LO0063	TOP (+z)	NOMINAL	YES
LO0064	TOP (+z)	MIN RISE RATE	YES
LO0053	SIDE (+y)	MAX RISE RATE	FT ONLY
LO0054	SIDE (+y)	NOMINAL	FT ONLY
LO0055	SIDE (+y)	MIN RISE RATE	FT ONLY
LO0056	TOP (-z)	MAX RISE RATE	FT ONLY
LO0057	TOP (-z)	NOMINAL	FT ONLY
LO0058	TOP (-z)	MIN RISE RATE	FT ONLY
LO0065	SIDE (-y)	MAX RISE RATE	FT ONLY
LO0066	SIDE (-y)	NOMINAL	FT ONLY
LO0067	SIDE (-y)	MIN RISE RATE	FT ONLY
LO0068	TOP (+z)	MAX RISE RATE	FT ONLY

LO0069	TOP (+z)	NOMINAL	FT ONLY
LO0070	TOP (+z)	MIN RISE RATE	FT ONLY
LO0071	SIDE (+y)	MAX RISE RATE	W/O SYM
LO0072	SIDE (+y)	NOMINAL	W/O SYM
LO0073	SIDE (+y)	MIN RISE RATE	W/O SYM
LO0074	TOP (-z)	MAX RISE RATE	W/O SYM
LO0075	TOP (-z)	NOMINAL	W/O SYM
LO0076	TOP (-z)	MIN RISE RATE	W/O SYM
LO0083	SIDE (-y)	MAX RISE RATE	W/O SYM
LO0084	SIDE (-y)	NOMINAL	W/O SYM
LO0085	SIDE (-y)	MIN RISE RATE	W/O SYM
LO0086	TOP (+z)	MAX RISE RATE	W/O SYM
LO0087	TOP (+z)	NOMINAL	W/O SYM
LO0088	TOP (+z)	MIN RISE RATE	W/O SYM

10.5.3 Results

Figure 10.5-1 though Figure 10.5-4 present selected results from the overpressure sensitivity study. For the full set of results, see Reference 25.

The following figures present the moment and shear loads as a percentage, or scale factor, of the published LC1a loads. The loads from the sensitivity study do not contain the 1.5 uncertainty factor on lateral load; while the LC1a loads they are scaled to do contain this factor. Thus, as long as the curves in Figure 10.5-1 and Figure 10.5-2 are below 1.0, the liftoff loads with overpressure do not exceed the published design loads, and the 1.5 uncertainty is adequate. The plots in Figure 10.5-1 and Figure 10.5-2 are typical of the other running forces in that they are enveloped by the LC1a forces (see Reference 25).

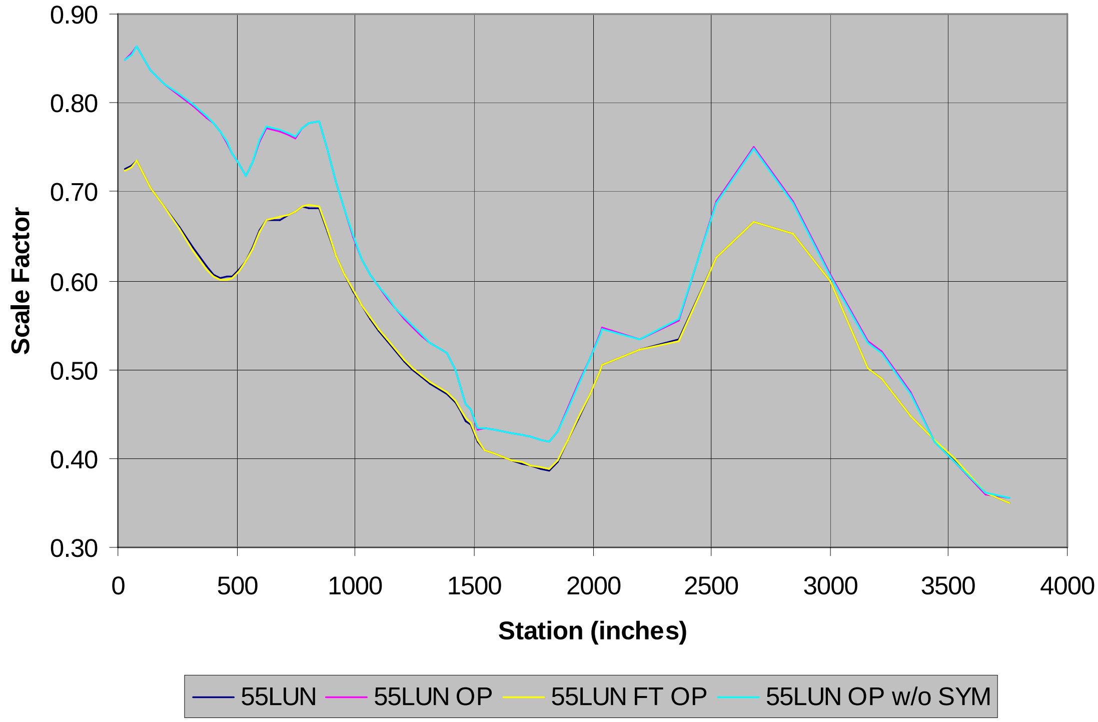

Figure 10.5-1, Z moment as a percentage of the LC1a design loads

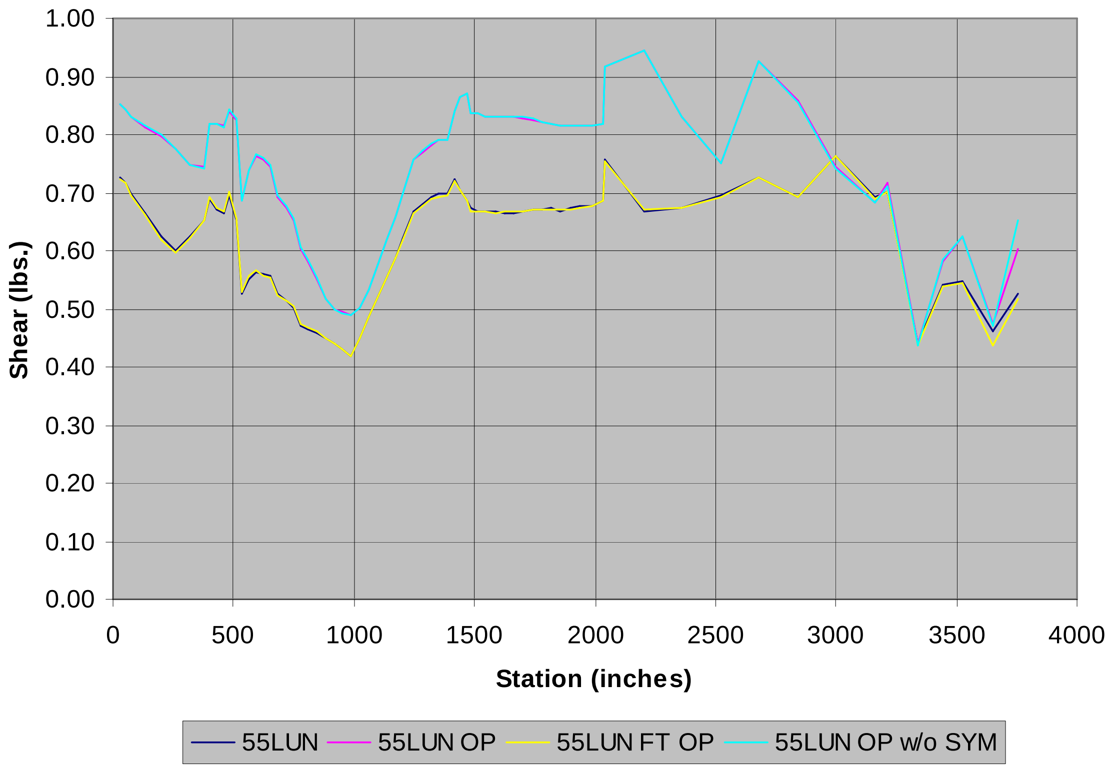

Figure 10.5-2, Y shear as a percentage of the LC1a design loads

Figure 10.5-3 and Figure 10.5-4 are plots of the Y and Z direction accelerations respectively, scaled to the LC1a accelerations. As can be seen, both of these plots show exceedances. While the causes for these exceedances are not fully understood, the following factors seem to be the most likely candidates;

1. The overpressure sensitivity results include more wind and dispersed thrust combinations than were run for the LC1a set. This is the primary reason for the small exceedances of Figure 10.5-3, where the extra combinations of wind and thrust dispersions caused minor differences in dynamic response.
2. The LC1a load set did not contain a load case with Y direction winds and thrust dispersions. The dispersed thrust loads, combined with the Y direction winds seem to have an unexpected affect on the behavior of the hold down post loads. For the Y wind with max thrust, the time between the separation of the "tension" posts and the "compression" posts is shorter. This seems to be exciting some higher frequency modes that the Z wind with max thrust, thus causing higher dynamic response.
3. The LC1a lateral accelerations do not contain the intended 1.5 uncertainty factor. Instead, a 1.1 uncertainty factor was mistakenly used. (The 1.1 uncertainty factor was correctly applied to the axial accelerations.)

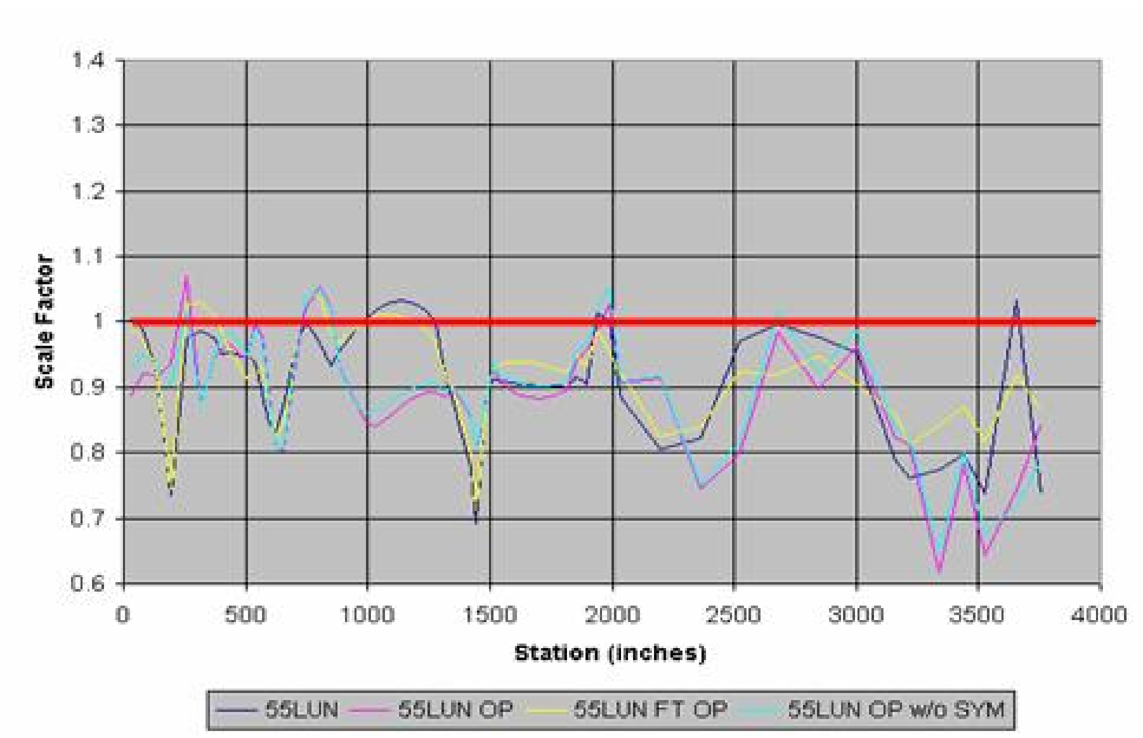

Figure 10.5-3, Z Direction Acceleration as a percentage of LC1a Y Acceleration

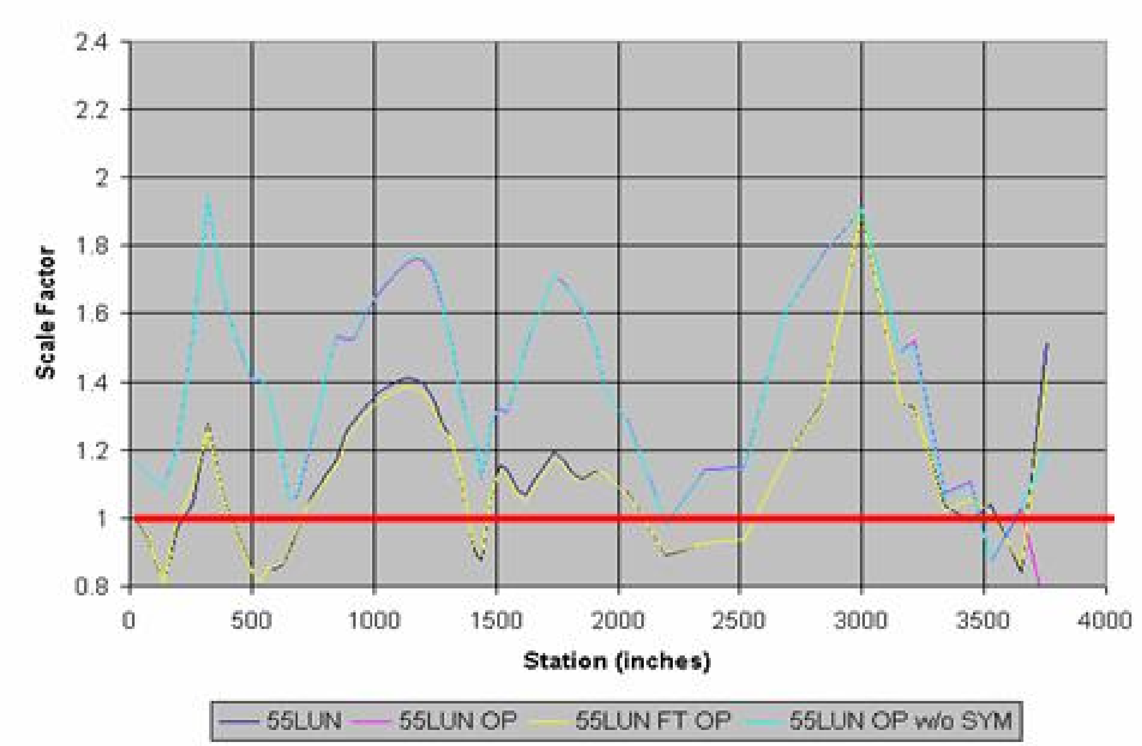

Figure 10.5-4, Y Direction Acceleration as a percentage of LC1a Y Acceleration

10.5.4 Conclusions and Future Work

By comparing the loads and accelerations from the LC1a published results, to the Liftoff Overpressure Sensitivity Study loads and accelerations, the following conclusions can be drawn:

1. Inclusion of the reciprocal incidence wind directions is necessary. Though the vehicle is symmetric, the overpressures are not. The interaction between the wind direction and overpressure timing can adversely affect vehicle loads.
2. Inclusion of symmetric overpressure has minimal effects. Symmetric overpressure source is the least important overpressure to loads.
3. Exclusion of RH SRB and SSME hole over pressure sources significantly reduces YSHEAR and ZMOMENT. RH SRB and SSME overpressure sources are the most important to loads.
4. All Overpressure Sensitivity Study liftoff section loads are covered by LC1a Design Loads.
5. All Overpressure Sensitivity Study liftoff accelerations are NOT covered by LC1a Design Loads.

Based on the findings of this study, it is apparent that using a reduced set of load cases in a highly dynamic environment such as liftoff, can miss some critical parameter interactions. Therefore, future liftoff analyses will consist of a full set of load cases, which will consider all possible combinations of the various parameter values (i.e. a full factorial Design Of

Experiments approach). Using this approach, the number of load cases can become very large, very fast, depending on the number of parameters, and parameter values considered. For this reason, efforts are underway to streamline the liftoff calculation so we may increase the number of load cases which may be handled in a reasonable amount of time.

Appendix A: Definition of Symbols, Acronyms, and Abbreviations

CLV - Crew Launch Vehicle
CEV - Crew Exploration Vehicle
FEM – Finite Element Model
FF-1STBO - Free-Free First stage Burn Out
FF-2NDIGN - Free-Free Second stage Ignition
FF-2NDBO - Free-Free Second stage Burn Out (i.e. Cutoff)
FSB - First Stage Booster
FSM - First Stage Motor
GLOW– Gross Liftoff Weight
KSC - Kennedy Space Center
LOX - Liquid Oxygen
LH2 - Liquid Hydrogen
MBPT - Mean Bulk Propellant Temperature
MPS – Main Propulsion System
MLP – Mobile Launch Platform
LUT – Launch Umbilical Tower
FSS – Flight Support Structure
LMS - Launch Management System
WIO – Wind Induced Oscillation
LAS - Launch Abort System
LAM - Launch Abort Motor
CM - Crew Module
SM - Service Module
SRB - Solid Rocket Booster
RSRM - Reusable Solid Rocket Motor
SSME - Space Shuttle Main Engine
SSP - Space Shuttle Program
ISS - International Space Station

Appendix B.1: Reference Mass Properties: “Memo1 FSB J2X.doc”

Dear Sirs:

Mass estimates for the Five Segment Booster (PBAND)/J2X CLV concept contained in Attachment 1 and 2 represent the best understanding of the Engineering Directorate at the initiation of DAC-0. These initial estimates were the developed in cooperation with the CLV Project Office and MSFCs Advanced Concepts Department. The bases of the estimates are also documented in Attachments 1 and 2. These target masses assume a Project Office margin of 15% of the estimated payload limit.

For the initial design verification cycle, the Project Offices have challenged Engineering to beat the target masses (also called “bogies”) noted in the far column of Attachment 3. For the Upper Stage Project, most target masses are subdivided into the Integrated Product Team (IPT) level. The exception is the Structures and Thermal IPT, where target masses are further subdivided into Spacecraft Adapter, Core Stage and Interstage.

Geoffrey Beech, PE
Systems Analysis Team Lead

Attachment 1

MASS PROPERTIES ACCOUNTING								
VEHICLE:	5 Segment-PBAN SRB with 1 J-2S+ Crew - Blk II							
STAGE:	First Stage FSB-PBAND							Basis of Estimate
	MASS SUBTOTALS			MASS	CENTERS OF GRAVITY			
	Tertiary	Secondary	Primary	TOTALS	CGx	CGy	CGz	
ITEM	lbm	lbm	lbm	lbm	x/blgth	y/bwidth	z/bwidth	
STAGE:	First 5 Segment SRB							
Forward Frustrum			24,185					provided by D. Blackwell 01/14/06
Structure								
Recovery System								
Separation System								
Avionics								
SRB (all other)			191,195					dry mass-frustrum mass
Segment Exit Cone								
Aft Skirt								
TVC								
BSMs								
Systems Tunnel								
Cabling								
Propellant								
DFI*								
STAGE DRY MASS W/O GROWTH				215,380				provided by D. Blackwell 01/14/06
Dry Mass Growth Allowance			5,123					
STAGE DRY MASS W/GROWTH (mdry)				220,503				
Residuals:			2,068					
Unburned Propellant		68						
Main propellant (slag retained)		2,000				TBD		
Inert expended			-8,132					
STAGE BURNOUT MASS (mbo)				214,439				
Total mass expelled:			1,397,785					
Motor Propellant		1,389,721						
Unburned Propellant		-68						
Inert mass		8,132						
FIRST STAGE GROSS LIFTOFF MASS (mgross)				1,612,224				
Interstage			9,070					
Second Stage Gross Liftoff Mass			317,261					
Launch Escape System			13,228					
Payload			55,140					
NET VEHICLE GROSS LIFTOFF MASS (mgross_veh)				2,006,922				

Attachment 2

New Nominal MASS PROPERTIES (01/15/2006 POST traj)					
	Tertiary	**Secondary**	**Primary**	**TOTALS**	**Basis of Estimation (BoE)**
Primary Body Structures:			14,336		sum
IU, CLV		790			UG VIPA/SA-CEV /Structure
Forward skirt		486			UG VIPA/FwdSkt/ Structure
Liquid Oxygen tank		3,298			INTROS
Intertank		1,811			INTROS
Liquid Hydrogen tank		5,757			INTROS
Aft compartment		0			INTROS
Thrust structure		2,195			UG VIPA/Thrust/ Structure
Secondary Structures:			700		sum
Base closeout structure		0			none
Propellant tank baffles:		700			sum
Liquid Oxygen slosh	376				**INTROS/Proj. Ofc / S. Cook**
Liquid Oxygen sump	245				**INTROS/Proj. Ofc / S. Cook**
Liquid Oxygen vortex	14				**INTROS/Proj. Ofc / S. Cook**
Liquid Hydrogen slosh	34				**INTROS/Proj. Ofc / S. Cook**
Liquid Hydrogen vortex	32				UG VIPA
Mounting Rings			0		
Access Doors			21		UG VIPA/Intertank/Door
Systems Tunnel			322		UG VIPA/Sys Tun/Structure
Separation Systems:			0		sum
Stage-to-Stage		0			none
Thermal Protection Systems (TPS):			144		sum
IU, CLV side		12			UG VIPA/SA-CEV /TPS
Forward skirt		6			UG VIPA/FwdSkt/ TPS
Intertank		72			UG VIPA/Intertank/TPS
Base closeout structure TPS		54			UG VIPA/Thrust/ TPS
Thermal Control Systems (TCS):			901		sum
Liquid Oxygen tank insulation		142			UG VIPA/LOXTank/TPS
Liquid Hydrogen tank insulation		487			UG VIPA/LH2 Tank/TPS
Internal insulation		0			none
Equipment cooling		0			none
Purge, vent, drain & haz gas dtn		272			INTROS
					sum
Intertank					UG VIPA
Main Propulsion System:			8,923		sum
Engine(s)		5,100			**Proj. Ofc / S. Cook**
Engine installation		12			UG VIPA/MPS/Gimbal seat,body,pin
TVC hardware		351			INTROS
Propellant feed systems group:		2,355			sum
Liquid Oxygen feed system	480				UG VIPA/MPS/LOXfeedline
Liquid Hydrogen feed system	1,875				UG VIPA/MPS/LH2feedline
Pressurization systems group:		148			sum
Liquid Oxygen press system	0				none
Liquid Hydrogen press system	147				UG VIPA/LH2Tank
RCS	1				UG VIPA/RCS
Fill and drain systems group:		307			sum
Liquid Oxygen fill and drain	192				UG VIPA/MPS/LOX f&d
Liquid Hydrogen fill and drain	115				UG VIPA/MPS/LH2 f&d
Gas vent systems group:		325			sum
Oxygen gas vent	150				UG VIPA/MPS/Vent Assy
Hydrogen gas vent	176				UG VIPA/MPS/Vent Assy
Engine pneumatic system		325			MPS IPT
Auxilary Propulsion System:			784		sum
RCS group:		784			UG VIPA/RCS/dry mass
APU			830		UG VIPA/Thrust/APU

Attachment 2 (cont'd)

Power - Electrical:			0		
Battery System:		0			
Battery cells	0				
Circuitry	0				
Power - Hydraulic:			248		sum
Hydraulic APUs		56			INTROS
Fuel storage & plumbing		17			INTROS
Conversion & distribution		111			INTROS
Cooling system		63			INTROS
Avionics:			733		**Proj. Ofc / S. Cook**
GN&C		n/a			
RF Communications		n/a			
Instrumentation		n/a			
Data mgmt/handling		n/a			
Range Safety (electronics)		n/a			
Miscellaneous:			153		sum
Range safety (ordinances)		153			sum
Liquid Oxygen LSC	50				INTROS
Liquid Hydrogen LSC	103				INTROS
STAGE DRY MASS W/O GROWTH				28,096	22,996
Dry mass growth allowance			3,449		15% (excludes Engine)
STAGE DRY MASS W/GROWTH				31,545	
Residuals:			2,917		sum
Main propellant (liquid residual)		2,589			
Prop Tank Pressurization Gases:		310			sum
Liquid Oxygen tank	118				MPS IPT
Liquid Hydrogen tank	192				INTROS
RCS propellant		6			INTROS
Subsystems		12			INTROS
Reserves:			2,448	5,364	sum
Main propellant		1,992			MPS IPT
Fuel bias		374			INTROS
RCS propellant		75			INTROS
APU reactants		6			INTROS
Inflight Fluid Losses:			41		sum
APU reactants		41			INTROS
Main Propulsion System:			8,923		sum
Engine(s)		5,100			**Proj. Ofc / S. Cook**
Engine installation		12			UG VIPA/MPS/Gimbal seat,body,pin
TVC hardware		351			INTROS
Propellant feed systems group:		2,355			sum
Liquid Oxygen feed system	480				UG VIPA/MPS/LOXfeedline
Liquid Hydrogen feed system	1,875				UG VIPA/MPS/LH2feedline
Pressurization systems group:		148			sum
Liquid Oxygen press system	0				none
Liquid Hydrogen press system	147				UG VIPA/LH2Tank
RCS	1				UG VIPA/RCS
Fill and drain systems group:		307			sum
Liquid Oxygen fill and drain	192				UG VIPA/MPS/LOX f&d
Liquid Hydrogen fill and drain	115				UG VIPA/MPS/LH2 f&d
Gas vent systems group:		325			sum
Oxygen gas vent	150				UG VIPA/MPS/Vent Assy
Hydrogen gas vent	176				UG VIPA/MPS/Vent Assy
Engine pneumatic system		325			MPS IPT
Auxilary Propulsion System:			784		sum
RCS group:		784			UG VIPA/RCS/dry mass
APU			830		UG VIPA/Thrust/APU
Miscellaneous:			0		
Crew and crew provisions		0			
STAGE BURNOUT MASS				37,250	

Attachment 2 (cont'd)

Main Ascent Propellant:			279,979		sum
Liquid Oxygen		236,506			INTROS
Liquid Hydrogen		43,474			INTROS
Engine purge helium			32		INTROS
RCS ascent propellant			300		UG VIPA
STAGE GROSS LIFTOFF MASS				317,261	
Stage start propellant			0		
STAGE PRELAUNCH GROSS MASS				317,261	
Interstage Cylinder					
Primary Body Structures:			2,654		
Interstage		2,654			UG VIPA
Separation Systems:			1,737		
Structure		810			UG VIPA
Separation Motors		927			UG VIPA
Thermal Protection Systems (TPS):			82		UG VIPA
Auxilary Propulsion System:			899		Popp
Roll Control group:		899			
INTERSTAGE DRY MASS W/O GROWTH				5,372	
Dry mass growth allowance			806		Modified from due to errors
INTERSTAGE DRY MASS W/GROWTH				6,178	
Roll Control Propellants:			2,199		sum
RCS propellant		2,189			Chapman
Roll Control press system		10			Chapman
Separation Systems:			693		sum
Separation Motor Propellant		693			VIPA
Miscellaneous:					
Crew and crew provisions		0			
INTERSTAGE GROSS MASS				9,070	28,368
2nd STAGE & INTERSTAGE GROSS MASS				326,331	

Legend

Structures and Thermal	20,897
Integrated Interstage	4,473
Integrated Main Propulsion System	3,472
Integrated Upper Stage Reaction Control System	785
Integrated First Stage Reaction Control System	899
Integrated Thrust Vector Control System - GRC	1,429
Integrated Avionics	886

Attachment 3

CLV 5-Segment SRB with J2-X Upper Stage Mass Bogies

38,750

Element	SUBTOTALS Secondary (lbm)	SUBTOTALS Primary (lbm)	Basic Mass (lbm)	Mass Growth Allowance (15%)	Predicted (Basic + MGA)	Design Challenge (MGA->Lv3, 5% ->Lv4)
First Stage						
Stage Dry Mass**		215,380	215,380	5,123	220,503	
Existing SRM,SRB inerts	191,195					n/a
Fwd Frustrum	24,185					TBD
Loaded Propellant		1,389,721				n/a
Residuals, etc		2,000				n/a
Upper Stage Dry Mass			28,369	4,255	32,624	27,018
Structures & Thermal		20,897	20,897	3,135	24,032	19,902
SC/Payload Adapter	1,074		1,074	161	1,235	1,023
Core Stage	15,350		15,350	2,303	17,653	14,619
Interstage Dry Mass	4,473		4,473	671	5,144	4,260
MPS		3,472	3,472	521	3,993	3,307
Upper Stage RCS		785	785	118	903	748
First Stage RCS		899	899	135	1,034	856
TVC (GRC)		1,429	1,429	214	1,644	1,361
Avionics		886	886	133	1,019	844
J2X Engine					5,100	TBD
Main Stage Propellant		279,877				n/a
FPR and Fuel Bias		2,468				n/a
Residuals		2,917				n/a
Upper Stage RCS Propellant		375				n/a
Other		79				n/a
Roll Control Propellant		2,199				n/a
Separation Motor Propellant		693				n/a
LAS						
Mass at Ignition **(minus Payload)**						
Throw Capability- Nominal Due East Crew		55,140				
Payload Allocation	47,948					
Margin (15% of Payload)	7,192					
Total Mass at Ignition						
***as calculated by POST on 01/15/06**						
****1% on existing hardware, 15% on Forward Skirt**						

Appendix B.2: Reference Mass Properties: "DAC0ExitMEL_Prop.xls"

Master Equipment List	BASIC MASS Tertiary	Secondary	Primary	Total	Basis of Estimation (BoE) (see MGA Depletion Chart)	MGA %	MGA	SubTotal	PREDICTED MASS
UPPER STAGE									
Structures and Thermal			22,161		sum	15%			25,510
Primary Body Structures		18,966			sum				
IU, CLV	865				SR: Struct & Mech-L	15%	130	995	
Forward skirt	478				SR: Struct & Mech-L	15%	72	550	
Liquid Oxygen tank	3,957				SR: Struct & Mech-L	15%	594	4,551	
Intertank	3,399				SR: Struct & Mech-L	15%	510	3,909	
Liquid Hydrogen tank	8,045				SR: Struct & Mech-L	15%	1,207	9,252	
Thrust structure	2,222				SR: Struct & Mech-L	15%	333	2,555	
Systems Tunnel		592			SR: Struct & Mech-L	15%	89	681	
IU Secondary Structures		671			sum				
Access Door	26				SR: Struct & Mech-L	15%	4	30	
Brackets & Panels, Avionics	540				SR: Struct & Mech-L	15%	81	621	
Avionics connector panels	30				SR: Struct & Mech-L	15%	5	35	
Utility Tray, misc. hardware	75				SR: Struct & Mech-L	15%	11	86	
Core Stage Secondary Struct		1105			sum				
Fwd Skirt Umby Plate, Sys Tun i/f	14				SR: Struct & Mech-L	15%	2	16	
Liquid Oxygen slosh baffles	394				SR: Struct & Mech-L	15%	59	453	
Liquid Oxygen anti-vortex	245				SR: Struct & Mech-L	15%	37	282	
Liquid Hydrogen slosh baffles	247				SR: Struct & Mech-L	15%	37	284	
Liquid Hydrogen anti-vortex	36				SR: Struct & Mech-L	15%	5	41	
LH2 Internal fasteners	108				SR: Struct & Mech-L	15%	16	124	
Intertank access door, fasteners	61				SR: Struct & Mech-L	15%	9	70	
Thermal Protection Systems (TPS):		205			sum				
IU, CLV side	38				JO: Thermal-L	18%	7	45	
Forward skirt	7				JO: Thermal-L	18%	1	8	
Intertank	85				JO: Thermal-L	18%	15	100	
Thrust Structure aft skirt	24				JO: Thermal-L	18%	4	28	
System Tunnel	51				JO: Thermal-L	18%	9	60	
Thermal Control Systems (TCS):		622			sum				
IU insulation (passive)	12				SR: Thermal-L	18%	2	14	
IU purge ducts (active)	15				SR: Thermal-L	18%	3	18	
Liquid Oxygen tank insulation	109				SR: Thermal-L	18%	20	129	
Liquid Hydrogen tank insulation	486				SR: Thermal-L	18%	87	573	
Main Propulsion System:			2,388		sum	10%			2,621
Pressurization systems:		490			sum				
O2 Tank Vent/Relief	87				MN: Propulsion-L	15%	13	100	
H2 Tank Vent/Relief	154				MN: Propulsion-L	15%	23	177	
H2 Tank Ground HE press	14				MN: Propulsion-L	15%	2	16	
H2 Tank MPS HE press	14				MN: Propulsion-L	15%	2	16	
H2 Tank GH2 press	78				MN: Propulsion-L	15%	12	90	
O2 Tank Ground HE press	14				MN: Propulsion-L	15%	2	16	
O2 Tank MPS HE press	14				MN: Propulsion-L	15%	2	16	
O2 Tank GH2 press	33				MN: Propulsion-L	15%	5	38	
Misc compnents, tertiary	82				MN: Built-in (20%)	0%	0	82	
O2 Systems:		396			sum				
O2 Fill and Drain	125				MN: Composite	5%	6	131	
Engine 02 Feed	136				MN: Composite	10%	14	149	
Engine O2 Conditioning	70				MN: Composite	10%	7	77	
Misc Compnents, tertiary	66				MN: Built-in (20%)	0%	0	66	
LH2 Systems:		1,034			sum				
LH2 Fill and Drain	110				MN: Composite	6%	7	117	
LH2 Recirculation Sys	91				MN: Composite	10%	9	100	
LH2 Feedline System	661				MN: Composite	14%	93	753	
Misc Compnents, tertiary	172				MN: Built-in (20%)	0%	0	172	
Pneumatic subsystem		468			sum				
HE fill	14				MN: Propulsion-L	15%	2	16	
HE Storage	170				MN: Propulsion-X	2%	3	173	
Engine/MPS Purge, Actuation	188				MN: Propulsion-L	15%	28	216	
H2,O2 Tank press HE Supply	6				MN: Propulsion-L	15%	1	7	
N2 Transfer	12				MN: Propulsion-L	15%	2	14	
Misc Compnents, tertiary	78				MN: Built-in (20%)	0%	0	78	
Upper Stage RCS (2 Modules)			890		sum				933
Prop/Press Tank	35				MD: Propulsion-L	15%	5	40	
Helium	1				MD: Propulsion-L	15%	0	1	
System Components	93				MD: Propulsion-L	15%	14	107	
Thrusters (6@ 100#)	124				MD: Propulsion-L	15%	19	142	
Support Structure	38				MD: Propulsion-L	15%	6	43	
Structure/Lines/Fittings	600				MD: Built-in growth	0%	0	600	

Thrust Vector Control			1,070			11%			1,185
Electro-Mechanical Actuators (2)	174				RT: Mechanisms-P	8%	14	188	
EMA Controllers (2)	150				RT: Heavy Avionics: E	15%	23	173	
High Voltage Power Control Unit (2)	168				RT: Heavy Avionics: E	15%	25	193	
Battery (2)	176				RT: Heavy Avionics: E	15%	26	202	
Electrical Cables/Harnesses	182				RT: SWAG	15%	27	209	
Secondary Structure	220				RT: built-in	0%	0	220	
Integrated Avionics			2,997		sum	10%			3,294
Electrical Power		1,355			sum				
Batteries	132				JW: Heavy Avionics: E	15%	20	152	
Power Distribution Units	192				JW: Heavy Avionics: E	15%	29	221	
Primary Power Cabling	231				JW: built in	0%	0	231	
E Integration Cabling (MSFC)	800				JW: built in	0%	0	800	
Communications		35			JW: Heavy Avionics: E	15%	5	40	
C&DH System		881			JW: Heavy Avionics: E	15%	132	1,013	
Operational Instrumentation		63			JW: Heavy Avionics: E	15%	9	73	
GN&C (IMU)		42			JW: Heavy Avionics: E	15%	6	48	
Control Electronics		138			JW: Heavy Avionics: E	15%	21	159	
Imaging System		135			JW: Heavy Avionics: E	15%	20	155	
Range Safety		348			sum				
UHF Command Sys	78				JW: Heavy Avionics: E	15%	12	90	
C-Band Radar Tracking	49				JW: Heavy Avionics: E	15%	7	56	
GPS Tracking Sys	14				JW: Light Avionics	30%	4	18	
Pyrotechnics	207				JW: Propulsion-E	15%	31	238	
UPPER STAGE DRY MASS (no Engine)			**BASIC**	29,506				**PREDICTED**	33,543
Upper Stage Engine (J2X)			5,500		KB: MGA, Margin included	0%	0	5,500	5500
Engine installation						0%			
UPPER STAGE DRY MASS (w/ Engine)			**BASIC**	35,006				**PREDICTED**	39,043
Residuals:			1,575		sum	n/a		1,575	
Main propellant (liquid residual)		1,249			MPS IPT	n/a			
Prop Tank Pressurization Gases:		310			sum	n/a			
Liquid Oxygen tank	118				MD	n/a			
Liquid Hydrogen tank	192				MD	n/a			
RCS propellant		5			INTROS	n/a			
Subsystems		12			INTROS	n/a			
Reserves:			2,823		sum	n/a		2,823	
Main propellant		2,823			MPS IPT	n/a			
Fuel bias		0			MPS IPT	n/a			
RCS propellant			150		MD	n/a		150	
APU reactants			6		INTROS	n/a		6	
Inflight Fluid Losses:			41		sum	n/a		41	
APU reactants		41				n/a			
UPPER STAGE BURNOUT MASS			**BASIC**	39,901				**PREDICTED**	43,638
Main Ascent Propellant:			282,345		sum	n/a		282,345	
Liquid Oxygen		238,907			INTROS	n/a			
Liquid Hydrogen		43,438			INTROS	n/a			
Engine purge helium			32		INTROS	n/a		32	
RCS ascent propellant			300		Danford	n/a		300	
UPPER STAGE GROSS LIFTOFF MASS			**BASIC**	322,278				**PREDICTED**	326,315
INTERSTAGE									
Interstage Structure:			10,360		sum	15%			11,914
Primary structure		7,579			SR: Built in (material selection)	15%	1,137	8,716	
Secondary (bracketry, doors, vents)		1,516			SR: Struct & Mech-L	15%	227	1,743	
BSM/RCS fairings, bracketry		283			SR: Struct & Mech-L	15%	42	325	
Separation Systems:		982			sum				
Separation rings	818				SR: Struct & Mech-L	15%	123	941	
Misc. hardware	164				SR: Struct & Mech-L	15%	25	189	
Thermal Protection Systems (TPS):			82		SR: Thermal-L	18%	15		97
BSM Motors (no prop)			927		MN: Prop-X	2%	19	945	945
Roll Control RCS			1,244		sum	8%			1,341
Prop/Press Tanks		230			MD: Prop-L	15%	35	265	
Helium		10			MD: Prop-L	15%	2	12	
System Components		129			MD: Prop-L	15%	19	148	
Thrusters (4 @800#)		192			MD: Prop-L	15%	29	221	
Misc. Hardware		83			MD: Prop-L	15%	12	95	
Structure/Lines/Fittings		600			MD: Built in growth	0%	0	600	
INTERSTAGE DRY MASS W/O GROWTH				12,613					14,297
Roll Control Propellants:			2,199		sum	n/a		2,199	
RCS propellant		2,189			MD	n/a			
Roll Control press system		10			MD	n/a			
Separation Systems:			693		sum			693	
Separation Motor Propellant		693			VIPA	n/a			
INTERSTAGE GROSS MASS			**BASIC**	15,505	36,619			**PREDICTED**	17,189

Appendix C: Ignition Overpressure Calculations

The ignition overpressure is a significant transient resulting from rapid acceleration of exhaust gases out of the engine / motor as well as afterburning at lift-off. The flow that is initiated after engine / motor ignition constitutes a source of mass, momentum, and energy. Compression and rarefaction waves are produced in the launch duct. These waves combine and impinge on the vehicle and neighboring structure. In addition, afterburning effects which cause a net volume change additionally cause an increase in the magnitude of the pulse.

The ignition overpressure model choice used for CLV predictions is the modified Broadwell and Tsu[1] methodology. This 1-D solution to the control volume form of the conservation equations provides a model that can be validated with the STS-1 ignition overpressure environment.

There are several models that describe IOP propagation and decay once outside of the duct. STS-1 solid rocket booster (SRB) ignition overpressure amplitude data has been fit using a nonlinear least squares method to give an accurate representation of the attenuation curve.[2] Other methods present curve fits to the data, but the methodology described in Casiano[2] uses physical relations and piecewise considerations to best fit the normalized curve to the data as a function of initial peak amplitude and distance from the source. The curve fits are represented in the far-field physically by using a linear R^{-1} correlation as would be expected for a spherical decay. In the near field where the decay is nonlinear, the best curve fit is of the nonlinear form R^{-2}.

1. Broadwell, J. E., and Tsu, C. N. An Analysis of Transient Pressures due to Rocket Starting in Underground Launchers. Space Technology Laboratories, Inc. June 29th, 1961.

2. Casiano, M. J. A Methodology for Predicting Ignition Overpressure and Attenuation Characteristics – MSFC NASA Internal Memorandum. ER42 (06-004).

Analysis assumptions:

- IOP prediction and launch/exhaust duct assumptions
    - Model is 1-D
    - Wave propagation is planar
    - Low Mach number flow
    - Low engine mass flow
    - Low thrust per area
    - Empirical corrections for afterburning
    - Empirical corrections for jet momentum loss
    - Momentum terms neglected (small compared to mass terms)
    - Mass flow rate is proportional to chamber pressure
    - Model uses 4 waves
    - Mass, momentum, energy source is reduced to a point (apparent source)
    - Source appears instantaneously (flow is not modeled through ignition)

- Attenuation propagation model
  - The predicted IOP waveform at the duct exit is regarded as a source
  - The far-field is linear spherical decay
  - The near field follows an R^{-2} decay

Other physical assumptions:

- Symmetric IOP out of launch duct
- No water suppression system
- No water bags to dissipate initial IOP pulse
- The model 'clvfsb05306' thrust profile is representative of actual 1st stage 5-segment booster thrust profile

There are assumptions in the analysis so that it is necessary to validate the prediction with STS-1 data. This implies an additional assumption:

- STS-1 fluid dynamic environment is similar to CLV fluid dynamic environment
  - STS-1 data contains fluid interactions with the solid rocket motor/external tank/orbiter acoustic
  - MLP geometry used with holes uncovered

Appendix D: Reference CEV Delivered FEM: "CEV_FEM_DAC2_summary.doc"

Crew Exploration Vehicle Finite Element Models
Command and Service Modules
B.E. Quasius
03 MAY 2006

The Lunar CEV Capsule, in conjunction with the Service Module and Launch Vehicle/Earth Departure Stage, is used to transport four crew members from Earth to lunar orbit and return them to Earth. The Capsule provides habitable volume for the crew, life support, docking and pressurized crew transfer to the LSAM, and atmospheric entry and landing capabilities.

The model, seen below, consists of 9758 nodes, 9488 elements, 15 concentrated masses, and 1426 MPCs (primarily connecting frame beam elements to shell elements). All nodes are modeled in the 4000000 or 4500000 coordinate systems which refer to CEV reference coordinate frame 4000100. The distance from the reference coordinate frame to the CLV/CEV interface is 327.379 inches.

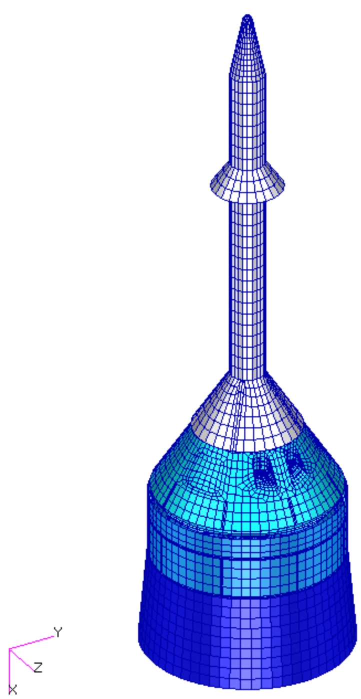

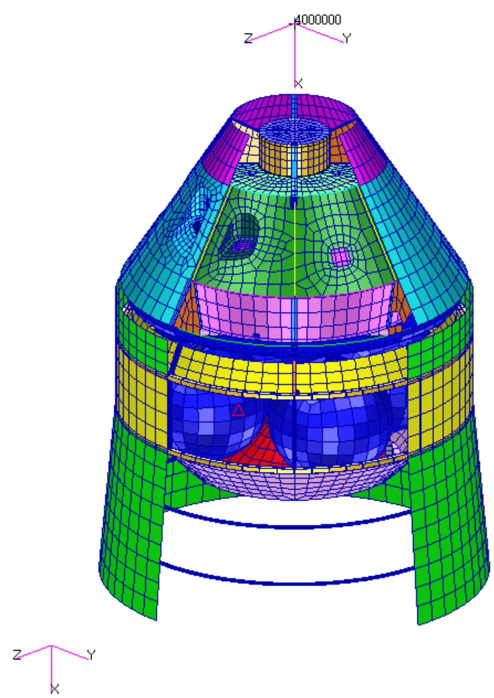

The following assumptions have been made:

1. Masses have generally been distributed as non-structural mass (NSM) where applicable, including TPS and most other NSM. Propellant, crew masses, and the engine were modeled as concentrated mass

2. Mass properties correlate to the JSC DAC2 Mass Allocations
    a. CEV weight: 50,785 lb
    b. Command Module weight: 17,300 lb
    c. Service Module weight: 29,870 lb
    d. LAS weight: 13,290 lb
3. Material properties were supplied by Ronald Baccus. Generic aluminum and steel and graphite (IM-7) composites are the principal materials, an idealized honeycomb core material is also used. All materials are located in the Cev13Materials.bulk file.
4. Honeycomb material properties are modeled with PCOMP cards.
5. Flanges are modeled with CBEAM/CBAR elements.
6. FEM ranges
    a. Nodes: 4, XXX,XXX
    b. Adapter interface nodes: 94,XXX,XXX
    c. Centerline nodes: 84,XXX,XXX
    d. Elements: 4, XXX,XXX
    e. RBEs: 4, XXX,XXX (unique IDs
    f. Material Ids: 4, XXX,XXX
    g. Property Ids: 4, XXX,XXX

Comments:
Model Verification
1. Mass and CG locations were verified.
2. Free-free mode checks were performed.
3. One-G Equilibrium checks were performed.
4. Unit cabin and tank pressure loads not examined this time
5. Determinate constraint thermal check was not performed.
6. Strain energy was checked with the GROUNDCHECK=YES. One direction marginally failed, but no modeling errors were discovered.

MODEL CHECKOUTS

GRAVITY CHECK

E Q U I L I B R I U M   C H E C K

RESULTANT LOADS IN BASIC COORDINATE SYSTEM

SUBCASE NO.	REFERENCE POINT	LOAD TYPE	T1	T2	T3	R1	R2	R3
1	ORIGIN	APP-LOAD	6.109080E+04	-5.015253E-15	4.931397E-15	1.209840E-12	-1.575212E+05	-2.256563E+02
		F-OF-SPC	-6.109080E+04	1.552536E-10	3.498409E-09	0.000000E+00	1.575212E+05	2.256563E+02
		F-OF-MPC	-1.972167E-11	-5.044853E-13	-2.944311E-12	-3.051758E-05	-2.441406E-04	1.525879E-05
			-------------	-------------	-------------	-------------	-------------	-------------
		TOTALS	-1.972167E-11	1.547441E-10	3.495469E-09	-3.051758E-05	-2.441406E-04	1.525879E-05
2	ORIGIN	APP-LOAD	-5.015253E-15	6.109080E+04	-3.084416E-14	1.575212E+05	5.328640E-12	7.560910E+06
		F-OF-SPC	-2.267006E-08	-6.109080E+04	-8.252135E-08	-1.575212E+05	-7.023547E-06	-7.560910E+06
		F-OF-MPC	-1.008749E-11	1.013234E-10	3.820944E-12	-2.441406E-04	7.629395E-06	3.906250E-02
			-------------	-------------	-------------	-------------	-------------	-------------
		TOTALS	-2.268016E-08	1.013234E-10	-8.251757E-08	1.538086E-02	6.058525E-07	-4.609375E-01
3	ORIGIN	APP-LOAD	4.931397E-15	-3.084416E-14	6.109080E+04	2.256563E+02	-7.560910E+06	-6.538480E-12
		F-OF-SPC	4.168214E-09	-8.641695E-08	-6.109080E+04	-2.256563E+02	7.560910E+06	7.801711E-06
		F-OF-MPC	-3.561380E-11	-1.581846E-12	1.548059E-10	0.000000E+00	-7.812500E-03	9.155273E-05
			-------------	-------------	-------------	-------------	-------------	-------------
		TOTALS	4.132605E-09	-8.641856E-08	1.548059E-10	0.000000E+00	4.921875E-01	9.935444E-05

FREE MODE CHECK

R E A L   E I G E N V A L U E S

MODE NO.	EXTRACTION ORDER	EIGENVALUE	RADIANS	CYCLES	GENERALIZED MASS	GENERALIZED STIFFNESS
1	1	-7.944618E-08	2.818620E-04	4.485973E-05	1.000000E+00	-7.944618E-08
2	2	-1.188891E-08	1.090363E-04	1.735367E-05	1.000000E+00	-1.188891E-08
3	3	-8.734787E-09	9.346008E-05	1.487463E-05	1.000000E+00	-8.734787E-09
4	4	-4.380126E-09	6.618253E-05	1.053328E-05	1.000000E+00	-4.380126E-09
5	5	3.332389E-09	5.772684E-05	9.187513E-06	1.000000E+00	3.332389E-09
6	6	1.507942E-08	1.227983E-04	1.954396E-05	1.000000E+00	1.507942E-08
7	7	1.134778E+03	3.368647E+01	5.361368E+00	1.000000E+00	1.134778E+03
8	8	1.179634E+03	3.434579E+01	5.466303E+00	1.000000E+00	1.179634E+03
9	9	5.442266E+03	7.377171E+01	1.174113E+01	1.000000E+00	5.442266E+03
10	10	6.769669E+03	8.227800E+01	1.309495E+01	1.000000E+00	6.769669E+03
11	11	7.991718E+03	8.939641E+01	1.422788E+01	1.000000E+00	7.991718E+03
12	12	1.194947E+04	1.093136E+02	1.739780E+01	1.000000E+00	1.194947E+04
13	13	1.246971E+04	1.116679E+02	1.777249E+01	1.000000E+00	1.246971E+04
14	14	1.305042E+04	1.142384E+02	1.818161E+01	1.000000E+00	1.305042E+04
15	15	1.357678E+04	1.165194E+02	1.854465E+01	1.000000E+00	1.357678E+04
16	16	1.387390E+04	1.177875E+02	1.874646E+01	1.000000E+00	1.387390E+04
17	17	1.712605E+04	1.308665E+02	2.082805E+01	1.000000E+00	1.712605E+04
18	18	1.795009E+04	1.339780E+02	2.132325E+01	1.000000E+00	1.795009E+04
19	19	1.940686E+04	1.393085E+02	2.217163E+01	1.000000E+00	1.940686E+04
20	20	2.010002E+04	1.417746E+02	2.256412E+01	1.000000E+00	2.010002E+04
21	21	2.039508E+04	1.428114E+02	2.272913E+01	1.000000E+00	2.039508E+04
22	22	2.044540E+04	1.429874E+02	2.275715E+01	1.000000E+00	2.044540E+04
23	23	2.129509E+04	1.459284E+02	2.322522E+01	1.000000E+00	2.129509E+04
24	24	2.214916E+04	1.488260E+02	2.368639E+01	1.000000E+00	2.214916E+04

GROUNDING/ELEMENT STRAIN ENERGY CHECK

Failed direction is close to passing. No modeling errors found in FEM

RESULTS OF RIGID BODY CHECKS OF MATRIX KGG (G-SET) FOLLOW:
PRINT RESULTS IN ALL SIX DIRECTIONS AGAINST THE LIMIT OF 5.713147E-03

DIRECTION	STRAIN ENERGY	PASS/FAIL
1	1.301624E-08	PASS
2	4.096942E-08	PASS
3	3.801360E-08	PASS
4	1.507628E-04	PASS
5	**7.574474E-03**	**FAIL**
6	5.209376E-04	PASS

SOME POSSIBLE REASONS MAY LEAD TO THE FAILURE:

1. CELASI ELEMENTS CONNECTING TO ONLY ONE GRID POINT;
2. CELASI ELEMENTS CONNECTING TO NON-COINCIDENT POINTS;
3. CELASI ELEMENTS CONNECTING TO NON-COLINEAR DOF;
4. IMPROPERLY DEFINED DMIG MATRICES;

MASS PROPERTY CHECKS

CEV Stack (LAS, CM, SM)- Origin at CM OML Cone Apex

E L E M E N T   P R O P E R T Y   S U M M A R Y   (BY PROPERTY TYPE / ID)

	STRUCT.MASS	NON-STR.MASS	TOTAL MASS	TM*WTMASS
SUBTOTAL MASS FOR ALL BAR ELEMENTS	2.39484E+01	2.97631E+01	5.37115E+01	5.37115E+01
SUBTOTAL MASS FOR ALL BEAM ELEMENTS	7.17058E-01	9.39859E+00	1.01157E+01	1.01157E+01
SUBTOTAL MASS FOR ALL CONM2 ELEMENTS	6.38123E+01	0.00000E+00	6.38123E+01	6.38123E+01
SUBTOTAL MASS FOR ALL SHELL ELEMENTS	2.32349E+01	7.22811E+00	3.04630E+01	3.04630E+01
SUBTOTAL MASS FOR ALL QUAD4 ELEMENTS	2.32314E+01	7.22811E+00	3.04595E+01	3.04595E+01
SUBTOTAL MASS FOR ALL TRIA3 ELEMENTS	3.50403E-03	0.00000E+00	3.50403E-03	3.50403E-03
TOTAL MASS FOR ALL SUPPORTED ELEMENT TYPES	1.11713E+02	4.63898E+01	1.58102E+02	1.58102E+02

```
     DIRECTION
MASS AXIS SYSTEM (S)     MASS             X-C.G.        Y-C.G.        Z-C.G.
        X           1.581025E+02      1.980396E-17  3.693785E-03 -2.578476E+00
        Y           1.581025E+02      1.237651E+02  8.722492E-17 -2.578476E+00
        Z           1.581025E+02      1.237651E+02  3.693785E-03 -1.070289E-16
                                          I(S)
                 *  4.865752E+05 -1.134165E+01 -4.859985E+03 *
                 * -1.134165E+01  3.061788E+06 -1.391663E+04 *
                 * -4.859985E+03 -1.391663E+04  3.023383E+06 *
                                          I(Q)
                 *  3.018878E+06                             *
                 *                4.865659E+05               *
                 *                              3.066302E+06 *
                                           Q
                 *  1.824232E-03  9.999982E-01  5.852729E-04 *
                 * -3.084501E-01  5.949195E-06  9.512405E-01 *
                 *  9.512388E-01 -1.915811E-03  3.084496E-01 *
```

CM- Origin at CM OML Cone Apex

	STRUCT.MASS	NON-STR.MASS	TOTAL MASS	TM*WTMASS
SUBTOTAL MASS FOR ALL BAR ELEMENTS	1.57168E+00	2.97631E+01	3.13348E+01	3.13348E+01
SUBTOTAL MASS FOR ALL CONM2 ELEMENTS	4.54710E+00	0.00000E+00	4.54710E+00	4.54710E+00
SUBTOTAL MASS FOR ALL SHELL ELEMENTS	2.94390E+00	5.93260E+00	8.87649E+00	8.87649E+00
SUBTOTAL MASS FOR ALL QUAD4 ELEMENTS	2.94039E+00	5.93260E+00	8.87299E+00	8.87299E+00
SUBTOTAL MASS FOR ALL TRIA3 ELEMENTS	3.50403E-03	0.00000E+00	3.50403E-03	3.50403E-03
TOTAL MASS FOR ALL SUPPORTED ELEMENT TYPES	9.06268E+00	3.56957E+01	4.47583E+01	4.47583E+01

```
     DIRECTION
MASS AXIS SYSTEM (S)     MASS             X-C.G.        Y-C.G.        Z-C.G.
        X           4.475835E+01      0.000000E+00  1.305437E-02 -9.108061E+00
        Y           4.475835E+01      1.343475E+02  0.000000E+00 -9.108061E+00
        Z           4.475835E+01      1.343475E+02  1.305437E-02  0.000000E+00
```

SM- Origin at CM OML Cone Apex

	STRUCT.MASS	NON-STR.MASS	TOTAL MASS	TM*WTMASS
SUBTOTAL MASS FOR ALL BAR ELEMENTS	2.10384E-01	0.00000E+00	2.10384E-01	2.10384E-01
SUBTOTAL MASS FOR ALL BEAM ELEMENTS	7.17058E-01	9.39859E+00	1.01157E+01	1.01157E+01
SUBTOTAL MASS FOR ALL CONM2 ELEMENTS	5.92652E+01	0.00000E+00	5.92652E+01	5.92652E+01
SUBTOTAL MASS FOR ALL SHELL ELEMENTS	6.41654E+00	1.29551E+00	7.71206E+00	7.71206E+00
SUBTOTAL MASS FOR ALL QUAD4 ELEMENTS	6.41654E+00	1.29551E+00	7.71206E+00	7.71206E+00
TOTAL MASS FOR ALL SUPPORTED ELEMENT TYPES	6.66092E+01	1.06941E+01	7.73033E+01	7.73033E+01

```
     DIRECTION
MASS AXIS SYSTEM (S)     MASS             X-C.G.        Y-C.G.        Z-C.G.
        X           7.730329E+01      4.050351E-17  1.527946E-05 -3.733709E-06
        Y           7.730329E+01      2.144795E+02  1.783944E-16 -3.733709E-06
        Z           7.730329E+01      2.144795E+02  1.527946E-05 -2.188979E-16
```

Appendix E: FSB Thrust Dispersions

This Appendix contains a draft memo with further details of the FSB thrust dispersion calculations.

April 14, 2006

ER (06-XXX)

TO: JP10/David Anderson

FROM: ER01/Carl P. Jones

THRU: ED04/Tim Ezell

THRU: JP20/Rick Burt

SUBJECT: Five Segment Booster Dispersion Model for DAC 1 Trajectory Analysis

REF:
(1) TR017186 "1st Stage Final Ballistic Prediction for Crew Launch Vehicle Design and Analysis Cycle Zero"
(2) ER20 (05-003) "Methodology Used to Create Booster Separation Motor Thrust-Time Traces for Critical Math Model CMM-193"
(3) NSTS 07700 Volume 10 Book 2 "Space Shuttle Flight and Ground System Specification: Environment Design, Weight and Performance, and Avionics Events"

The purpose of this memo is to document a recommended Five Segment Booster (FSB) performance dispersion model for CLV DAC 1 use.

The recommended model consists of separate representations for Loads analysts and Trajectory analysts. For Loads analysis, bounding motor performance traces will be described that represent the highest and lowest thrust that the vehicle will experience. For Trajectory analysis, a scaling algorithm will be described that is capable of generating motor performance at any Propellant Mean Bulk Temperature (PMBT), burn rate, and propellant weight.

FSB Dispersion Analysis

The nominal FSB performance (CLVFSB-05306) has previously been documented. Dispersions about that nominal motor performance are required for Loads, Trajectory, and other disciplines analysis work.

MSFC ER and ATK have performed preliminary dispersion analysis of the FSB motor configuration. The analysis is preliminary because no actual FSB motor data exists. All analysis has been based on RSRM data with engineering judgment used to extrapolate results to the FSB motor configuration. An agreed to goal of the preliminary dispersion analysis was to synchronize CLV analysis/certification dispersion levels with the FSB motor Contract End Item (CEI) specification dispersion levels. This goal is a result of the subtle disconnect that exists today on the Space Shuttle program. The Space Shuttle Vehicle (SSV) is currently certified to an environment that tighter than the motor CEI specification allows. A good example of this is the web time difference between motor pairs (web time is a burn rate indicator). The SSV is certified to a 1.2% web time difference between pairs. ATK's CEI specification allows a 2% web time difference between pairs. It is desirable to resolve such ambiguities in the CLV program.

MSFC ER's approach to FSB dispersion analysis was to provide moderate margin on a standard statistical analysis of the RSRM dispersion data. ER's standard dispersion recommendation is to provide coverage for 99.73% of the population at 90% confidence. 99.73% population coverage covers the range from -3 standard deviations to +3 standard deviations in a normally distributed data set. A confidence level must be specified since the data used is considered a sample of a larger population. ER traditionally uses 90% confidence in its analysis. For FSB preliminary dispersion analysis, ER's approach was to increase population coverage to 99.9% coverage at 95% confidence and to then add an additional 10% on top of that dispersion. This larger population coverage and 10% "pad" was felt appropriate for the unknowns that may occur with the FSB motor development.

Concurrent to ER's effort, ATK approached the FSB preliminary dispersion analysis using two analysis methods. For the first analysis method, ATK investigated their manufacturing process capability and derived a dispersion estimate based on 2*Cpk. Cpk is the process capability index and is a measure of both centeredness and spread of a manufacturing process. A Cpk of 1.0 indicates the process variability is at a specification limit. Manufacturers typically target a Cpk of 1.33 or higher which indicates a manufacturing process is well within specification limits. For the second analysis method, ATK performed a more formal dispersion analysis by breaking the dispersions up into burn rate contributors and trace shape contributors. ATK applied a root-sum-square technique to arrive at the total dispersion level and added some additional "pad" by allowing the nominal motor to vary by an additional 0.003 ips in burn rate.

ER and ATK converged to similar recommended steady-state dispersion levels. Table 1 shows the results of ER and ATK along with the final agreed to dispersion level recommendations and the current RSRM CEI Specification limits.

CEI Individual Motor Performance @ 60 Deg. F	ER22 99.9% Prob @95% Conf + 10% (%)	ATK Rb, Shape + 3 mils/s Rb (%)	**Final Recommended FSB Dispersions (%)**	RSRM CEI (%)
Interval Web Time (sec)	3.61	3.55	**3.7**	5.0
Interval Action Time (sec)	3.73	3.66	**3.7**	6.5
Interval Web Time Average Pressure (psia)	3.62	3.68	**3.7**	5.3
Maximum Head-End Pressure (psia)	4.17	4.21	**4.2**	6.5
Maximum Sea-Level Thrust (Mlbf)	3.55	3.81	**3.8**	6.2
Interval Web Time Average Vac Thrust (Mlbf)	3.62	3.67	**3.8**	5.3
Vacuum Delivered Specific Impulse (sec)	0.80	0.78	**1.0**	0.7
Interval Web Time Vac Total Impulse (Mlbf-sec)	1.01	0.87	**1.0**	1.0
Interval Action Time Vac Total Impulse (Mlbf-sec)	0.80	0.77	**1.0**	1.0

Table 1 FSB Steady-State Dispersion Analysis Results

In addition to the steady-state dispersion levels, dispersions on ignition parameters and a few miscellaneous parameters are requires. For the ignition parameters, ER applied the same 99.9% coverage at 95% confidence plus 10% approach while ATK recommended RSRM nominal values +/- 4 standard deviations on the data. ATK used a different approach since burn rate doesn't affect the ignition parameters as readily as it does the steady-state parameters. Table 2 shows the results of the ER and ATK analysis. ER agreed to adopt the ATK results.

Ignition Requirements		ER22 99.9% Prob @95% Conf + 10%	ATK 4 Std Dev	**Final Recommended FSB Dispersions**	RSRM CEI
Pressure Rise Rate (psi/10 ms)	MIN	57.5	63.1	**63.1**	65.7
	NOM	90.9	90.8	**90.8**	90.8
	MAX	129.8	118.6	**118.6**	115.9
Ignition Interval (secs)	MIN	182	0.202	**0.202**	0.202
	NOM	230	0.230	**0.230**	0.232
	MAX	284	0.259	**0.259**	0.262
Thrust Rise Rate (lbf/10 ms)	MIN	129600	156082	**156000**	154000
	NOM	253000	253014	**253000**	252000
	MAX	398200	349946	**350000**	350000

Table 2 FSB Ignition Parameter Dispersion Analysis Results

Two other miscellaneous parameters were determined and agreed to. Motor Inert Weight dispersions remain at 0.85% (same as RSRM). Motor Propellant Weight dispersions were set at 0.25%, up from RSRM value of 0.21%. The increased Propellant Weight dispersion reflects some increased conservatism (RSRM has always been close to the edge of this specification limit) and the effect of an additional segment.

Dispersed Performance Trace Generation: Loads Analysis

Tables 1 and 2 give values of the steady-sate and ignition parameter dispersions for the FSB. From this information performance traces need to be generated for use by the Loads analysis community. For the Space Shuttle Program, ER (via Boeing) provides the Ascent Performance community with FORTRAN subroutines that the user can link into their analysis codes. These subroutines provide dispersed performance traces given inputs on desired dispersion levels. For CLV, subroutines such as used on Shuttle are not available.

Dispersions About the Nominal Motor Trace

Scaling Model for DAC 1 Trajectory Use

Based on the above nominal and dispersion results, the following is the recommended DAC 1 FSB Dispersion Model for Trajectory Analysis use. Random variables for the model are as follows.

Rb	$= 0.337 + \sigma_{rb} * 0.0037$	(inches/sec)
PMBT	= f(month,day)	(deg F)
WP	$= 1380508 * (1.0 + \sigma_{wp} * 0.00083)$	(lbm)
FM	$= 1.0 + \sigma_{isp} * 0.0033$	(non-dimensional)

In the above equations, σ represents the desired dispersion sigma-level multiplier (-3 to 3) on the standard deviation.

Individual FSB performance traces can be created from these dispersion values, the nominal FSB performance trace, and the performance scaling equations documented in the SPAD (NSTS 08209, Vol 1). These equations are shown below.

$$P_{scaled} = P*\exp[0.0011*(\mathbf{PMBT}-60) + 0.001063*(1474.274*LN\{\mathbf{RB}/0.368\})]*(\mathbf{WP}/1106059)^{1.53846}$$

$$F_{scaled} = FM*F*\exp[0.0011*(\mathbf{PMBT}-60) + 0.001063*(1474.274*LN\{\mathbf{RB}/0.368\})]*(\mathbf{WP}/1106059)^{1.53846}$$

$$W_{scaled} = W*\exp[0.001063*(\mathbf{PMBT}-60) + 0.001063*(1474.274*LN\{\mathbf{RB}/0.368\})]*(\mathbf{WP}/1106059)^{1.53846}$$

$$T_{scaled} = T*\exp[-0.001063*(\mathbf{PMBT}-60) - 0.001063*(1474.274*LN\{\mathbf{RB}/0.368\})]*(\mathbf{WP}/1106059)^{-0.53846}$$

Where P is pressure, F is thrust, W is flowrate, and T is time.

Dispersion Model Usage, Limitations, and Improvements Needed

Questions on this analysis should be directed to the ER22/Tim Olive at (256) 544-1509.

Original Signed by

Carl P. Jones
Director
MSFC Propulsion Directorate

cc:
JP20/Rick Burt
JP20/Zena Hester
MP41/David Ricks
MP51/Sam Ortega
ED04/Tim Ezell
EI21/Robert Cooper
ER01/Carl P. Jones
ER20/Robert Garcia
ER22/Bobby Taylor
ER22/Ben Hayashida
ER22/Jennifer Stevens
ER22/Karen Bishop-Behel
ER22/Tim Olive
EV10/John Hutt
EV12/Don Krupp
EV40/Steve Ryan
EV42/Mark Phillips
EV42/Greg Dukeman